Target Detection Architecture for Resource Constrained Wireless Sensor Networks within Internet of Things

Bolisetti Siva Karteek

A thesis submitted in partial fulfilment of the requirement of Staffordshire University for the degree of Doctor of Philosophy

August 2017

Abstract

Wireless sensor networks (WSN) within Internet of Things (IoT) have the potential to address the growing detection and classification requirements among many surveillance applications. RF sensing techniques are the next generation technologies which offer distinct advantages over traditional passive means of sensing such as acoustic and seismic which are used for surveillance and target detection applications of WSN. RF sensing based WSN within IoT detect the presence of designated targets by transmitting RF signals into the sensing environment and observing the reflected echoes. In this thesis, an RF sensing based target detection architecture for surveillance applications of WSN has been proposed to detect the presence of stationary targets within the sensing environment.

With multiple sensing nodes operating simultaneously within the sensing region, diversity among the sensing nodes in the choice of transmit waveforms is required. Existing multiple access techniques to accommodate multiple sensing nodes within the sensing environment are not suitable for RF sensing based WSN. In this thesis, a diversity in the choice of the transmit waveforms has been proposed and transmit waveforms which are suitable for RF sensing based WSN have been discussed. A criterion have been defined to quantify the ease of detecting the signal and energy efficiency of the signal based on which ease of detection index and energy efficiency index respectively have been generated. The waveform selection criterion proposed in this thesis takes the WSN sensing conditions into account and identifies the optimum transmit waveform within the available choices of transmit waveforms based on their respective ease of detection and energy efficiency indexes.

A target detector analyses the received RF signals to make a decision regarding the existence or absence of targets within the sensing region. Existing target detectors which are discussed in the context of WSN do not take the factors such as interference and nature of the sensing environment into account. Depending on the nature of the sensing environment, in this thesis the sensing environments

are classified as homogeneous and heterogeneous sensing environments. Within homogeneous sensing environments the presence of interference from the neighbouring sensing nodes is assumed. A target detector has been proposed for WSN within homogeneous sensing environments which can reliably detect the presence of targets. Within heterogeneous sensing environments the presence of clutter and interfering waveforms is assumed. A target detector has been proposed for WSN within heterogeneous sensing environments to detect targets in the presence of clutter and interfering waveforms. A clutter estimation technique has been proposed to assist the proposed target detector to achieve increased target detection reliability in the presence of clutter. A combination of compressive and two-step target detection architectures has been proposed to reduce the transmission costs. Finally, a 2-stage target detection architecture has been proposed to reduce the computational complexity of the proposed target detection architecture.

List of Published Work

J02 S.K. Bolisetti, M. Patwary, M.N. Soliman, and M. Abdel-Maguid, "RF Sensing Based Target Detector for Smart Sensing within Internet of Things in Harsh Sensing Environments," IEEE Access, July, 2017

C02 S.K. Bolisetti, M. Patwary, M.N. Soliman, and M. Abdel-Maguid, "Energy Efficient Target Detection Through Waveform Selection for Multi-Sensor RF Sensing Based Internet of Things," (Under Review, IEEE PIMRC, 2017)

J01 S.K. Bolisetti, M. Patwary, K. Ahmed, M.N. Soliman, and M. Abdel-Maguid, "Subspace compressive GLRT detector for MIMO radar in the presence of clutter," In Scientific World Journal, vol. 2015, Article ID 341619, 8 pages, 2015.

C01 S.K. Bolisetti, K. Ahmed, M. Patwary, and M. Abdel-Maguid, "Compressive parametric glrt detector for airborne mimo radar," In International Conference on Wireless Communications and Signal Processing, WCSP, pages 1-5, nov. 2011. doi:10.1109/WCSP.2011.6096735.

Acknowledgements

Undertaking this PhD has been a memorable and life-changing experience for me. It has been a long journey and I am honoured to have met many people along the way who have supported my academically and emotionally. It would not have been possible for me to get here without all the support that I received from my supervision team and colleagues.

I would like to first thank my principle supervisor Prof. Mohammad Patwary for all the invaluable support he gave me throughout my PhD. He encouraged to me to pursue my PhD and has always stood by me to support and guide me along the right path. He has always believed in my abilities and always encouraged me to follow my ideas.

I would also like to thank Dr. Abdel-Hamid Soliman for his kind support. He is one of the most helpful persons I have met and I am grateful have him in my supervision team.

I greatly appreciate the support I received from Prof. Mohamed Abdel-Maguid for his valuable support and guidance especially during the first phase of my PhD.

I would also like to thank all my friends and colleagues. They have made my time here a truly memorable one. Special thanks to Kamran Naeem, Anas Amjad, Masum Billah and Raouf Abozariba for their friendship and support.

I would finally like to say a heart felt thank you to my loving sister, mom and my dad, Mr. Haribabu Bolisetti who stood by me during the good and bad times with their love, motivation and support. With their unconditional support, they have always motivated to follow my dreams.

Contents

List of Figures

List of Tables

Abbreviations

ABORT	**A**daptive **B**eam-forming **O**rthogonal **R**ejection **T**est
ACE	**A**daptive **C**oherence **E**stimator
ADC	**A**nalog-to-**D**igital **C**onverter
AIE	**A**daptive to **I**nterference **E**stimator
AMF	**A**daptive **M**atched **F**ilter
APP	**A** **P**osteriori **P**robability
ASB	**A**daptive **S**idelobe **B**lanker
AWGN	**A**dditive **W**hite **G**aussian **N**oise
C-AIE	**C**ompressive-**A**daptive to **I**nterference **E**stimator
C-GLRT	**C**ompressive-**G**eneralised **L**ikelihood **R**atio **T**est
CC	**C**ross-**C**orrelation
CFAR	**C**onstant **F**alse **A**larm **R**ate
DVS	**D**ynamic **V**oltage **S**caling
GLRT	**G**eneralised **L**ikelihood **R**atio **T**est
IoT	**I**nternet **o**f **T**hings
ISM	**I**ndustrial, **S**cientific and **M**edical
MAC	**M**ultiple **A**ccess **C**hannel
MAP	**M**aximum **A**posteriori **P**robability
MDL	**M**aximum **D**escription **L**ength
MIMO	**M**ultiple **I**nput **M**ultiple **O**utput
ML	**M**aximum **L**ikelihood
MLE	**M**aximum **L**ikelihood **E**stimator

MPI	**M**ost **P**owerful **I**nvariant
NP	**N**eyman-**P**earson
P_d	**P**robability of **D**etection
P_{fa}	**P**robability of **F**alse **A**larm
PAC	**P**arallel **A**ccess **C**hannel
QoS	**Q**uality **o**f **S**ervice
SCM	**S**imple **C**ovariance **M**atrix
SCR	**S**ignal to **C**lutter **R**atio
SD	**S**ubspace **D**etector
SINR	**S**ignal to **I**nterference and **N**oise **R**atio
SIR	**S**ignal to **I**nterference **R**atio
SNR	**S**ignal to **N**oise **R**atio
UWB	**U**ltra **W**ide **B**and
WSN	**W**ireless **S**ensor **N**etwork

Symbols

P_t	Transmit signal power
P_r	Received signal power
λ_w	Wavelength
N_s	Number of sensing nodes
$\mathbf{y}_i$	Received signal at the i^{th} sensing node
$\bar{\mathbf{y}}_i$	Compressed received signal at the i^{th} sensing node
N_y	Number of received signal samples
$\mathbf{s}$	Transmit waveform
$\mathbf{S}$	Transmit waveform convolution matrix
N_t	Transmit signal length
$\mathbf{h}$	Interfering waveform
$\mathbf{H}$	Interfering waveform convolution matrix
t_n	Number of targets
$\mathbf{a}$	Target impulse response
$\mathbf{A}$	Convolution matrix for target impulse response
N_a	Target impulse response length
b_n	Number of interfering waveforms
$\mathbf{b}$	Interfering signal impulse response
$\mathbf{B}$	Convolution matrix for impulse response of Interfering signal
c_n	Number of clutter scatterers
$\mathbf{w}$	AWGN noise
$\boldsymbol{\sigma}^2$	Noise variance

$\mathbf{d}$	Disturbance vector
$\mathbf{R}_d$	Disturbance covariance matrix
δ	Ease of detection index
η	Energy efficiency Index
α	Scaling factor
$*$	Convolution operator
$Q(\,)$	Marcum Q function
$Q^{-1}(\,)$	Inverse marcum Q function
$f(\,)$	Probability density function
$\Gamma(\,)$	Log-likelihood function
$\hat{(\,)}$	Maximum likelihood estimate
$\bar{(\,)}$	Compressed data
$\mathbb{T}$	Test statistic
γ	Detection threshold
$\boldsymbol{\phi}_i$	Measurement matrix at the i^{th} sensing node
$\boldsymbol{\phi}$	Measurement matrix at the control centre
μ	Compression ratio
ς	Clutter texture
λ_i	i^{th} Eigenvalue
$\boldsymbol{\Phi}_i$	i^{th} Eigenvector
r	Rank of a matrix
$\mathbf{K}$	Projection matrix for interfering signal
$\boldsymbol{\nabla}$	Measurement coefficient
χ	Test statistic coefficient

Chapter 1

Introduction

1.1 Introduction to Wireless Sensor Networks as Internet of Things

Internet of Things (IoT) is a network of devices, which have the ability to sense and gather data and then share the information over the internet with other devices where it can be utilised for various applications. A visual representation of IoT [1] is shown in Figure 1.1. The sensing devices within the IoT perform the primary and the most important function of sensing and collecting the desired information. Depending on the nature of the application, the sensing devices within IoT can be inter-connected to form a network of sensing nodes, which are referred to as Wireless Sensor Networks (WSNs). WSNs are the key technologies within IoT, which enables reliable and energy efficient operation of the desired task. WSNs have been widely considered to be one of the most important emerging technologies in the recent times. In this research, WSNs are considered to be a part of one of the elements within IoT.

Recent advancements in microprocessing and wireless communication technologies allowed development of compact, low-cost and energy efficient sensing nodes. Once deployed within the sensing region, the sensing nodes coordinate among themselves and perform tasks such as assigned. Depending on the nature of the

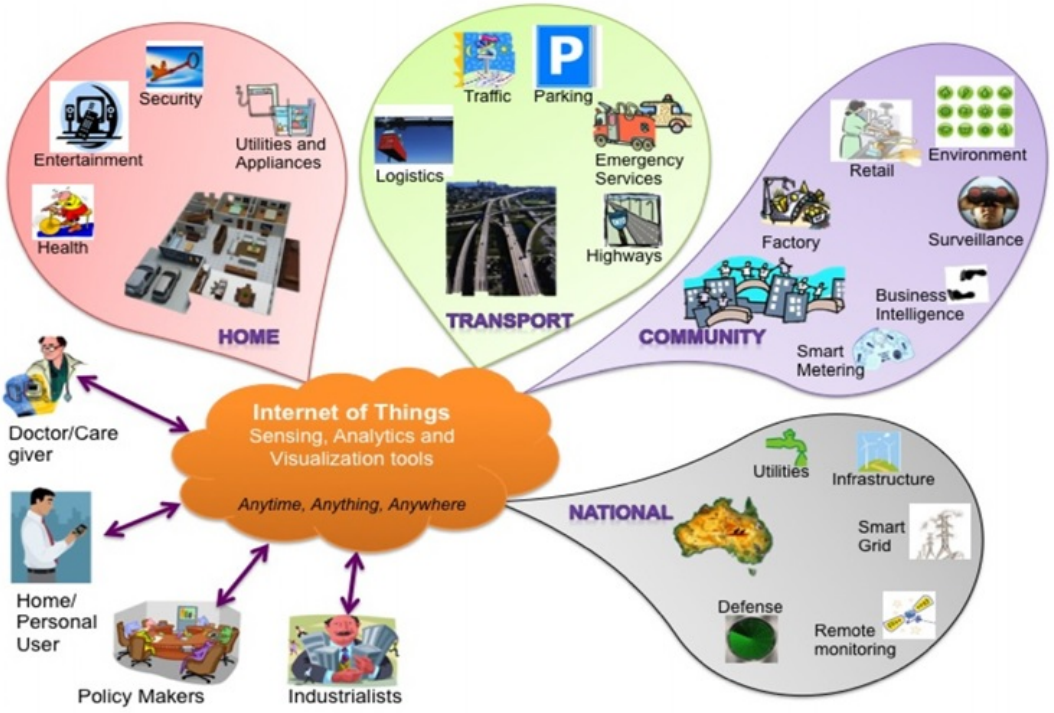

FIGURE 1.1: Applications of Internet of Things

application, the sensing nodes can be deployed either in an organised fashion or randomly within inaccessible or hostile environments. Once deployed within the sensing region, the sensing nodes collect data which is necessary to perform the desired applications. The sensing nodes are equipped with sensing devices with limited power, processing and communication capabilities. Sensing nodes collectively monitor the sensing region and respond to the occurrence of unexpected events or relay the information to a centralised control centre. The control centre, which is usually equipped with additional power and processing resources, collects the data from all the sensing nodes and makes a decision regarding the occurrence of an event.

WSN have attracted the attentions of researchers worldwide due to their potential applications in wide range of military and civilian applications. A WSN typically consists of a large number of low-cost, low-power, multi-functional sensing nodes which are linked through a wireless channel. The sensing nodes are usually equipped with one or more sensing devices. The other components within sensing

nodes include microprocessor, transceiver, flash storage, power supply [2]. Depending on the nature of the sensing devices, the sensing nodes monitor the sensing region and collect information regarding designated events. Besides sensing, the sensing nodes also perform tasks such as data processing and communication. To optimise the lifetime and performance of a WSN, the characteristics of the sensing nodes such as reliability, energy consumption, computation and communication must be optimised. Some of the characteristics and constraints which are typical to WSN are

- *Node Deployment:* Depending on the requirement of the sensing application sensing nodes can be either densely deployed or widely scattered. Identifying the optimum number of sensing nodes which are required to be deployed is the key to optimise the efficiency and lifetime of a WSN. Within accessible environments, placement of the sensing nodes can be investigated so that the ideal positions to deploy the sensing nodes, which optimises the performance of the WSN, can be identified. However, within inaccessible sensing environments, planned deployment of sensing nodes may not always be possible due to inaccessibility within those environments. In such scenarios, the sensing nodes can be randomly scattered across the sensing region.

- *Power Supply:* Sensing nodes are usually battery powered with limited energy supply. Sensing nodes rely on this limited available power to perform all the required tasks. In most of the scenarios involving harsh and hostile sensing environments, human intervention to restore the power supply not feasible.

- *Computation and Storage:* Depending the network topology, the sensing nodes can either transmit all the received signal data to the control centre or perform preliminary signal processing operations before transmitting the data. The sensing nodes are equipped with a processing unit with limited computational capabilities. Necessary signal processing algorithms are stored in a flash storage device within the sensing node. The storage unit

with limited storage capacity can also store other information such as received data, event logs, etc. Within an event driven network, the sensing nodes transmit the detected information to the control centre upon occurrence of the designated event. Within an on-demand network, the sensing nodes store the detected information within the storage unit for future use and transmit the information to the control centre periodically or upon request.

- *Self-Configurability:* In most of the scenarios, the sensing nodes are randomly scattered across the sensing region. Instead of communicating directly with the control centre, the sensing nodes, which act as an ad-hoc network, relay the information to the control centre. For efficient network operation, the sensing nodes are required to be aware of its neighbouring nodes in order to reduce energy consumption and interference within the network.

- *Application:* The components with the sensing nodes and the network topology is usually application specific. Depending on the nature of the sensing application, the design requirements of the WSN change. The communication and sensing node deployment strategies need to be planned accordingly to optimise the reliability, performance and lifetime of the WSN.

- Reliability and Data Redundancy: Once deployed, the sensing nodes are expected to operate on their own to perform the designated tasks. The low-cost sensing nodes are susceptible to random failures. Moreover, due to limited processing capabilities of the sensing nodes, the detection reliabilities of the sensing nodes are low. Within WSN with densely deployed sensing nodes, the detected information by multiple sensing nodes is usually closely correlated which results in transmitting multiple copies of similar data. Such redundant data is required to be eliminated to reduce the energy consumption during wireless transmissions.

1.2 Challenges

Compared to traditional communication systems, the sensing nodes within WSN are subject to unique characteristics and constraints, which have a significant impact on the reliability and performance of a WSN. These characteristics and constraints present several challenges in the design of WSN. In this section, some of the most significant challenges of WSN are addressed.

1.2.1 Design

The main objective of designing a sensing node is to create a compact, low-cost and energy efficient device. Diverse applications and increasing processing requirements pose significant challenge in the design of sensing nodes. However, the need for compact size and low energy consumption restricts the choice of components such as transmitter, microprocessor and flash storage which can be integrated within the sensing nodes. Constraints in the choice of processor and memory units restrict the choice of operating softwares which could provide improves reliability and resource management. Moreover, lack of sufficient processing and storage capabilities prevent implementation efficient sensing algorithms, which restrict the detection reliability of the sensing nodes.

1.2.2 Energy

Energy is one of the most commonly addressed resource constraint in the context of resource constrained WSN. Typically, the sensing nodes which constitute the WSN are powered by batteries. Depending on the amount of power consumption within the sensing nodes, the batteries are required to be either recharged or replaced periodically. Within small scale WSNs, it is possible to recharge the depleted batteries. However, in certain scenarios the sensing nodes may not be accessible or frequently accessed to restore the depleted batteries. In such scenarios, the deployed sensing nodes are discarded and replaced with new operational sensing nodes, which significantly adds to operational costs. In such scenarios, it

is desirable achieve extended sensing node life times. Typically, a sensing node is at required to be functional until it can be replaced or objective is fulfilled and the minimum required operational time depends on the type of the application. Hence, the most important design challenge within a WSN is energy efficiency of the sensing nodes and all the other aspects of the WSN such as network design and communication protocols are related to the energy constraints of the sensing nodes. Most of the energy consumption within the processing unit of a sensing node is attributed to switching energy and leakage energy. Leakage energy, which is caused due to energy dissipated from the hardware components can be reduced by progressive shutdown of idle components and through software-based techniques such as Dynamic Voltage Scaling (DVS) [3].

1.2.3 Adaptability

Once deployed, the sensing nodes are required to coordinate among themselves to perform the desired tasks. In most of the sensing applications which involve random deployment, the sensing nodes must have the ability to configure themselves into a communications network and identify their immediate neighbours to relay information. During network operation, in case of a random sensing node failure, the sensing nodes can reconfigure among themselves to identify optimum relay path. The sensing nodes are also required to operate in rapidly change dynamic sensing environments. The sensing nodes must be equipped with sufficient intelligence so that they are adaptable to the changes in sensing conditions such as channel and sensing environment.

1.2.4 Security

For applications such as surveillance and border management, the sensing nodes detect and transmit information, which is vulnerable interceptions. Within such applications, deployment of the sensing nodes at a significant distance from the control centre increases the chances of their exposure to intrusions and attacks.

Moreover, wireless communications give the intruders an opportunity to intercept the transmitted information, which could then be manipulated. If the locations of the sensing nodes are identified, the sensing nodes can also be remotely subjected to a variety of attacks such as jamming where high-powered RF signals are used to disrupt the operational characteristics of the sensing nodes, which could severely impact the reliability of the WSN. In the existing literature, numerous wireless security protocols have been proposed to address these challenges. However, sensing nodes with limited processing and storage capabilities could not handle these protocols. New solutions need to be developed to address these issues in the context of resource constrained WSN.

1.3 Applications of WSNs

The sensing nodes con be equipped with one or more sensing devices to detect or monitor different parameters such as RF or infrared signals, motion, sound, light, temperature, pressure and others. Compared to conventional wired sensors, wireless sensors have a significant advantage since they offer mobility and can be applied to a wide range of applications and sensing environments. The ease of deployment and self-organising nature of the low-cost, low-powered sensing nodes that constitutes a WSN has attracted the interest of the scientific community to explore their deployment in a variety of applications [4]. Some of the major areas of interest for WSN applications are

1.3.1 Surveillance and Security Applications

Compact size and easy to deploy nature have made WSN an attractive venture for numerous surveillance and security applications within IoT. For surveillance and security applications, WSN can use a wide range of sensing devices such as RF, acoustic, seismic, video, IR and other kinds of sensors [5] and are capable of detecting events such as intrusions, seismic and acoustic activities, metallic objects and movements as shown in Figure 1.2. Sensing nodes can be easily installed in

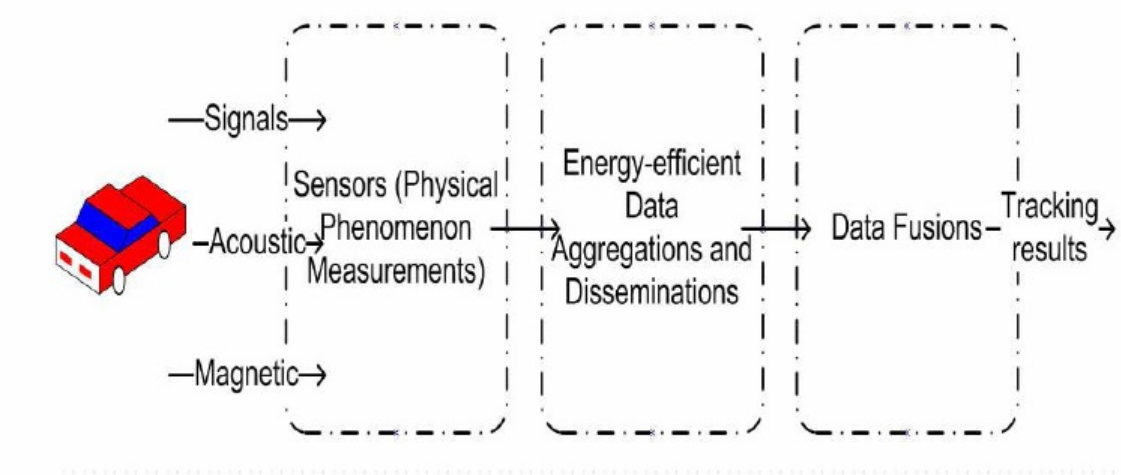

FIGURE 1.2: Surveillance and security architecture of WSN within IoT

places such as buildings, airports, power plants and have the ability to detect and track the intruders. WSN are also attracting various military applications such as information collection, surveillance, target tracking, border patrol [6, 7]. Due to the nature of surveillance and security applications, the sensing nodes are mostly expected to gather the data and communicate the information back to the control centre. Use of WSN for surveillance and security applications ensures constant and reliable surveillance without the need for human involvement.

- *Battlefield Monitoring:* Within battlefields, protecting military sites and installations is of utmost importance. However, such hostile environments pose a serious threat to the safety of the security personnel and constantly moving troops to and from these locations involve a lot of costs. WSN provide a cost-effective solution to provide surveillance within such locations. For battlefield monitoring, to protect military sites and installations, the sensing nodes can be equipped with one or more sensing devices such as RF, acoustic, seismic, etc. to monitor and track the movements of the troops, vehicles, etc. and conduct close surveillance on the opposing forces.

- *Infrastructure Monitoring:* With the increasingly evolving threats, many of the infrastructures such as airports, power plants, nuclear sites, communication centres are extremely vulnerable to attacks. These locations cover

vast areas and providing surveillance within such locations is extremely challenging. Apart from the difficulties, large number of security personnel are required which is extremely expensive. WSNs can offer a low cost and reliable solution to this problem. Sensing nodes can be deployed for remote sensing of such sensitive infrastructures to provide surveillance and perform tasks such as intrusion detection and tracking.

- In some of the surveillance applications such as infrastructure monitoring and remote sensing, target detection and tracking is one of the most important objective. However, under such circumstances multiple objects may pass through the sensing region that are of no interest. For example, within military applications, it is necessary to identify to detect and track enemy troops and vehicles while any wild animals passing through the sensing region are of no interest. Under such scenarios, target recognition is required to be performed to distinguish between targets and non-targets before initialising the tracking procedure. Target recognition involves two stages, which are target detection and target classification. During target detection, the sensing nodes detect the signals, which are expected to be emitted from the target based on which a decision is made regarding the existence or absence of the targets. During target classification, the sensing nodes use a target classification algorithm to match the received signals to the expected target signatures and makes a distinction between targets and non-targets.

1.3.2 Environmental Monitoring

Environmental monitoring is one of the widely used civilian applications of WNS. In environmental monitoring, sensing nodes are deployed to monitor a wide range of environmental conditions such as temperature, pressure, soil composition and air or water quality [8]. WSN for environmental monitoring has a wide range of applications in scientific, industrial and agricultural sectors. Some of the applications of WSN for environmental monitoring include,

- Sensing nodes can be deployed to remotely monitor the conditions of wild life, plants and the environmental parameters of their natural habitats without direct human intervention.
- Sensing nodes can be deployed in smart cities to monitor air and water quality and provide the relevant authorities with constant stream of data.
- Sensing nodes can be installed in research facilities to detect biological, chemical or other hazardous agents and initiate necessary counter measures.
- Sensing nodes can be deployed in locations which are vulnerable to natural calamities such as forest fires, fires, earthquakes and alert the inhabitants with early warnings so that necessary safety and preventive measures can be initiated.

1.4 Target Detection for Surveillance Applications

Due to low-cost and cooperative nature of sensing nodes, WSN is well suited for surveillance applications [9, 10]. Some of the surveillance applications of WSN include battlefield surveillance, remote monitoring in urban environments, intrusion detection, etc. Sensing nodes can be deployed in hazardous battlefield environments to monitor enemy activities while keeping the human operator at safety. Traditionally, target detection is performed through passive means of sensing. Unlike the traditional passive sensing devices such as temperature sensor, seismic detector, etc., in [11] authors have discussed the introduction of active sensing nodes within the sensing region. Active sensing nodes actively interact with the sensing region by transmitting a short RF signal into the sensing region. Upon existence of a target, the sensing nodes receive a reflected echo based on which a decision is made regarding the existence of the target. While active sensing nodes allow aggressive sensing strategies for increased reliability, the increased

power consumption within resource limited sensing nodes must be taken into account while designing the network. Within the existing literature, limited research has been done towards developing RF sensing based WSN. For WSN deployed in harsh sensing environments, there is a need to develop robust target detectors, which provide reliable target detection rates while being computationally efficient. Most often within WSN, the sensing nodes are required to operate in harsh sensing environments in the presence of clutter and interfering signals. While clutter is caused due to undesirable reflections of the transmitted signal, interference is caused due to interfering signals from the neighbouring sensing nodes. The sensing nodes while co-existing with the other sensing nodes are required to provide reliable target detection rates while using the limited available power and processing capabilities.

1.5 Aim & Objectives

The aim of this research is to develop RF sensing based target detection architecture for resource constrained wireless sensor networks. Transmit signals and their characteristics are required to be investigated to integrate a waveform selection criterion within the target detection architecture to optimise the detection performance. Nature of the sensing environments such as noise, interference and clutter are required to be investigated. Mathematical models for adaptable target detectors are required to be derived which can dynamically adapt to the changing sensing conditions and optimise the target detection performance. Various resource constraints within WSN are required to be investigated in the context of RF sensing based surveillance applications and optimise the proposed target detectors to optimise the energy efficiency and reduce the operational complexities. Objectives of this research are as follows

- To conduct research on distributed surveillance applications of WSN and identify application specific operational, performance and resource constrains and the potential trade-offs with the QoS of the WSN.

- To investigate various properties of the signals and sensing environments in the context of surveillance and security applications of RF sensing based WSN and analyse their impact on the target detection reliability.

- To investigate various existing target detection models and statistical estimation techniques and identify the optimisation parameters, which are suitable for resource constrained WSN.

- To propose an optimised target detection architecture for distributed surveillance applications of RF sensing based WSN and identify the operational natures of the sensing environment.

- To develop mathematical models for the proposed target detection architecture, which are dynamically adaptable to changes in operational and sensing environments and provide reliable target detection performance.

- To simulate different sensing conditions in the context of WSN and to test and validate through simulation, the robustness of the proposed target detection models under changing conditions within the sensing environments.

1.6 Research Contributions

The main contributions of this research are found below

- RF sensing based target detection architecture has been proposed for surveillance applications of resource constrained WSN. To address the resource constraints of WSN, a two-stage target detection model has been proposed where the target detection procedure is performed in two stages at the sensing node and at the control centre respectively. The proposed two-step target detection model reduces the computational burden on the resource constrained sensing nodes within the WSN and restricts the amount of data transfer between the sensing nodes and the control centre.

- A transmit waveform selection criterion for RF sensing in the presence of interfering waveforms has been proposed. Transmit waveforms which are suitable for RF sensing within resource constrained WSN have been discussed and their impact on the target detection reliability of the WSN have been investigated to formulate a target detection optimisation procedure in the context of the expected sensing conditions within resource constrained WSN.

- A target detector has been proposed for target detection within homogeneous sensing conditions has been proposed. Sensing and operational characteristics of WSN in homogeneous sensing conditions are investigated and a mathematical model has been derived to optimise the target detection reliability.

- An optimised target detector for WSN in heterogeneous sensing conditions has been mathematically derived. Harsh sensing conditions within heterogeneous sensing conditions in the context of RF sensing based surveillance applications have been investigated and unknown parameter estimation procedure has been formulated to obtain increased target detection reliability.

- A resource optimisation procedure has been proposed and the impact of the optimisation procedure on the target detection reliability has been investigated. Some of the most significant resource constraints within RF sensing based WSN have been identified to be computational and power constraints. A dual-phase estimation procedure namely; initialisation and operational phases have been proposed to reduce the computational burden. To address power constraints, compressive sensing based target detection architecture has been proposed which is expected to reduce the power consumption associated with the data transmission and a target detector is mathematically modelled to optimise reliability of the compressive sensing based target detection procedure.

1.7 Thesis Organisation

The rest of the thesis is organised as follows:

In Chapter 2, various characteristics of WSN and respective challenges in the context of RF sensing based surveillance applications are discussed. State of the art in target detection architectures has been discussed and their relevance in the context of resource constrained WSN has been investigated.

In Chapter 3, characteristics of the wireless sensing nodes and their relevance to the operational constraints of the RF sensing based target detection applications of WSN has been presented. Transmit waveforms which are suitable for RF sensing based applications of WSN have been proposed. Operational nature of the sensing environment has been established and a waveform selection criterion has been proposed to optimise the target detection reliability of the WSN. Simulation results are presented and the target detection performance of the WSN has been analysed for various choices of transmit waveforms.

In Chapter 4, a target detection architecture for RF sensing based WSN in homogeneous sensing environment has been proposed. The system model and the expected received signal models for the proposed target detection architecture has been presented. Relevant target detection algorithms have been proposed for primary and secondary detectors. Simulation results have been presented to analyse the performance of the proposed target detectors under various sensing and operational conditions.

In Chapter 5, a new target detection architecture of RF sensing based WSN in heterogeneous sensing conditions has been proposed. The expected received signal models and relevant operational constraints have been presented. A computationally efficient procedure to estimate the clutter statistics from the secondary data has been presented. A hybrid matched filter based detector has been proposed for primary detection and a target detector, which has the capability to adaptively estimate the interfering signal strengths has been proposed for secondary detection. Simulation results have been presented to compare the performances of the

proposed target detectors under various sensing conditions.

Finally, in Chapter 6, concluding remarks have been given and future directions of the proposed research have been summarised.

1.8 Summary

A summary of the key points discussed in various sections of this chapter is provided in Table 1.1.

Section	Summary
Section 1.2: Challenges	Various challenges and constraints in the context of RF sensing based WSN such as Sensing node design, Energy availability, adaptability to sensing conditions and network security are introduced in this section.
Section 1.3: Applications	Various RF sensing based surveillance and security applications of WSN such as infrastructure monitoring, battlefield monitoring and environmental monitoring are introduced in this section.
Section 1.4: Target Detection	An introduction to the target detection architectures for RF sensing based surveillance applications of WSN within IoT has been provided in this section.
Section 1.5: Aim & Objectives	In this section the aim and objectives of this research are summarised.
Section 1.6: Research Contributions	Various contributions of this research are summarised in this section.

TABLE 1.1: Summary of key points discussed in Chapter 1

Chapter 2

State of the Art in WSN Technologies and Target Detection

2.1 Introduction

In this chapter, the literature review of the state of the art in target detection architectures for WSN has been discussed.

2.2 WSN for Surveillance and Security Applications

The ability of the sensing nodes to detect the occurrence of an event is related to the distance of the event from the sensing node, nature of the sensing event and sensitivity of the sensing device within the sensing node. Most of the existing applications of WSNs involve deployment of passive sensing nodes. While passive sensing nodes consume relatively less power, they are also prone to false alarms and miss detections. Active sensing nodes, while being less energy efficient than passive sensing nodes, are also expected to provide more reliable target detection

performances. WSNs for surveillance and security applications are known to use infrared, acoustics, optics and ultrasonics for active sensing. In the existing literature, RF sensing based WSN has been considered by the authors in [12–15]. Within this research, to address the problem of target detection for surveillance and security applications, we consider the deployment of low powered active sensing nodes with RF sensing capabilities. Upon detecting the occurrence of the event, the sensing nodes gather the required information and transmit the information to the control centre for further processing. While in certain scenarios where short-range communications maybe sufficient to transfer the data to the control centre, in other cases, various multi-hop relay strategies are used to route the information back to the control centre. Depending on the number of hops required to transmit data from the sensing nodes to the base station, a WSN can be classified as single-hop or multi-hop networks. Most of the existing research on WSNs is focussed on network operation, energy efficient communication schemes and network security. [16–22]. While the existing detection strategies are incompatible with WSNs due to limited availability of power, storage and processing capabilities, limited research has been done towards developing robust signal processing techniques for target detection.

2.3 Characteristics of WSN

WSN are used to remotely monitor a given sensing region do detect the occurrence of events and transmit the detected information to the control centre. A WSN consists of multiple sensing nodes, which are deployed within the sensing region and have the ability to coordinate among themselves to perform the pre-defined task. The characteristics of the WSN such as sensing devices, coverage, data processing, etc. have a crucial role to ensure efficient completion of the desired tasks within the surveillance region. In this section, some of the characteristics of WSN have been discussed.

2.3.1 Sensing Node Architecture

The sensing nodes are the primary components within a WSN, which monitor the sensing region. Depending on the nature of the sensing application, the sensing nodes are required to be equipped with necessary sensing devices to perform the desired task. For RF sensing based surveillance applications, the necessary components within the sensing nodes are; an antenna for receiving the RF signals, RF sensor, processor, communications transceiver and power supply. In [15], authors have performed a study on feasibility of RF sensing based WSN. The RF sensor within the sensing node which is considered in [15], is equipped with an oscillator, RF amplifier, LF amplifier and an Analog-to-Digital Convertor (ADC). Authors have used an oscillator, which consists of a low loss coaxial resonator with a high Q factor for improving the noise characteristics and an RF transistor with a capacitive feedback network. The centre frequency of the RF sensing platform is 2.45GHz in an ISM band with an output power of -5dBm and a low barrier Schottky diode has been used for demodulating the transmitted RF signals, which are reflected to the sensing node. In their work, authors have observed that the RF sensing node has a power consumption of 5mA at 3V and achieved a sensing range of 10m for human targets which indicates that RF sensing based sensing nodes are feasible within resource constrained WSN. In [14], authors have used a TWR-ISM-002 sensor which is obtained from [23] as a RF sensing platform within the sensing node. TWR-ISM-002 is a motion sensor with a maximum sensing range of 20 meters, which can be adjusted using a potentiometer. The sensing node consumes less than 1mA at 3.4v to 6V power supply. Authors have used binary hypothesis testing based Neyman-Pearson detector for target detection.

Observation: While the RF sensing nodes meet the power consumption requirements for resource constrained WSN, the sensing strategies proposed by the authors does not take into account, the presence of clutter which results in increased false alarm rates.

2.3.2 Coverage and Deployment

The combined range of the sensing nodes within a WSN denotes the amount of coverage provided within the sensing region. To provide coverage efficiently, the problem of the number of sensing nodes which are required to provide sufficient coverage and the deployment strategies for the sensing nodes need to be addressed. The number of sensing nodes, which are required to provide sufficient coverage within the sensing region, varies depending on the application and nature of the sensing devices. It also depends on the sensing conditions within which the sensing nodes are expected to operate. Within a given set of sensing conditions, coverage within the sensing region can be provided through proper deployment of sensing nodes. Depending on the nature of the sensing region, the sensing nodes can be deployed either randomly or deterministically.

2.3.2.1 Deterministic Deployment

Within small scale sensing environments and if the sensing environments are easily accessible, deterministic placement of the sensing nodes allows development of efficient sensing and communication strategies. The placement of the sensing nodes has a significant impact in the reliability of the WSN. In [24], authors have addressed the problem of identifying the optimal placement of the sensing nodes within the sensing region to design a robust WSN with optimal lifetime. Through optimised placement of the sensing nodes, the number of sensing nodes, which are required to provide reliable coverage within the sensing region, can be reduced thereby, reducing the cost of the WSN. Organised deployment of the sensing nodes allows a greater degree of control over the operation of the WSN. However, due to the presence of limited number of sensing nodes within the WSN, any unexpected failures of the sensing nodes may disrupt the connectivity of the WSN. In [25], authors have addressed the coverage problems and developed an obstacle resistant sensing node deployment algorithm. In [26], authors have addressed the problem

of increasing the life time of the sensing nodes through organising the sensing nodes into several set covers which are activated successively.

Observation: Due to known location of the sensing nodes, the distances and locations of the sensing nodes are known to the control centre, which helps to achieve increased target detection reliability. The sensing conditions within which WSN is expected to operate can also be accurately predicted. However, deterministic deployment strategies may not always be available for inhospitable sensing environments.

2.3.2.2 Random Deployment

To provide coverage within a large scale or inaccessible sensing region, random deployment of sensing nodes can be implemented. This method of sensing node deployment is suitable for military or hostile sensing environments where manual access of the sensing region is restricted. Through random deployment, the sensing nodes can be easily deployed within the sensing region by randomly scattering the sensing nodes. However, homogeneous deployment of the sensing nodes cannot be ensured. Due to the unbalanced distribution of the sensing nodes, sufficiently large number of sensing nodes are required to be deployed to provide reliable coverage, which increases the hardware costs. In [27], authors have addressed the problem of identifying and repairing any gaps in the connectivity within the WSN. For RF sensing based WSN, as a consequence of random deployment, the unknown locations of the sensing nodes pose a serious challenge. In [28], authors have proposed a location support system to estimate the locations of the sensing nodes within the cluster. Authors have proposed a beacon node with known position, which transmits an RF and an ultrasonic signal simultaneously. Due to difference in the prorogation speeds of RF and ultrasonic signals, the sensing nodes receive the two transmitted signals at different instances and the locations of the sensing nodes are estimated based on the time difference between the arrival times of the two signals. Within RF sensing based WSN, the control centre may act as a beacon node and estimate the locations of the sensing nodes within its cluster. In [29],

authors have proposed ENSBox, which is a self-localisation scheme. In the proposed system, the control centre transmits an acoustic chirp signal and broadcasts the transmit time of the chirp signal through RF channel. The receiving nodes measure the time taken for the chirp signal to arrive to identify their locations in the context of the control centre.

Observation: Unknown locations of the sensing nodes within the cluster increases the target detection complexity. The sensing conditions are hard to predict which has a significant impact on the target detection reliability of the WSN. However, existing range detection techniques for WSN can be used to predict the locations of the sensing nodes with reasonable accuracy to increase the efficiency of the WSN.

2.3.3 Data Processing

The objective of a WSN is to monitor the given sensing region to detect the occurrence of predefined events. The sensing devices within the sensing nodes periodically collect relevant information regarding the event based on which a decision is made regarding the occurrence or non-occurrence of the event. Depending on the detection strategy and nature of the sensing application, the sensing nodes may either perform preliminary signal processing operations or transmit the received data to a centralised control centre for further processing. The detection strategy can be classified as decentralised detection and centralised detection.

2.3.3.1 Decentralised Detection

In decentralised detection strategy [30–33], the sensing nodes perform signal processing operations locally based on which a decision is made regarding the occurrence or non-occurrence of the event of interest. All the sensing nodes within the cluster make a local decision independently and transmit the respective decisions to the control centre. The control centre receives all the individual decisions from the sensing nodes and makes a final decision regarding the occurrence of the event.

One of the main advantage of decentralised detection strategy is that it reduces the amount of data transfer between the sensing nodes and the control centre, which reduces the power consumption, thereby increasing the lifetime of the WSN. In [32], authors have proposed a decentralised intrusion detection strategy for WSN. Authors have defined a set of rules, which are applied to the received data based on which intrusions within the sensing region are detected locally by the sensing nodes. In [33], authors have proposed a decentralised detection strategy for the detection of deterministic RF signals in additive white Gaussian noise. Authors have addressed the case where the WSN is constrained by the capacity of the wireless channel over which the sensing nodes transmit the received information to the control centre. Authors have demonstrated that when the observations are independent and identically distributed, having multiple sensing nodes sending limited observations based on decentralised detection is more beneficial than each sensing node transmitting detailed information to the control centre.

Observation: In decentralised detection, the sensing nodes perform preliminary screening to ignore the redundant information. As a result the power consumption is reduced due to limited amount of data transfer between the sensing nodes and the control centre. However during certain scenarios of RF sensing applications, the resource constrained sensing nodes may not have sufficient processing capabilities to perform the preliminary operations. A trade-off between target detection reliability and power consumption must be taken into account while choosing a suitable detection strategy.

2.3.3.2 Centralised Detection

During centralised detection strategy, the sensing nodes transmit the received data to the control centre. The control centre is expected to have significantly more power and processing resources that the sensing nodes within the cluster. For surveillance applications within harsh sensing applications, centralised detection strategies may be implemented to achieve high detection reliabilities. The control centre can take advantage of the higher available processing capabilities to

implement efficient algorithms to achieve increased detection reliabilities than decentralised detection scheme. However, this is achieved at the cost of increased transmission costs since the sensing nodes are required to transmit more data to the control centre. In [34], authors have proposed a centralised detection strategy for WSN where the sensing nodes are grouped into clusters where each cluster is headed by a control centre. In [35], authors have proposed a centralised detection strategy for detection of deterministic signals in correlated Gaussian noise. In contrast to traditional Parallel Access Channel (PAC), authors have explored Multiple Access Channel (MAC) for transmitting the sensing node observations to the control centre and it has been observed that MAC significantly reduces the bandwidth requirement or detection delay.

Observation: Centralised detection for RF sensing applications requires significantly large amounts of data transfer between sensing nodes and the control centre. While centralised detection increases the target detection reliability, this is achieved at the cost of reduced lifetime of the sensing nodes. With limited capacity of the wireless communications channel, excessive data transfer may lead to congestion, which may lead to delays or sensing errors. With multiple sensing nodes sharing the communications channel, it is desirable to identify the sensing nodes which contain useful information and prioritise them over the others.

2.3.4 Communication

The sensing nodes, which are usually scattered across a large sensing area, are required to transmit the detected information to a centralised control centre. Within sensing nodes, a significantly large portion of the available power is consumed during data transmission. Sensing nodes with limited power and hardware usually have limited communications range. Ad hoc routing techniques increase the communication range by allowing the sensing nodes to relay the information between one another. When significantly large number of sensing nodes are deployed within

a sensing region, the communications range of the sensing nodes is limited to reduce the power consumption and interference. The communications range of the sensing nodes is limited to its immediate neighbours. To avoid parts of the WSN loosing connectivity due to obstacles or sensing node failures, multihop techniques are introduced where the power ranges of the sensing nodes are adaptively adjusted so that each sensing has multiple orders of neighbouring nodes [36]. It has been observed that multihop communication in WSN reduces the power consumption when compared to single hop transmissions [37]. Multihop communications also allow to limit the transmission powers to lower levels, which is of significant importance to surveillance applications which require covert operations.

2.4 WSN for Target Detection

Sensing the presence or absence of a target is one of the primary objectives of WSN for surveillance applications. Traditionally, WSN used infrared, magnetic, seismic, acoustics, optics, etc. as primary means of sensing. Intrusion detection for surveillance applications is a problem, which is well suited for WSN. However, RF sensing based target detection within WSN has not yet been widely researched [14, 15]. RF sensing involves transmitting RF signals into the sensing region and detecting reflected components of the transmitted signals to detect the presence of targets [14, 15, 38]. Some of the major advantages of using RF sensing are no line-of-sight requirement, ability to distinguish between targets and non-targets, ability to operate through obstacles, ability to estimate range and velocity of the targets [12]. Commercial widespread applications of RF sensing have not yet been possible due to limitations over power consumption and processing requirements. With the development of micro-power impulse radios, RF sensing based WSN has become a possibility. UWB technology was developed at Lawrence Livermore National Labs [12] which uses micropower impulses as against to conventional narrowband transmissions. Micropower impulses in UWB technology are transmitted for a short duration of time and hence contain little energy. In [15], authors designed

a low-power RF sensing platform based on UWB technology and investigated the power budget and energy breakdown for the sensing node. These sensing nodes are compact and low powered which makes them ideal for WSN. Subsequent developments [39] resulted in designing RF sensing based autonomous network of sensing nodes with significant improvements in sensing range and power consumption. An autonomous sensor network is expected to have the ability to gather the sensing data and use intelligent design framework to support autonomous decision capabilities to detect and track targets within the sensing range.

Power consumption is one of the main design constraints within a sensing node. In [15] authors have designed a sensing node for RF sensing based applications which consumes 10mA at 3V and provides a sensing range up to 10m. While working prototypes have already been developed, extensive research is yet to be done in developing a reliable and computationally efficient target detector. In [14] authors have considered Neyman-Pearson based binary hypothesis detector to be a suitable target detector. In [40, 41] authors have proposed a target detector, which uses the average signal strength as measured by the sensing nodes to detect the presence of targets. While such methods are simple to implement and computationally less complex, their target detection reliabilities are poor due to high false alarm rates. In many of the practical surveillance applications, WSN are required to operate in harsh sensing environments and the low complexity target detectors proposed for WSN exhibit increased false detection rates and reduced reliability. Real time experiments on Mica2 motes showed that the false alarm rates of the decisions taken based on the data from a single sensing node can be as high as 60 percent [42]. In [39] authors have proposed a WSN with multiple sensing nodes distributed within the sensing region. In [43] authors have discussed data fusion to improve the target detection reliability. A network of distributed sensing nodes as designed in [44–46] where the sensing nodes are grouped together by a control centre which can adopt joint scheduling approach [47] can provide improved sensing coverage and connectivity with efficient energy consumption. A

distributed network of sensing nodes can be seen as a multiple-input multiple-output (MIMO) system that transmits a waveform of known shape and detects the reflected echoes from the target. The presence of multiple sensing nodes within the sensing region increases the probability of detecting the presence of targets. However, the signals transmitted from the neighbouring sensing nodes interfere with each other and hence reduces the target detection reliability. In the existing literature, various target detectors [48–53] have been proposed by the authors to provide improved target detection performance. However, the proposed target detectors are computationally intense and incompatible with resource constrained WSN. RF sensing based WSN rely on detecting the reflected components of the known transmitted signals to detect the presence of the targets. However, the presence of objects within the sensing region, which interact with the transmitted signal, results in clutter returns. Since clutter returns appear similar to the target returns, the presence of clutter leads to increased the false detection rates and reduced reliability.

Observation: The existing target detectors which are proposed for WSN have not taken some of the crucial sensing conditions such as interference and clutter into account. Optimised target detection strategies need to be developed for resource constrained WSN which are reliable and computationally efficient.

2.5 Optimisation Goals

Once deployed, WSN are expected to operate on their own without the need for human intervention are perform the designated task reliably. Longevity of the sensing nodes within the WSN is crucial to ensure continued operation over extended periods of time. However, the sensing nodes are constrained by limited available power and therefore, to optimise the lifetime, the sensing nodes are required to operate efficiently to perform the desired tasks. In the existing literature, energy consumption within WSN has been investigated by the authors [54, 55]. To reduce energy consumption, authors have investigated WSN aspects such as

network topology, sleep scheduling, data aggregation, etc. [56–61]. Unlike the other aspects of WSN which involve the networking techniques, compressive sensing techniques for data aggregation significantly reduces the amount of data, which is required to be transferred. It has been observed in the existing literature that a significant share of the limited available power within the sensing nodes is consumed during data transmission. The lifetime of the sensing nodes can therefore be increased by restricting the amount of data transfer between the sensing nodes and the control centre.

Within an event driven network, the sensing nodes transmit the received data to the control centre if the presence of a target is detected. Therefore, reliable detection strategies can improve the detection reliability and reduce the amount of data transfer between the sensing nodes and the control centre. Within the context of RF sensing, the nature of the sensing environment has a significant impact on the target detection reliability. RF sensing based WSN rely on detecting the existence of desired RF signals to detect the existence of targets within the sensing region. Due to the nature of the sensing region, the received signals may be corrupted by noise, interference, clutter, etc., which reduce the target detection reliability.

2.5.1 Compressive Sensing

Energy efficient data collection and transfer is a crucial factor, which needs to be addressed to optimise the energy consumption and lifetime of WSN. Compressive sensing is a burgeoning signal processing technique, which is being increasingly applied to WSN. Compressive sensing allows the desired signal to be reconstructed from a linear combination of small number of random measurements. Compressive sensing has attracted significant attention for distributed compression in WSN to increase the energy efficiency of the WSN [62, 63]. Compressive sampling reduces the amount of data, which is required to be transmitted to the control

centre. However, necessary conditions for successive implementation of compressive sensing are not always met. Compressive sensing requires selecting a suitable transformation to make the target signal sparse, which is not always applicable to RF signals, which are oscillatory in nature. [64], authors have proposed directional wave atoms, which allows sparse representation of oscillatory patterns. However, within RF sensing based WSN, most often, only a small amount of the received signal parameters carry information regarding the target. Therefore, compressive sensing can be used to reduce the amount of data transmission, computational complexity and power consumption within the sensing nodes. In [65–67], authors have proposed compressive sensing for RF applications by exploiting the sparse nature of the received signals.

2.5.2 Noise

Noise is one of the major factors, which contribute to the corruption of the received signal data. In the existing literature there are many proposed solutions [68–70] to reduce or suppress noise. However, most of the proposed solutions are application specific and too complex for other applications such as WSN, which have limited power and computational resources. For successful noise reduction, in [68] and [70] authors proposed a constant estimation of the noise spectrum. Authors have considered different types of noise such as white and colored noise. However, this noise estimation process may interfere with target detection and imposes additional burden on the sensing node processor. Alternatively, opportunistic estimation of the noise spectrum can be done while there is an explicit knowledge of non-existence of the target. Moreover, the existing algorithms are complex and unsuitable for resource constrained WSN.

2.5.3 Interference

Within a large WSN, with multiple sensing nodes operating simultaneously, the signals transmitted by the neighbouring sensing nodes interfere with each other.

Within an RF sensing based WSN where the sensing nodes rely on RF signals as the primary means of sensing, the presence of interfering signals severely deteriorates the reliability of the WSN. To achieve reliable surveillance, the problem of interference is required to be addressed. In [71], authors have proposed conflict graph construction using bandwidth tests. However, it is a static application, which is developed for communications interface of IEEE 802.11, multi-hop WSN and therefore not dynamic RF sensing based surveillance applications. In [72], authors have proposed a figure of merit for outage probability which is a scalar value which denotes the ability of the detector targets based on the density of nodes and the waveform parameters. In [73], a cross-matched filtering-based interference suppression algorithm has been proposed which uses an iterative filtering algorithm to suppress interferences. However, to implement the proposed solutions, the sensing nodes require additional hardware and extensive computational capabilities.

2.5.4 Clutter

Clutter is comprised of all the scatterers within the sensing region, which reflect transmitted RF signals to the sensing nodes. Clutter returns appear on the same domain as the target returns. The presence of clutter is known to cause increased false alarms and hence reduce the target detection reliability of the WSN [51]. In the existing literature, authors proposed using Doppler shift caused due to moving targets to negotiate clutter [74, 75]. While this approach yields performance gains in the case of fast moving targets, alternative approaches need to be investigated for target detectors for slow moving or static targets. Clutter estimation techniques have been addressed in [76–83] where the statistical distribution of clutter is estimated from the secondary data which is obtained during calibration of the system. Detection of targets in the presence of cluttered background has been addressed in [84–86]. However, the proposed solutions involve complex numerical computations, which are unsuitable for resource constrained WSN.

2.6 Waveform Selection

RF sensing based active sensing nodes transmit RF signals into the sensing region and detect the presence of targets by observing the received echoes [14, 15]. The choice of an appropriate transmit waveform is an important design parameter for RF sensing based surveillance applications of WSN. For RF sensing based surveillance applications, the choice of transmit waveform has a significant impact on the detection performance and reliability of the WSN. Waveform design to optimise the target detection performance in the presence of interfering waveforms has been addressed in [87–89]. Optimum waveform design techniques for clutter mitigation have been addressed in [90, 91]. Authors have resorted to eigen-analysis to design suitable transmit waveforms and optimise the target detection reliability. However, the proposed waveform design schemes are complex and only suitable for narrowband waveforms.

Transmission of RF signals by the active sensing nodes is associated with significant increase in the power consumption within the sensing nodes with limited available power. While longevity of WSN is desirable, optimum choice of a transmit waveform within WSN must fulfil the necessary criterion to achieve the desired target detection reliability while operating within the constraints of the available resources. Brevity of the transmit pulses is required to reduce the transmission costs. To reduce the signal processing complexities, the choice of a transmit waveform with good correlation properties is desirable. Recent advancements in UWB [9, 12] technologies allowed development of low-cost devices, which can transmit relatively short UWB pulses. Due to ultra-short nature of the UWB pulse, it is required to transmit significantly lower power for these pulses. This has made RF sensing techniques possible for resource constrained WSN. UWB waveforms which are suitable for surveillance applications of RF sensing based WSN have been discussed in [92–95].

Observation: The existing waveform design techniques are not suitable for resource constrained WSN due to computational complexities involved in designing

the waveforms and transmission complexities. Narrowband waveforms, which are suitable for long-range communications are usually associated with high transmission costs and low resolution. For short-range surveillance applications of WSN, short UWB pulses are beneficial due to low transmission costs and high sensing resolution. However, with multiple sensing nodes deployed within the sensing region, sufficient diversity in the choice of UWB waveforms is required. Suitable waveform selection algorithms in the context of resource constrained WSN need to be developed to optimise the target detection performance.

2.7 Operational Spectrum

Unlike the traditional narrowband systems, UWB systems generate ultra short pulses in the time domain with pulse widths not exceeding a few nanoseconds. Generation of these ultra short pulses allow transmitting the desired RF waveforms with reduced transmission costs. The operational spectrum of a UWB system depends of various factors such as pulse width, bandwidth and centre frequency [93–95]. According to theoretical fourier transform [96], for a transmit pulse width τ in the time domain, the operational bandwidth in the frequency domain is given by $1/\tau$. The amount of spectrum occupied by a UWB signal for RF sensing applications is usually at least 25% of the centre frequency. Therefore to achieve a pulse width of 0.5 ns, the required bandwidth is 2 GHz and the centre frequency for RF sensing applications is 8 GHz. This is a microwave frequency in the centimeter-wave region. In the existing literature authors have designed low powered sensing nodes which operate in the microwave region of the spectrum [12, 15, 93–95].

2.8 Signal Processing Architectures

Sensing environment and signal properties are the most influential factors that affect the performance of a target detector [97, 98]. The characteristics of the sensing environment vary depending on the area of application. The other factors

that influence the performance of a target detector are noise, clutter, multipath, interference, signal strength, attenuation, etc. Noise can be attributed to all the unwanted signals and disturbances, which are superimposed on the signal of interest and hence corrupting the inherent properties of the signal. Depending on the sensing environment, the received signal component can be either the signal of interest superimposed by noise or only a random noise component. It is the responsibility of target detector to decide if the received signal consists of the signal of interest or otherwise. The degree of difficulty of detecting signal component is related to the knowledge of the signal, which is to be detected at the receiver and the knowledge of the sensing environment. Different detection models have been proposed in [99–103] and their design considerations vary depending on their assumptions regarding the availability of the knowledge over the statistical properties of the received signal as well as sensing environment. The most commonly addressed signal detection techniques in the context of resource constrained WSNs are Matched Filter, Spectrum sensing / Energy Detector and Cyclostationary Feature Detector.

Energy detection has been addressed in [97, 104, 105] which is widely used for signal detection when the target signal subspace is a priori unknown. While being less complex, these existing models need to be optimised for applications involving WSN. In [69, 106] a detection scheme with low computational complexity is proposed and is based on constant estimation of background noise. However, the proposed techniques are relatively complex for resource constrained WSN. Moreover, during continuous estimation of noise samples, some desired signal components may be embedded within the noise samples which cannot be separated and may subsequently deteriorate the desired signal quality during noise reduction; since, the desired signal components, which are included in the noise samples may be considered as noise and eliminated. In [107] authors addressed the minimum signal to noise ratio, which is required for efficient target detection. The problem of detecting a signal corrupted by noise with limited number of samples has been addressed in [108, 109]. Most recent advances regarding this problem are addressed

in [107] and [110]. While, this issue involving white noise is addressed in [110], the same issue regarding coloured noise has been addressed in [107].

Generally, detection models can be classified into, primary and hybrid detection models. While, primary detection models are derived from a root idea of solving a particular detection problem, hybrid detection models are a combination of the principles of primary detection models to provide a better performance for a considered detection problems. Neyman-Pearson detector and Bayesian test detectors are the basic target detection models and form the basis for most of the modern target detectors. Neyman-Pearson detector has been addressed by authors in [111–114] where, it makes a decision over the presence or absence of the desired signal based on likelihood ratio test. In a Bayesian test detector [115, 116], the general target detection problem is to decide between the two hypothesis H_0, which indicate the absence of the desired signal and H_1, which designate the presence of the desired signal in the received signal component. Bayesian test detector considers unknown parameters to be different under both the hypothesis, which are estimated based on multidimensional integrations. The final test statistic is generated based on likelihood ratio test. A Posteriori Probability (APP) estimation based detector has been addressed in [117] which is a Bayesian theorem based target detector where the unknown parameters are estimated based on their conditional probabilities generated from secondary data. Another Bayesian detector called Maximum Aposteriori Probability (MAP), which is similar to APP detector, has been addressed in [118] where the unknown parameters are estimated based on Maximum likelihood estimates of their Posteriori distributions. Some of the widely accepted detection models are, Generalised Likelihood Ratio Test (GLRT) detector[48, 52, 99, 119–122], RAO Test detector[100, 100, 123, 124], WALD Test detector[101, 125–127], Adaptive Matched Filter (AMF) detector[100, 125, 128]. Other popular detection models are, Adaptive Side-lobe Blanker (ASB)[129], Subspace Detector (SD)[130, 131], Most Powerful Invariant (MPI) detector, Adaptive Beam-forming Orthogonal Rejection Test (ABORT) detector[132], etc. GLRT

[119] is modelled considering the problem of detecting a signal of unknown amplitude and in the presence of Gaussian noise at a Constant False Alarm Rate (CFAR). GLRT assumes availability of sufficient training data and sufficient number of available signal samples. The performance of the GLRT detector degrades considerably when this assumption is violated. The performance of a RAO detector [100] is commensurate with that of a GLRT but this is conditional on sufficient availability of the training data. For a mismatched signal, a RAO detector exhibits better performance than GLRT. Alternatively, a computationally more complex parametric RAO detector [124] may be considered which requires relatively lesser number of training data than a GLRT detector. ABORT detector has the ability to reduce the impacts of signal array mismatches caused due to several mechanical inconsistencies such as antenna positioning, shape, calibration, etc. ABORT while specifically designed to perform in such type of scenarios but lacks robustness. In such scenarios where precise knowledge over the dimensions of the signal statistics are unavailable, a target detection model called Minimum Description Length (MDL) detector [109, 127, 133] has been proposed. MDL principle is based on Maximum Likelihood (ML) principle but has the ability to tolerate the problem of unknown parameter dimensions. However, a WALD test based detector has been presented in [126] whose performance is commensurate with that of MDL but at a reduced complexity.

A two-step GLRT detector has been proposed by the authors in [100] which is adaptive in nature. It is widely referred to as an AMF detector. In [100], a GLRT as an AMF has been presented where, in the first phase of target detection, the unknowns are estimated based on GLRT detector while, in the second phase of detection, the covariance matrix is replaced by its estimate based on the secondary data or training data. In [125], authors proposed a WALD test detector as an AMF detector where the first phase of target detection is done based on WALD test detector. Similar to its counterpart, AMF detector also displays CFAR property and at the same time, it is faster and has a better detection performance than a GLRT detector. However, AMF detector relies on the training data to suppress

interference. However, if the statistics do not match, AMF detector tends to have increased rate of false alarms. In the presence of application specific external factors such as clutter, multi-path or jammers, AMF detectors display increased false alarm rate. In [134] and [135], authors proposed an Adaptive Coherence Estimator (ACE) detector. In an ACE detector, the primary covariance matrix is replaced by the Sample Covariance Matrix (SCM), which is estimated from the training data. The estimation procedure has been addressed by the authors in [134, 135]. It has proven applications in radar, sonar and other telecommunications networks in the presence of coloured noise. ACE detector is more adaptive to environments, which are particularly non-homogeneous in nature than its counterparts such as GLRT and RAO detectors. It also displays better rejection capabilities during signal mismatches thus reducing false alarms.

In [129], authors proposed a hybrid target detector called, ASB detector. It is a hybrid target detection model, which is realised as a combination of an AMF detector and ACE detector. The signal is processed in the first phase based on an AMF detector. It needs to be noted that an AMF detector has a high false alarm rate in non-homogeneous environments. As a way around this problem, based on the decision of the AMF detector, the signal is then forwarded to ACE detector, which displays better performance in non-homogeneous environments. The final decision over the existence of the signal is made only if both the detectors agree on the existence of the signal. Alternatively, it can be bluntly stated as an "AND" operation between both the detectors. Authors have claimed that by using an ACE detector reduced false alarm rates can be achieved, however at the cost of increased miss detections. A hybrid detection model as a combination of AMF and RAO detector has been proposed by the authors in [100]. The idea behind this hybrid detection model is to reduce the influence of low training samples on the performance of RAO detector but on the other hand, retaining the rejection capabilities of RAO detector. A new hybrid detection model has been proposed in [123] which is a combination of an SD and a RAO detector which has increased robustness.

For the resource constrained WSN, one of the major constrain that influences the lifetime of a sensing node is available power. It has been observed that more power is consumed during transmission than any other process. Compressive sensing has been proposed by the authors in [136–142] where a target detection model is proposed to detect the target from compressed received signal samples. Hence, by taking advantage of compressive sensing in the context of resource constrained WSN where, it is possible to transmit lesser number of data bits and hence saving power, thereby increasing the lifetime of the sensing node. A relatively new compressive sensing technique namely Subspace Compressive detection has been addressed by the authors in [138]. In subspace compressive sensing, the authors have proposed to exploit the known sparse nature of the signal subspace to achieve a more reliable target detection performance while retaining the signal compressibility. Compressive sensing based on signal sparsity is addressed by the authors in [52, 143].

Observations: In the existing literature, many target detection challenges have been addressed by researchers and different solutions have been proposed. However, the proposed solutions correspond to a specific target detection problem and may not be feasible with the solutions of other detection problems. In most of the scenarios, the existing solutions to the target detection problems involve complex and computationally intense numerical integrations and require large amounts of data to be collected. This imposes a fundamental limit on the application of these solutions in practical scenarios in the context of resource constrained WSN where, the target detector faces multiple detection challenges. Hence, it is necessary to develop an efficient target detection model which is suitable for resource constrained WSN.

2.9 Summary

In the section, current state of the art in WSN technologies and target detection has been discussed. Characteristics of the WSN have a significant impact on the

reliability with which WSN can perform a desired operation. Existing research on various operational characteristics of WSN have been discussed in the context of RF sensing based applications. Resource constraints of the WSN limit the fast-growing potentials of WSN. Existing resource constraints have been discussed and the optimisation goals for RF sensing based applications have been presented. Various design characteristics of the existing RF sensing based target detection architectures have been discussed and their relevance to the resource constrained WSN has been analysed. In Chapter 3, the sensing node characteristics and their impact on operational characteristics of RF sensing based WSN has been mathematically analysed. A waveform selection procedure has been proposed to optimise the target detection reliability and energy efficiency of WSN. A summary of the key points discussed in various sections of this chapter is provided in Table 2.1.

Section	Summary
Section 2.2: WSN for Surveillance and Security Applications	Existing literature which address the problem RF sensing based target detection applications of WSN within IoT has been discussed in this section.
Section 2.3: Characteristics of WSN	Constraints on various characteristics of WSN such as sensing node architecture, node deployment, data processing and communication which have a significant impact on energy efficiency and reliability of WSN have been discussed in this section. Various solutions addressed in the existing literature and their compatibility with RF sensing based applications of WSN have been discussed.
Section 2.4: WSN for Target Detection	Existing literature which addresses the problem of RF sensing based target detection within WSN has been discussed in this section. However authors have resorted to simple Neyman-Pearson based detectors which are unreliable. Reliable target detection strategies are proposed in this thesis to achieve increased target detection reliability.
Section 2.5: Optimisation Goals	Existing literature on various constraints such as transmit data, noise, interference and clutter which are required to be addressed to optimise the target detection reliability and energy efficiency have been discussed in this section. An analysis of compatibility of the existing solutions within resource constrained WSN has been provided.
Section 2.6: Waveform Selection	Waveform design and selection techniques for target detection which are addressed in the existing literature have been discussed in this section. The complexity of the existing techniques in the context of resource constrained WSN has been discussed.
Section 2.7: Operational Spectrum	The operational spectrum of the proposed UWB system for RF sensing applications and various factors which influence the choice of the operational spectrum are discussed in this section.
Section 2.8: Signal Processing Architectures	In his section the existing signal processing architectures for target detection have been discussed. Various limitations of the existing techniques in the context of resource constrained WSN have been addressed.

TABLE 2.1: Summary of key points discussed in Chapter 2

Chapter 3

Target Detection Optimisation Through Waveform Selection for RF Sensing Based Wireless Sensor Networks

3.1 Introduction

A WSN consists of low-cost, easy-to-deploy network of sensing nodes, which are deployed within the sensing region. Once deployed, the sensing nodes coordinate among themselves to perform tasks such as surveillance, data collection, etc. and relay the data back to the control centre. A block diagram representing the operation of a WSN is shown in Figure 3.1. The sensing nodes are equipped with one or more sensing devices with limited power, processing and communication capabilities. Depending on the nature of the sensing devices, the sensing nodes can either passively monitor or actively interact with the sensing environment. In most of the existing literature, authors have addressed passive detection techniques for surveillance applications of WSN. RF sensing based active detection techniques provide increased reliability and higher target detection rates. RF sensing based

active sensing nodes transmit RF signals into the sensing region and detect the presence of targets by observing the received echoes [14, 15, 38]. However, existing RF sensing based target detection strategies are computationally intense for resource constrained sensing nodes within WSN. Transmission of RF signals by the active sensing nodes is associated with significant increase in the power consumption within the sensing nodes with limited available power. Recent advancements in UWB [15, 39] technologies allowed development of low-cost devices, which can transmit very short UWB pulses. Due to ultra-short nature of the UWB pulse, very little power is required to transmit these pulses. This has made RF sensing techniques possible for resource constrained WSN. However, as a consequence of low transmit power and subsequent propagation losses; the received echoes are associated with very low energies. Within the received signal components, detecting the presence of these echoes, which are usually corrupted by noise and interference is extremely challenging. Efficient target detection strategies need to be developed to provide reliable target detection rates.

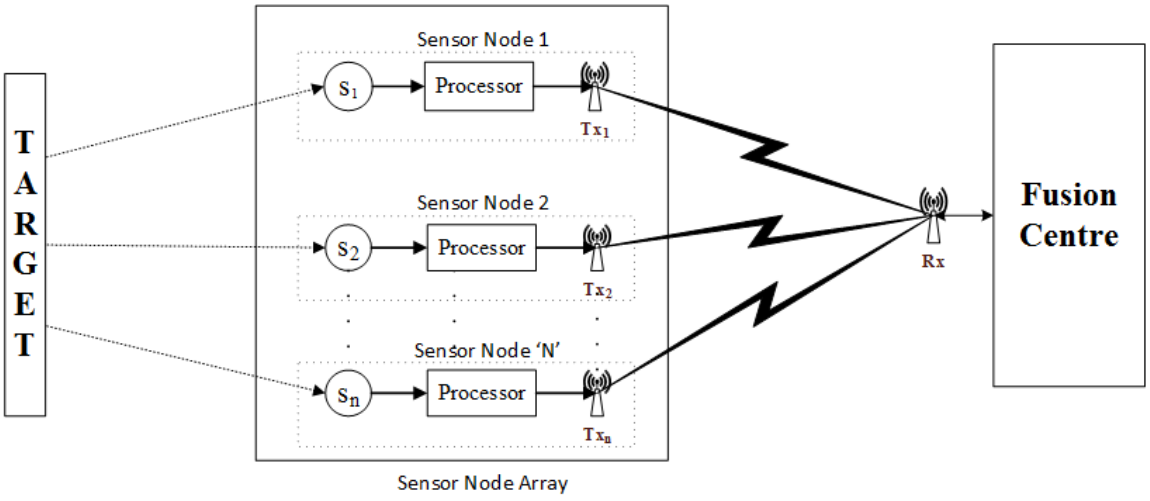

FIGURE 3.1: Block diagram of a wireless sensor network

3.2 Operational Characteristics of Wireless Sensor Networks

Sensing nodes are the primary operating elements within a WSN. The primary task of a sensing node is to monitor the sensing region and detect the occurrence or non-occurrence of the target. Sensing nodes, which actively interact with the sensing region are classified as active sensing nodes. Active sensing nodes use sensing devices such as RF sensors, infrared sensors to detect the presence of targets. Passive sensing nodes use passive sensing devices such as seismic, temperature sensors and others to detect the presence of targets by passively monitoring the sensing region. Sensing nodes are equipped with one or more of the functional components such as a sensing device, processor, flash memory, communication device, actuator, energy source, etc. A block diagram of the typical functional components within a sensing node is shown in Figure 3.2. In this section, some of the operating constraints of the WSN have been introduced.

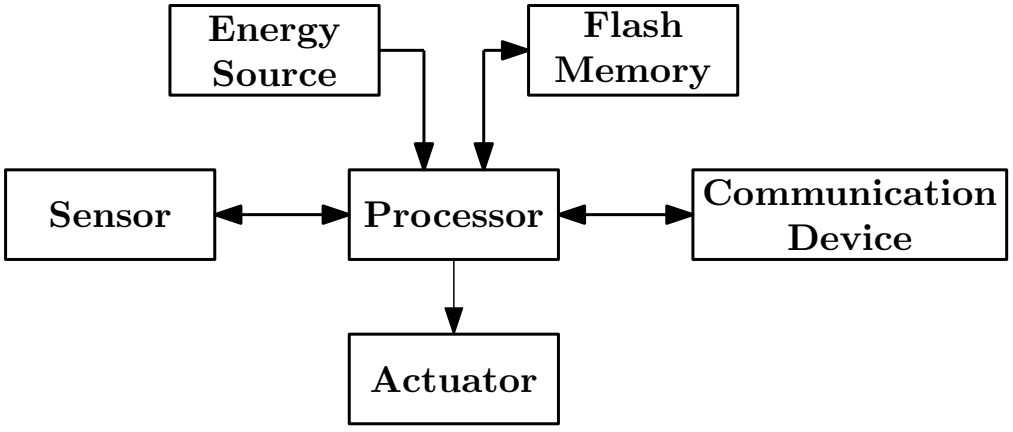

FIGURE 3.2: Essential components within a sensing node

3.2.1 Processing Device

The processing unit within a sensing node typically consists of an ADC, micro controller and flash memory. ADC converts the analog output signal from the sensor transducer into a digital signal. The micro controller is capable to perform local signal processing operations on the received signal as required and generates a stream of data, which is either stored in the local memory or transmitted to the control centre. Flash memory is also used to store the application programs, which are required to perform various tasks within the sensing node.

3.2.2 Sensing and Communication

The communication devices within the sensing node transmit and receive the desired RF signals and are responsible for all the data transfer between sensing nodes and the control centre. The communication and operational characteristics of a sensing node are greatly driven by its power constraints. The operational characteristics of the sensing node are classified as periodic, on-demand sensing and event-driven [144]. In periodic sensing mode, the sensing nodes periodically communicate with the control centre, in on-demand sensing mode the sensing nodes communicate only upon a request from the control centre. In event-driven sensing mode, the sensing nodes communicate with the control centre upon the occurrence of the target.

The sensor within the sensing node gathers the data regarding the desired event and generates an electrical response signal, which is transferred to the processing device. Within an RF sensing based WSN, the event of interest is the existence of the RF signal, which is reflected from the target, which is existent within the sensing region. The received signal power as observed by the sensing nodes is a function of the transmit power, distance of the target from the sensing node, target reflectivity and the characteristics of the sensing environment. Assuming a free space path loss model, the signal power P_r at a distance R from the sensing

node can be measured as

$$P_r = \frac{P_t G_l \sigma_s \lambda_w^2}{(4\pi)^3 R^n L} \tag{3.1}$$

where P_t is the transmit power, G_l is the effective antenna gain, σ_s accounts for the target reflectivity, L is a scalar accounting for losses and n is the path loss exponent. Due to size and power budget constraints, sensing nodes are limited to short range radio communications. The size of the antenna as related to the operating wavelength of the signal can be written as [145, 146],

$$d_{min} \geq \frac{\lambda_w}{4} \tag{3.2}$$

where d_{min} is the minimum size of the antenna and λ_w is the operating wavelength. It can be observed from Equation 3.2 that the limited size of the sensor antenna imposes constraints on the choice of operating wavelength. Substituting Equation 3.2 in Equation 3.1 and rearranging the terms, a relationship between antenna size and communication range of the sensing node can be observed as

$$R \leq \left[\frac{P_t G_l \sigma_s d_{min}^2}{4\pi^3 P_r L} \right]^{\frac{1}{n}} \tag{3.3}$$

Under the operating conditions for a given d_{min}, the required communication range R and the required received signal power can be achieved by dynamically adjusting the transmit power at the cost of reduced life time of the sensing nodes.

3.2.3 Sensing Range

The sensing range is the maximum distance from the sensing node where the existence of the target can be reliably detected. For RF sensing based WSN, the probability of detecting a target increases with the increase in received Signal to Noise Ratio (SNR). The received SNR at the i^{th} sensing node can be written as

$$SNR_i = \frac{P_r}{P_n} = \frac{P_t G_l \sigma_s \lambda_w^2}{(4\pi)^3 R^4 P_n L} \tag{3.4}$$

where P_n is the noise power. For a 3-dimensional deployment of sensing nodes within the sensing region as shown in Figure 3.3, the range of the target which is located at the coordinates (X_t, Y_t, Z_t) from the i^{th} sensing node located at (X_i, Y_i, Z_i) is measured as

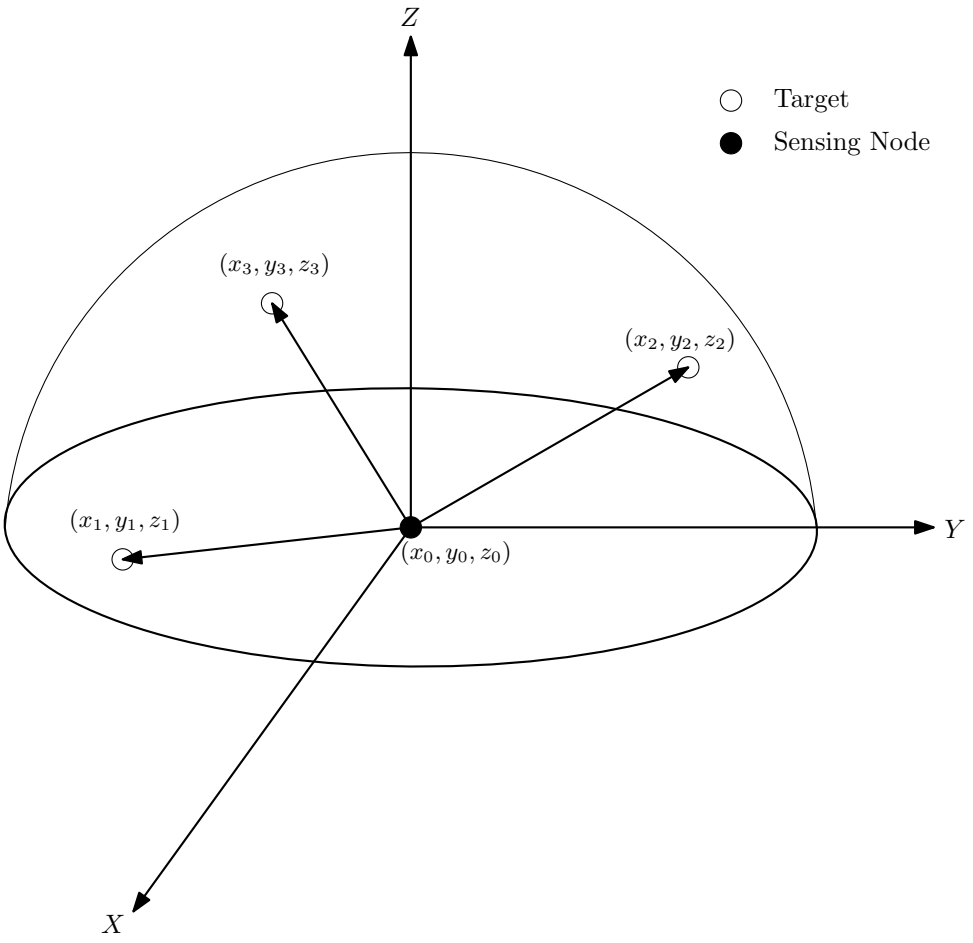

FIGURE 3.3: 3-dimensional target distribution relative to the sensing nodes within the sensing region

$$d_i = \sqrt{(X_i - X_t)^2 + (Y_i - Y_t)^2 + (Z_i - Z_t)^2} \tag{3.5}$$

For a given transmit power and minimum detectable SNR, the sensing range at which the target can possibly exist can be divided into three regions as shown in Figure 3.4. The probability of detecting the target as related to the distance d_t of the target from the sensing node can be expressed as

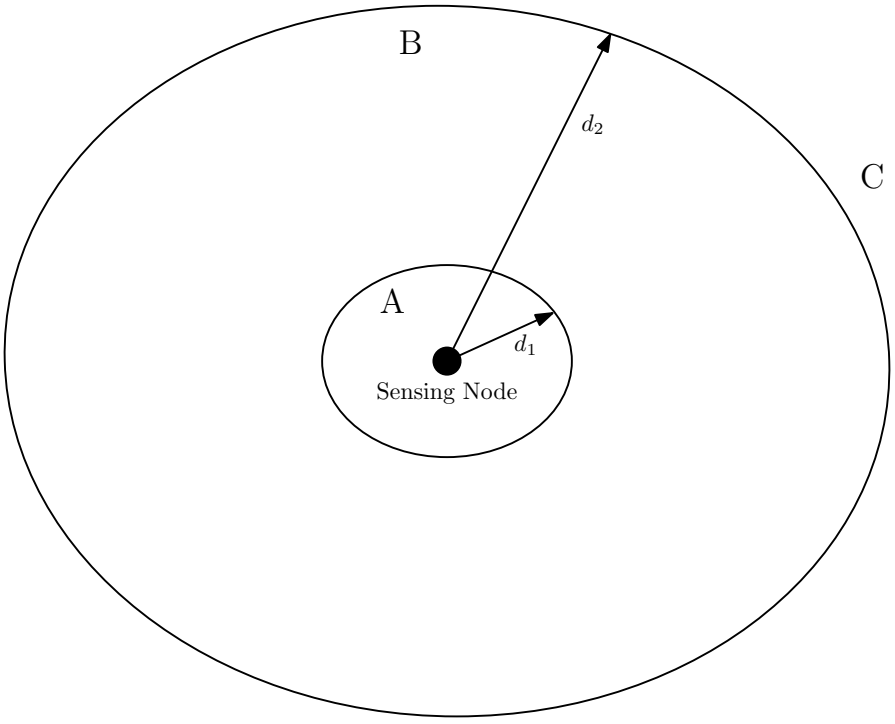

FIGURE 3.4: Detection probability distribution of a sensing node relative to the sensing range

$$P_d = \begin{cases} 1 & d_t < d_1 \\ P(d_t, snr) & d_1 < d_t < d_2 \\ 0 & d_t > d_2 \end{cases} \tag{3.6}$$

While the ability of a sensing node to detect the presence of a target is a function of the range and received SNR, the reliability of the target detection procedure can be significantly improved by implementing suitable signal processing techniques which are robust to sensing and noise characteristics.

3.2.4 Target Detection

A target detector analyses the received signal data, which is received by the sensing nodes to make a decision regarding the existence or absence of a target. However,

the received signal samples are usually corrupted by noise. Hence the target faces a binary hypothesis testing problem which is characterised by hypothesis H_0 and hypothesis H_1 where hypothesis H_0 indicates absence of the target and hypothesis H_1 indicates the presence of a target within the sensing region. Energy detection is a commonly used technique for surveillance applications. Energy detection technique, though suboptimal to matched filter based detection has been considered for the target detection due to its relatively low complexity and hence suitable for wireless sensing nodes with limited power and processing capabilities.

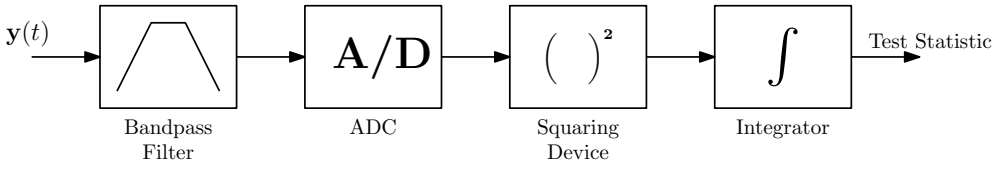

FIGURE 3.5: Implementation of the Energy Detector

Depending on the nature of the sensing conditions, a time frame for the receiving window is defined and during this period the received signal samples are collected. The energy detector consists of a bandpass filter which is then followed by an ADC to generate discrete received signal samples. The discrete received signal samples are subjected to a squaring device and integrator to generate the test statistic. The test statistic is a monotonic function of the integrator output. A time domain implementation of an energy detector is shown in Figure 3.5. For received signal $\mathbf{y}_i$ at the i^{th} sensor node, the test statistic for the energy detector can be written as

$$\mathbb{T}_i = \sum_{n=1}^{N} \mathbf{y_i} \mathbf{y_i}^H \tag{3.7}$$

where N is the number of received signal samples. For a sufficiently large number of observations, by central limit theorem, the test statistic under hypothesis H_0 and H_1 can be approximated as

$$H_0 : \quad \mathbb{T}_i \sim \mathcal{N}(N\sigma_w^2, 2N\sigma_w^4) \tag{3.8}$$

$$H_1 : \quad \mathbb{T}_i \sim \mathcal{N}\big(N(\sigma_x^2 + \sigma_w^2), 2N(\sigma_x^2 + \sigma_w^2)^2\big) \tag{3.9}$$

For a channel gain $\mathbf{H_g}$, the received SNR at the sensing node receiver is given as

$$SNR = \frac{|H_g|^2\sigma_x^2}{\sigma_w^2} \tag{3.10}$$

where σ_x^2 is the received target signal power and σ_w^2 is the Additive White Gaussian Noise (AWGN) power. The detector makes a decision regarding the existence or absence of the target by comparing the test statistic $\mathbb{T}$ with a predefined threshold γ i.e., $H_0 : \mathbb{T} < \gamma$ and $H_1 : \mathbb{T} > \gamma$. The performance of the target detector is measured based on two parameters which are Probability of False Alarm (P_{fa}) which is defined as $P(\mathbb{T} > \gamma|H_0)$ and Probability of Detection (P_d) which is defined as $P(\mathbb{T} > \gamma|H_1)$. P_d and P_{fa} of the energy detector under a given set of sensing conditions can be measured as

$$P_{fa} = Q\left(\frac{\gamma - N\sigma_w^2}{\sqrt{2N\sigma_w^4}}\right) \tag{3.11}$$

$$P_d = Q\left(\frac{\gamma - N(\sigma_x^2 + \sigma_w^2)}{\sqrt{2N(\sigma_x^2 + \sigma_w^2)^2}}\right) \tag{3.12}$$

where Q(.) is the modified Bessel function which is defined as

$$Q(x) = \frac{1}{\sqrt{2\pi}} \int_x^\infty exp(\frac{-t^2}{2})dt$$

For an acceptable false alarm rate P_{fa}, the threshold γ is calculated from Equation 3.11 as

$$\gamma = \sqrt{2N}\sigma_w^2 Q^{-1}(P_{fa}) + N\sigma_w^2 \tag{3.13}$$

It can be observed from Equation 3.10, Equation 3.12 and Equation 3.13 that

to achieve a desired P_d at a given P_{fa}, a relationship can be obtained between required SNR and minimum number of received signal samples. Equation 3.12 can be rearranged as

$$Q^{-1}(P_d) = \frac{\gamma - N(\sigma_x^2 + \sigma_w^2)}{\sqrt{2N(\sigma_x^2 + \sigma_w^2)^2}} \tag{3.14}$$

Substituting Equation 3.13 and after subsequent mathematical manipulations, Equation 3.14 can be written as

$$N = 2\left[\frac{\sigma_w^2 Q_{-1}(P_{fa}) - (\sigma_x^2 + \sigma_w^2)Q_{-1}(P_d)}{\sigma_x^2}\right]^2 \tag{3.15}$$

Using Equation 3.10, the minimum number of received signal samples that are required to achieve a desired target detection performance at a given SNR can be estimated as

$$N_{min} = 2\left(\frac{|H_g|^2}{SNR}\left(Q^{-1}(P_{fa}) - Q^{-1}(P_d)\right) - Q^{-1}(P_d)\right)^2 \tag{3.16}$$

3.3 Waveform Selection for Wireless Sensor Networks

The choice of transmit waveform has a significant impact on the target detection performance of WSN. With multiple sensing nodes deployed within the sensing region, the problem of the waveforms transmitted from the neighbouring sensing nodes interfering with each other need to be addressed [147]. Conventional multi-user communication techniques are not suitable for RF sensing applications. Within the existing literature, orthogonal waveform design techniques have been addressed to allow multiple access [92, 93, 95]. However, transmitting these orthogonal waveforms require complex transmitting devices which are usually unavailable within resource constrained sensing nodes. Due to event driven nature of the sensing nodes within WSN, the transmission cycles of independent sensing

nodes may not always be synchronised and hence the choice of orthogonal waveforms may not always be the optimal solution. A simple and resource efficient solution in the choice of transmit waveforms is required which guarantees reliable target detection rates within the constraints of the given sensing conditions. In this section, the choice of transmit waveforms which are suitable for RF sensing based applications of WSN and relevant waveform selection strategies to optimise the target detection reliability within the resource constraints of WSN have been discussed.

3.3.1 Problem Formulation

The problem of interest is RF sensing based WSN whose primary objective is to provide surveillance within the sensing region. The proposed WSN as shown in Figure 3.6, consists of clusters of sensing nodes which are distributed within the sensing region. Each cluster consists of a primary node which, acts as the cluster-head and a group of receiving nodes. The primary node within each cluster transmits the desired RF signal into the sensing region. In the event of existence of a target within the sensing region, the receiving nodes attempt to detect the reflected echoes of the known transmitted signal. The primary node is assumed to have sufficient resources to transmit the desired RF waveforms.

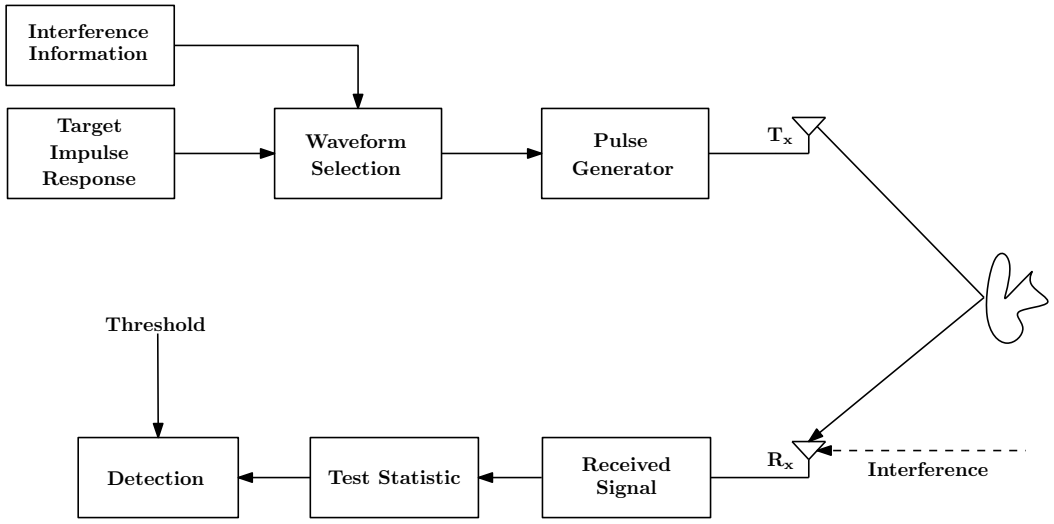

FIGURE 3.6: Proposed target detection model For WSN

To meet the power constraints low-power UWB pulses are transmitted with short transmit durations. As a result of high bandwidth and ultra-short nature of the transmit pulses, the reflected echoes are characterised by the impulse response of the target. For a target impulse response of length N_a and transmit UWB waveform $\mathbf{s}(t)$, the reflected echo from the target can be written as

$$\Omega(t) = \mathbf{a}(t) * \mathbf{s}(t) \tag{3.17}$$

where $*$ indicates the convolution operator and $\mathbf{a}$ is the target impulse response. It is assumed that WSN has the knowledge of the target's impulse response. In the presence of noise and interfering waveforms, the received target echo at the i^{th} sensing node can be written as

$$\mathbf{y}_i(n) = \mathbf{A}\mathbf{s}_i(n) + \mathbf{B}\mathbf{h}_i(n) + \mathbf{w}_i(n) \tag{3.18}$$

where $\mathbf{y}$ is the $N_y \times 1$ received signal data, $\mathbf{s}_i$ is the $N_t \times 1$ transmitted waveform by the i^{th} sensing node. $\mathbf{A}$ is the $N_y \times N_t$ convolution matrix for the target impulse response. $\mathbf{h}_i$ is interfering waveform at the i^{th} sensing node and $\mathbf{n}_i$ is thermal

noise. $\mathbf{B}$ is $N_y \times N_t$ convolution matrix for the channel impulse response.

$$\mathbf{A} = \begin{bmatrix} \mathbf{a}(1) & 0 & \dots & \dots & 0 \\ \mathbf{a}(2) & \mathbf{a}(1) & \ddots & \dots & 0 \\ \vdots & \vdots & \ddots & \ddots & 0 \\ \mathbf{a}(N_a) & \mathbf{a}(N_a-1) & \dots & \dots & 0 \\ 0 & \mathbf{a}(N_a) & \mathbf{a}(N_a-1) & \dots & \mathbf{a}(1) \\ \vdots & 0 & \mathbf{a}(N_a) & \dots & \mathbf{a}(2) \\ \vdots & \vdots & 0 & \ddots & \vdots \\ 0 & 0 & \dots & 0 & \mathbf{a}(N_a) \end{bmatrix} \tag{3.19}$$

here $N_y = N_t + N_a$ - 1. The channel convolution matrix $\mathbf{B}$ can be written similarly as shown in Equation 3.19. The convolution matrices allow continuous representation of the time convolution operator in discrete form. Estimation of channel impulse response has been addressed by the authors in the existing literature [148, 149] and it is assumed to be known to the target detector.

3.3.2 UWB Waveforms

The choice of an appropriate transmit waveform is an important design parameter for RF sensing based surveillance applications of WSN. While longevity of WSN is extremely desirable, optimum choice of a transmit waveform within WSN must fulfil the necessary criterion to achieve the desired target detection reliability while operating within the constraints of available resources. Brevity of the transmit pulses is required to meet the power constraints. However, for sensing nodes with limited hardware capabilities, the complexities involved in generating and transmitting these ultra-short pulses must also be considered. To reduce the signal processing complexity, the transmit waveform must possess good correlation properties which makes it easily detectable at the target detector. In this section, some of the transmit waveforms which are suitable for WSN and their correlation properties have been discussed.

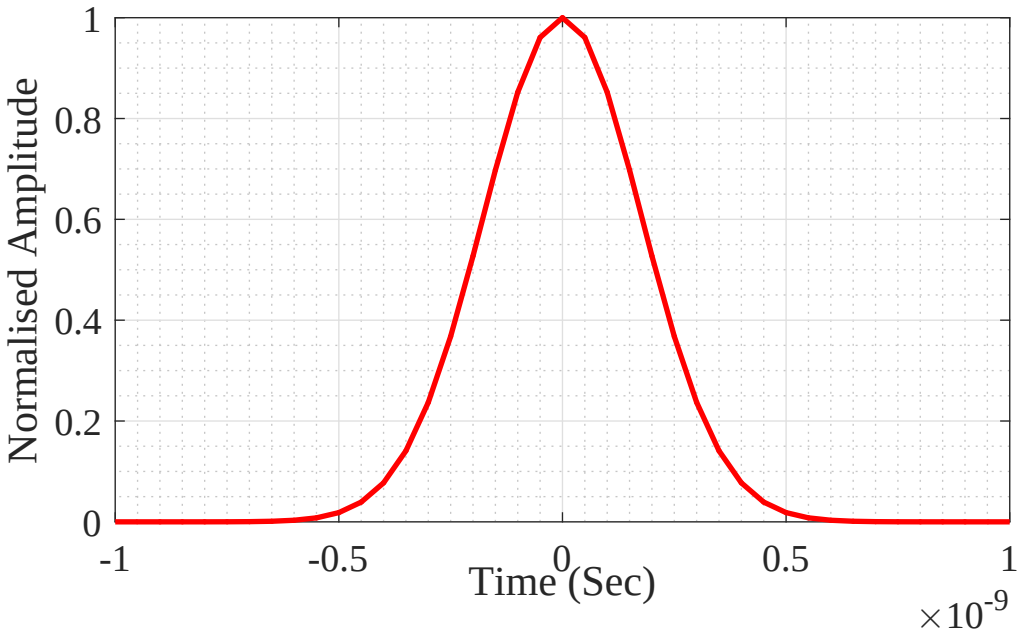

FIGURE 3.7: Time domain representation of Gaussian Pulse

Gaussian pulse is one of the most commonly discussed waveforms. In the time domain, very short Gaussian pulses can be generated which can be used for resource constrained WSN. The time domain expression of a Gaussian pulse shown in Figure 3.7 can be written as

$$\mathbf{g}(t) = Ae^{(\frac{-t}{\tau})^2} \tag{3.20}$$

where A is maximum amplitude and τ is the pulse width. The first derivative of the Gaussian pulse gives a Monocycle pulse, which is another commonly discussed waveform. A monocycle pulse shown in Figure 3.8 can be mathematically expressed as

$$\mathbf{m}(t) = A(\frac{t}{\tau})e^{-(\frac{t}{\tau})^2} \tag{3.21}$$

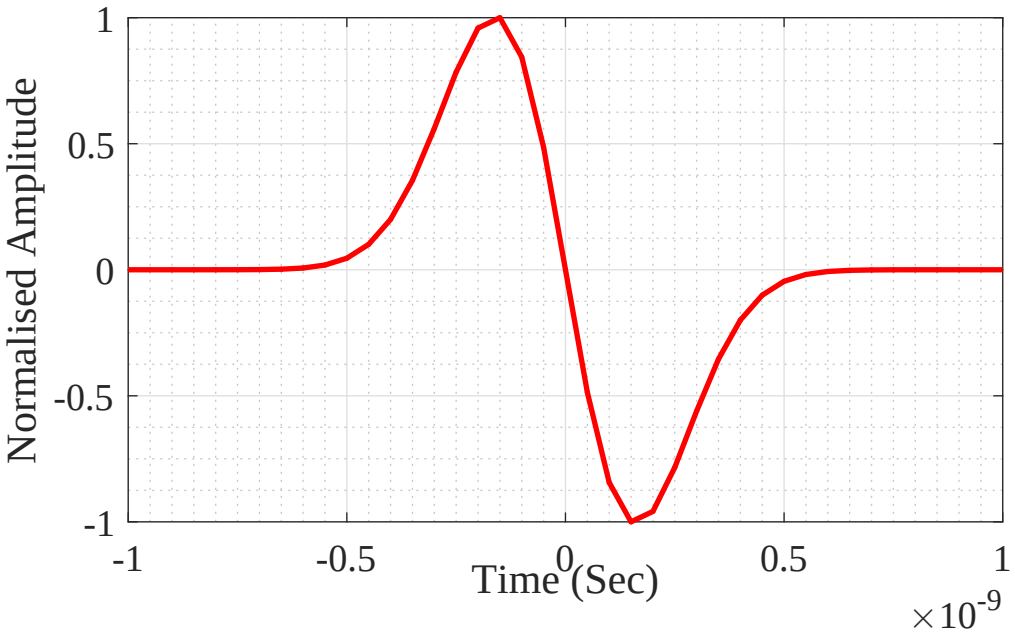

FIGURE 3.8: Time domain representation of Monocycle Pulse

Due to simplicity and ease of generation, the Gaussian and monocycle pulses can be used within WSN with very low computational cost. However, within a large sensing region with multiple transmitting nodes the target detection rates severely deteriorate due to interference from the neighbouring sensing nodes. Hence, a degree of diversity in the choice of waveforms among the transmitting nodes is required.

In [92–95], orthogonal waveforms based on Gegenbauer and Hermite polynomials are discussed. Waveforms generated based on modified Gegenbauer and Hermite polynomials can be used to generate short UWB pulses and the diversity in the available waveforms provides a simple solution to also allow multiple access. Gegenbauer polynomials are defined in the interval [-1,1]. The recurrence equation for the n^{th} order Gegenbauer polynomial is written as

$$\mathcal{G}_n(\beta,t) = \frac{2(n+\beta-1)}{n} t G_{n-1}(\beta,t) - \frac{(n+2\beta-2)}{n} G_{n-2}(\beta,t) \tag{3.22}$$

where n is the order of the Gegenbauer polynomial and β is the shape parameter. The first 5 orders of Gegenbauer polynomials are expressed in Equation 3.23 as

$$
\begin{aligned}
\mathcal{G}_0(\beta,t) &= 1 \\
\mathcal{G}_1(\beta,t) &= 2\beta t \\
\mathcal{G}_2(\beta,t) &= \beta[-1+2(1+\beta)t^2] \\
\mathcal{G}_3(\beta,t) &= \beta(1+\beta)[-2t+(2+\beta)\frac{4t^3}{3}] \\
\mathcal{G}_4(\beta,t) &= \beta(1+\beta)[\frac{1}{2}-2(2+\beta)t^2+(2+\beta)(3+\beta)\frac{2t^4}{3}]
\end{aligned}
\tag{3.23}
$$

Modified Gegenbauer polynomials use a weight function $\mathbf{w}(t)$ to facilitate the generation of ultra-short pulses. Modified Gegenbauer functions are written as

$$
\begin{aligned}
\mathbf{G}(\beta,t) &= \sqrt{\mathbf{w}(t)}\mathcal{G}_n(\beta,t) \\
\mathbf{w}(t,\beta) &= (1-t^2)^{\beta-\frac{1}{2}} \qquad \beta > \tfrac{-1}{2}
\end{aligned}
\tag{3.24}
$$

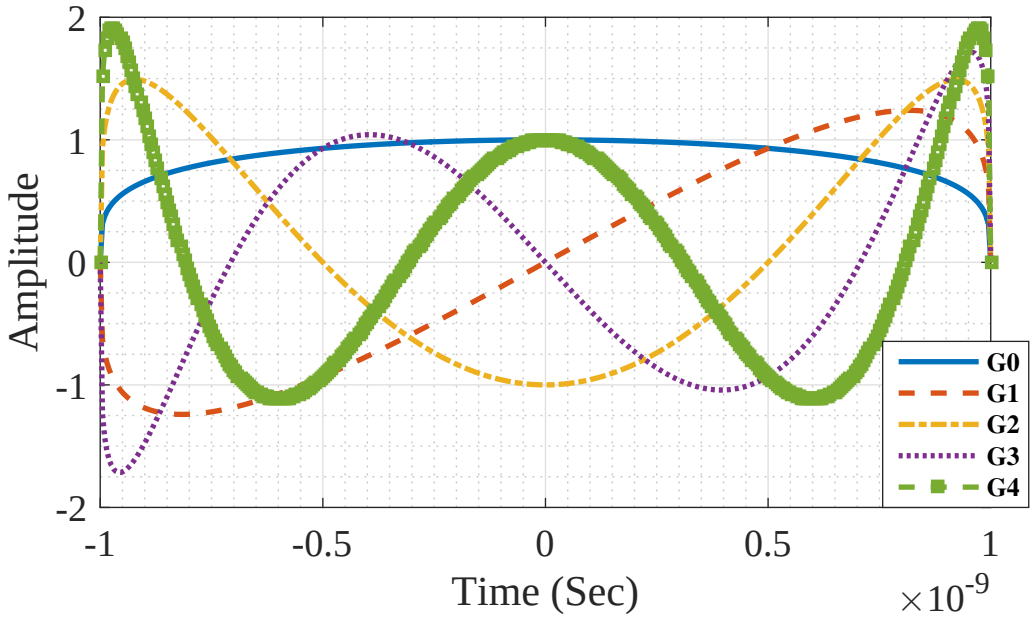

FIGURE 3.9: Modified Gegenbauer functions of orders n = 0, 1, 2, 3 and 4

The time domain representation of the first five modified Gegenbauer polynomials is shown in Figure 3.9 with the value of $\beta = 1$. Modified Hermite polynomials are defined in the interval $[-\infty\ ,\ \infty]$. n^{th} order Hermite polynomial can be written as

$$\begin{aligned} h_{e_n}(t) &= (-1)^n e^{\frac{t^2}{2}} \frac{d^n}{dt^n}(e^{\frac{-t^2}{2}}) \quad n \neq 0 \\ h_{e_0}(t) &= 1 \end{aligned} \tag{3.25}$$

From Equation 3.25, the first 5 orders of Hermite polynomials are expressed by the following equations,

$$\begin{aligned} h_{e_0}(t) &= 1 \\ h_{e_1}(t) &= t \\ h_{e_2}(t) &= t^2 - 1 \\ h_{e_3}(t) &= t^3 - 3t \\ h_{e_4}(t) &= t^4 - 6t^2 + 3 \end{aligned}$$

Modified Hermite polynomials are obtained by multiplying Hermite polynomials with $e^{\frac{-t^2}{4}}$. The first 5 orders of the modified Hermite pulses are plotted in Figure 3.10. n^{th} order Modified Hermite function can be expressed as

$$h_n(t) = e^{\frac{-t^2}{4}} h_{e_n}(t) \tag{3.26}$$

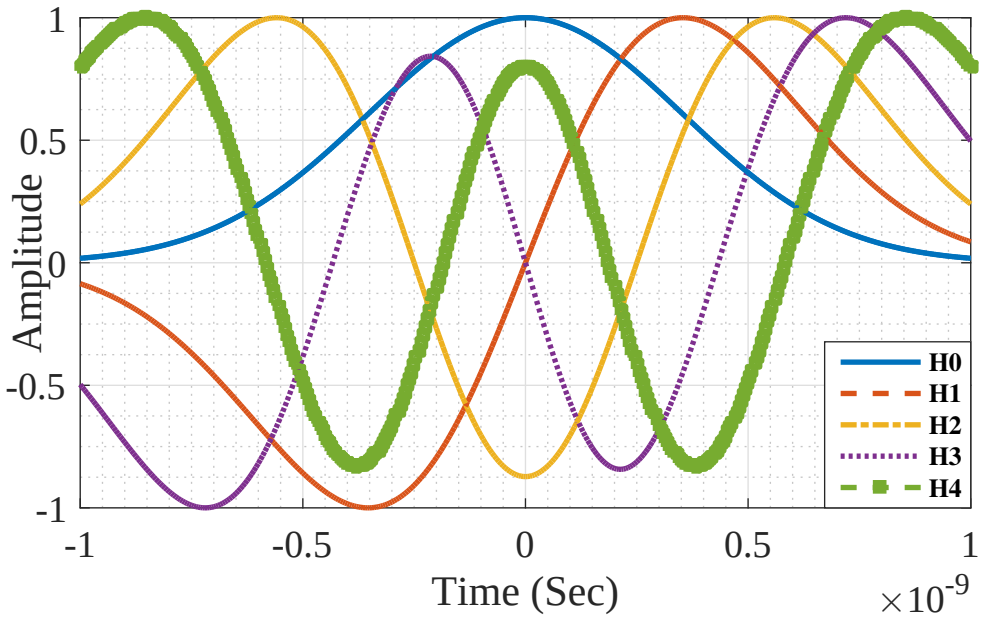

FIGURE 3.10: Modified Hermite functions of orders n = 0, 1, 2, 3 and 4

TABLE 3.1: Comparison of Dynamics and Peak widths of the waveforms discussed

Waveform	Dynamics (D)	Peak Width (W)
Gaussian Pulse	1	142
Monocycle Pulse	1	114
G_0	1	386
G_1	1	150
G_2	0.7	88
G_3	0.63	62
G_4	0.62	46
Hm_0	1	234
Hm_1	1	124
Hm_2	0.61	94
Hm_3	0.58	74
Hm_4	0.50	58

The transmit waveforms discussed in this section are easy to generate and does not require complex transmitting devices. They also provide diversity within the choice of transmit waveforms. These proposed waveforms which are suitable for UWB communications, can be transmitted as short pulses with reduced transmission costs. In [147] authors have proposed a criterion based on dynamics and peak width of the autocorrelation functions to identify optimum transmit waveforms. Dynamics is the difference between amplitudes of the main lobe and peak side lobes of the autocorrelation function and peak width is width of the main lobe at -3dB amplitude over a given period of time. Within RF sensing applications, to provide reliable target detection, transmit waveforms whose autocorrelation functions display main lobes, which are significantly stronger than the side lobes

are desirable. Transmit waveforms with lower peak widths provide improved range resolution. Dynamics and peak widths of some of the waveforms discussed in this section are summarised in Table 3.1 where G_i represents i^{th} order Gegenbauer pulse and Hm_i represents i^{th} order Hermite pulse. For WSN whose primary objective is to detect the occurrence of any intrusions, transmit waveforms with high dynamics would be a suitable choice. For surveillance applications of WSN, to be able to detect the presence of multiple targets, transmit waveforms with high dynamics to peak width ratio are desirable.

3.3.3 Waveform Selection for Target Detection Optimisation

The performance measure of a WSN as a surveillance system while dedicated to detecting the existence or non-existence of targets is the degree of reliability on such decision-making process. The two possible outcomes of this decision-making process are hypothesis H_0 and hypothesis H_1 which are modelled as a binary hypothesis testing problem where H_0 represents absence of a target and H_1 represents the existence of a target. The possible received signal models $\mathbf{y}_i$ corresponding to hypothesis H_0 and H_1 are,

$$H_0 : \begin{cases} H_{00}\text{: } \mathbf{y}(n) = \mathbf{w}(n) \\ H_{01}\text{: } \mathbf{y}(n) = \mathbf{Bh}(n) + \mathbf{w}(n) \end{cases} \tag{3.27}$$

$$H_1 : \begin{cases} H_{10}\text{: } \mathbf{y}(n) = \mathbf{As}(n) + \mathbf{w}(n) \\ H_{11}\text{: } \mathbf{y}(n) = \mathbf{As}(n) + \mathbf{Bh}(n) + \mathbf{w}(n) \end{cases} \tag{3.28}$$

Equation 3.27 and Equation 3.28 represent possible received signal models under hypothesis H_0 and H_1 which are characterised by existence and absence of target and interfering waveforms. A Cross-Correlation (CC) based detector is a popular technique, which is used to detect the existence of known waveforms within the

received signal component. A CC detector performs cross-correlation between the received signal and the target signal to make a decision regarding the existence of the target waveform.

$$r(\Delta T) = \sum_{n=-\infty}^{\infty} \mathbf{s}(n - \Delta T)\mathbf{y}(n) \tag{3.29}$$

where $r(\Delta T)$ is cross correlation between the received signal and the target signal after a time delay ΔT corresponding to a given range bin. However, as a consequence of the ultra-wide band nature of the transmit signal and target impulse response; the reflected echoes undergo shape transformations. Hence the optimal detector should match the scattered waveform in Equation 3.17 with the received signal. If matched filter impulse response is $\mathbf{f}$, then the matched filtered output of the received signal is given by,

$$\mathbf{x} = \mathbf{f}^H\mathbf{y} = \mathbf{f}^H\mathbf{A}\mathbf{s} + \mathbf{f}^H\mathbf{B}\mathbf{h} + \mathbf{f}^H\mathbf{w} \tag{3.30}$$

Signal to Interference and Noise Ratio (SINR) at the matched filter output is given by,

$$SINR = \frac{|\mathbf{f}^H\mathbf{A}\mathbf{s}|^2}{E[|\mathbf{f}^H\mathbf{B}\mathbf{h}|^2] + E[|\mathbf{f}^H\mathbf{w}|^2]} \tag{3.31}$$

From [150], the matched filter impulse response that maximises the SINR at the receiver can be written as

$$\mathbf{f} = \alpha(\mathbf{B}\mathbf{h}\mathbf{h}^H\mathbf{B}^H + \mathbf{R}_w)^{-1}\mathbf{A}\mathbf{s} \tag{3.32}$$

where α is a scaling parameter and $\mathbf{R}_w$ is the noise covariance matrix. However, the matched filter in Equation 3.32 only produces the maximum attainable SINR under the constraints of the transmitted waveform. From Equation 3.30 and Equation 3.32, the optimum transmit waveform that maximises the target return at the matched filter output has been derived in [151] as

$$\hat{\mathbf{s}} = \max_{\mathbf{s}} \mathbf{s}^H \mathbf{A}^H (\mathbf{B}\mathbf{h}\mathbf{h}^H \mathbf{B}^H + \mathbf{R}_w)^{-1} \mathbf{A}\mathbf{s} \tag{3.33}$$

$$\delta = \alpha \frac{(\max(\mathbf{f}^H \star \mathbf{A}\mathbf{s}) - \max(\mathbf{f}^H \star \mathbf{B}\mathbf{h}))(\max(\mathbf{f}^H \star (\mathbf{A}\mathbf{s} + \mathbf{B}\mathbf{h})) - \max(\mathbf{f}^H \star \mathbf{B}\mathbf{h}))}{\max(\mathbf{f}^H \star \mathbf{B}\mathbf{h})} \tag{3.34}$$

The solution to Equation 3.33 can be obtained through eigen-analysis. The transmit waveform that maximises the matched filter output is the eigenvector corresponding to the maximum eigenvalue of $\mathbf{A}^H(\mathbf{B}\mathbf{h}\mathbf{h}^H\mathbf{B}^H + \mathbf{R}_w)^{-1}\mathbf{A}$. However, the optimised waveform obtained in Equation 3.33 is associated with transmission complexities and the resource constrained sensing nodes within the WSN may not have sufficient resources to transmit these waveforms. To reduce the transmitting complexity, the transmit waveforms discussed in Section 3.3.2 have been considered. While the waveforms discussed in Section 3.3.2 do not optimise the matched filter output, suitable waveform may be chosen which maximises the matched filter output within the constraints of the available transmit waveforms. However, maximising SINR is not the sufficient condition to optimise the target detection performance of WSN.

The matched filter compares the received signal with the expected target return to detect the existence of the target echo. A reliable decision regarding the existence or absence of a target can be made when the matched filter outputs under hypothesis H_0 and H_1 are clearly distinguishable. To measure the ability of the matched filter to make this distinction an Ease of Detection Index (δ) has been defined in Equation 3.34 which is measured at 3dB Signal-to-Interference Ratio (SIR). Here $\star$ represents correlation operator and α is a scalar accounting for equality constraint. When the sensing conditions are known, the transmit waveform which maximises (δ) gives optimum reliability among the available transmit waveforms. Within resource constrained WSN, the amount of transmit power has a significant impact on the lifetime of the sensing nodes. The choice of transmit waveform while achieving high δ, must also be energy efficient to ensure longevity of the

sensing nodes. The amount of transmit power required to guarantee the desired SIR at the receiver is related to various factors such as prorogation losses, target impulse response, target range, etc. For a given sensing conditions, the energy efficiency of the transmit waveform is defined by Energy Efficiency Index (η). η is the ratio of the amount of transmit power (P_{Tm}) required to guarantee desired SIR at the matched filter output to the amount of transmit power (P_{Tr}) required to guarantee desired SIR at the sensing node receiver which is given as

$$\eta = \frac{P_{Tm}}{P_{Tr}} = \frac{max(\mathbf{f}^H \star \mathbf{Bh})(\mathbf{As})^H(\mathbf{As})}{max(\mathbf{f}^H \star \mathbf{As})(\mathbf{Bh})^H(\mathbf{Bh})} \tag{3.35}$$

Energy efficiency index denotes the factor by which the transmit power may be reduced while ensuring desired SINR at the matched filter output. To identify the transmit waveform which provides a measure of balance between δ and η, a selection criterion has been defined which is given by the ratio δ/η. Therefore, for given sensing conditions the transmit waveform which maximises δ/η optimises the target detection reliability of WSN.

3.4 Performance Analysis

3.4.1 Analysis of the Sensing Criterion

In this section the operational constraints of the WSN which are discussed in Section 3.2 have been analysed. To fulfil the objective of target detection, the sensing nodes rely on the received echoes from the targets and make a decision regarding the existence of absence of the targets. However, the energy of the transmit pulses deteriorates with distance travelled. Moreover, the received data is usually corrupted by noise. The received signal-to-noise ratio at the receiver is therefore measured as the ratio between the received signal power and the noise power. SNR is measured as defined in Equation 3.10. For simplicity, the values of antenna gain, radar cross section and loss factor as 1. The operating frequency is assumed to be 10GHz and the transmit power to be 1 Watt. For different

noise powers at the receiver, the expected received SNR at varying locations of the target locations from the sensing node is plotted in Figure 3.11.

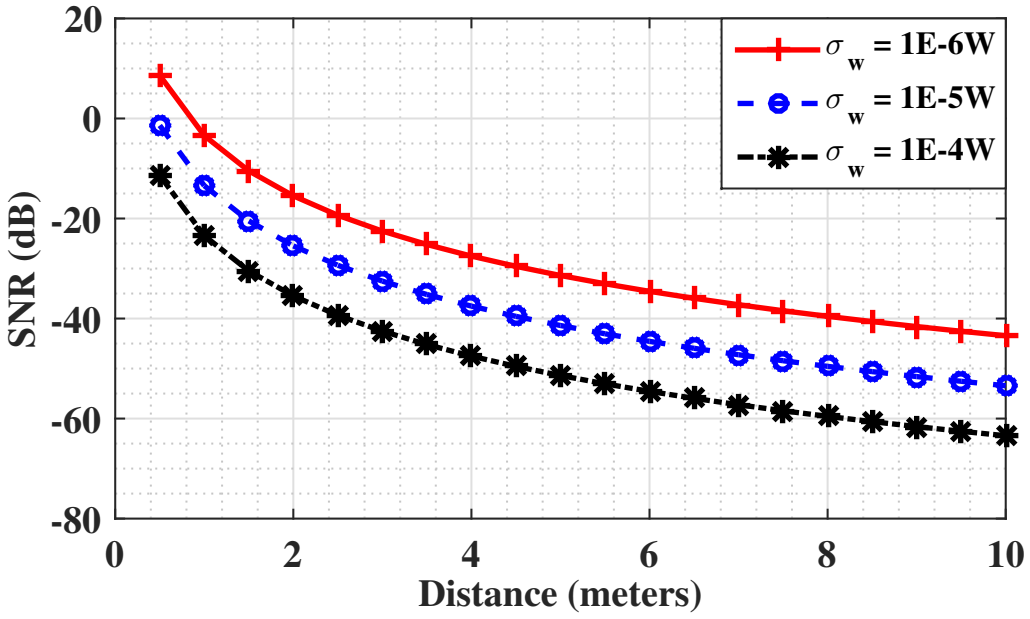

FIGURE 3.11: Received SNR vs Distance at different noise powers

In Figure 3.12, the target detection performance of the Energy Detector discussed in Section 3.2.4 is plotted. The results are obtained from the mathematical equations discussed in Equation 3.12 and Equation 3.13. The simulations are performed over varying distances 'd' of the target from the sensing node and the impact of the number of received signal samples on the target detection reliability is shown. A Gaussian channel is assumed with constant noise power and the results are plotted at a false alarm rate of 10^{-4}. From the results, it can be observed that the target detection reliability of the Energy Detector for wireless sensor network can be increased by increasing the length of the observation window. However, the increased reliability is achieved as a consequence of increased transmission costs and computational complexity.

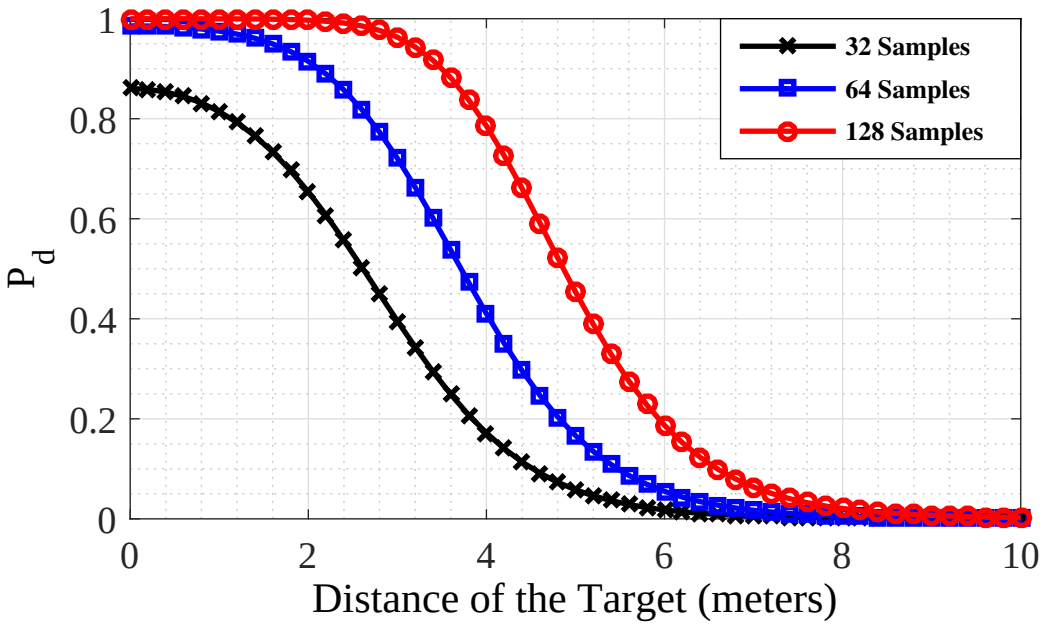

FIGURE 3.12: Target detection performance vs distance of the target

In Equation 3.16, a relationship between the observation window and the desired probability of detection and probability of false alarm for energy detector has been derived. In Figure 3.13, the number of received signal samples required to achieve a desired detection rate is plotted. The channel gain is assumed to be 1. From the figure, it can be observed that a direct correlation existed between probability of detection and the number of received signal samples at a given sensing range. In Figure 3.14 the probability of detection vs the received SNR for different lengths of observation windows are plotted. The results are obtained based on Equation 3.12 and Equation 3.13

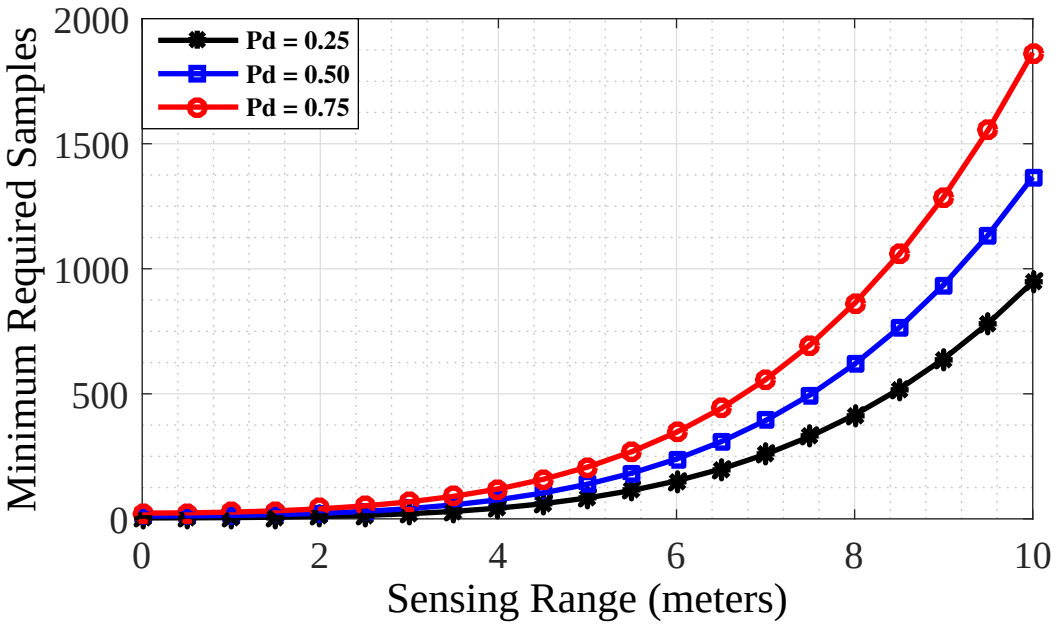

FIGURE 3.13: Sensing range vs length of the observation window

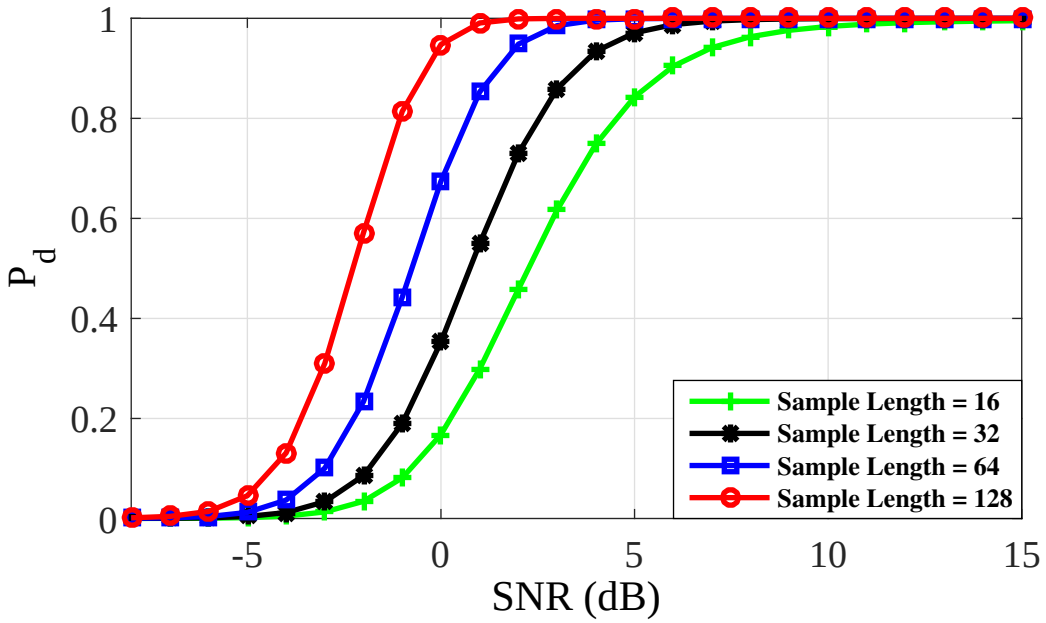

FIGURE 3.14: P_d vs SNR with unknown target signal

TABLE 3.2: Comparison of δ and η of the waveforms discussed with interfering Monocycle waveform

Waveform	EDI (δ)	EEI (η)	(δ/η) at $\alpha = 1$
Gaussian Pulse	0.4553	0.2277	1.9995
G_0	0.4045	0.2214	1.8272
G_1	0.3906	0.3789	1.0309
G_2	0.0357	0.5609	0.0636
G_3	0.4180	0.1440	2.9024
G_4	1.2945	0.0843	15.3645
Hm_0	0.1969	0.4029	0.4888
Hm_1	-0.0333	1.3813	-0.0241
Hm_2	0.3603	0.2523	1.4281
Hm_3	1.2444	0.0958	12.9957
Hm_4	1.2675	0.0857	14.7904

3.4.2 Performance Analysis of the Proposed Waveform Selection Criterion

In this section, the optimality criterion for the waveforms discussed in Section 3.3.2 have been compared. For simulations, the interfering waveform is assumed to be a Monocycle pulse and the presence of white Gaussian noise is assumed. WSN is assumed to be deployed to detect the presence of a target with known impulse response. A uniform indoor sensing environment is considered and an estimate of the channel impulse response is assumed to be known. In Table 3.2, δ and η of the waveforms considered under the given sensing conditions is summarised. High value of Ease of Detection Index indicates greater target detection reliability and lower value for Energy Efficiency Index indicates improved transmission efficiency.

From Table 3.2 it can be observed that for the simulated sensing conditions, G_4 and Hm_4 waveforms generated high δ/η ratios compared to the other waveforms. Similarly, δ/η ratio of Hm_1 waveform is less than zero which indicates that for the given sensing conditions Hm_1 waveform is unsuitable for transmission.

Matched Filter Output: In Figure 3.15 and Figure 3.16, the matched filter outputs of the received signal models under hypothesis H_0 and H_1 with transmit waveforms being G_4 and Hm_4 respectively are plotted. The transmission periods of individual sensor nodes within WSN are assumed to be unsynchronised. The matched filter outputs for all 4 cases of received signal models in Equation 3.27 and Equation 3.28 are plotted. H_{00} indicates the received signal model under hypothesis H_0 where the target and interfering waveforms are absent. Similarly, H_{01} refers to the received signal under hypothesis H_0 in the presence of interfering waveform. Similarly, H_{10} and H_{11} refer to the received signal models under hypothesis H_1 in the absence and presence of interfering waveform. From the plots, it can be observed that, when G_4 and Hm_4 waveforms are transmitted respectively, a clear distinction existed between matched filter outputs under hypothesis H_0 and H_1 which indicates greater detection reliability. Similarly, in Figure 3.17, the matched filter output is plotted when G_3 waveform is transmitted. In this case at 3dB SINR, while the matched filter output is maximised under hypothesis H_1, a reduced distinction can be observed between hypothesis H_0 and H_1 along with lower dynamics which leads to reduced detection reliability. In Figure 3.18, the matched filter output is plotted when Hm_1 waveform is transmitted. In this case, no distinction between matched filter outputs under hypothesis H_0 and H_1 can be observed which indicates an uncertainty in the decision-making process.

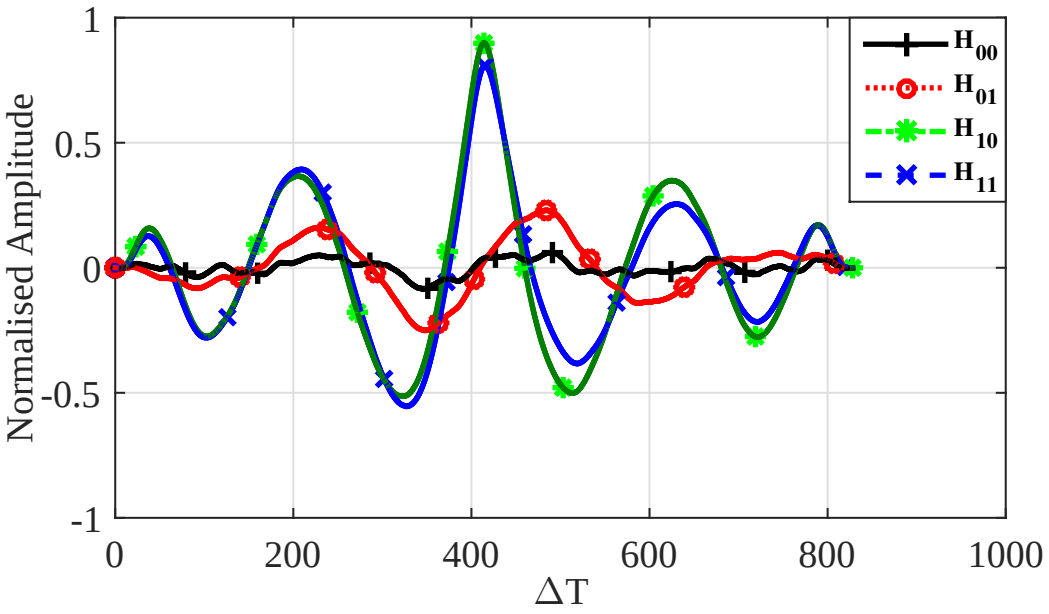

FIGURE 3.15: Matched filter output for G_4 transmit waveform and interfering monocycle pulse

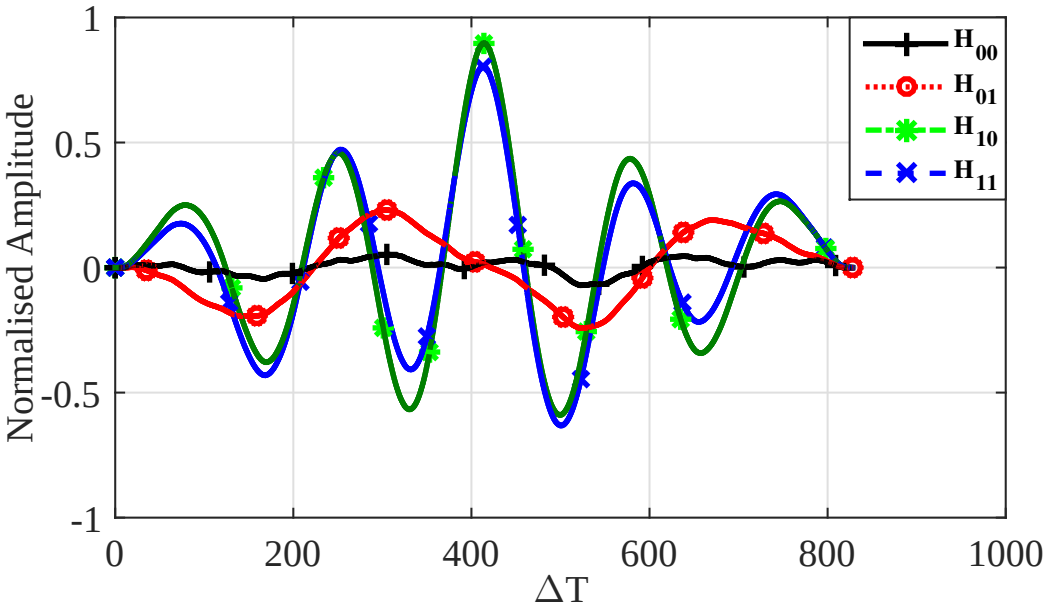

FIGURE 3.16: Matched filter output for Hm_4 transmit waveform and interfering monocycle pulse

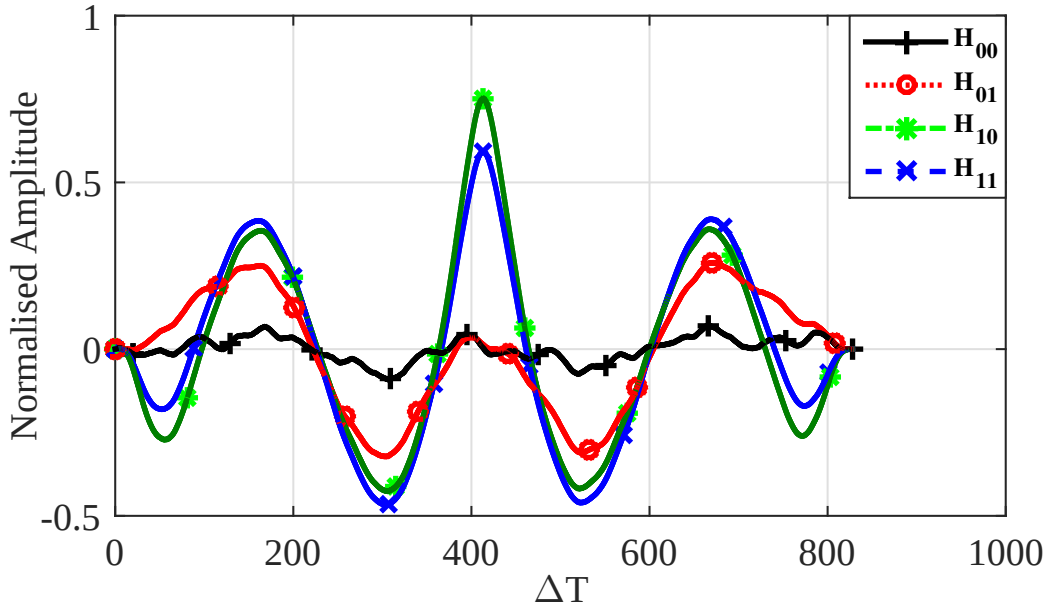

FIGURE 3.17: Matched filter output for G_3 transmit waveform and interfering monocycle pulse

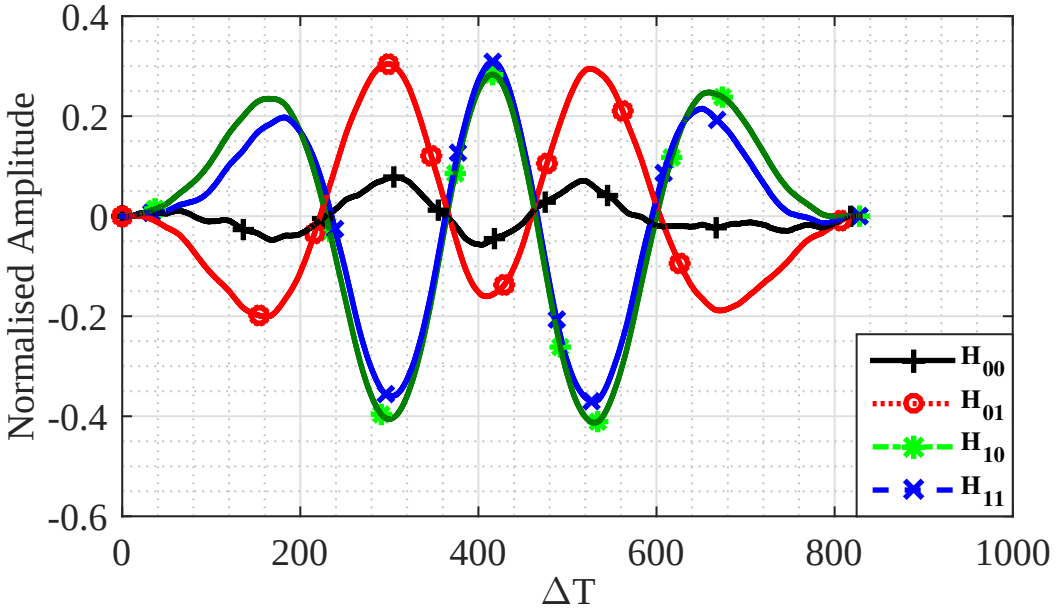

FIGURE 3.18: Matched filter output for Hm_1 transmit waveform and interfering monocycle pulse

Target Detection Performance: To make a decision regarding the existence of targets, a test statistic $\mathbb{T}$ is generated based on likelihood ratio test which is

compared to a pre-defined threshold γ. The test statistic for the detection problem based on matched filter output as discussed in [152, 153] can be written as

$$\mathbb{T} = \frac{\mathbf{f}^H \mathbf{y}}{\mathbf{y}^H \mathbf{y} - \mathbf{f}^H \mathbf{y}} \underset{H_0}{\overset{H_1}{\gtrless}} \gamma \tag{3.36}$$

where γ is usually chosen such that the maximum P_{fa} remains within an acceptable limit. For simulations, γ is chosen to ensure a maximum allowable P_{fa} of 10^{-3}. Monte-Carlo techniques have been implemented for simulations with $10/P_{fa}$ independent simulations with $N_y = 415$ received signal samples. The target impulse response vector length N_a is assumed to be 15. According to the results summarised in Table 3.2 and simulation results for the matched filter outputs discussed in this section, within the given sensing conditions, G_4 waveform is expected to provide optimum target detection performance. To verify the observations, in Figure 3.19 the target detection performances of the proposed target detector have been compared when G_4 and Hm_1 waveforms are transmitted respectively. The corresponding false alarm rates are plotted in Figure 3.20. Clearly, when G_4 waveform is transmitted the target detector outperformed its counterpart when Hm_1 waveform is used. Similarly, in Figure 3.21, the target detection performances are compared when G_4 and G_3 waveforms are transmitted. While G_3 provided a significant improvement in target detection performance when compared to Hm_1, G_4 outperformed G_3 by a significant margin. Finally, in Figure 3.23, the target detection performances are compared when G_4 and Hm_4 waveforms are transmitted. From Table 3.2 it can be observed that the difference between δ/η ratios of G_4 and Hm_4 waveforms are comparable which is validated through simulations in Figure 3.23 with G_4 slightly outperforming Hm_4. The corresponding false alarm rates are shown in Figure 3.24.

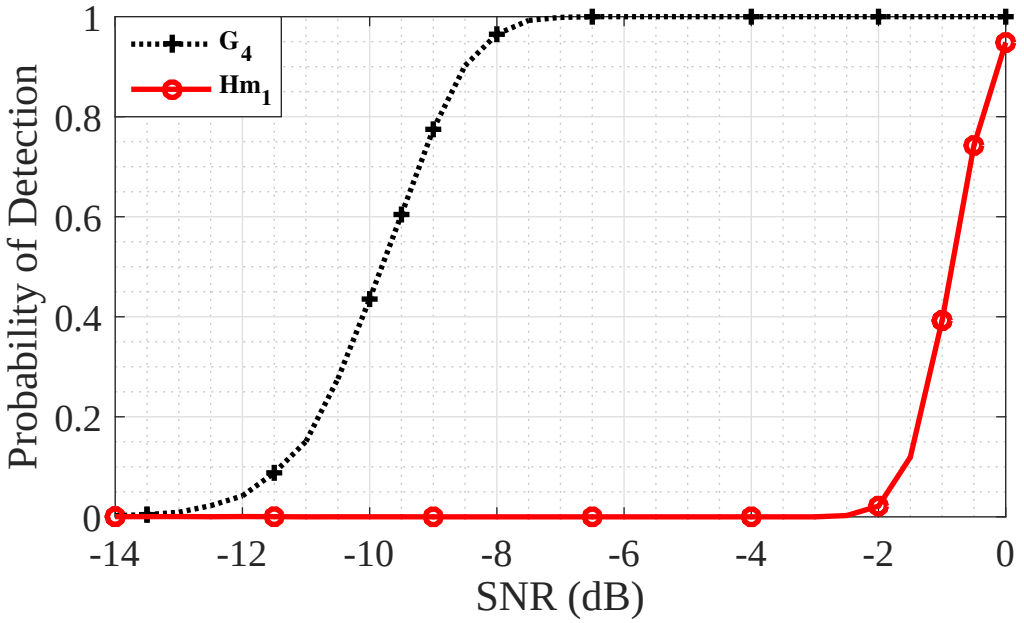

FIGURE 3.19: Comparison of target detection performance when G_4 and H_1 waveforms are transmitted

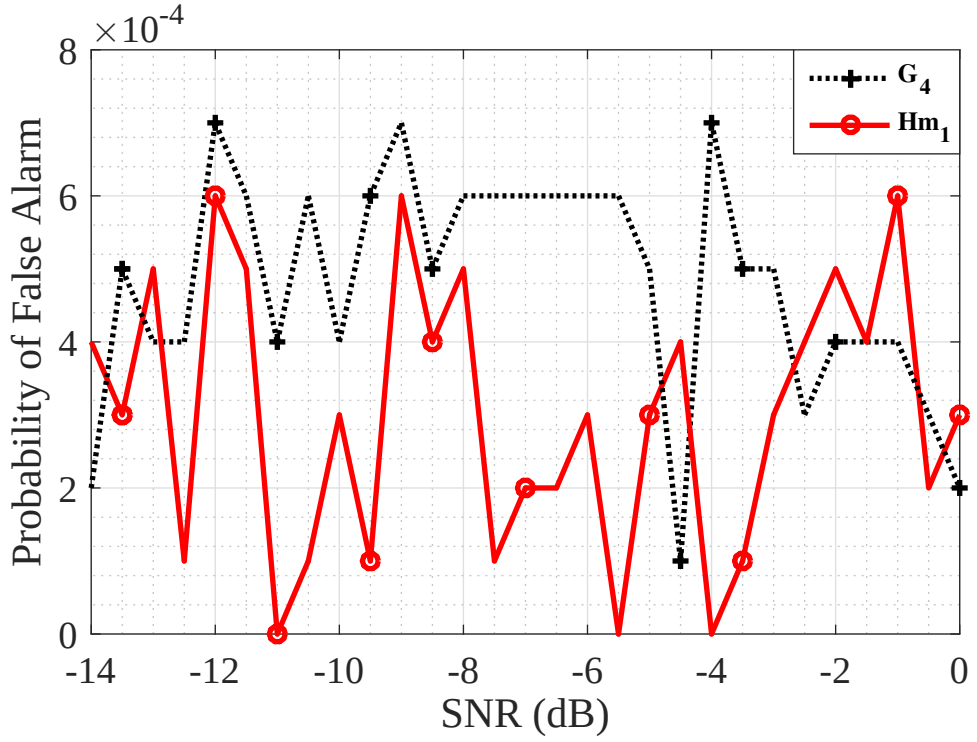

FIGURE 3.20: Comparison of false alarm rates when G_4 and H_1 waveforms are transmitted

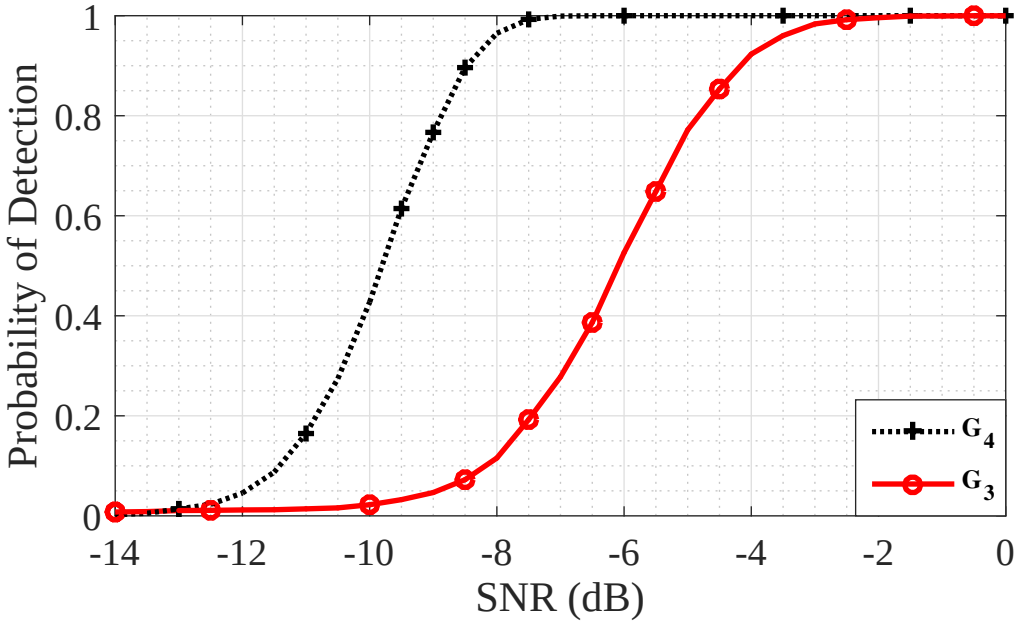

FIGURE 3.21: Comparison of target detection performance when G_4 and G_3 waveforms are transmitted

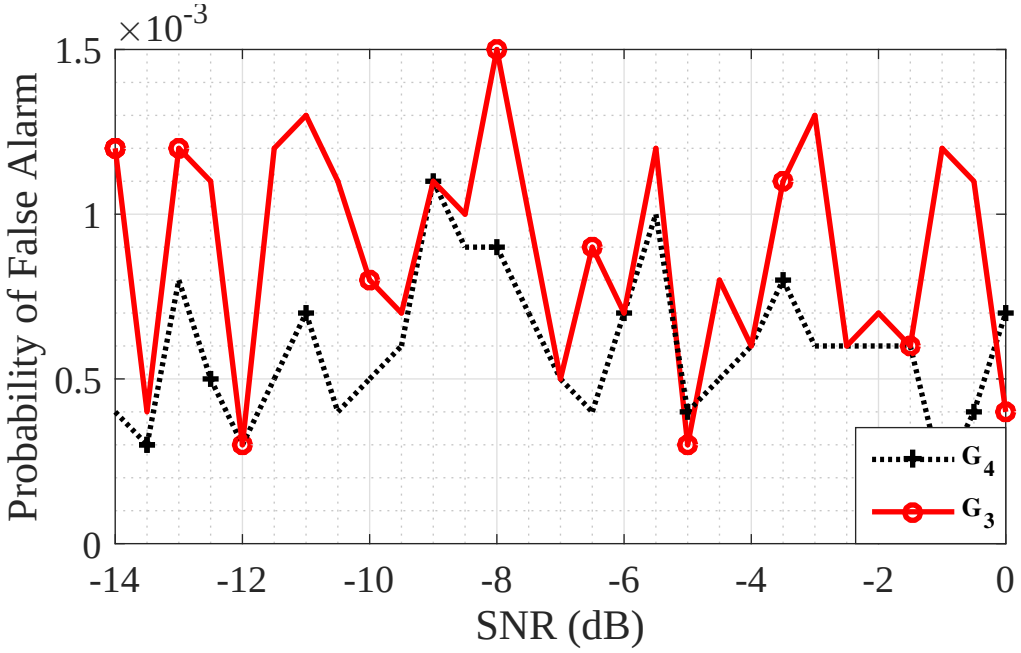

FIGURE 3.22: Comparison of false alarm rates when G_4 and G_3 waveforms are transmitted

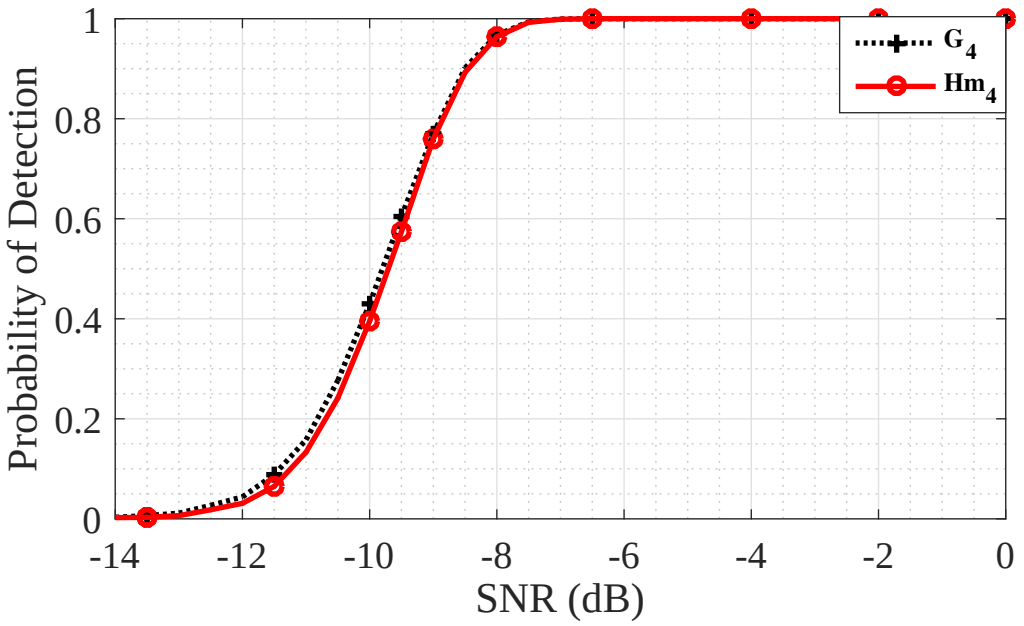

FIGURE 3.23: Comparison of target detection performance when G_4 and H_4 waveforms are transmitted

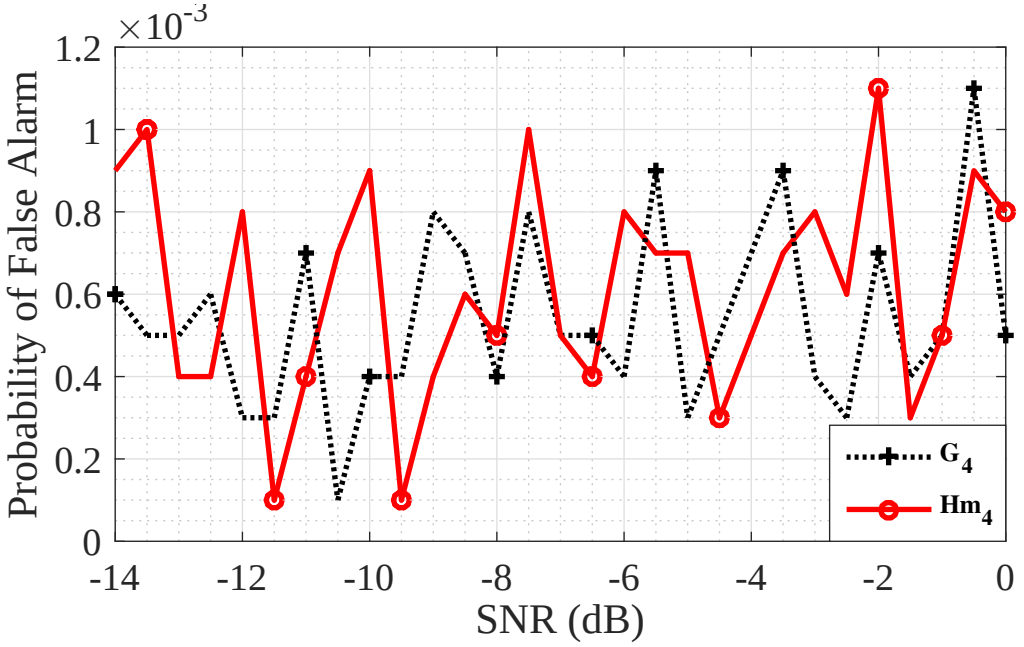

FIGURE 3.24: Comparison of false alarm rates when G_4 and H_4 waveforms are transmitted

Hence, for a given set of sensing conditions and known target impulse response, the selection of waveform will have to consider expected available energy consumption

as well as the targeted P_{fa} to attain. The proposed framework to measure the δ/η ratio is expected to provide with an indicative benchmark on the suitability of a certain waveform. To calibrate a detection system the highest possible value of such threshold is to be preferred.

3.5 Summary

In this chapter, a RF sensing based wireless sensor network has been considered for surveillance applications. Sensing node deployment and various operational constraints of RF sensing based WSN have been established. Relationships between various operational parameters, which influence the target detection reliability of the sensing nodes have been derived. Waveform selection criterion in the context of energy efficiency and detection reliability within RF sensing based WSN for surveillance applications has been investigated. The amount of power consumed during RF signal transmission is one of the major disadvantages of RF sensing when considered for low-powered device based WSN. Transmit waveforms within the range of UWB technologies which are suitable for resource constrained WSN have been explored. Various received signal models in the context of multi-sensor UWB based WSN have been discussed. Within an event driven WSN, where the transmission periods of individual sensor nodes are unsynchronised, a waveform selection criterion to optimise the target detection reliability has been proposed. The proposed waveform selection criterion takes into account the nature of the target and sensing conditions to generate ease of detection index and energy efficiency index for all available transmit waveforms. Numerical results show the target detection performances of the proposed WSN for different choices of transmit waveforms and show that the proposed waveform selection criterion optimised the target detection reliability of WSN under the constraints of available choices of transmit waveforms. In Chapter 4, a novel target detection architecture has been proposed for RF sensing based WSN within homogeneous sensing environments.

Chapter 4

Target Detection Architecture for RF Sensing Based WSN for Homogeneous Sensing Environments

4.1 Introduction

Sensing environment has a significant role in determining the target detection reliability of a WSN. Within a RF sensing based WSN, the sensing nodes rely on detecting the presence of the known RF signals within the received signal components to detect the presence of targets. Upon existence of a target within the sensing region, the sensing nodes are expected to receive the reflected components of the transmitted signal. However, existence of interference from the neighbouring sensing nodes leads to increased false detection rates and reduced target detection reliability. In this chapter, a homogeneous sensing environment without clutter has been considered with organised deployment of sensing nodes. Under such scenarios, the neighbouring sensing nodes inflicts the same amount of interference on any other sensing nodes. In this chapter, a novel target detection architecture has

been proposed for resource constrained WSN under such scenarios. The proposed target detection architecture is designed provide improved target detection reliability and simulation results have been provide to validate the claims. Compressive sensing has been proposed to reduce the transmissions costs where the sensing nodes are only required to transmit compressed received signal samples to the control centre and the control centre has the ability to make a decision regarding the existence or absence of the targets compressed received signal samples.

4.2 Proposed System Model

In this chapter, a homogeneous sensing environment with tactical deployment of sensing nodes has been considered. The proposed system model for distributed target detection using a WSN is shown in Figure 4.1. The proposed system model is suitable for indoor sensing environments where clutter is usually absent. Wireless sensing nodes with 3D coverage, which are deployed within the sensing region in an organised fashion, are expected to provide surveillance by monitoring the sensing region for the designated targets by detecting the presence of the known components of the reflected/transmitted RF signals from the target. As shown in Figure 4.1, to address problem of detecting the presence of targets using a WSN, a network of wireless sensing nodes within the sensing region are assumed to act as a bistatic MIMO receiver. A generalised k-coverage scenario is considered where each point within the sensing region is assumed to be within the sensing range of at least k number of sensing nodes. A cluster of N_s sensing nodes are assumed to be deployed within the sensing region which are within the sensing range of the target. Each cluster consists of a control centre and a group of N_s receiving nodes. The control centre, which is assumed to be equipped with sufficient power and computational resources, transmits the desired RF signal into the sensing region and the receiving sensing nodes attempt to detect the reflected components of the transmitted signal. The transmitting and the receiving elements coordinate among themselves to act as a MIMO system.

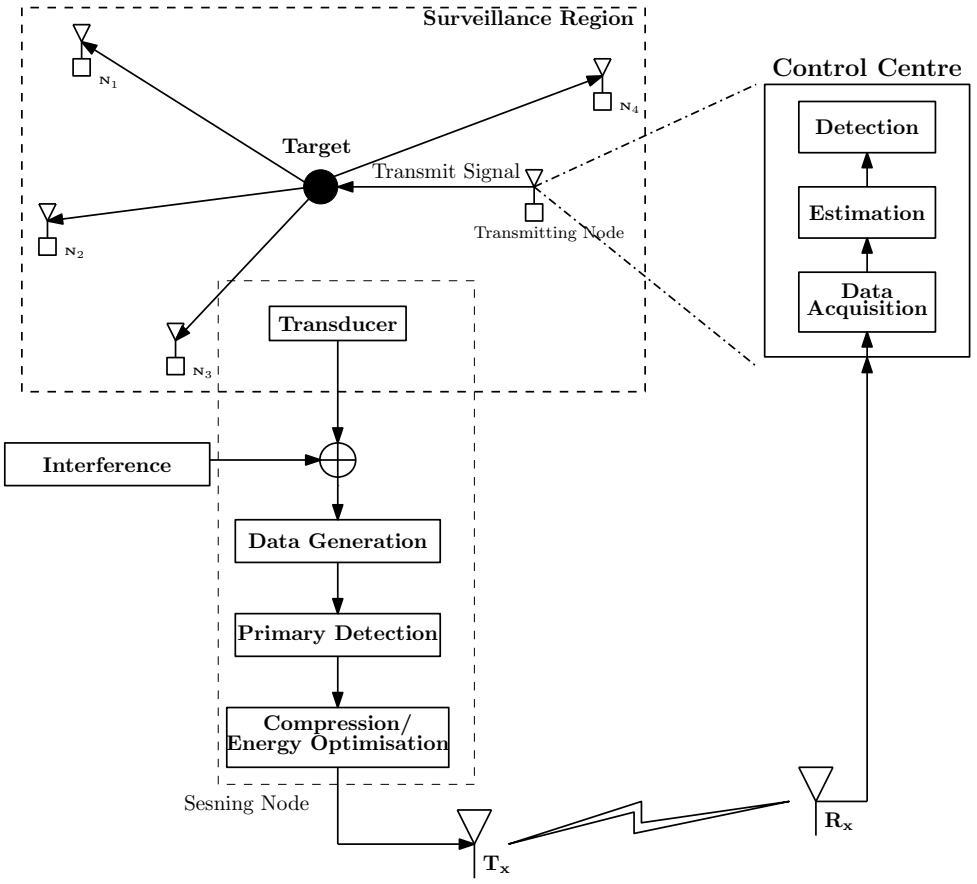

FIGURE 4.1: Proposed system model for WSN surveillance applications

If the signal is transmitted for a time period of T sec $0 \leq t \leq T$, at a sampling rate of f_s, let $\mathbf{s}$ be a $N_t \times 1$ vector representing the time-limited, finite energy transmit signal. Therefore, total energy allocated to each transmission period is

$$E = \int_0^T \mathbf{s}^2(t)dt = \sum_{i=1}^{N_t} \mathbf{s}^2(i) = \mathbf{s}^H\mathbf{s} \tag{4.1}$$

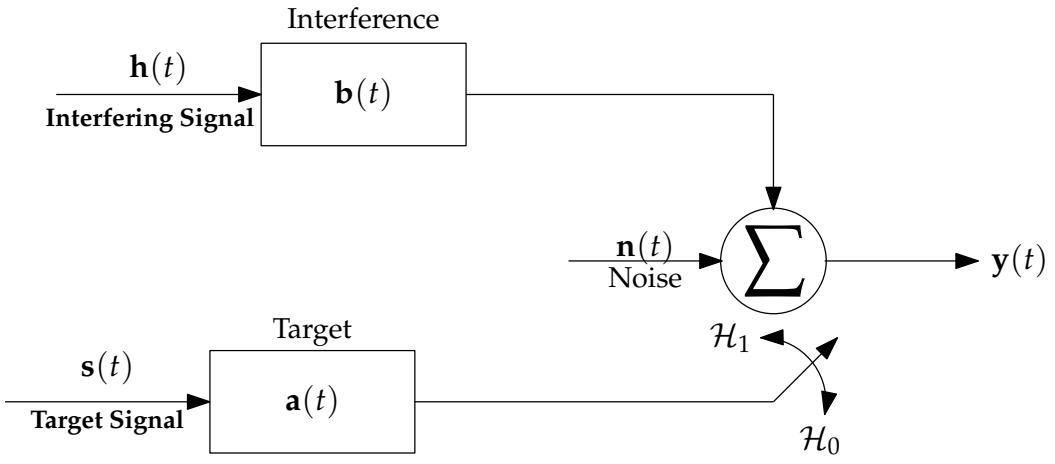

FIGURE 4.2: Received Signal Model at the Sensing Nodes Under Hypothesis H_0 and H_1

When a waveform $\mathbf{s}(t)$ is transmitted, the receiving nodes are expected to receive a direct arrival and reflected components of the transmitted signal where the reflected components are characterised by a time delay. It is assumed that the transmitting and receiving nodes are synchronised through a communications channel so that the reflected signals can be distinguished from the direct arrivals. The sensing nodes also receive interfering signals from the neighbouring clusters Figure 4.2. The control centre is assumed to have the knowledge of the transmitting waveforms from the neighbouring clusters. If $\mathbf{y}_i(t)$ is the received signal at the i^{th} sensing node, it can be written as

$$\mathbf{y}_i(t) = \mathbf{s}(t) * \mathbf{a}_i(t) + \mathbf{h}(t) * \mathbf{b}_i(t) + \mathbf{w}_i(t), \qquad 0 \leq t \leq T_y \tag{4.2}$$

where $*$ denotes convolution operator. T_y is the total time period over which the received signal samples are collected, $\mathbf{s}(t)$ is the reference transmit waveform, $\mathbf{a}(t)$ is the impulse response of the target return. $\mathbf{h}(t)$ is the is the interfering signal, $\mathbf{b}(t)$ is the impulse response corresponding to the interfering signal and $\mathbf{w}(t)$ is the thermal noise.

Let the impulse response of the target return be negligible for a time duration of T_a. Hence, the received signals have to be observed for an extended duration of time which is given by $T_y = T + T_a$. The discrete $N_y \times 1$ received signal data at the i^{th} sensing node is represented as

$$\begin{aligned} \mathbf{y}_i[n] &= \mathbf{S}\mathbf{a}_i[n] + \mathbf{H}\mathbf{b}_i[n] + \mathbf{w}_i[n] \\ \mathbf{a}_i &= [a_1, a_2, \ldots, a_{N_a}]^T \ , \ i = 1,2 \ldots N_s \\ \mathbf{b}_i &= [b_1, b_2, \ldots, b_{N_a}]^T \ , \ i = 1,2 \ldots N_s \end{aligned} \tag{4.3}$$

where $\mathbf{y}_i$ is the $N_y \times 1$ received signal data at the i^{th} receiving node where $N_y = N_t + N_a$ - 1. $\mathbf{a}_i$ is the $N_a \times 1$ unknown impulse response associated with the target return at the i^{th} receiving node; $\mathbf{b}_i$ is the $N_a \times 1$ unknown impulse response of the interfering signal at the i^{th} receiving node; Noise is assumed to be AWGN with unknown variance. $\mathbf{S}$ is the $N_y \times N_a$ convolution matrix of $\mathbf{s}(t)$, $\mathbf{H}$ is the $N_y \times N_a$ convolution matrix of $\mathbf{h}(t)$ and can be written as in [154, 155],

$$\mathbf{S} = \begin{bmatrix} s(1) & 0 & \ldots & \ldots & 0 \\ s(2) & s(1) & \ddots & \ldots & 0 \\ \vdots & \vdots & \ddots & \ddots & 0 \\ s(N_t) & s(N_t-1) & \ldots & s(1) & 0 \\ 0 & s(N_t) & s(N_t-1) & \ldots & s(1) \\ \vdots & 0 & s(N_t) & \ldots & s(2) \\ \vdots & \vdots & 0 & \ddots & \vdots \\ 0 & 0 & \ldots & 0 & s(N_t) \end{bmatrix} \tag{4.4}$$

The convolution matrices $\mathbf{S}$ and $\mathbf{H}$ allow continuous representation of the time convolution operator $(*)$ in Equation 4.2 into discrete form. In Equation 4.3 while the impulse responses $\mathbf{a}$, $\mathbf{b}$ and noise variance are unknown but deterministic and the estimation of these unknown parameters is addressed in the later sections.

$$\mathbf{H} = \begin{bmatrix} h(1) & h(0) & h(-1) & \dots & h(2-N_a) \\ h(2) & h(1) & \ddots & \dots & \vdots \\ \vdots & \vdots & \ddots & \ddots & \vdots \\ h(N_t) & h(N_t-1) & \dots & h(1) & \vdots \\ \vdots & h(N_t) & h(N_t-1) & \dots & h(1) \\ \vdots & h(0) & h(N_t) & \dots & h(2) \\ \vdots & \vdots & h(0) & \ddots & \vdots \\ h(N_y) & h(N_y-1) & h(N_y-2) & h(0) & h(N_t) \end{bmatrix} \tag{4.5}$$

In the presence of a target with existence of background interference, the received signal at each receiver element can be expressed as a combination of target return, interference and noise.

4.3 Proposed Target Detection Model

Within a WSN as a surveillance system, a target detector is dedicated to detecting the existence or absence of the targets within the sensing region. To make a decision regarding the existence or nonexistence of a target, the i^{th} sensing node faces a binary hypothesis testing problem where hypothesis H_0 indicates absence of the target and hypothesis H_1 indicates the existence of a target. The measure of performance of a target detector is the degree of reliability of such decision-making process. As shown in Figure 4.2, the received signal at the i^{th} sensing node under hypothesis H_0 and H_1 can be mathematically modelled as

$$H_0 : \begin{cases} \mathbf{y}_i = \mathbf{H}\mathbf{b}_i + \mathbf{w}_i \\ \text{Absence of the Target} \end{cases} \tag{4.6}$$

$$H_1 : \begin{cases} \mathbf{y}_i = \mathbf{S}\mathbf{a}_i + \mathbf{H}\mathbf{b}_i + \mathbf{w}_i \\ \text{Existence of the Target} \end{cases} \tag{4.7}$$

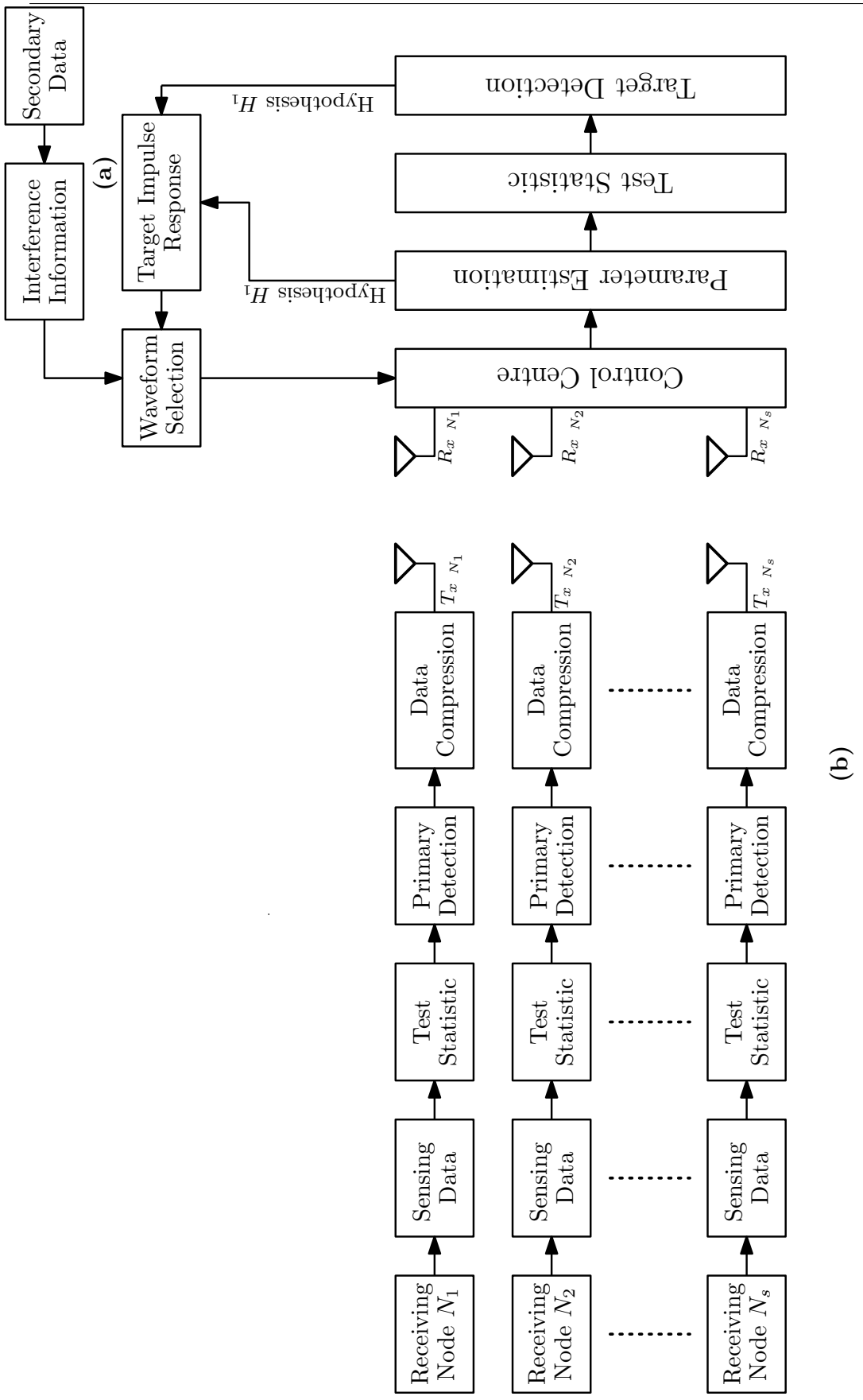

FIGURE 4.3: Proposed RF sensing based target detection architecture for surveillance applications. (a) Initialisation phase. (b) Operational Phase

Based on the operational nature of the WSN, the target detection procedure can be classified as: (i) Decentralised detection (ii) Centralised detection. In decentralised detection, the target detection procedure is performed at the sensing nodes where the individual sensing nodes within the cluster make an independent decision regarding the existence or absence of the target and the sensing nodes transmit the hypothesis testing decision to the control centre. In centralised detection, the sensing nodes transmit the received data to the control centre and the control centre makes a decision regarding the existence of the target based on the aggregated data from all the sensing nodes within the cluster.

In the case decentralised detection, with the reduced computational capabilities of the sensing nodes, the choice of the target detector is limited based on the complexity of the target detection procedure. As a consequence, while being computationally less complex, the target detection reliability of the decentralised detection is usually poor. In the case of centralised detection, due to availability of sufficient computational resources, efficient target detection procedures can be implemented to achieve desired target detection reliabilities. However, within centralised detection, excessive data transfer is required to be performed periodically between the sensing nodes and the control centre, which has a significant impact on the lifetime of the sensing nodes with limited available power. The transmission costs at the sensing nodes can be reduced by avoiding the undesirable data transfers between the sensing nodes and the control centre which ensures longevity of the sensing nodes. The proposed target detection architecture for resource constrained WSN adopts a balanced compromise between both centralised and decentralised detection procedures. A hybrid detection procedure has been proposed where the sensing nodes make a preliminary decision regarding the existence of the targets, which is referred to as primary detection and the control centre makes a final decision based on the received data from all the sensing nodes, which is referred to as secondary detection. The proposed target detection architecture is shown in Figure 4.3. Due to operational nature of WSN, it is expected that the sensing conditions remain stationary over a given period of time. Therefore, the sensing

procedure is performed in two stages namely; Initialisation phase and Operational phase. During initialisation phase, the sensing nodes gather preliminary data regarding the sensing environment, which is used during the operational phase where the target detection procedure is performed.

4.4 Proposed Target Detectors for Primary Detection

The objective of performing primary detection is to reduce the amount of data transfer between the sensing nodes and the control centre. As shown in Equation 4.6 and Equation 4.7, in the absence of a target, the received signal data at the sensing nodes consists of noise and interfering components which are of no interest to the control centre. Ideally, it is desirable for the sensing nodes to transmit the received signal data only in the presence of a target. The objective of the primary detector is to make a preliminary decision regarding the existence or absence of the target by analysing the received signal data. Due to limited processing capabilities of the sensing nodes, the primary detector is required to be energy efficient and computationally less complex. Hence, to meet the computational constraints, simple, low-complexity target detectors are considered for primary detection while tolerating reduced reliability.

4.4.1 Energy Detector

Energy detection is one of the commonly used sensing technique for surveillance applications of WSN. The test statistic for an energy detector is obtained by measuring the energy of the received signal data. The test statistic is compared to a pre-defined threshold γ based on which a decision is made regarding the existence or absence of a target. As discussed in Chapter 3.2.4, for received signal at the i^{th} sensing node, the test statistic for the energy detector is be written as

$$\zeta_i = \sum_{n=1}^{N_y} \mathbf{y_i} \mathbf{y_i}^H \tag{4.8}$$

When received signal, interference and noise powers are defined by σ_s^2, σ_i^2 and σ_w^2 respectively, for sufficiently large number of observations, the distribution of the test statistic under hypothesis H_0 and H_1 can be expressed as

$$H_0 : \quad \zeta_i \sim \mathcal{N}(N_y(\sigma_i^2 + \sigma_w^2), 2N_y(\sigma_i^2 + \sigma_w^2)^2) \tag{4.9}$$

$$H_1 : \quad \zeta_i \sim \mathcal{N}\big(N_y(\sigma_s^2 + \sigma_i^2 + \sigma_w^2), 2N_y(\sigma_s^2 + \sigma_i^2 + \sigma_w^2)^2\big) \tag{4.10}$$

The probability of false alarm P_{fa} and probability of detection P_d for the energy can be estimated as

$$P_{fa} = Q\left(\frac{\gamma - N_y(\sigma_i^2 + \sigma_w^2)}{\sqrt{2N_y}(\sigma_i^2 + \sigma_w^2)}\right) \tag{4.11}$$

$$P_d = Q\left(\frac{\gamma - N_y(\sigma_s^2 + \sigma_i^2 + \sigma_w^2)}{\sqrt{2N_y}(\sigma_s^2 + \sigma_i^2 + \sigma_w^2)}\right) \tag{4.12}$$

From Equation 4.11, it can be observed that the threshold for the energy detector is chosen based on the expected noise and interfering signal powers. Therefore, the energy detector is highly susceptible to any changes in the noise and interfering signal powers and lead to significantly high false alarm rates. In Figure 4.4, the target detection performance of energy detector is shown. The received signal power is assumed to be constant during simulations while the noise and interference powers are varying. It is evident from Figure 4.4 that the energy detector while being computationally less complex, is highly unreliable due to high false alarm rates.

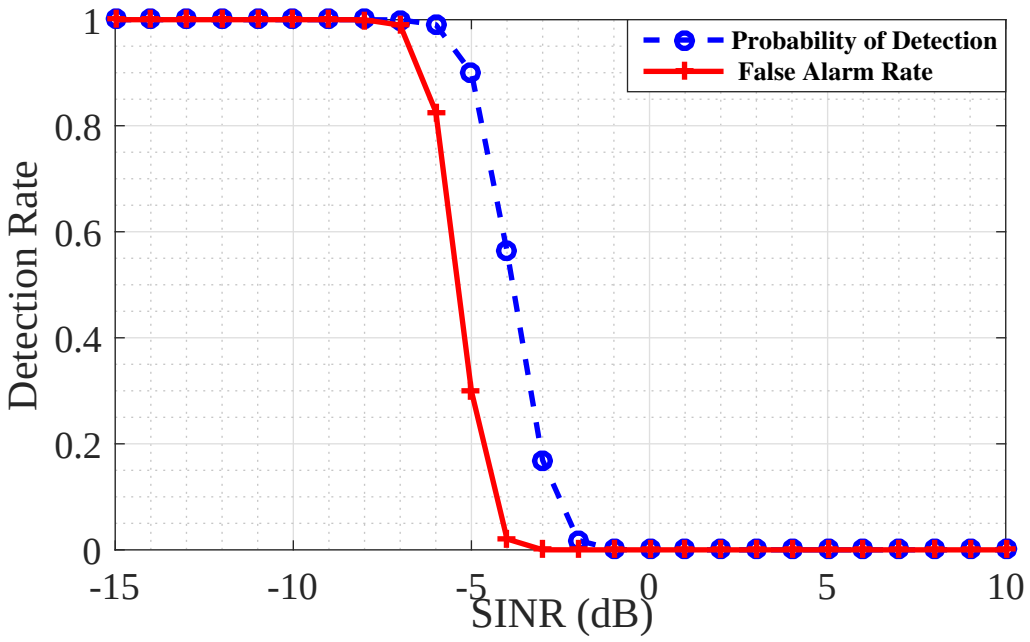

FIGURE 4.4: Target detection performance of Energy Detector

4.4.2 Matched Subspace Detector

In this section, a computationally efficient target detector has been proposed which is expected to provide improved target detection reliability than an energy detector. It is assumed that the sensing nodes does not have the knowledge of the interfering waveforms. Therefore, for this case, received signal models under hypothesis H_0 and H_1 are written as

$$\begin{aligned} H_0 &: \mathbf{y}_i = \mathbf{d}_i \\ H_1 &: \mathbf{y}_i = \mathbf{S}\mathbf{a}_i + \mathbf{d}_i \end{aligned} \tag{4.13}$$

where $\mathbf{d}_i$ is the disturbance vector given by $\mathbf{d}_i = \mathbf{H}\mathbf{b}_i + \mathbf{w}_i$. The disturbance covariance matrix which is estimated during initialisation phase is given by $\sigma^2\mathbf{R}_d$. Here σ^2 represents the variations in the disturbance signal power under initialisation and operational phases. When $\mathbf{R}_d$ is known, the received signal data can be whitened by projecting it onto $\mathbf{R}_d^{-1/2}$ where the distribution of the whitened disturbance signal is, $\mathbf{d} \sim \mathcal{N}\left(0, \sigma^2\mathbf{I}\right)$

The probability density functions of the whitened received signal data under hypothesis H_0 and H_1 are,

$$f(\mathbf{y}_i|\sigma^2, H_0) = \left(\frac{1}{\pi\sigma^2}\right)^{N_y/2} exp\left(\frac{-1}{2\sigma^2}\mathbf{y}_i^H\mathbf{y}_i\right) \tag{4.14}$$

$$f(\mathbf{y}_i|\mathbf{a}, \sigma^2, H_1) = \left(\frac{1}{\pi\sigma^2}\right)^{N_y/2} exp\left(\frac{-1}{2\sigma^2}(\mathbf{y}_i - \mathbf{S}\mathbf{a}_i)^H(\mathbf{y}_i - \mathbf{S}\mathbf{a}_i)\right) \tag{4.15}$$

The test statistic can be obtained based on the conventional likelihood ratio test where the unknown parameters are replaced by their maximum likelihood estimates. The test statistic for the proposed matched subspace detector at the i^{th} sensing node can be expressed as

$$\mathbb{T} = \frac{\mathbf{y}_i^H\mathbf{y}_i}{(\mathbf{y}_i - \mathbf{S}\hat{\mathbf{a}}_i)^H(\mathbf{y}_i - \mathbf{S}\hat{\mathbf{a}}_i)} \tag{4.16}$$

here $\hat{\mathbf{a}}_i$ is the maximum likelihood estimate of the target impulse response at the i^{th} sensing node which is given by $(\mathbf{S}^H\mathbf{S})^{-1}\mathbf{S}^H\mathbf{y}_i$. Substituting $\hat{\mathbf{a}}_i$ in Equation 4.16 and subsequent mathematical manipulations gives the final detection rule which is written as

$$\mathbb{T} = \frac{\mathbf{y}_i^H(\mathbf{I} - \mathbf{S}(\mathbf{S}^H\mathbf{S})^{-1}\mathbf{S}^H)\mathbf{y}_i}{\mathbf{y}_i^H\mathbf{S}(\mathbf{S}^H\mathbf{S})^{-1}\mathbf{S}^H\mathbf{y}_i} \underset{H_1}{\overset{H_0}{\gtrless}} \gamma \tag{4.17}$$

here $\mathbf{S}(\mathbf{S}^H\mathbf{S})^{-1}\mathbf{S}^H$ is the signal subspace and γ is the detection threshold. The threshold γ is chosen to ensure that the maximum false alarm rate does not exceed the pre-defined acceptable rate. At any given instant, the value of threshold is chosen based on the sensing conditions such as noise and clutter and operating conditions such as number of received signal samples and compression. Therefore, the test statistic for the matched subspace detector can be obtained by projecting the received signal data on to the expected target signal subspace and the corresponding null subspace.

4.5 Secondary Detector Design

The target detector at the control centre performs secondary detection. The sensing nodes within the cluster, which detect the presence of a target after primary detection, transmit the received signal data to the control centre. The control centre is expected to possess increased power and processing capabilities than the individual sensing nodes within the cluster and the secondary target detector is designed to exploit the processing resources, which are available at the control centre to provide desired target detection reliability within the operating conditions of the WSN. As shown in Figure 4.3 during initialisation phase, the control centre gathers the information regarding the interfering waveforms from the neighbouring clusters. Due to homogeneous nature of the sensing environment, the total interference at the sensing nodes is measurable with variations in the received power over a given period of time. In this section, a mathematical model for the proposed secondary detector is derived to optimise the target detection reliability of the WSN in the presence of interfering waveforms. The amount of received signal data that is required to be transmitted by the sensing nodes regulates to lifetime of the wireless sensor network. Moreover, the processing complexity of the target detector increases with the increase in the number of received signal samples. Depending on the sensing environment; noise and interfering signal strengths at any given instant, the sensing nodes may transmit raw data or compressed received signal data. A mathematical model for a new target detector has been proposed which has the ability to process the compressed received signal samples from the sensing nodes to detect the presence of the targets.

4.5.1 Proposed Target Detector in the Presence of Interference

In this section, the known knowledge of the interfering waveforms has been exploited to derive a mathematical model for the proposed secondary detector at the control centre. From the received signal models described in Equation 4.6 and

Equation 4.7, the joint probability density functions for the unknown parameters under hypothesis H_0 and H_1 can be written as

$$f(\mathbf{y}|\mathbf{b},\sigma^2,H_0) = \left(\frac{1}{\pi\sigma^2}\right)^{N_yN_s/2} exp\left(\frac{-1}{2\sigma^2}(\mathbf{y}-\mathbf{Hb})^H(\mathbf{y}-\mathbf{Hb})\right) \tag{4.18}$$

$$f(\mathbf{y}|\mathbf{a},\mathbf{b},\sigma^2,H_1) = \left(\frac{1}{\pi\sigma^2}\right)^{N_yN_s/2} exp\left(\frac{-1}{2\sigma^2}(\mathbf{y}-\mathbf{Sa}-\mathbf{Hb})^H(\mathbf{y}-\mathbf{Sa}-\mathbf{Hb})\right) \tag{4.19}$$

In Equation 4.2, while the knowledge of the transmitted and interfering waveforms is available, the target detector does not have the knowledge of the noise power and the impulse responses of interference and target returns which vary over time and with location of the target. The test statistic for the proposed target detector is generated based on the likelihood ratio test and the unknown parameters are replaced by their ML estimates. The ML estimates of these unknown parameters under hypothesis H_0 and H_1 are obtained from their corresponding log-likelihood functions denoted by Γ which are obtained from Equation 4.18 and Equation 4.19 as

$$\Gamma(\mathbf{y}|\mathbf{b},\sigma^2,H_0) = -\frac{N_yN_s}{2}log(\pi\sigma^2) - \frac{1}{2\sigma^2}(\mathbf{y}-\mathbf{Hb})^H(\mathbf{y}-\mathbf{Hb}) \tag{4.20}$$

$$\Gamma(\mathbf{y}|\mathbf{a},\mathbf{b},\sigma^2,H_1) = -\frac{N_yN_s}{2}log(\pi\sigma^2) - \frac{1}{2\sigma^2}(\mathbf{y}-\mathbf{Sa}-\mathbf{Hb})^H(\mathbf{y}-\mathbf{Sa}-\mathbf{Hb}) \tag{4.21}$$

Log-likelihood functions are used here to simplify ML estimation procedure and have no impact on the outcome of the ML estimator.

4.5.1.1 Estimation of Noise Variance

The estimates of the noise variance under hypothesis H_0 and H_1 are denoted by $\hat{\sigma}_0^2$ and $\hat{\sigma}_1^2$ which are obtained by differentiating the corresponding log-likelihood

functions in Equation 4.20 and Equation 4.21 with respect to σ^2 while treating the other parameters as constants as shown in Equation 4.22 and Equation 4.23.

$$\frac{\partial}{\partial \sigma^2}\Big(\Gamma(\mathbf{y}:\mathbf{b},\sigma^2,H_0)\Big)=0 \tag{4.22}$$

$$\frac{\partial}{\partial \sigma^2}\Big(\Gamma(\mathbf{y}:\mathbf{a},\mathbf{b},\sigma^2,H_1)\Big)=0 \tag{4.23}$$

Solving Equation 4.22 and Equation 4.23 gives the ML estimates of σ^2 under hypothesis H_0 and H_1 which are summarised as

$$\hat{\sigma}_0^2=\frac{1}{N_yN_s}(\mathbf{y}-\mathbf{Hb})^H(\mathbf{y}-\mathbf{Hb}) \tag{4.24}$$

$$\hat{\sigma}_1^2=\frac{1}{N_yN_s}(\mathbf{y}-\mathbf{Sa}-\mathbf{Hb})^H(\mathbf{y}-\mathbf{Sa}-\mathbf{Hb}) \tag{4.25}$$

4.5.1.2 Estimation of Interference Impulse Response

From Equation 4.6 and Equation 4.7, it can be observed that the presence of interfering signal exists under hypothesis H_0 and H_1 and therefore the unknown impulse response of the interfering signal is required to be estimated under both the hypothesis. The estimates of the unknown impulse responses of the interfering signal under hypothesis H_0 and H_1 are denoted by $\hat{\mathbf{b}}_0$ and $\hat{\mathbf{b}}_1$ respectively. The corresponding ML estimates are obtained by differentiating the relevant log-likelihood functions under hypothesis H_0 and H_1 in Equation 4.20 and Equation 4.21 with respect to $\mathbf{b}$ which are given by,

$$\frac{\partial}{\partial \mathbf{b}}(\Gamma(\mathbf{y}:\mathbf{b},H_0)=0 \tag{4.26}$$

$$\frac{\partial}{\partial \mathbf{b}}(\Gamma(\mathbf{y}:\mathbf{a},\mathbf{b},H_1))=0 \tag{4.27}$$

To obtain the ML estimate of $\mathbf{b}$ under hypothesis H_1, Equation 4.27 can be solved as

$$\begin{aligned} 0 &= \frac{\partial}{\partial \mathbf{b}}(\mathbf{y}^H\mathbf{y} - \mathbf{y}^H(\mathbf{Sa}) - \mathbf{y}^H(\mathbf{Hb}) - (\mathbf{Sa})^H\mathbf{y} + (\mathbf{Sa})^H(\mathbf{Sa}) + (\mathbf{Sa})^H(\mathbf{Hb}) \\ &\qquad - (\mathbf{Hb})^H\mathbf{y} + (\mathbf{Hb})^H(\mathbf{Sa}) + (\mathbf{Hb})^H(\mathbf{Hb})) \\ &= -\mathbf{y}^H\mathbf{H} + (\mathbf{Sa})^H\mathbf{H} + \hat{\mathbf{b}}_1^H(\mathbf{H}^H\mathbf{H}) \end{aligned}$$

Therefore, the estimate of the unknown impulse response of the interfering signal under hypothesis H_1 can be obtained as

$$\hat{\mathbf{b}}_1^H = (\mathbf{H}^H\mathbf{H})^{-1}\mathbf{H}^H(\mathbf{y} - \mathbf{Sa}) \tag{4.28}$$

Hypothesis H_0 represents the scenario where the target return is absent; i.e., $\mathbf{a} = 0$. Therefore, the estimate of the unknown impulse response of the interfering signal under hypothesis H_0 can be obtained by substituting $\mathbf{a} = 0$ in Equation 4.28 which gives,

$$\hat{\mathbf{b}}_0^H = (\mathbf{H}^H\mathbf{H})^{-1}\mathbf{H}^H\mathbf{y} \tag{4.29}$$

4.5.1.3 Estimation of Target Return

Hypothesis H_1 assumes the existence of a target return within the received signal component, while hypothesis H_0 assumes the absence of the target return. While the transmitted RF waveform is known to the target detector, the impulse response, $\mathbf{a}$ associated with the target return is unknown. The impulse response of the target return can be estimated from the log-likelihood function of the received signal under hypothesis as shown in Equation 4.21. Substituting the ML estimates σ_1^2 and $\hat{\mathbf{b}}_1$ which are obtained in Equation 4.25 and Equation 4.28 respectively in Equation 4.21 gives the log-likelihood function under hypothesis H_1 which is written as

$$\begin{aligned}\Gamma(\mathbf{y}|\mathbf{a}, H_1) &= -N_y N_s log\bigg(\frac{\pi}{N_y N_s}(\mathbf{y}-\mathbf{Sa}-\mathbf{H}(\mathbf{H}^H\mathbf{H})^{-1}\mathbf{H}^H(\mathbf{y}-\mathbf{Sa}))^H(\mathbf{y}-\mathbf{Sa}- \\ &\qquad \mathbf{H}(\mathbf{H}^H\mathbf{H})^{-1}\mathbf{H}^H(\mathbf{y}-\mathbf{Sa}))\bigg) - N_y N_s \\ &= -N_y N_s log\bigg(\frac{\pi}{N_y N_s}(\mathbf{y}-\mathbf{Sa})^H(\mathbf{I}-\mathbf{H}(\mathbf{H}^H\mathbf{H})^{-1}\mathbf{H}^H)^H(\mathbf{I}- \\ &\qquad \mathbf{H}(\mathbf{H}^H\mathbf{H})^{-1}\mathbf{H}^H)(\mathbf{y}-\mathbf{Sa})\bigg) - N_y N_s\end{aligned}$$

here the interfering signal subspace which is denoted by $\mathbf{S}_h$ can be written as

$$\mathbf{S}_h = \mathbf{H}(\mathbf{H}^H\mathbf{H})^{-1}\mathbf{H}^H \tag{4.30}$$

Therefore, the log-likelihood function under hypothesis H_1 is,

$$\Gamma(\mathbf{y}|\mathbf{a}, H_1) = -N_y N_s log\bigg(\frac{\pi}{N_y N_s}(\mathbf{y}-\mathbf{Sa})^H(\mathbf{I}-\mathbf{S}_h)^H(\mathbf{I}-\mathbf{S}_h)(\mathbf{y}-\mathbf{Sa})\bigg) - N_y N_s \tag{4.31}$$

Finally, impulse response which is associated with the target return which is denoted by $\hat{\mathbf{a}}$ can be estimated as

$$\frac{\partial}{\partial \mathbf{a}}(\Gamma(\mathbf{y}:\mathbf{a}, H_1)) = 0 \tag{4.32}$$

Solving Equation 4.32 gives,

$$\begin{aligned}0 &= \frac{\partial}{\partial \mathbf{a}}\bigg((\mathbf{y}-\mathbf{Sa})^H(\mathbf{I}-\mathbf{S}_h)^H(\mathbf{I}-\mathbf{S}_h)(\mathbf{y}-\mathbf{Sa})\bigg) \\ &= -\mathbf{y}^H(\mathbf{I}-\mathbf{S}_h)^H(\mathbf{I}-\mathbf{S}_h)\mathbf{S} + \mathbf{a}^H\mathbf{S}^H(\mathbf{I}-\mathbf{S}_h)^H(\mathbf{I}-\mathbf{S}_h)\mathbf{S}\end{aligned} \tag{4.33}$$

Solving Equation 4.33, the unknown impulse response of the target return can be expressed as

$$\hat{\mathbf{a}} = (\mathbf{S}^H(\mathbf{I} - \mathbf{S}_h)^H(\mathbf{I} - \mathbf{S}_h)\mathbf{S})^{-1}\mathbf{S}^H(\mathbf{I} - \mathbf{S}_h)^H(\mathbf{I} - \mathbf{S}_h)\mathbf{y} \tag{4.34}$$

4.5.1.4 Test Statistic

The test statistic for the proposed target detector is obtained from the probability density functions of the received signal models which are given in Equation 4.18 and Equation 4.19. To make a decision regarding the existence or absence of the target; i.e., to choose between hypothesis H_1 and H_0 respectively, the test statistic, $\mathbb{T}$ is generated based on the likelihood ratio test which is written as

$$\mathbb{T} = \frac{\max\limits_{\sigma^2, \mathbf{b}} f(\mathbf{y}|\sigma^2, \mathbf{b}, H_0)}{\max\limits_{\sigma^2, \mathbf{a}, \mathbf{b}} f(\mathbf{y}|\sigma^2, \mathbf{a}, \mathbf{b}, H_1)} \underset{H_1}{\overset{H_0}{\gtrless}} \gamma \Big|_{P_{fa}} \tag{4.35}$$

here γ is the decision threshold which is chosen to ensure that the maximum false rate P_{fa} does not exceed the permissible limit. The obtained test statistic is compared to the threshold, γ and hypothesis H_1 is chosen if the test statistic exceeds γ and hypothesis H_0 is chosen otherwise. Therefore, substituting the estimates of the unknown parameters in Equation 4.35 gives,

$$\mathbb{T} = \frac{\mathbf{y}^H\mathbf{P}\mathbf{y} - \mathbf{y}^H\mathbf{P}\mathbf{S}(\mathbf{S}^H\mathbf{P}\mathbf{S})^{-1}\mathbf{S}^H\mathbf{P}\mathbf{y}}{\mathbf{y}^H(\mathbf{I} - \mathbf{S}_H)\mathbf{y}} \underset{H_1}{\overset{H_0}{\gtrless}} \gamma \Big|_{P_{fa}} \tag{4.36}$$

where $\mathbf{P} = (\mathbf{I} - \mathbf{S}_h)^H(\mathbf{I} - \mathbf{S}_h)$. It needs to be noted that the test statistic is obtained after substituting all the ML estimates in their corresponding probability density functions and subsequent mathematical manipulations. The proposed target detector named as Adaptive Interference Estimator (AIE) dynamically adapts to the changes within the known knowledge of the interfering waveforms and generates the test statistic based on which a final decision is made regarding the existence or absence of the targets within the sensing region.

4.5.2 Proposed Compressive Target Detector in the Presence of Interference

In Section 4.5.1, a test statist for AIE detector has been derived to detect the presence of targets in the presence of interfering waveforms. The amount of received signal data, which is required to be transmitted by the sensing nodes to the control centre, has a significant impact on the operating lifetime of the wireless sensor network. Moreover, increase in the amount of received signal data at the control centre from individual sensing nodes within the cluster, increases the complexity in implementing the target detection procedure. With limited energy and computational capacity, such increase in processing complexity may lead towards resource saturation. Hence, to ensure longevity of the wireless sensor network as a surveillance system, it is desirable to reduce the amount of data transfer between the sensing nodes and the control centre. Therefore, under favourable sensing conditions, the sensing nodes may compress the received signal data before transmitting it to the control centre using a pre-defined measurement matrix. When the knowledge of the measurement matrix used by the individual sensing nodes is available, the ability of the target detector at the control centre to reliably utilise the compressed received signal data to detect the presence of targets, reduces the processing complexity. In this section, a new target detector namely Compressive Adaptive Interference Estimator (CAIE) has been derived, which has the ability to process the compressed received signal samples to detect the presence of targets within the sensing region.

4.5.2.1 Compressive Received Signal Model

During compressive detection, the sensing modes compresses the received signal data by projecting it onto a pre-defined measurement matrix before transmitting it to the control centre. For the received signal $\mathbf{y}_i$ and a measurement matrix $\boldsymbol{\phi}_i$ at the i^{th} sensing node, the compressed data is written as $\bar{\mathbf{y}}_i = \boldsymbol{\phi}_i\ \mathbf{y}$, where $\bar{\mathbf{y}}_i$ is the compressed data at the i^{th} sensing node. The dimensions $M \times N_y$ of

$\boldsymbol{\phi}_i$ are chosen such that $M \ll N_y$. $\boldsymbol{\phi}_i$ is usually orthogonal i.e., $\boldsymbol{\phi}_i \boldsymbol{\phi}_i^H = \mathbf{I}$. A compression ratio $\mu = \frac{M}{N_y}$ is defined which is a measure of compressibility. The choice of compression ratio μ is chosen as a trade-off between the transmission costs and target detection reliability. The compressed received signal data at the control centre can be written as

$$\begin{aligned} \bar{\mathbf{y}} &= [\boldsymbol{\phi}_1 \mathbf{y}_1, \boldsymbol{\phi}_2 \mathbf{y}_2, \ldots, \boldsymbol{\phi}_{Ns} \mathbf{y}_{Ns}]^T \\ &= [\bar{\mathbf{y}}_1, \bar{\mathbf{y}}_2, \ldots, \bar{\mathbf{y}}_{Ns}]^T \end{aligned}$$

When the projection matrices used by the individual sensing nodes are known to the control centre, the projection matrix at the control centre can be reconstructed as

$$\boldsymbol{\phi} = \begin{bmatrix} \boldsymbol{\phi}_1 & 0 & \ldots & 0 \\ 0 & \boldsymbol{\phi}_2 & \ddots & 0 \\ \vdots & 0 & \ddots & \vdots \\ 0 & \ldots & 0 & \boldsymbol{\phi}_{Ns} \end{bmatrix} \tag{4.37}$$

Therefore, the compressed received signal models at the control centre under hypothesis H_0 and H_1 can be written as

$$H_0 : \left\{ \; \bar{\mathbf{y}} = \boldsymbol{\phi}\mathbf{H}\mathbf{b} + \boldsymbol{\phi}\mathbf{w} \right. \tag{4.38}$$

$$H_1 : \left\{ \; \bar{\mathbf{y}} = \boldsymbol{\phi}\mathbf{S}\mathbf{a} + \boldsymbol{\phi}\mathbf{H}\mathbf{b} + \boldsymbol{\phi}\mathbf{w} \right. \tag{4.39}$$

From the received signal models and the corresponding unknown parameters described in Equation 4.38 and Equation 4.39, the joint probability density functions

for the unknown parameters under hypothesis H_0 and H_1 are,

$$f(\bar{\mathbf{y}} : \mathbf{b}, \sigma^2, H_0) = \left(\frac{1}{\pi\sigma^2}\right)^{N_y N_s/2} exp\left(\frac{-1}{2\sigma^2}(\bar{\mathbf{y}} - \boldsymbol{\phi}\mathbf{Hb})^H(\boldsymbol{\phi}\boldsymbol{\phi}^H)^{-1}(\bar{\mathbf{y}} - \boldsymbol{\phi}\mathbf{Hb})\right) \quad (4.40)$$

$$f(\bar{\mathbf{y}} : \mathbf{a}, \mathbf{b}, \sigma^2, H_1) = \left(\frac{1}{\pi\sigma^2}\right)^{N_y N_s/2} exp\left(\frac{-1}{2\sigma^2}(\bar{\mathbf{y}} - \boldsymbol{\phi}\mathbf{Sa} - \boldsymbol{\phi}\mathbf{Hb})^H(\boldsymbol{\phi}\boldsymbol{\phi}^H)^{-1}(\bar{\mathbf{y}} - \boldsymbol{\phi}\mathbf{Sa} - \boldsymbol{\phi}\mathbf{Hb})\right) \quad (4.41)$$

As discussed in Section 4.5.1, the test statistic for CAIE is generated based on the likelihood ratio test which is obtained from the probability density functions of the received signal under hypothesis H_0 and H_1 which are given in Equation 4.40 and Equation 4.41. The estimates of the unknown parameters within the probability density functions are obtained from the corresponding log-likelihood functions of the probability density functions under hypothesis H_0 and H_1. The corresponding log-likelihood functions under hypothesis H_0 and H_1 respectively are,

$$\Gamma(\bar{\mathbf{y}} : \mathbf{b}, \sigma^2, H_0) = -\frac{N_y N_s}{2} log(\pi\sigma^2) - \frac{1}{2\sigma^2}\left((\bar{\mathbf{y}} - \boldsymbol{\phi}\mathbf{Hb})^H(\boldsymbol{\phi}\boldsymbol{\phi}^H)^{-1}(\bar{\mathbf{y}} - \boldsymbol{\phi}\mathbf{Hb})\right) \quad (4.42)$$

$$\Gamma(\bar{\mathbf{y}} : \mathbf{a}, \mathbf{b}, \sigma^2, H_1) = -\frac{N_y N_s}{2} log(\pi\sigma^2) - \frac{1}{2\sigma^2}\left((\bar{\mathbf{y}} - \boldsymbol{\phi}\mathbf{Sa} - \boldsymbol{\phi}\mathbf{Hb})^H(\boldsymbol{\phi}\boldsymbol{\phi}^H)^{-1}(\bar{\mathbf{y}} - \boldsymbol{\phi}\mathbf{Sa} - \boldsymbol{\phi}\mathbf{Hb})\right) \quad (4.43)$$

4.5.2.2 Estimation of Noise Variance

The estimates of the noise variance, σ^2 under hypothesis H_0 and H_1 which denoted by $\hat{\sigma}_0^2$ and $\hat{\sigma}_1^2$ respectively are obtained by performing partial differentiation with respect to σ^2 on the corresponding log-likelihood functions in Equation 4.42 and Equation 4.43 which can be shown as

$$\frac{\partial}{\partial \sigma^2}\Big(\Gamma(\bar{\mathbf{y}} : \mathbf{b}, \sigma^2, H_0)\Big) = 0 \tag{4.44}$$

$$\frac{\partial}{\partial \sigma^2}\Big(\Gamma(\bar{\mathbf{y}} : \mathbf{a}, \mathbf{b}, \sigma^2, H_1)\Big) = 0 \tag{4.45}$$

Solving Equation 4.44 and Equation 4.45 gives the ML estimates of σ^2 under hypothesis H_0 and H_1 which are summarised as

$$\hat{\sigma}_0^2 = \frac{1}{N_y N_s}\Big((\bar{\mathbf{y}} - \boldsymbol{\phi}\mathbf{H}\mathbf{b})^H(\boldsymbol{\phi}\boldsymbol{\phi}^H)^{-1}(\bar{\mathbf{y}} - \boldsymbol{\phi}\mathbf{H}\mathbf{b})\Big) \tag{4.46}$$

$$\hat{\sigma}_1^2 = \frac{1}{N_y N_s}\Big((\bar{\mathbf{y}} - \boldsymbol{\phi}\mathbf{S}\mathbf{a} - \boldsymbol{\phi}\mathbf{H}\mathbf{b})^H(\boldsymbol{\phi}\boldsymbol{\phi}^H)^{-1}(\bar{\mathbf{y}} - \boldsymbol{\phi}\mathbf{S}\mathbf{a} - \boldsymbol{\phi}\mathbf{H}\mathbf{b})\Big) \tag{4.47}$$

4.5.2.3 Estimation of Interference Impulse Response

The unknown impulse responses of the interfering signal under hypothesis H_0 and H_1 are estimated from the corresponding log-likelihood functions of the compressed received signal models. The estimates of the unknown impulse responses of the interfering waveform under hypothesis H_0 and H_1 which denoted by $\hat{\mathbf{b}}_0$ and $\hat{\mathbf{b}}_1$ respectively, are obtained by differentiating Equation 4.42 and Equation 4.43 with respect to $\mathbf{b}$ and equating the result to zero.

$$\frac{\partial}{\partial \mathbf{b}}(\Gamma(\bar{\mathbf{y}} : \mathbf{b}, H_0)) = 0 \tag{4.48}$$

$$\frac{\partial}{\partial \mathbf{b}}(\Gamma(\bar{\mathbf{y}} : \mathbf{a}, \mathbf{b}, H_1)) = 0 \tag{4.49}$$

Solving Equation 4.48 and Equation 4.49 as discussed in Section 4.5.1.2 gives the ML estimate of the interference impulse responses $\hat{\mathbf{b}}_0$ and $\hat{\mathbf{b}}_1$ under hypothesis H_0 and H_1 respectively which can be written as

$$\hat{\mathbf{b}}_0 = ((\boldsymbol{\phi}\mathbf{H})^H(\boldsymbol{\phi}\boldsymbol{\phi}^H)^{-1}(\boldsymbol{\phi}\mathbf{H}))^{-1}(\boldsymbol{\phi}\mathbf{H})^H(\boldsymbol{\phi}\boldsymbol{\phi}^H)^{-1}\bar{\mathbf{y}} \tag{4.50}$$

$$\hat{\mathbf{b}}_1 = ((\boldsymbol{\phi}\mathbf{H})^H(\boldsymbol{\phi}\boldsymbol{\phi}^H)^{-1}(\boldsymbol{\phi}\mathbf{H}))^{-1}(\boldsymbol{\phi}\mathbf{H})^H(\boldsymbol{\phi}\boldsymbol{\phi}^H)^{-1}\big(\bar{\mathbf{y}} - \boldsymbol{\phi}\mathbf{S}\mathbf{a}\big) \tag{4.51}$$

4.5.2.4 ML Estimate of Target Return

Hypothesis H_0 represents the scenario where the target is absent within the sensing region. Therefore, under hypothesis H_0, the impulse response associated with the target return is zero. To measure the target impulse response under hypothesis H_1, the new log-likelihood function of the received signal under hypothesis H_1 is obtained by substituting $|hat\sigma^2$ and $hat\mathbf{b}_1$ in Equation 4.43 which gives,

$$\begin{aligned}
\Gamma(\bar{\mathbf{y}}|\mathbf{a}, H_1) &= -N_yN_s log\Bigg(\frac{\pi}{N_yN_s}\big(\bar{\mathbf{y}} - \bar{\mathbf{S}}\mathbf{a} - \bar{\mathbf{H}}(\bar{\mathbf{H}}^H(\boldsymbol{\phi}\boldsymbol{\phi}^H)^{-1}\bar{\mathbf{H}})^{-1}\bar{\mathbf{H}}^H(\boldsymbol{\phi}\boldsymbol{\phi}^H)^{-1} \\
&\quad (\bar{\mathbf{y}} - \bar{\mathbf{S}}\mathbf{a})\big)^H(\boldsymbol{\phi}\boldsymbol{\phi}^H)^{-1}\big(\bar{\mathbf{y}} - \bar{\mathbf{S}}\mathbf{a} - \bar{\mathbf{H}}(\bar{\mathbf{H}}^H(\boldsymbol{\phi}\boldsymbol{\phi}^H)^{-1}\bar{\mathbf{H}})^{-1}\bar{\mathbf{H}}^H(\boldsymbol{\phi}\boldsymbol{\phi}^H)^{-1} \\
&\quad (\bar{\mathbf{y}} - \bar{\mathbf{S}}\mathbf{a})\big)\Bigg) - N_yN_s \\
&= -N_yN_s log\Bigg(\frac{\pi}{N_yN_s}(\bar{\mathbf{y}} - \bar{\mathbf{S}}\mathbf{a})^H(\mathbf{I} - \bar{\mathbf{H}}(\bar{\mathbf{H}}^H(\boldsymbol{\phi}\boldsymbol{\phi}^H)^{-1}\bar{\mathbf{H}})^{-1}\bar{\mathbf{H}}^H(\boldsymbol{\phi}\boldsymbol{\phi}^H)^{-1})^H \\
&\quad (\boldsymbol{\phi}\boldsymbol{\phi}^H)^{-1}(\mathbf{I} - \bar{\mathbf{H}}(\bar{\mathbf{H}}^H(\boldsymbol{\phi}\boldsymbol{\phi}^H)^{-1}\bar{\mathbf{H}})^{-1}\bar{\mathbf{H}}^H(\boldsymbol{\phi}\boldsymbol{\phi}^H)^{-1})(\bar{\mathbf{y}} - \bar{\mathbf{S}}\mathbf{a})\Bigg) \\
&\quad -N_yN_s
\end{aligned} \tag{4.52}$$

where $\bar{\mathbf{H}} = \boldsymbol{\phi}\mathbf{H}$ and $\bar{\mathbf{S}} = \boldsymbol{\phi}\mathbf{S}$. Here the term $\bar{\mathbf{H}}(\bar{\mathbf{H}}^H(\boldsymbol{\phi}\boldsymbol{\phi}^H)^{-1}\bar{\mathbf{H}})^{-1}\bar{\mathbf{H}}^H(\boldsymbol{\phi}\boldsymbol{\phi}^H)^{-1}$ represents the interference subspace for compressive measurements which is represented by $\bar{\mathbf{S}}_h$. To simplify the computational process, let $\bar{\mathbf{P}}$ be defined as

$$\bar{\mathbf{P}} = (\mathbf{I} - \bar{\mathbf{S}}_h)^H(\boldsymbol{\phi}\boldsymbol{\phi}^H)^{-1}(\mathbf{I} - \bar{\mathbf{S}}_h) \tag{4.53}$$

Therefore, the log-likelihood function under hypothesis H_1 can be written as

$$\Gamma(\bar{\mathbf{y}}|\mathbf{a}, H_1) = -N_yN_s log\Bigg(\frac{\pi}{N_yN_s}(\bar{\mathbf{y}} - \bar{\mathbf{S}}\mathbf{a})^H\bar{\mathbf{P}}(\bar{\mathbf{y}} - \bar{\mathbf{S}}\mathbf{a})\Bigg) - N_yN_s \tag{4.54}$$

Finally, as discussed in Section 4.5.1.3, the unknown impulse response of the target return can be estimated as

$$\frac{\partial}{\partial \mathbf{a}}(\Gamma(\bar{\mathbf{y}} : \mathbf{a}, H_1)) = 0 \tag{4.55}$$

Solving Equation 4.55 gives the ML estimate of the target impulse response which is denoted by $\hat{\mathbf{a}}$.

$$\hat{\mathbf{a}} = (\bar{\mathbf{S}}^H \mathbf{P} \bar{\mathbf{S}})^{-1} \bar{\mathbf{S}}^H \mathbf{P} \bar{\mathbf{y}}$$

4.5.2.5 Test Statistic

The test statistic for the proposed CAIE detector is obtained from the probability density functions of the received signals under hypothesis H_0 and H_1 which are defined in Equation 4.40 and Equation 4.41. The test statistic, $\mathbb{T}$ for the proposed detector is written as

$$\mathbb{T} = \frac{\underset{\sigma^2, \mathbf{b}}{\max} f(\bar{\mathbf{y}}|\sigma^2, \mathbf{b}, H_0)}{\underset{\sigma^2, \mathbf{a}, \mathbf{b}}{\max} f(\bar{\mathbf{y}}|\sigma^2, \mathbf{a}, \mathbf{b}, H_1)} \underset{H_1}{\overset{H_0}{\gtrless}} \gamma \Big|_{P_{fa}} \tag{4.56}$$

Therefore, substituting the estimates of the unknown parameters in Equation 4.56 gives the final test statistic which is,

$$\mathbb{T} = \frac{\bar{\mathbf{y}}^H \big(\mathbf{P}(\mathbf{I} - \bar{\mathbf{S}}_s)\big)\bar{\mathbf{y}}}{\bar{\mathbf{y}}^H \big((\boldsymbol{\phi}\boldsymbol{\phi}^H)^{-1}(\mathbf{I} - \bar{\mathbf{S}}_h)\big)\bar{\mathbf{y}}} \underset{H_1}{\overset{H_0}{\gtrless}} \gamma \Big|_{P_{fa}} \tag{4.57}$$

$\bar{\mathbf{S}}_s$ is the target signal subspace for compressive measurements which is defined by $\bar{\mathbf{S}}(\bar{\mathbf{S}}^H \mathbf{P} \bar{\mathbf{S}})^{-1} \bar{\mathbf{S}}^H \mathbf{P}$

4.6 Performance Analysis

The performance of a WSN as a surveillance system is a measure of reliability with which the target detection procedure can be performed within the bounds of the

resource constraints of WSN. To achieve reliability of target detection procedure is quantised in terms of two parameters which are; P_d and P_{fa}. Probability of detection is defined as the rate at which the existence of the targets within the sensing region can be detected while probability of the false alarm defines the rate at which the target detector falsely detects the presence of targets. A reliable target detector is expected to have low false alarm rate and high target detection rate within a given range of sensing conditions. In this section, the target detection performance of the proposed target detectors, which are discussed in this chapter have been analysed.

4.6.1 Primary Detection

In Section 4.4, energy detector and matched subspace detectors have been proposed for primary detection. In this section, their target detection performances have been analysed. Energy detector relies on detecting the energy of the reflected signals to detect the presence of the targets within the sensing range. It has already been shown in Section 4.4 that energy detector is highly susceptible to any changes in the sensing conditions. In Section 4.4.2, a Matched subspace detector has been proposed which exploits the knowledge of the target signal subspace to provide reliable target detection performance which is robust against changes within the sensing conditions. The test statistic for the proposed MSD is given in Equation 4.17. The performances of the energy detector and the matched subspace detectors within the sensing conditions discussed in this chapter are compared through simulations and thresholds are chosen to ensure that the maximum false alarm rate does not exceed 10^{-4}. For simulations the length of the transmit signal, N_t is assumed to be 32 and 64 samples long and it is assumed that the target impulse response, $N_a = 4$. Therefore, as discussed previously in this chapter, the length of the received signal samples is given by, $N_y = N_t + N_a$ - 1 which gives us 35 and 67 samples respectively. In Figure 4.5, the target detection performances of ED and MSD with 35 received signal samples are plotted. While ED slightly

outperformed the proposed MSD, however, it must be noted that under changing sensing conditions, ED suffers severe deterioration in target detection reliability while the proposed MSD has the ability to identify the existence of the target returns. In Figure 4.6, the corresponding false alarm rates during the simulations are plotted. For fair analysis of the target detection performances, the thresholds for the energy detector are adjusted to ensure that the false alarm rates are restricted within a permissible range. In Figure 4.7, the simulations are repeated with increased number of received signal samples and corresponding false alarm rates are plotted in Figure 4.8. At 67 received signal samples, the proposed MSD outperformed the conventional ED. As discussed in Figure 4.3, under suitable sensing conditions, compressive sensing can be adopted to reduce the power and processing requirements. The target detection performances of the compressive matched subspace detectors are also shown in Figure 4.5 and Figure 4.7.

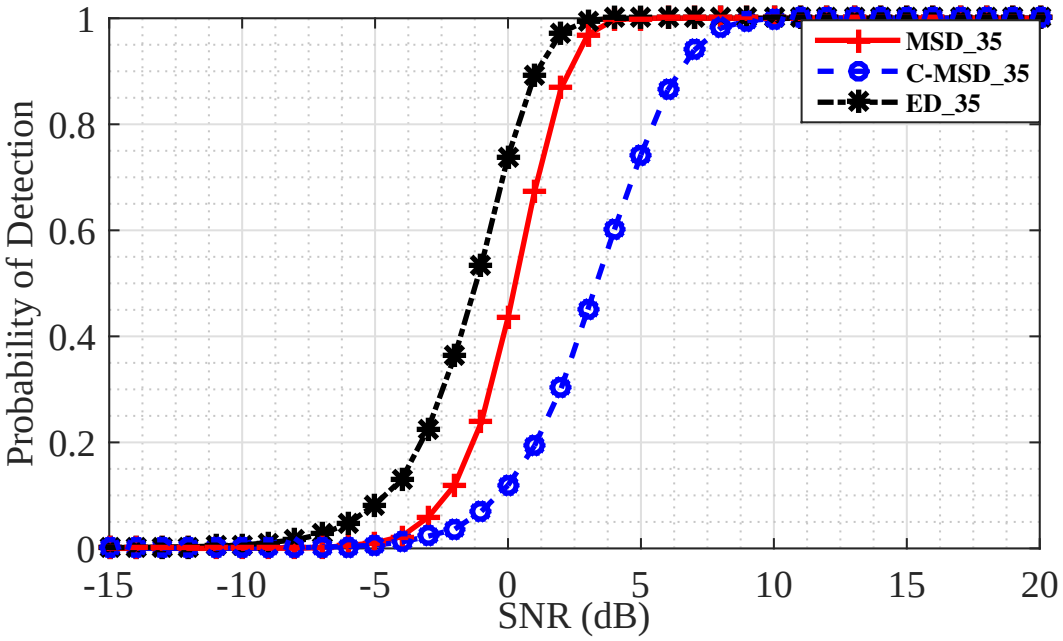

FIGURE 4.5: Target detection performances of ED and MSD with 35 received signal samples

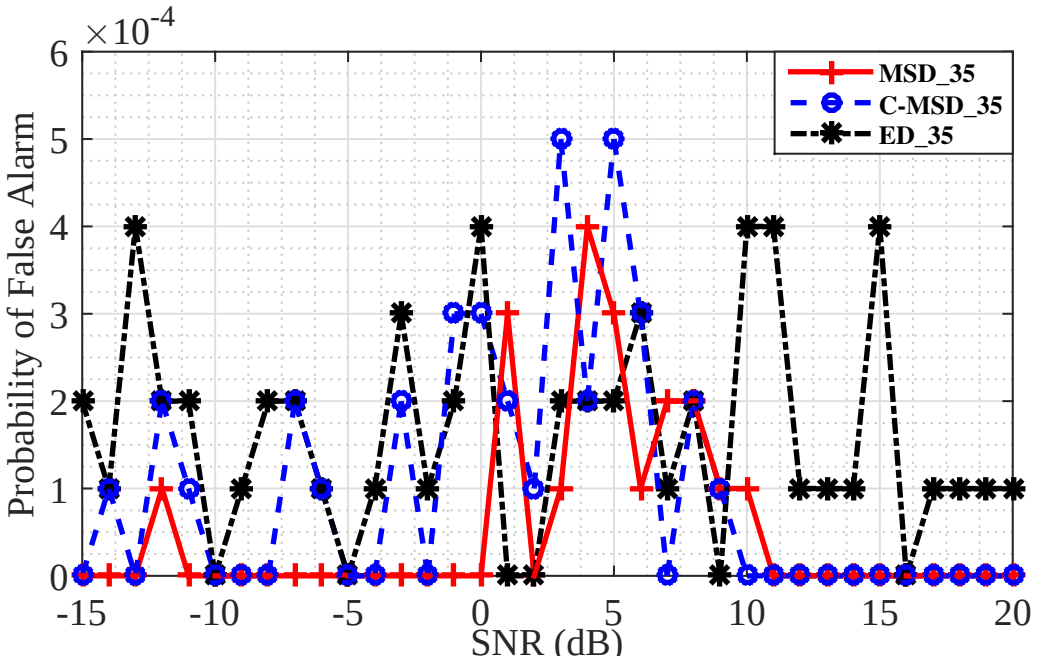

FIGURE 4.6: False alarm rates of ED and MSD with 35 received signal samples

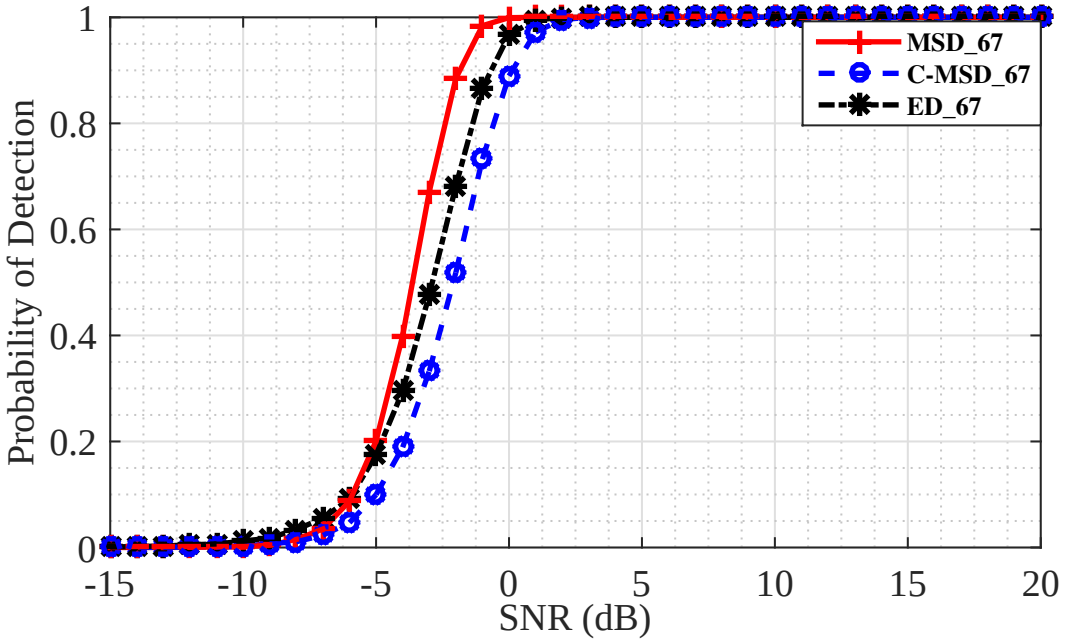

FIGURE 4.7: Target detection performances of ED and MSD with 67 received signal samples

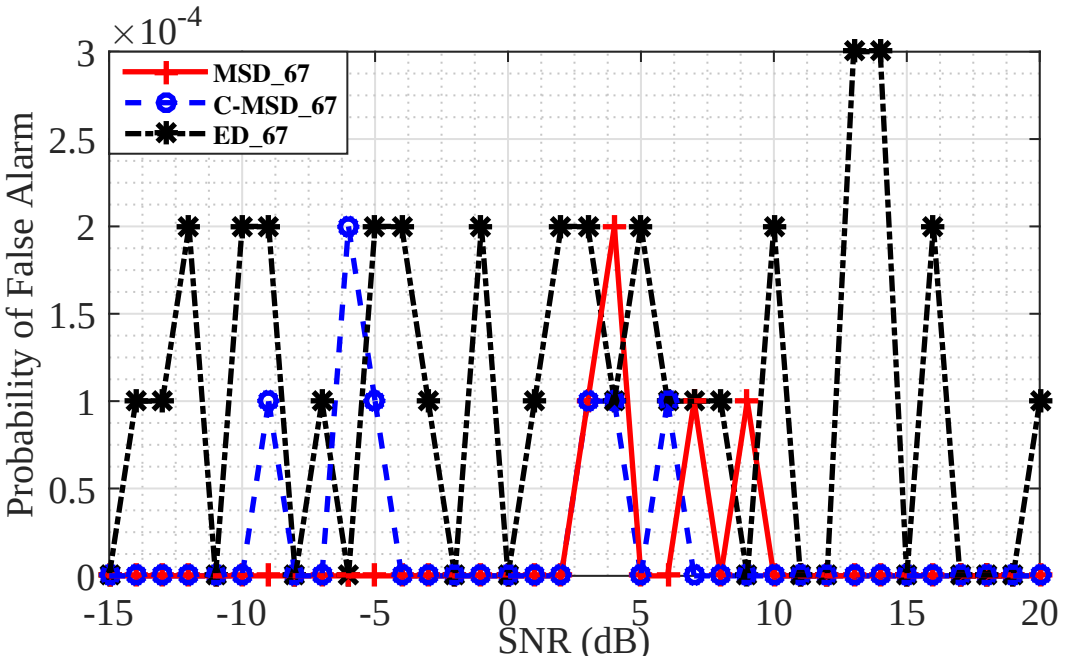

FIGURE 4.8: False alarm rates of ED and MSD with 67 received signal samples

4.6.2 Secondary Detection

In this section, the target detection performance of the proposed AIE for WSN has been analysed. Under similar sensing conditions, the target detection performance of the proposed detector is compared to the performance of a conventional GLRT based target detector, which is considered to be a suitable candidate for WSN. C-AIE detector has been proposed in Section 4.5.2 which has the ability to detect the existence of the targets using compressed received signal samples from the sensing nodes. The test statistic for the proposed AIE detector is given in Equation 4.36. Compressive sensing has been introduced to reduce the computational complexity and transmission costs between sensing nodes and the control centre. Simulations are performed at 40% compression ratio. The test statistic for the proposed C-AIE detector is given in Equation 4.57. For simulations, a single transmitting source is considered i.e., $N_T = 1$ which is transmitting the desired RF waveform into the sensing region. The transmitting node in this case is the control centre, which is assumed to transmit a Monocycle pulse. N_r sensing nodes are assumed to be deployed within the cluster which receive the reflected echoes of the known

transmitted waveform. It is assumed that the length of the target impulse response vector, $N_a = 4$. Each sensing node is assumed to collect, $N_y = 35$ independent target signal samples which are corrupted by Gaussian noise and interference. Acceptable false alarm is assumed to be $P_{fa} = 10^{-4}$. A summary of assumptions made within simulations is provided in Table 4.1.

Parameter	Assumption
N_T	1
N_a	4
N_t	32, 64
N_y	35, 67
P_{fa}	10^{-4}
N_s	1, 2, 3
μ	0.4, 0.6

TABLE 4.1: Summary of assumptions within simulations

In Figure 4.9, the simulation results are plotted for the target detection performance of the proposed AIE, C-AIE detectors, which are compared to the performances of the conventional GLRT and Compressive-GLRT (C-GLRT) detectors. For simulations in Figure 4.9, it is assumed that only one sensing node within the cluster detected the presence of the target after primary detection. The interfering waveform is assumed to be a fourth order modified Gegenbauer pulse which is discussed in Section 3.3.2. From the results, it can be observed that both AIE significantly outperformed the GLRT detector and C-AIE detector outperformed the conventional C-GLRT detector. Similarly, in Figure 4.10, the simulation results are plotted assuming that two sensing nodes detected the target echoes, i.e., $N_s = 2$. With two sensing nodes receiving the target echoes, the proposed AIE detector has shown an improvement in the target detection performance by about 3.5dB at 80% probability of detection. Similarly, in Figure 4.11, the simulation results are plotted assuming that three sensing nodes detected the target echoes, i.e., $N_s = 3$. In this scenario, the proposed AIE detector has shown a significant improvement in the target detection performance by about 5dB at 80% probability of detection when compared to the performance in the case of $N_s = 1$. According to the

waveform selection criterion summarised in Table 3.2, when a Monocycle pulse is transmitted, fourth order modified Gegenbauer pulse from the neighbouring cluster causes the least significant amount of interference. Similarly, a moderately low compatibility has been observed between Monocycle and 3^{rd} order modified Hermite pulses.

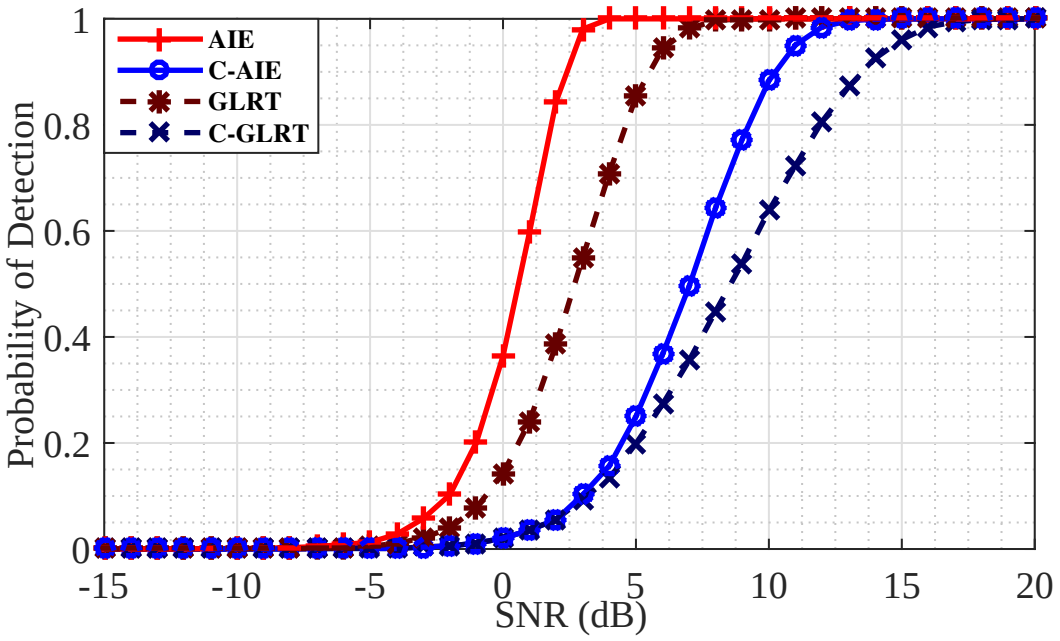

FIGURE 4.9: Target detection performances of AIE and CAIE detectors with 1 receiving nodes in the presence of G_4 interference

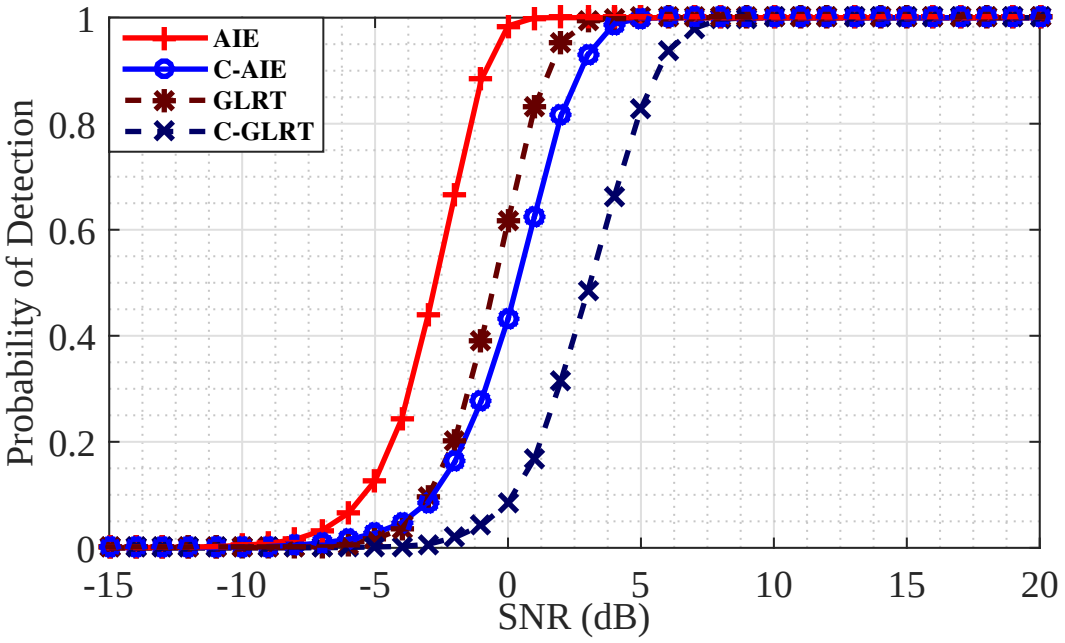

FIGURE 4.10: Target detection performances of AIE and CAIE detectors with 2 receiving nodes in the presence of G_4 interference

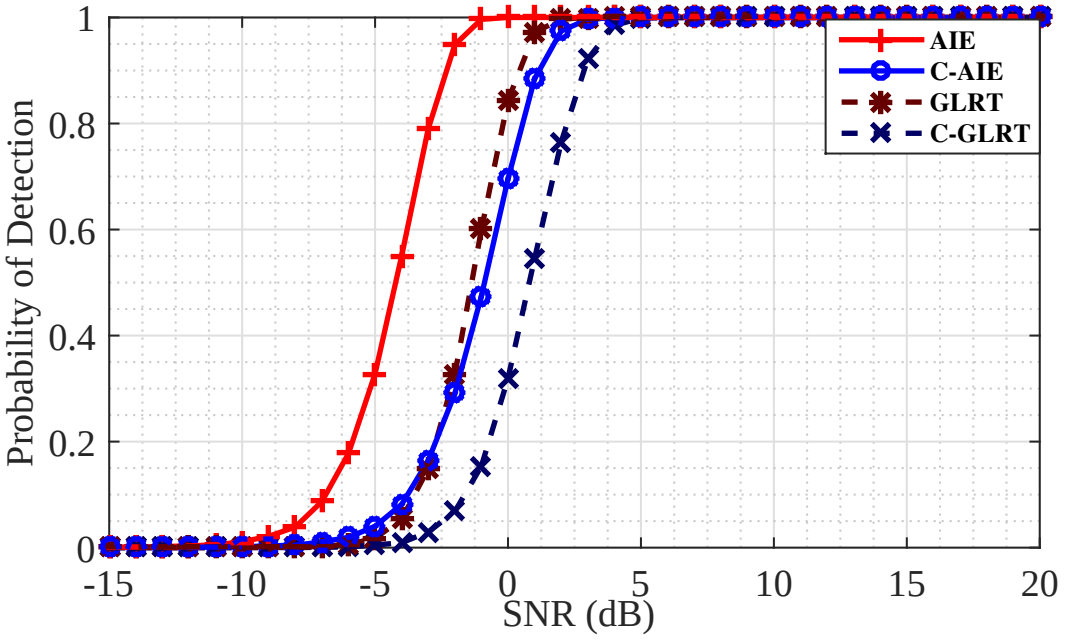

FIGURE 4.11: Target detection performances of AIE and CAIE detectors with 3 receiving nodes in the presence of G_4 interference

In Figure 4.12, the target detection performance of the proposed AIE and C-AIE detectors are plotted when the target signal is a Monocycle Pulse and the interfering waveform is a Hm_3 pulse as discussed in Section 3.3.2. $N_s = 1$ sensing nodes are assumed to detect the target echoes. In the presence of Hm_3 interfering waveform, a significant reduction in the target detection performance can be observed when compared to the similar scenario with G_4 interfering waveform. However, the performance of the proposed target detectors remained significantly robust when compared to the conventional detectors with C-AIE detector nearly matching the performance of a GLRT detector while the C-GLRT detector completely failed to perform. In Figure 4.13 and Figure 4.14, performances proposed detectors with two and three receiving nodes are plotted and the corresponding gains in the target detection performance can be observed. Under these sensing conditions, the proposed AIE detector can be implemented when detection rates are crucial and since C-AIE detector matched the performance of the GLRT detector, it can be implemented to reduce the power and processing burden on the WSN without any significant performance loss.

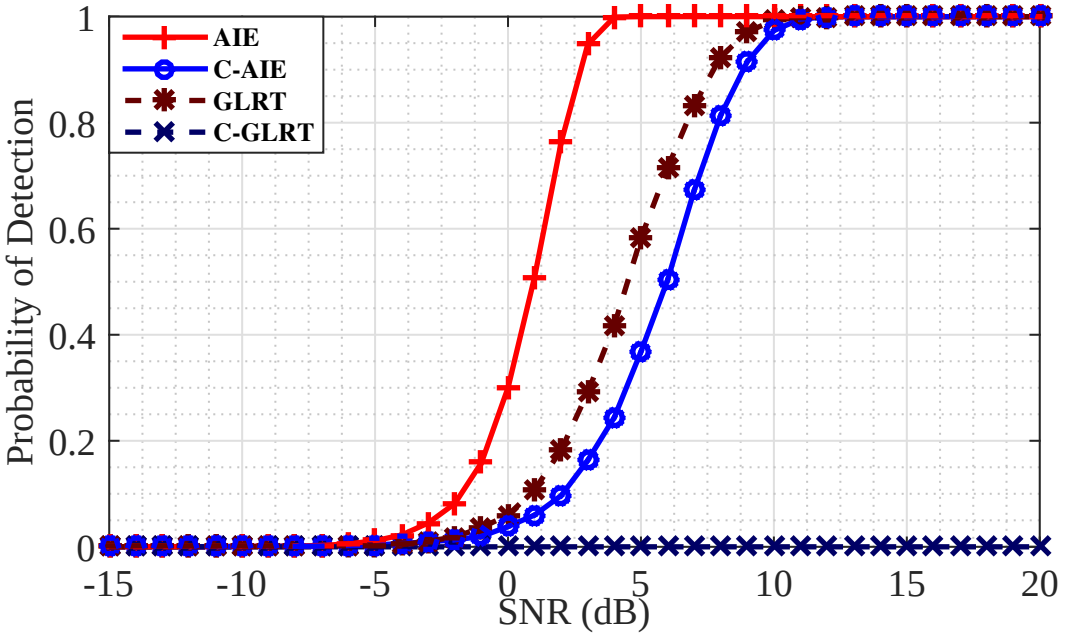

FIGURE 4.12: Target detection performances of AIE and CAIE detectors with 1 receiving nodes in the presence of Hm_3 interference

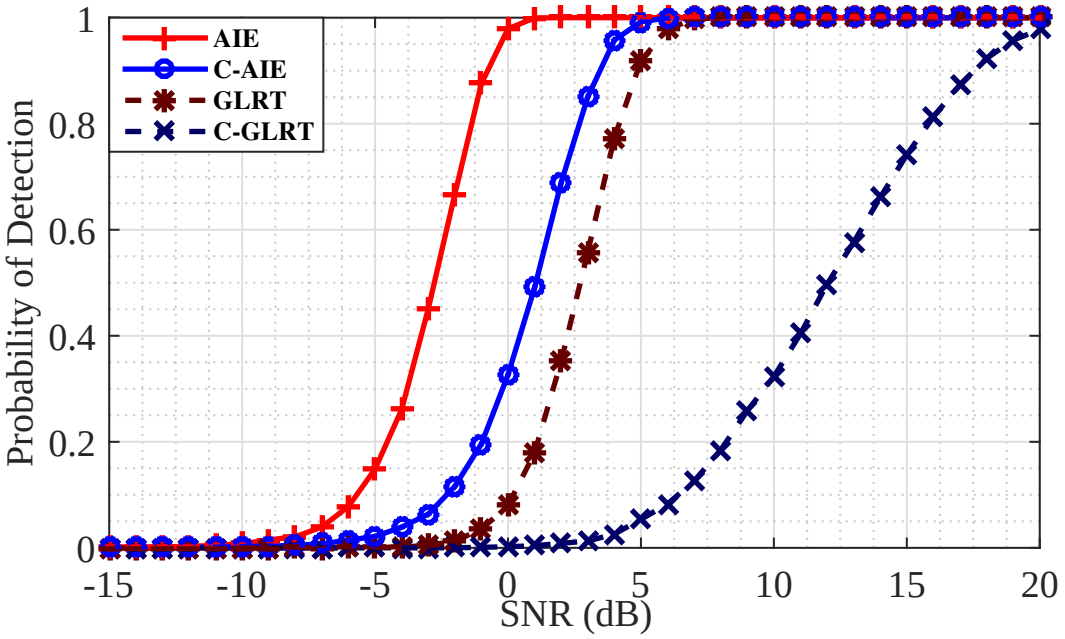

FIGURE 4.13: Target detection performances of AIE and CAIE detectors with 2 receiving nodes in the presence of Hm_3 interference

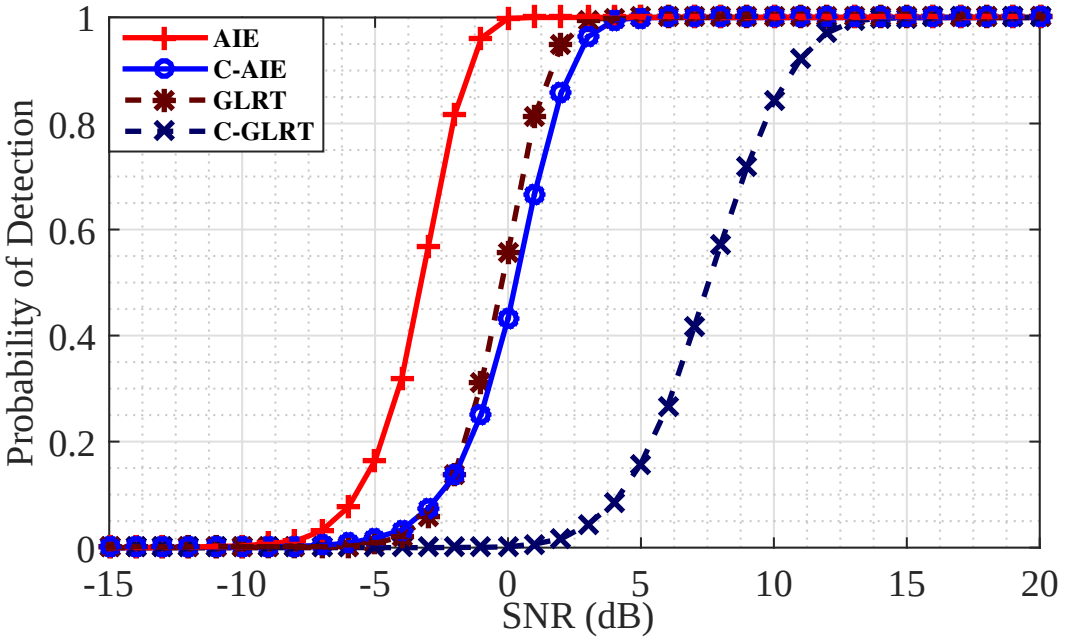

FIGURE 4.14: Target detection performances of AIE and CAIE detectors with 3 receiving nodes in the presence of Hm_3 interference

To obtain fair comparison between the performances of the proposed target detector for different transmit waveforms, in Figure 4.15, the target detection performances of the proposed AIE are plotted when G_4, Hm_4, Hm_3 and G_4 waveforms are transmitted respectively. The simulation results correlate with the results summarised in Table 3.2. The simulations are performed again with compressive sensing and the results are plotted in Figure 4.16. It can be observed that, with compressive sensing, the choice of transmit waveform has become more significant and between the four waveforms which are simulated, up to 4dB gain in target detection performance can be obtained through proper selection of a transmit waveform.

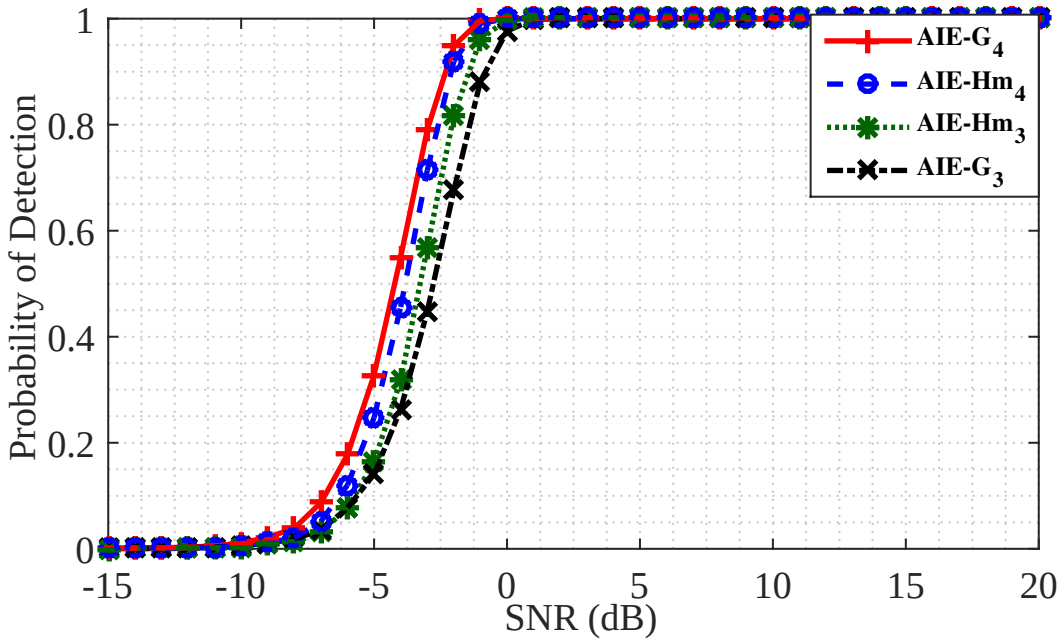

FIGURE 4.15: Target detection performances of proposed AIE detector with changing interfering waveforms

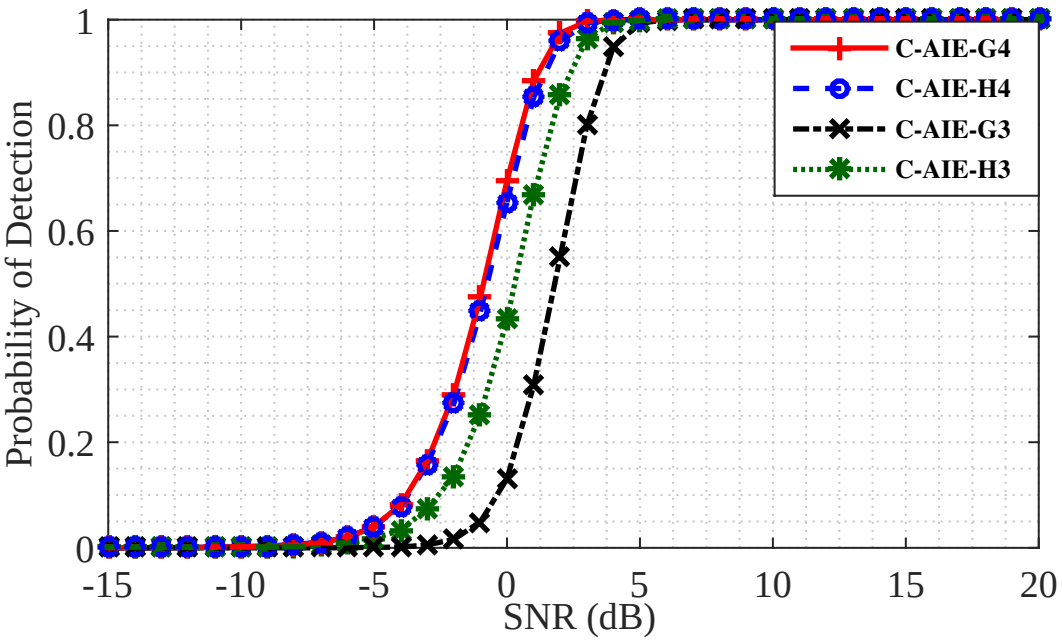

FIGURE 4.16: Target detection performances of proposed C-AIE detector with changing interfering waveforms

Effect of sample size on the performance of the proposed AIE detector is shown in Figure 4.17. For theoretical analysis, a comparison of the target detection performance of the proposed detector with other existing detectors is provided in Figure 4.18. Simulations are performed under the assumption that there are N_s = 3 receiving nodes and SIR = 3dB and SNR = -3dB. The corresponding ROC curves for sensitivity analysis are shown in Figure 4.19.

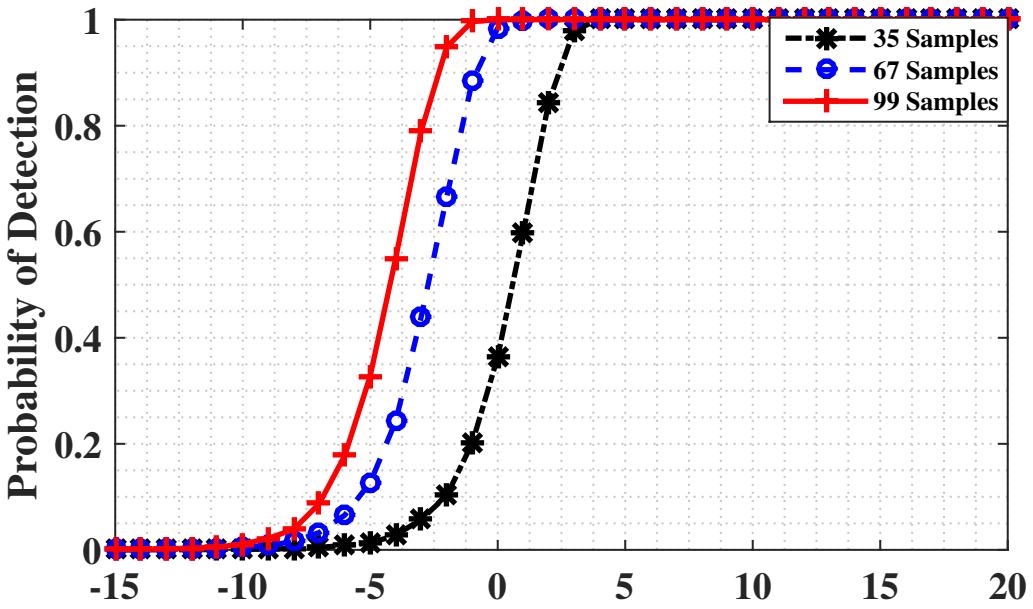

FIGURE 4.17: Effect of sample size on the target detection performance of the proposed AIE detector

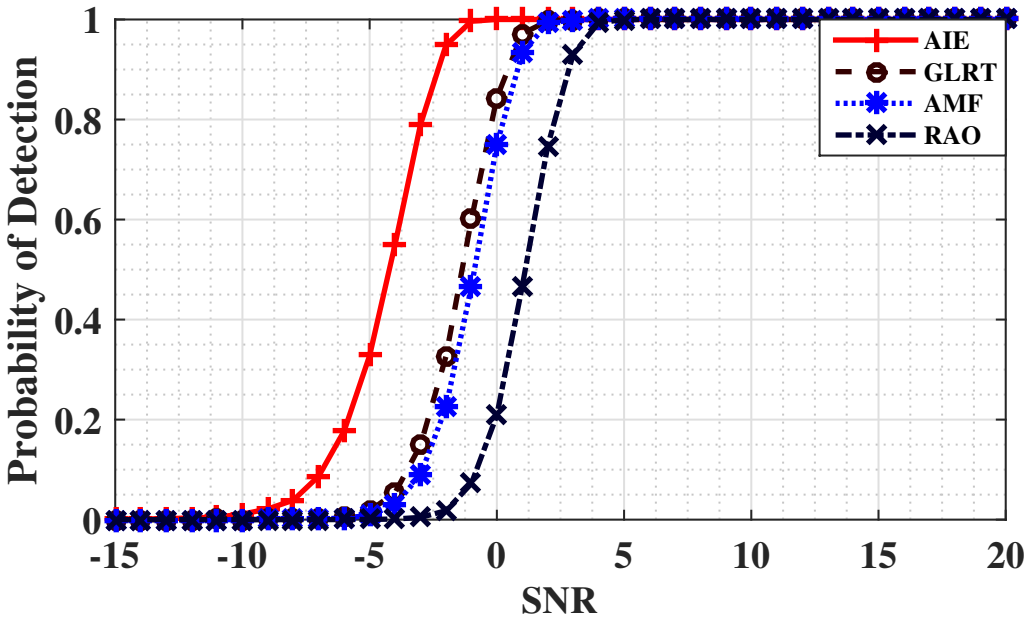

FIGURE 4.18: Target detection performances of proposed AIE compared with other existing detectors

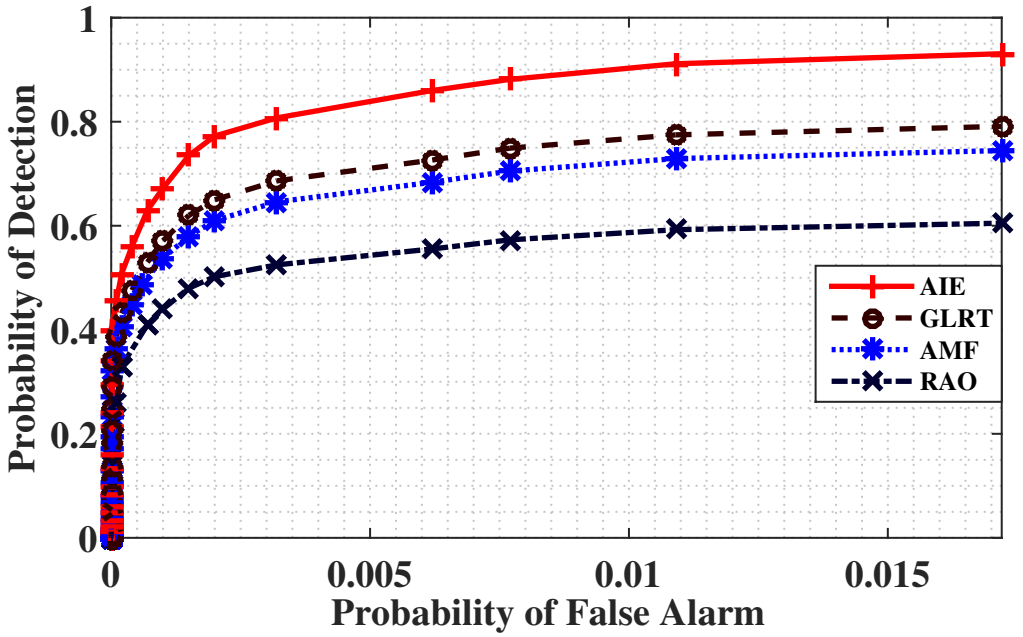

FIGURE 4.19: Sensitivity analysis of AIE, GLRT, AMF and RAO detectors

4.6.3 Computational Complexity

Computational complexity is a measure of the amount of processing burden on the WSN. Computational complexity defines the amount of resources such as power, processing, storage, etc. that are required by the sensing node to perform the required task. Depending on the nature of the processing system, the complexity can be measured based on different parameters such as processing time, storage requirement, amount of communication, number of processing operations, etc. In this research, the computational complexity is measured to estimate the processing burden on the sensing nodes. The computational complexity at the sensing node processor is defined as the number of arithmetic operations which are required to perform a desired task. From the mathematical models discussed in this chapter, it can be observed that the sensing nodes are required to perform various arithmetic operations involving matrix addition and matrix multiplications. Given two matrices M1 of dimensions $[X_1 \times Y_1]$ and M2 of dimensions $[X_2 \times Y_2]$, the number of arithmetic operations required to perform matrix addition i.e., M1+M2 is

measured as

$$\text{Computational Complexity} = X_1 Y_2 \tag{4.58}$$

Similarly the number of arithmetic operations required to perform matrix multiplication i.e., M1*M2 is measured as

$$\text{Computational Complexity} = Y_1 Y_2 X_1 + (Y_1 - 1) Y_2 X_1 \tag{4.59}$$

The computational complexity of the target detection procedure is the sum of all the arithmetic operations required to generate the final test statistic. In Figure 4.20, the computational complexities of the proposed AIE and C-AIE detectors are compared at different compression ratios.

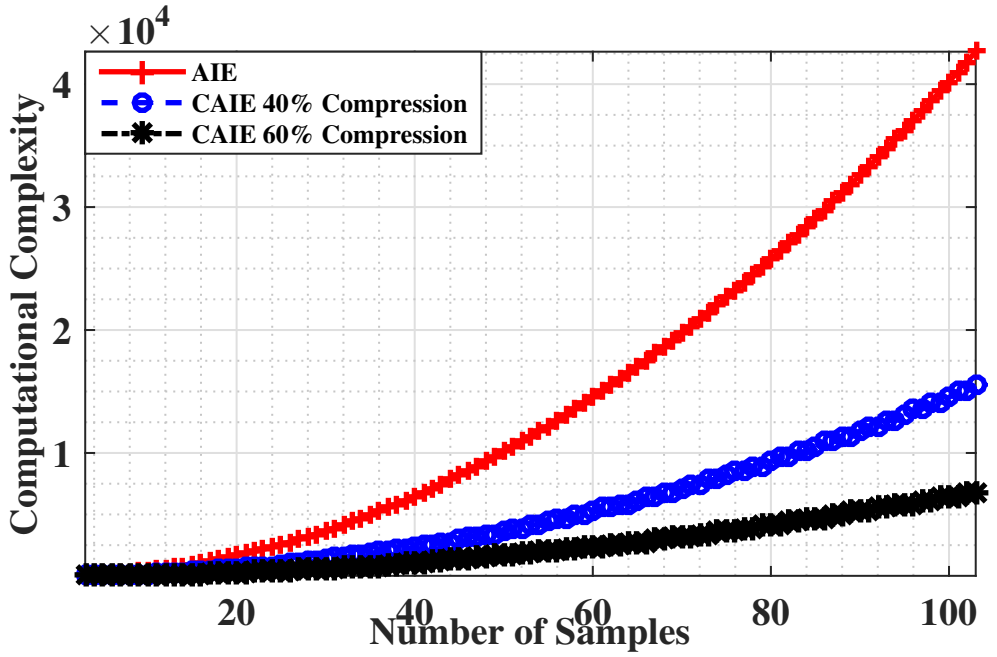

FIGURE 4.20: Computational Complexities of the proposed AIE detector at different compression ratios

4.7 Summary

In this chapter, a target detection architecture for surveillance applications of WSN within homogeneous sensing environments has been proposed. Within WSN with

resource constrained sensing nodes, reliable target detection algorithms cannot be implemented due to lack of sufficient computational capabilities. A distributed target detection architecture has been proposed where the sensing nodes transmit the received data to a centralised control centre, which has sufficient processing resources to make a reliable decision regarding the existence of the targets. To reduce the power consumption during data transmission, a two-stage hybrid target detection architecture has been proposed. A target detector with relatively low complexity is implemented at the sensing nodes to make a preliminary decision regarding the existence of the targets. The sensing nodes only transmit the received data to the control centre only upon detecting the existence of the targets. Random false alarms are tolerated at this stage. At the control the proposed target detector is implemented which is shown to provide reliable and significantly high target detection rates compared to the existing target detectors. In Chapter 5, a new target detection architecture has been proposed for RF sensing based WSN which is deployed in relatively harsher, heterogeneous sensing environments with the presence of clutter and interfering signals.

Chapter 5

Target Detection Architecture for RF Sensing Based WSN for Heterogeneous Sensing Environments

5.1 Introduction

In this section, a WSN, which is deployed in heterogeneous sensing environment has been considered. Most often within WSN, the sensing nodes are required to operate in harsh sensing environments in the presence of clutter and interfering signals. Due to heterogeneous nature of the sensing environment, the interfering signal strengths from the neighbouring sensing nodes vary. The sensing nodes while co-existing with the other sensing nodes, are required to provide reliable target detection rates while using the limited available power and processing capabilities. The proposed target detector is expected to give an energy efficient solution to the problem of target detection under these sensing conditions. To optimise the target detector, the target detection procedure is divided into initialisation and

operational phases. Preliminary time-invariant estimations are performed in initialisation phase and the final decisions are made using the received signal samples obtained during the operational phase. Amount of data transfer between the sensing nodes and the control centre has a severe impact on the lifetime of a sensing nodes. Compressive sensing has been proposed to reduce the transmissions costs.

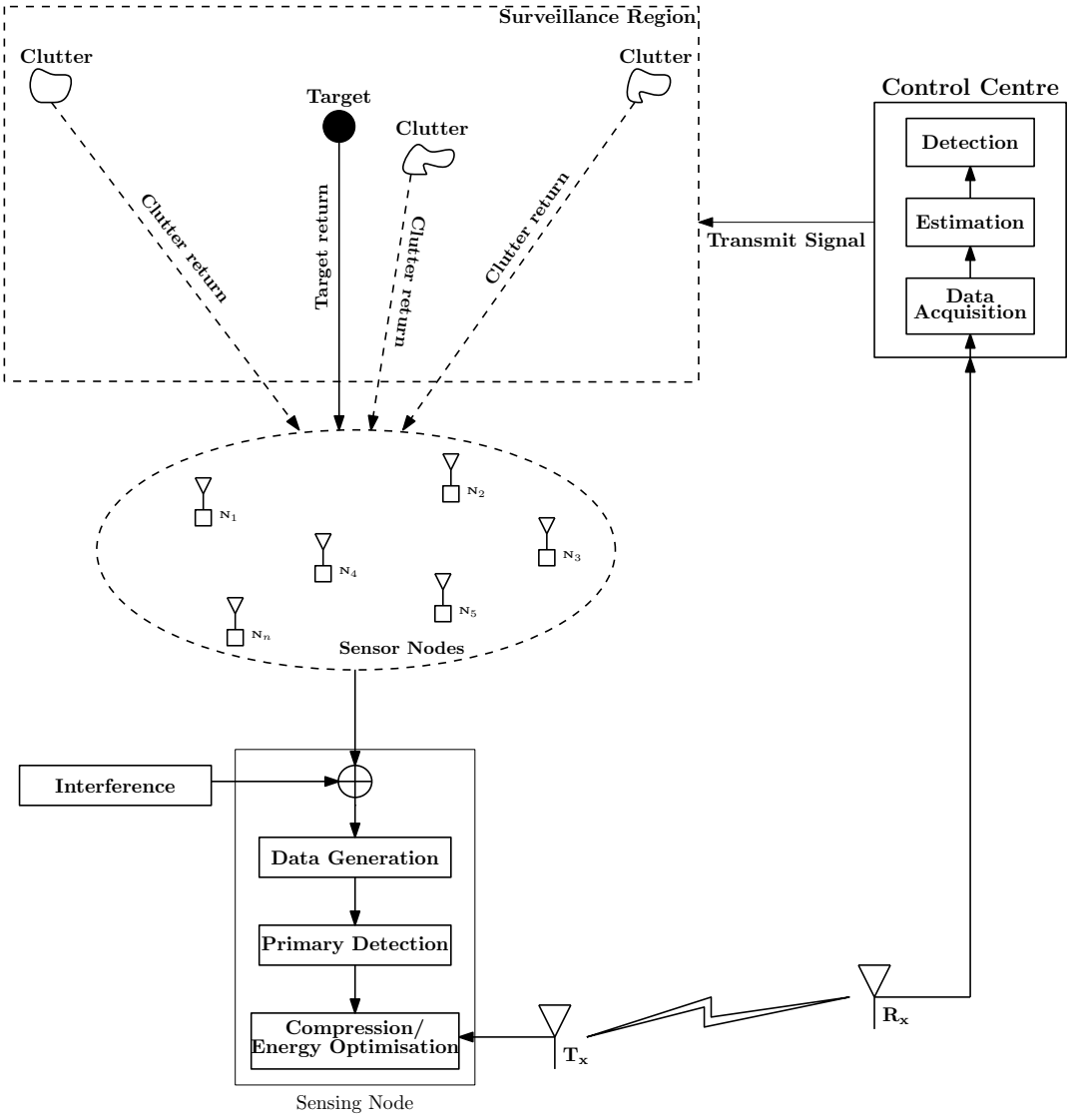

FIGURE 5.1: Proposed system model for WSN surveillance applications within cluttered heterogeneous sensing environment

5.2 Proposed System Model

In this chapter, a low power surveillance system has been considered which is supported by WSN. To achieve increased reliability within the low power applications of WSN, RF sensing has been considered to be the primary means of sensing. The proposed wireless sensor network consists of clusters of sensing nodes, which are distributed within the sensing region. Each cluster consists of a control centre and a group of receiving nodes, which are distributed randomly within the sensing region. It is assumed that the control centre is equipped with sufficient resources to transmit the desired RF signal into the sensing region. The sensing environment is considered to be heterogeneous in nature with harsh sensing conditions. The system model for the proposed WSN as a surveillance system is shown in Figure 5.1. When a waveform is transmitted from the control centre, the sensing nodes receive a direct arrival and reflected components of the transmitted signal. It is assumed that the sensing nodes are synchronised with the control centre and have the ability to distinguish between the direct arrivals and the reflected components. The heterogeneous sensing environment is assumed to be cluttered in nature. Therefore, when a waveform $\mathbf{s}(t)$ is transmitted by the control centre, in the presence of a target within the sensing region, the sensing nodes receive components of the transmitted signal which are reflected from the target and clutter. Moreover, with multiple clusters of sensing nodes operating independently within the sensing region, the sensing nodes may receive interfering waveforms from the neighbouring clusters. The received signal $\mathbf{y}_i(t)$ at the i^{th} sensing node as shown in Figure 5.2 can be written as

$$\mathbf{y}_i(t) = \sum_{k=1}^{t_n} \mathbf{s}(t) * \mathbf{a}_{ik}(t) + \sum_{k=1}^{b_n} \mathbf{h}_k(t) * \mathbf{b}_{ik}(t) + \sum_{k=1}^{c_n} \mathbf{c}_{ik}(t) + \mathbf{w}_i(t), \qquad 0 \leq t \leq T_y \quad (5.1)$$

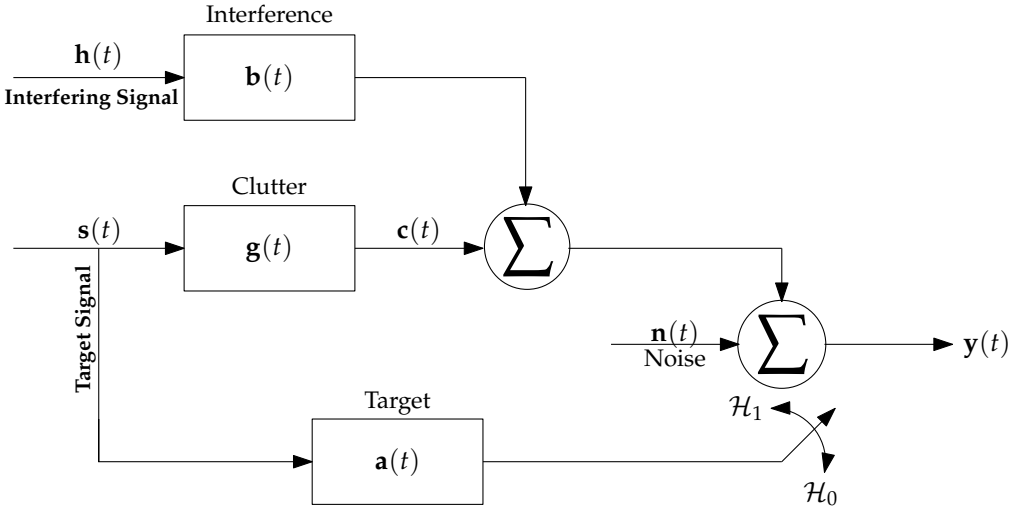

FIGURE 5.2: Received signal model at the sensing nodes under hypothesis H_0 and H_1

where $*$ denotes convolution operator. T_y is the total time period over which the received signal samples are collected, $\mathbf{s}(t)$ is the reference transmit waveform, $\mathbf{a}_k(t)$ is the impulse response corresponding to the k^{th} target return and t_n is the number of targets within the range bin. $\mathbf{h}_k(t)$ is the is the k^{th} interfering signal, $\mathbf{b}_k(t)$ is the impulse response corresponding to the k^{th} interfering signal and b_n is the number of interfering nodes. $\mathbf{w}(t)$ is the thermal noise. If the impulse response of the target is known to exist for a time duration of T_a, the received signal samples within a given range bin are required to be observed for an extended duration of time which is given by, $T_y = T + T_a$. The discrete $N_y \times 1$ received signal data at the i^{th} sensing node is written as

$$\mathbf{y}_i[n] = \sum_{k=1}^{t_n} \mathbf{S}\mathbf{a}_{ik}[n] + \sum_{k=1}^{b_n} \mathbf{H}_k \mathbf{b}_{ik}[n] + \sum_{k=1}^{c_n} \mathbf{c}_{ik}[n] + \mathbf{w}_i[n] \tag{5.2}$$

$$\mathbf{a}_i = [a_1, a_2, \ldots, a_{N_a}]^T \ , \ i = 1,2 \ldots N_s$$

$$\mathbf{b}_i = [b_1, b_2, \ldots, b_{N_a}]^T \ , \ i = 1,2 \ldots N_s$$

where $\mathbf{y}_i$ is the $N_y \times 1$ received signal data at the i^{th} receiving node, $N_y = N_t + N_a$ - 1. $\mathbf{a}_i$ is the $N_a \times 1$ unknown impulse response associated with the target return at the i^{th} receiving node; $\mathbf{b}_i$ is the $N_a \times 1$ unknown impulse response of the interfering signal at the i^{th} receiving node; $\mathbf{c}_i$ is the clutter return at the i^{th} receiving node. Noise is assumed to be AWGN with unknown variance. $\mathbf{S}$ is the $N_y \times N_a$ convolution matrix of $\mathbf{s}(t)$, $\mathbf{H}$ is the $N_y \times N_a$ convolution matrix of $\mathbf{h}(t)$. The convolution matrices $\mathbf{S}$ and $\mathbf{H}$ are discussed in Chapter 4 in Equation 4.4 and Equation 4.5. Due to cooperative nature of the sensing nodes within the WSN, the control centre is assumed to have the knowledge of the interfering waveforms which are transmitted by the neighbouring clusters. In Equation 5.2, while $\mathbf{S}$ and $\mathbf{H}$ are known quantities, the impulse responses $\mathbf{a}$, $\mathbf{b}$ and noise variance are unknown but deterministic. However, clutter is unknown. To achieve reliable target detection performance in the presence of clutter, sufficient knowledge of the statistical distribution of clutter is necessary which is discussed in the following section.

5.3 Clutter Model

In this section, the problem of unknown clutter has been addressed. Clutter is considered to be comprised of all the fixed scatterers within the sensing region. Due to the nature of sensing nodes with short range sensing capabilities, the dominant scatterers, which contribute to clutter, are assumed to be non-varying over extended periods of time. The cluttered nature of the sensing environment produces additional transmit signal echoes, which arrive at the sensing nodes along with the target returns. The vector $\mathbf{c}_i$ in Equation 5.2 is a $N_y \times 1$ vector containing the clutter returns. In the existing literature, authors have proposed modelling clutter as a Compound-Gaussian process [156–158] i.e., as a product of two independent random variables.

$$\mathbf{c} = \sqrt{\varsigma}\mathbf{g} \tag{5.3}$$

here the speckle, $\mathbf{g}$ is a complex Gaussian with covariance matrix $\mathbf{\Sigma}$ and ς is the clutter texture component and is usually a real nonnegative scalar. In [152, 159–161], authors have addressed the problem of target detection in the presence of clutter with known covariance structure but unknown level. However, the presence of a noise component whose power is independent of clutter is largely ignored. In this section, a disturbance vector consisting of noise and clutter signals, which can be estimated from secondary data, has been considered which is written as

$$\mathbf{d} = \sqrt{\varsigma}\mathbf{g} + \mathbf{w} \tag{5.4}$$

$$\mathbf{R}_d = \varsigma\mathbf{\Sigma} + \sigma^2\mathbf{I} \tag{5.5}$$

where $\mathbf{d}$ is the disturbance vector and $\mathbf{R}_d$ is the disturbance covariance matrix. $\mathbf{I}$ is a $N_c \times N_c$ identity matrix where N_c is the length of the received signal vector. $\mathbf{\Sigma}$ is the clutter covariance matrix which is unknown to the target detector. Noise which varies with time, is assumed to be additive white Gaussian in nature whose variance σ^2 is unknown but deterministic. Clutter covariance estimation has been addressed by the authors in the existing literature [79, 81, 82]. If clutter texture is gamma-distributed with mean μ and order ν, texture distribution function can be written as

$$f(\varsigma) = \frac{1}{\Gamma(\nu)}\left(\frac{\nu}{\mu}\right)^{\nu}\varsigma^{\nu-1}e^{-\frac{\nu}{\mu}\varsigma} \qquad \varsigma \geq 0 \tag{5.6}$$

where $\Gamma(\nu)$ is the gamma function of order ν. The unconditional probability density function (pdf) of the disturbance vector $\mathbf{d}$ can be obtained by averaging $f(\mathbf{d}|\varsigma)$ with respect to its texture distribution $f(\varsigma)$ [83].

$$f(\mathbf{d}) = \int_0^{\infty} \frac{1}{\pi^{N_y N_s}|\varsigma\mathbf{\Sigma} + \sigma^2\mathbf{I}|} exp\Big[- \mathbf{d}^H(\varsigma\mathbf{\Sigma} + \sigma^2\mathbf{I})^{-1}\mathbf{d}^H\Big] f(\varsigma)d\varsigma \tag{5.7}$$

However, the detection strategy based on this clutter model is difficult to implement within resource constrained WSN as it involves unknown parameters and

computationally intense numerical integrations with respect to clutter texture distribution. It can be recalled that the disturbance covariance matrix $\mathbf{R}_d$ is the sum of unknown stationary clutter and random noise. The clutter covariance matrix, $\varsigma\mathbf{\Sigma}$ is assumed to have a known structure whose rank r is significantly less than N_c which is usually true in many practical applications. Let λ_{di} and $\mathbf{\Phi}_{di}$ $(i = 1, 2 \ldots N_c)$ be the i^{th} eigenvalue and the corresponding i^{th} normalised eigenvector respectively of the disturbance covariance matrix $\mathbf{R}_d$. Since $\mathbf{R}_d$ is symmetric, the disturbance covariance matrix can be expressed as $\mathbf{\Phi}_d\boldsymbol{\lambda}_d\mathbf{\Phi}_d^H$. Similarly let λ_{ci} and $\mathbf{\Phi}_{ci}$ be the i^{th} eigenvalue and the corresponding i^{th} normalised eigenvector respectively of the clutter covariance matrix $\mathbf{\Sigma}$. It must be noted that $\boldsymbol{\lambda}_c$ and $\mathbf{\Phi}_c$ here are unknown. From Equation 5.5, $\boldsymbol{\lambda}_d$ can be written as $\boldsymbol{\lambda}_d = \varsigma\boldsymbol{\lambda}_c + \sigma^2\mathbf{I}$. Therefore, $\mathbf{R}_d$ can be expressed as

$$\mathbf{R}_d = \mathbf{\Phi}_d(\varsigma\boldsymbol{\lambda}_c + \sigma^2\mathbf{I})\mathbf{\Phi}_d^H \tag{5.8}$$

Finally, inverse covariance matrix is given by,

$$\mathbf{R}_d^{-1} = (\mathbf{\Phi}_d^H)^{-1}(\varsigma\boldsymbol{\lambda}_c + \sigma^2\mathbf{I})^{-1}(\mathbf{\Phi}_d)^{-1} \tag{5.9}$$

$$= \mathbf{\Phi}_d(\varsigma\boldsymbol{\lambda}_c + \sigma^2\mathbf{I})^{-1}\mathbf{\Phi}_d^H \tag{5.10}$$

To solve Equation 5.10, the inverse of $(\varsigma\boldsymbol{\lambda}_c + \sigma^2\mathbf{I})$ is required to be estimated. Clearly $(\sigma^2\mathbf{I})^{-1}$ and $(\varsigma\boldsymbol{\lambda}_c + \sigma^2\mathbf{I})^{-1}$ always exists. Fundamental matrix inversion lemma may be used to solve this problem if the rank of $\boldsymbol{\lambda}_c$ is 1. However, based on the previous assumption, when the rank of $\boldsymbol{\lambda}_c$ is r such that $1 \leq r \ll N_c$, matrix inversion lemma may not always be applicable. Here $(\sigma^2\mathbf{I})$ is a full rank matrix and $\varsigma\boldsymbol{\lambda}_c$ is a diagonal matrix of rank r i.e., $\varsigma\boldsymbol{\lambda}_c$ can only have up to r non zero elements. Following the results from [162], the matrix $\varsigma\boldsymbol{\lambda}_c$ can be decomposed into

a sum of matrices of rank one i.e.,

$$\begin{aligned} \varsigma\boldsymbol{\lambda}_c &= \sum_{k=1}^{r} \boldsymbol{\delta}_k \\ \boldsymbol{\delta}_i\boldsymbol{\delta}_j &= \mathbf{0}_{N_c\times N_c} \qquad i \neq j \end{aligned} \tag{5.11}$$

here $\boldsymbol{\delta}_k$ is a null matrix where only the k^{th} diagonal element is non-zero and the rank of $\boldsymbol{\delta}_k$ is one. Since, $\sigma^2\mathbf{I}$ and $(\sigma^2\mathbf{I} + \varsigma\boldsymbol{\lambda}_c)$ are non-singular, inverse of $(\sigma^2\mathbf{I} + \varsigma\boldsymbol{\lambda}_c)$ is given by,

$$\begin{aligned} (\sigma^2\mathbf{I} + \varsigma\boldsymbol{\lambda}_c)^{-1} &= \boldsymbol{\kappa}_r^{-1} - v_r\boldsymbol{\kappa}_r^{-1}\boldsymbol{\delta}_r\boldsymbol{\kappa}_r^{-1} \\ v_k &= \frac{1}{1 + tr(\boldsymbol{\kappa}_k^{-1}\boldsymbol{\delta}_k)} \\ \boldsymbol{\kappa}_{k+1}^{-1} &= \boldsymbol{\kappa}_k^{-1} - v_k\boldsymbol{\kappa}_k^{-1}\boldsymbol{\delta}_k\boldsymbol{\kappa}_k^{-1} \\ \boldsymbol{\kappa}_1 &= \sigma^2\mathbf{I} \end{aligned} \tag{5.12}$$

The solution to the problem of $(\sigma^2\mathbf{I} + \varsigma\boldsymbol{\lambda}_c)^{-1}$ can be obtained by solving Equation 5.12 recursively. Based on the initial conditions of Equation 5.12, the first order recursive inverse coefficients can be obtained as

$$\begin{aligned} \boldsymbol{\kappa}_1 &= \sigma^2\mathbf{I} \\ \boldsymbol{\kappa}_1^{-1} &= \sigma^{-2}\mathbf{I} \\ v_1 &= \frac{1}{1 + trace(\boldsymbol{\kappa}_1^{-1}\boldsymbol{\delta}_1)} \end{aligned} \tag{5.13}$$

Since $\boldsymbol{\delta}_1$ is a diagonal matrix with only one non-zero diagonal element which is λ_{c1}, $trace(\boldsymbol{\kappa}_1^{-1}\boldsymbol{\delta}_1) = \lambda_{c1}/\sigma^2$. Therefore, the first order recursive inverse coefficient can be written as

$$v_1 = \frac{\sigma^2}{\sigma^2 + \lambda_{c1}} \tag{5.14}$$

Substituting Equation 5.14 in Equation 5.12, the second order recursive inverse coefficients are obtained as

$$\begin{aligned} \boldsymbol{\kappa}_2^{-1} &= \boldsymbol{\kappa}_1^{-1} - v_1 \boldsymbol{\kappa}_1^{-1} \boldsymbol{\delta}_1 \boldsymbol{\kappa}_1^{-1} \\ &= \sigma^{-2}\mathbf{I} - \frac{\sigma^{-2}}{\sigma^2 + \lambda_{c1}} \boldsymbol{\delta}_1 \\ &= \sigma^{-2}\left(\mathbf{I} - \frac{\boldsymbol{\delta}_1}{\sigma^2 + \lambda_{c1}}\right) \end{aligned} \tag{5.15}$$

$$\begin{aligned} v_2 &= \frac{1}{1 + trace(\boldsymbol{\kappa}_2^{-1}\boldsymbol{\delta}_2)} \\ &= \frac{1}{1 + trace\left(\sigma^{-2}(\mathbf{I} - \frac{\boldsymbol{\delta}_1}{\sigma^2 + \lambda_{c1}})\boldsymbol{\delta}_2\right)} \end{aligned}$$

From Equation 5.11, it may be recalled that $\delta_1\delta_2$ is a null matrix. Therefore, the second order recursive coefficient, v_2 can be obtained as

$$\begin{aligned} v_2 &= \frac{1}{1 + trace(\sigma^{-2}\boldsymbol{\delta}_2)} \\ &= \frac{\sigma^2}{\sigma^2 + \lambda_{c2}} \end{aligned} \tag{5.16}$$

Similarly, from Equation 5.15 and Equation 5.16, the third order recursive inverse coefficients are obtained as

$$\begin{aligned} \boldsymbol{\kappa}_3^{-1} = \sigma^{-2}\left(\mathbf{I} - \frac{\boldsymbol{\delta}_1}{\sigma^2 + \lambda_{c1}}\right) - \frac{\sigma^2}{\sigma^2 + \lambda_{c2}}\sigma^{-2}\Bigg(\mathbf{I} - \\ \frac{\boldsymbol{\delta}_1}{\sigma^2 + \lambda_{c1}}\Bigg)\boldsymbol{\delta}_2\sigma^{-2}\left(\mathbf{I} - \frac{\boldsymbol{\delta}_1}{\sigma^2 + \lambda_{c1}}\right) \end{aligned} \tag{5.17}$$

As mentioned previously in Equation 5.11, since $\boldsymbol{\delta}_i\boldsymbol{\delta}_j = \mathbf{0}_{N_c \times N_c}$ when $i \neq j$, Equation 5.17 can be simplified as

$$\kappa_3^{-1} = \sigma^{-2}\left(\mathbf{I} - \frac{\boldsymbol{\delta}_1}{\sigma^2 + \lambda_{c1}} - \frac{\boldsymbol{\delta}_2}{\sigma^2 + \lambda_{c2}}\right) \tag{5.18}$$

To obtain $(\varsigma\boldsymbol{\lambda}_c + \sigma^2\mathbf{I})^{-1}$, $(r+1)^{th}$ order recursive inverse coefficients are required. Observing Equations (5.18,5.15,5.13) and using the principle of induction, the $(r+1)^{th}$ order recursive inverse coefficient can be obtained which gives the solution to $(\varsigma\boldsymbol{\lambda}_c + \sigma^2\mathbf{I})^{-1}$ as

$$(\sigma^2\mathbf{I} + \varsigma\boldsymbol{\lambda}_c)^{-1} = \sigma^{-2}\left(\mathbf{I} - \frac{\boldsymbol{\delta}_1}{\sigma^2 + \lambda_{c1}} - \frac{\boldsymbol{\delta}_2}{\sigma^2 + \lambda_{c2}} \cdots - \frac{\boldsymbol{\delta}_r}{\sigma^2 + \lambda_{cr}}\right) \tag{5.19}$$

Substituting Equation 5.19 in Equation 5.10, $\mathbf{R}_d^{-1}$ can be written as

$$\mathbf{R}_d^{-1} = \sigma^{-2}\boldsymbol{\Phi}_d\left(\mathbf{I} - \frac{\boldsymbol{\delta}_1}{\sigma^2 + \lambda_{c1}} - \frac{\boldsymbol{\delta}_2}{\sigma^2 + \lambda_{c2}} \cdots - \frac{\boldsymbol{\delta}_r}{\sigma^2 + \lambda_{cr}}\right)\boldsymbol{\Phi}_d^H \tag{5.20}$$

Usually the clutter returns are significantly stronger than noise power at the sensing nodes. Under such scenarios, the following approximation can be made; $\sigma^2 + \lambda_{ci} \approx \lambda_{ci}$. Since $\boldsymbol{\Phi}_d\boldsymbol{\Phi}_d^H = \mathbf{I}$, Equation 5.20 can be rewritten as

$$\begin{aligned} \mathbf{R}_d^{-1} &\approx \sigma^{-2}\left(\mathbf{I} - \sum_{i=1}^{r}\boldsymbol{\Phi}_{di}\boldsymbol{\Phi}_{di}^H\right) \\ \mathbf{R}_d^{-1} &\approx \sigma^{-2}\mathbf{C} \end{aligned} \tag{5.21}$$

here $\mathbf{C}$ is the clutter projection matrix which is given by,

$$\mathbf{C} = \mathbf{I} - \sum_{i=1}^{r}\boldsymbol{\Phi}_{di}\boldsymbol{\Phi}_{di}^H \tag{5.22}$$

When clutter returns are significantly stronger than noise, the dominant eigenvalues in $\boldsymbol{\lambda}_d$ which correspond to the clutter returns can be distinguished from the remaining eigenvalues of $\boldsymbol{\lambda}_d$. The clutter projection matrix $\mathbf{C}$ can be easily obtained from the eigenvectors corresponding to the dominant eigen values of $\mathbf{R}_d$.

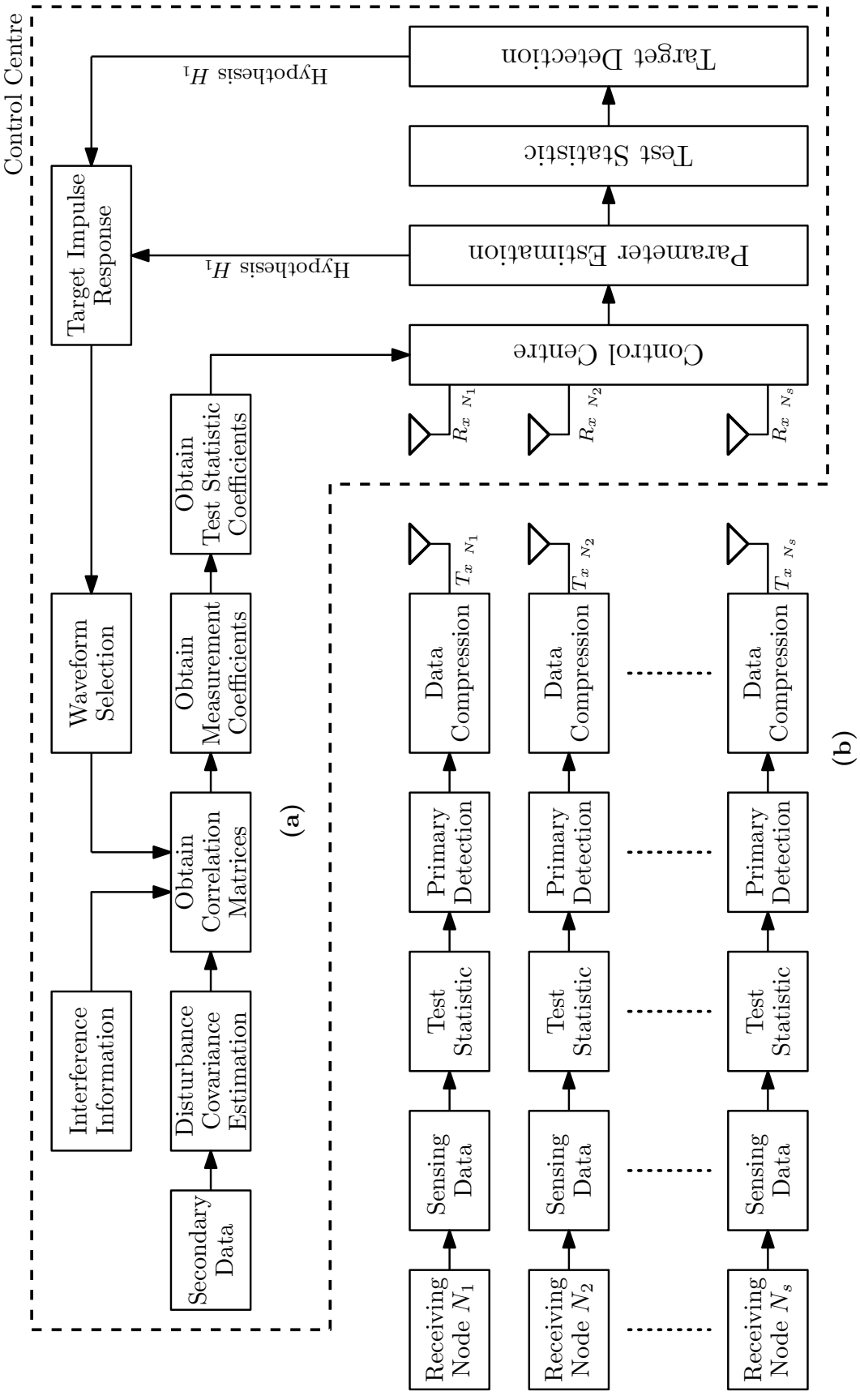

FIGURE 5.3: Proposed RF sensing based target detection architecture for surveillance applications. (a) Initialisation phase. (b) Operational Phase

5.4 Proposed Target Detection Model

In this section, the proposed target detection architecture for RF sensing based WSN has been discussed. The proposed target detection architecture is suitable for WSN, which is deployed for surveillance applications in harsh sensing conditions with the presence of clutter within the sensing environment. Clutter constitutes to all the scatterers within the sensing region, which reflect the transmitted RF signal. Clutter returns appear in the same subspace as the target return, which leads to increased false alarm rates. The proposed target detection architecture is expected to provide increased target detection reliability than the conventional target detectors in the presence of clutter. As shown in Figure 5.2, the target detector faces a binary hypothesis testing problem and the received signal models under hypothesis H_0 and H_1 are,

$$H_0 : \begin{cases} \mathbf{y}_i = \sum_{k=1}^{b_n} \mathbf{H}_k \mathbf{b}_{ki} + \mathbf{d}_i \\ \text{Absence of the Target} \end{cases} \tag{5.23}$$

$$H_1 : \begin{cases} \mathbf{y}_i = \sum_{k=1}^{t_n} \mathbf{S}\mathbf{a}_{ki} + \sum_{k=1}^{b_n} \mathbf{H}_k \mathbf{b}_{ki} + \mathbf{d}_i \\ \text{Existence of the Target} \end{cases} \tag{5.24}$$

It may be recalled from Equation 5.4 that the disturbance vector $\mathbf{d}$ constitutes of clutter and noise. The proposed target detection architecture consists of the sensing nodes, which perform primary detection and secondary detection at the control centre. Given the harsh sensing conditions and intense computational requirements, the target detection procedure is divided between initialisation and operational phases as shown in Figure 5.3.

5.5 Hybrid Matched Filter Detector for Primary Detection

In this section, a matched filter based target detector has been derived for primary detection at the sensing nodes. To reduce the amount of data transfer between the sensing nodes and the control centre, the primary detector at the sensing nodes is required to make a preliminary decision regarding the existence of the target with a certain degree of reliability. However, within a cluttered background environment, the primary detector must be able to reliably distinguish between clutter returns and the target returns. The probability density functions of the received signal models under hypothesis H_0 and H_1 are,

$$f(\mathbf{y}|\mathbf{R}_d, H_0) = \left(\frac{1}{\pi|\mathbf{R}_d|}\right)^{N_y/2} exp\left[\frac{-1}{2}\left(\mathbf{y}^H\mathbf{R}_d^{-1}\mathbf{y}\right)\right] \tag{5.25}$$

$$f(\mathbf{y}|\mathbf{a}, \mathbf{R}_d, H_1) = \left(\frac{1}{\pi|\mathbf{R}_d|}\right)^{N_y/2} exp\left[\frac{-1}{2}\left(\mathbf{y} - \sum_{k=1}^{t_n}\mathbf{S}\mathbf{a}_k\right)^H\mathbf{R}_d^{-1}\left(\mathbf{y} - \sum_{k=1}^{t_n}\mathbf{S}\mathbf{a}_k\right)\right] \tag{5.26}$$

here $\mathbf{R}_d$ is the disturbance covariance matrix which is obtained during the initialisation phase. Within the disturbance covariance matrix, clutter is static. However, the noise power at the sensing nodes may vary with time, which is required to be estimated to achieve reliable target detection. Using $\mathbf{R}_d$ from Equation 5.21, the modified probability density functions under hypothesis H_0 and H_1 can be written as

$$f(\mathbf{y}|\sigma^2, H_0) = \left(\frac{1}{\pi\sigma^2|\mathbf{C}^{-1}|}\right)^{N_y/2} exp\left[\frac{-1}{2\sigma^2}\left(\mathbf{y}^H\mathbf{C}\mathbf{y}\right)\right] \tag{5.27}$$

$$f(\mathbf{y}|\mathbf{a}, \sigma^2, H_1) = \left(\frac{1}{\pi\sigma^2|\mathbf{C}^{-1}|}\right)^{N_y/2} exp\left[\frac{-1}{2\sigma^2}(\mathbf{y} - \sum_{k=1}^{t_n}\mathbf{S}\mathbf{a}_k)^H\mathbf{C}(\mathbf{y} - \sum_{k=1}^{t_n}\mathbf{S}\mathbf{a}_k)\right] \tag{5.28}$$

here the unknown parameters are target impulse response, $\mathbf{a}$ and noise variance, σ^2. The test statistic based on likelihood ratio test can be written as

$$\mathbb{T}_0 = \frac{\max\limits_{\sigma^2} f(\mathbf{y}|\sigma^2, H_0)}{\max\limits_{\mathbf{a},\sigma^2} f(\mathbf{y}|\mathbf{a}, \sigma^2, H_1)} \tag{5.29}$$

The value of σ^2 that maximises the pdf under hypothesis H_0 is obtained by nulling the derivative with respect to σ^2 which gives,

$$\hat{\sigma}_0^2 = \frac{1}{N_y}\left(\mathbf{y}^H\mathbf{C}\mathbf{y}\right) \tag{5.30}$$

Similarly, maximising the pdf hypothesis H_1 with respect to σ^2 gives,

$$\hat{\sigma}_1^2 = \frac{1}{N_y}\left((\mathbf{y} - \sum_{k=1}^{t_n}\mathbf{S}\mathbf{a}_k)^H\mathbf{C}(\mathbf{y} - \sum_{k=1}^{t_n}\mathbf{S}\mathbf{a}_k)\right) \tag{5.31}$$

Substituting the ML estimates $\hat{\sigma}_0^2$ and $\hat{\sigma}_1^2$, the probability density functions under hypothesis H_0 and H_1 can be rewritten as

$$f(\mathbf{y}|\sigma^2, H_0) = \left(\frac{1}{\frac{\pi}{N_y}\left(\mathbf{y}^H\mathbf{C}\mathbf{y}\right)|\mathbf{C}^{-1}|}\right)^{N_y/2} exp(-N_y) \tag{5.32}$$

$$f(\mathbf{y}|\mathbf{a}, \sigma^2, H_1) = \left(\frac{1}{\frac{\pi}{N_y}\left((\mathbf{y} - \sum_{k=1}^{t_n}\mathbf{S}\mathbf{a}_k)^H\mathbf{C}(\mathbf{y} - \sum_{k=1}^{t_n}\mathbf{S}\mathbf{a}_k)\right)|\mathbf{C}^{-1}|}\right)^{N_y/2} exp(-N_y) \tag{5.33}$$

Substituting Equation 5.32 and Equation 5.33 in Equation 5.29 and after subsequent mathematical manipulations, the modified test statistic is obtained as

$$\mathbb{T} = \frac{(\mathbf{y} - \sum_{k=1}^{t_n}\mathbf{S}\mathbf{a}_k)^H\mathbf{C}(\mathbf{y} - \sum_{k=1}^{t_n}\mathbf{S}\mathbf{a}_k)}{\mathbf{y}^H\mathbf{C}\mathbf{y}} \underset{H_1}{\overset{H_0}{\gtrless}} \gamma \tag{5.34}$$

Obtaining the ML estimate of $\mathbf{a}$ in Equation 5.34 is a common weighted least-square problem the solution to which can be written as

$$\hat{\mathbf{a}} = (\mathbf{S}^H\mathbf{C}\mathbf{S})^{-1}\mathbf{S}^H\mathbf{C}\mathbf{y} \tag{5.35}$$

Substituting the estimate of $\mathbf{a}$ and after subsequent mathematical manipulations, Equation 5.34 can be rewritten as

$$\mathbb{T} = \frac{\mathbf{y}^H\mathbf{C}\mathbf{y} - \mathbf{y}^H\mathbf{C}\mathbf{S}\hat{\mathbf{a}} - (\mathbf{S}\hat{\mathbf{a}})^H\mathbf{C}\mathbf{y} + (\mathbf{S}\hat{\mathbf{a}})^H\mathbf{C}(\mathbf{S}\hat{\mathbf{a}})}{\mathbf{y}^H\mathbf{C}\mathbf{y}} \tag{5.36}$$

However, it can be observed that,

$$\mathbf{y}^H\mathbf{C}\mathbf{S}\hat{\mathbf{a}} = (\mathbf{S}\hat{\mathbf{a}})^H\mathbf{C}\mathbf{y} = (\mathbf{S}\hat{\mathbf{a}})^H\mathbf{C}(\mathbf{S}\hat{\mathbf{a}}) = \mathbf{y}^H\mathbf{C}\mathbf{S}(\mathbf{S}^H\mathbf{C}\mathbf{S})^{-1}\mathbf{S}^H\mathbf{C}\mathbf{y} \tag{5.37}$$

Therefore, substituting Equation 5.37 in Equation 5.36 and after subsequent transformations, the test statistic can be written as

$$\mathbb{T} = \frac{\mathbf{y}^H\mathbf{C}\mathbf{y} - \mathbf{y}^H\mathbf{C}\mathbf{S}(\mathbf{S}^H\mathbf{C}\mathbf{S})^{-1}\mathbf{S}^H\mathbf{C}\mathbf{y}}{\mathbf{y}^H\mathbf{C}\mathbf{S}(\mathbf{S}^H\mathbf{C}\mathbf{S})^{-1}\mathbf{S}^H\mathbf{C}\mathbf{y}} \underset{H_1}{\overset{H_0}{\gtrless}} \gamma \tag{5.38}$$

When the output of the receiver filter is matched to $\mathbf{C}\mathbf{S}(\mathbf{S}^H\mathbf{C}\mathbf{S})^{-1/2}$, Equation 5.38 reduces to,

$$\mathbb{T} = \frac{\mathbf{y}^H\mathbf{C}\mathbf{y} - (\mathbf{f}^H\mathbf{y})^H(\mathbf{f}^H\mathbf{y})}{(\mathbf{f}^H\mathbf{y})^H(\mathbf{f}^H\mathbf{y})} \underset{H_1}{\overset{H_0}{\gtrless}} \gamma \tag{5.39}$$

The hybrid test statistic in Equation 5.39 is an energy detector followed by a matched filter.

5.6 Secondary Detector Design

Within harsh sensing environments with multiple clusters of sensing nodes operating simultaneously, the sensing nodes face the challenge of detecting the existence of targets in the presence of clutter and interfering waveforms. Under such harsh sensing conditions, the reliability of the target detection procedure is significantly reduced. Due to heterogeneous nature of the sensing environment, predicting the nature of the interference at the sensing nodes is a complex procedure. Within a dynamic sensing environment, the sensing nodes are required to gather large

amounts of secondary data constantly to keep up with the fast changing conditions. This imposes a huge power and processing burden on the resource constrained WSN. The sensing nodes are assumed to coordinate among themselves and have the knowledge of waveforms, which are transmitted from the neighbouring clusters. However, due to heterogeneous nature of the sensing environment, the interfering waveforms from different cluster are subjected to different impulse responses. The objective is to develop a target detector which has the ability to make a distinction between hypothesis H_0 and H_1 based on the received signal samples which are corrupted by noise, clutter and interfering signals. In this section, a mathematical model for a computationally efficient target detector is derived which is implemented at the control centre. The proposed target detector exploits the cooperative nature of WSN and reduces the need to collect secondary data. From the received signal models described in Equation 5.23 and Equation 5.24, the probability density functions for the received signal under hypothesis H_0 and H_1 respectively are,

$$f(\mathbf{y}|\mathbf{b},\sigma^2,H_0) = \left(\frac{1}{\pi\sigma^2|\mathbf{C}^{-1}|}\right)^{N_yN_s/2} exp\left[\frac{-1}{2\sigma^2}\left((\mathbf{y}-\sum_{k=1}^{b_n}\mathbf{H}_k\mathbf{b}_k)^H\mathbf{C}(\mathbf{y}-\sum_{k=1}^{b_n}\mathbf{H}_k\mathbf{b}_k)\right)\right] \tag{5.40}$$

$$f(\mathbf{y}|\mathbf{a},\mathbf{b},\sigma^2,H_1) = \left(\frac{1}{\pi\sigma^2|\mathbf{C}^{-1}|}\right)^{N_yN_s/2} exp\left[\frac{-1}{2\sigma^2}\left((\mathbf{y}-\sum_{k=1}^{t_n}\mathbf{S}\mathbf{a}_k-\sum_{k=1}^{b_n}\mathbf{H}_k\mathbf{b}_k)^H\mathbf{C}(\mathbf{y}-\sum_{k=1}^{t_n}\mathbf{S}\mathbf{a}_k-\sum_{k=1}^{b_n}\mathbf{H}_k\mathbf{b}_k)\right)\right] \tag{5.41}$$

5.6.1 Case 1: Detector Design With Known σ^2 and 1 Interfering Node

In this case it is assumed that the noise variance is known to that target detector and only one neighbouring sensing node is contributing to interference i.e., $b_n = 1$. This is applicable to the scenario where sensing nodes are widely scattered and the interference from the other sensing nodes is negligibly weak. The test statistic, $\mathbb{T}$ for the proposed target detector is obtained from the probability density functions defined in Equation 5.40 and Equation 5.41 where the unknown parameters are replaced by their MLEs which is written as

$$\mathbb{T} = \frac{\max\limits_{\mathbf{b}} f(\mathbf{y}|\mathbf{b}, H_0)}{\max\limits_{\mathbf{a},\mathbf{b}} f(\mathbf{y}|\mathbf{a}, \mathbf{b}, H_1)} \underset{H_1}{\overset{H_0}{\gtrless}} \gamma \tag{5.42}$$

The MLEs of the unknown parameters are obtained by differentiating the exponential arguments of the pdfs in Equation 5.40 and Equation 5.41 with respect to the corresponding unknown parameter. The corresponding derivatives under hypothesis H_0 and H_1 are equated to zero to obtain the ML estimate. Since $\mathbf{C}$ is Hermitian, differentiating the exponential term in the Equation 5.41 with respect to $\mathbf{b}$ gives,

$$\mathbf{H}^H\mathbf{C}\mathbf{H}\hat{\mathbf{b}}_1 = \mathbf{H}^H\mathbf{C}\mathbf{y} - \mathbf{H}^H\mathbf{C}\mathbf{S}\sum_{k=1}^{t_n}\hat{\mathbf{a}}_k \tag{5.43}$$

here $\hat{\mathbf{b}}_1$ denotes the ML estimate of interference impulse response under hypothesis H_1 and $\hat{\mathbf{a}}$ represents the ML estimate of the target impulse response, which is unknown at this stage. Similarly, from Equation 5.40 the ML estimate of $\mathbf{b}$ under hypothesis H_0 can be obtained as

$$\mathbf{H}^H\mathbf{C}\mathbf{H}\hat{\mathbf{b}}_0 = \mathbf{H}^H\mathbf{C}\mathbf{y} \tag{5.44}$$

here $\hat{\mathbf{b}}_0$ denotes the ML estimate of $\mathbf{b}$ under hypothesis H_0. With the knowledge

of the transmit and the interfering waveforms available to the control centre, the reference correlation matrices are generated as

$$\mathbf{R_s} = \mathbf{S}^H\mathbf{CS} \tag{5.45}$$

$$\mathbf{R_h} = \mathbf{H}^H\mathbf{CH} \tag{5.46}$$

$\mathbf{R_s}$ and $\mathbf{R_h}$ can be interpreted as the transmit and interfering signal correlation matrices respectively. Similarly $\mathbf{R_{hs}}$ which is the reference cross-correlation matrix between the transmit and the interfering signals is defined as

$$\mathbf{R_{hs}} = \mathbf{H}^H\mathbf{CS} \tag{5.47}$$

Finally the cross-correlation matrices for received signal with respect to the transmit and the interfering signals which are $\mathbf{R_{sy}}$ and $\mathbf{R_{hy}}$ respectively are defined as

$$\mathbf{R_{hy}} = \mathbf{H}^H\mathbf{Cy} \tag{5.48}$$

$$\mathbf{R_{sy}} = \mathbf{S}^H\mathbf{Cy} \tag{5.49}$$

Using the correlation matrices, Equation 5.43 and Equation 5.44 can be rewritten as

$$\mathbf{R_h}\hat{\mathbf{b}}_1 = \mathbf{R_{hy}} - \mathbf{R_{hs}}\hat{\mathbf{a}} \tag{5.50}$$

$$\mathbf{R_h}\hat{\mathbf{b}}_0 = \mathbf{R_{hy}} \tag{5.51}$$

Using Equation 5.50, the ML estimate of the unknown target impulse response is obtained by differentiating the exponential argument in Equation 5.41 with respect to $\mathbf{a}$ and equating it to zero. Solving this differential equation gives,

$$\mathbf{S}^H\mathbf{Q}\mathbf{S}\sum_{k=1}^{t_n}\hat{\mathbf{a}}_k = \mathbf{S}^H\mathbf{Q}\mathbf{y} \tag{5.52}$$

where

$$\mathbf{Q} = \left(\mathbf{I} - \mathbf{H}{\mathbf{R_h}}^{-1}\mathbf{H}^H\mathbf{C}\right)^H \mathbf{C}\left(\mathbf{I} - \mathbf{H}{\mathbf{R_h}}^{-1}\mathbf{H}^H\mathbf{C}\right) \tag{5.53}$$

here $\hat{\mathbf{a}}$ represents the ML estimate of the target impulse response under hypothesis H_1. The test statistic for the proposed target detector in this case is obtained from Equation 5.42 as

$$\mathbb{T} = exp\left[\frac{-1}{2\sigma^2}\left(\left(\mathbf{y}-\sum_{k=1}^{t_n}\mathbf{S}\hat{\mathbf{a}}_k-\mathbf{H}\hat{\mathbf{b}}_1\right)^H\mathbf{C}\left(\mathbf{y}-\sum_{k=1}^{t_n}\mathbf{S}\hat{\mathbf{a}}_k-\mathbf{H}\hat{\mathbf{b}}_1\right)-\left(\mathbf{y}-\mathbf{H}\hat{\mathbf{b}}_0\right)^H\mathbf{C}\left(\mathbf{y}-\mathbf{H}\hat{\mathbf{b}}_0\right)\right)\right] \tag{5.54}$$

To solve Equation 5.54 logarithm is applied on both sides, and use the correlation matrices defined in equations Equation 5.46 to Equation 5.49 which gives the desired test statistic,

$$ln\,\mathbb{T} = \frac{-1}{2\sigma^2}\Big(\hat{\mathbf{a}}^H\mathbf{R_{hs}}^H{\mathbf{R_h}}^{-1}\mathbf{R_{hs}}\hat{\mathbf{a}} - {\mathbf{R_{sy}}}^H\hat{\mathbf{a}} - \hat{\mathbf{a}}^H\mathbf{R_{sy}} + \hat{\mathbf{a}}^H\mathbf{R_s}\hat{\mathbf{a}} + {\mathbf{R_{hy}}}^H\hat{\mathbf{b}}_1 + \hat{\mathbf{b}}_1^H\mathbf{R_{hy}} - 2\hat{\mathbf{b}}_1^H\mathbf{R_h}\hat{\mathbf{b}}_1\Big) \underset{H_0}{\overset{H_1}{\gtrless}} ln\,\gamma \tag{5.55}$$

To optimise the test statistic derived in Equation 5.55, a two-stage target detection model has been adopted. The proposed two-stage design model for WSN is summarised in Figure 5.4. Considering the operational nature of WSN with static clutter and known interfering waveforms, target detection procedure is performed in two stages which are, 1) Initialisation stage and 2) Operational stage. In the initialisation phase, the known knowledge of clutter and interference statistics are exploited to generate the measurement and test statistic coefficients. Since the

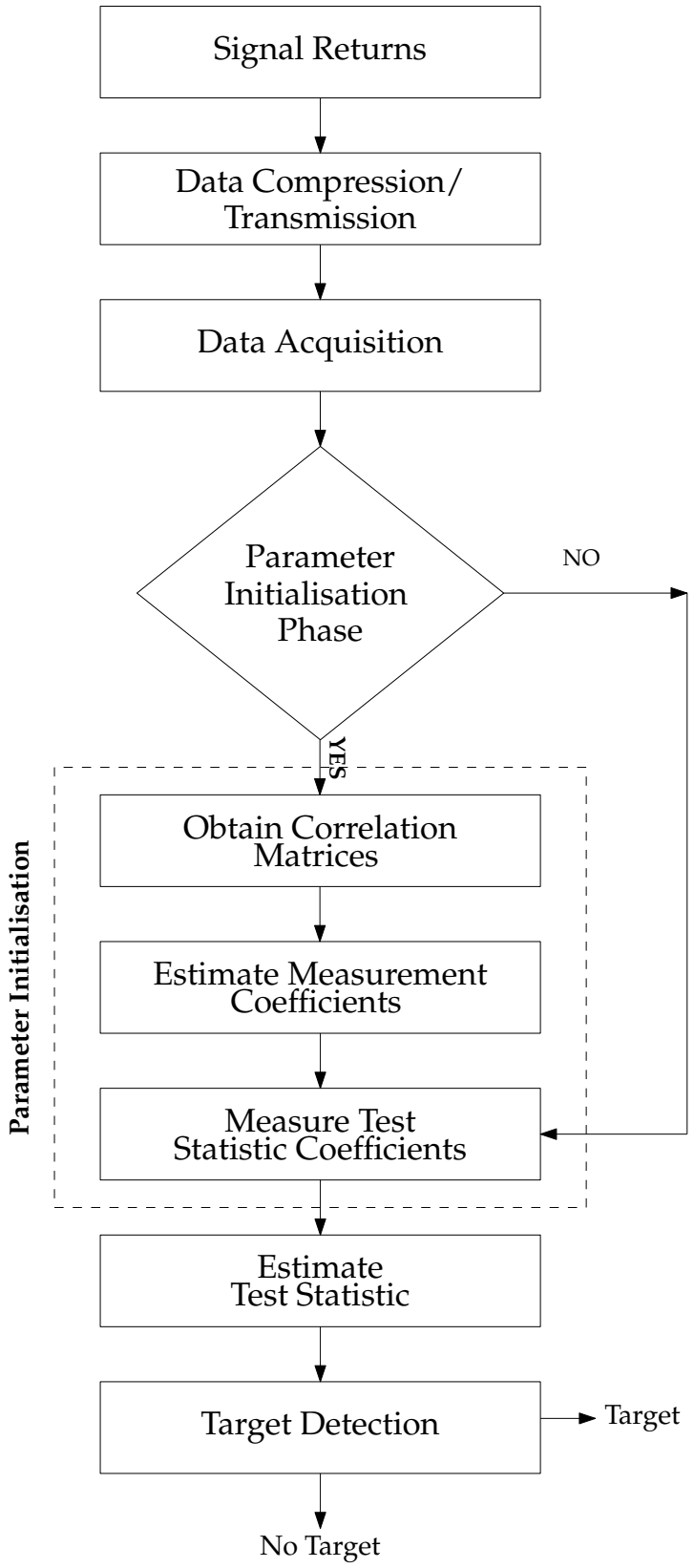

FIGURE 5.4: Operational principle of the proposed 2-stage target detection model

sensing conditions are expected to be static over a significant period of time, the initialisation phase is only required to be performed periodically. In the operational phase, the test statistic coefficients and the received signal data are used to generate the actual measurable test statistic based on which a final decision is made regarding the existence or absence of the target. The measurement coefficients are written as

$$\begin{bmatrix} \boldsymbol{\nabla}_1 & \boldsymbol{\nabla}_2 \\ \\ \boldsymbol{\nabla}_3 & \boldsymbol{\nabla}_4 \end{bmatrix} = \begin{bmatrix} (\mathbf{QS})(\mathbf{S}^H\mathbf{QS})^{-1} & \mathbf{R_h}^{-1}\mathbf{H}^H\mathbf{C} \\ \\ \boldsymbol{\nabla}_1\mathbf{R_{hs}}^H\boldsymbol{\nabla}_2 & \boldsymbol{\nabla}_1\mathbf{S}^H\mathbf{C} \end{bmatrix} \tag{5.56}$$

Using the ML estimates of $\hat{\mathbf{a}}$ and $\hat{\mathbf{b}}$ and the measurement coefficients in Equation 5.56, the optimised test statistic for the proposed target detector can be obtained as

$$ln\,\mathbb{T} = \mathbf{y}^H\boldsymbol{\chi}\mathbf{y} \underset{H_1}{\overset{H_0}{\gtrless}} - 2\sigma^2 ln\,\gamma \tag{5.57}$$

$$\boldsymbol{\chi} = (\boldsymbol{\nabla}_3^H + \boldsymbol{\nabla}_3) - (\boldsymbol{\nabla}_4^H + \boldsymbol{\nabla}_4) - (\boldsymbol{\nabla}_3 - \boldsymbol{\nabla}_4)\mathbf{C}^{-1}\boldsymbol{\nabla}_4^H \tag{5.58}$$

where $\boldsymbol{\chi}$ is the test statistic coefficient. Since $\boldsymbol{\chi}$ and the measurement coefficients are independent of the received signal data, they can be generated during the initialisation phase which reduces the computational complexity during the operational phase.

5.6.2 Case 2: Detector Design With Unknown σ^2 and 1 Interfering Nodes

In this case, it is assumed that the noise variance is unknown to the target detector. The presence of only one interfering node is assumed. The estimates of the unknown parameters $\mathbf{a}$ and $\mathbf{b}$ are obtained as explained in Equation 5.50 to Equation 5.52. The ML estimates of σ^2 under hypothesis H_0 and H_1 are obtained

by differentiating Equation 5.40 and Equation 5.41 respectively with respect to σ^2 as

$$\hat{\sigma}_0^2 = \frac{1}{N_y N_s}\left(\mathbf{y}^H\mathbf{C}\mathbf{y} - \mathbf{R_{hy}}^H\hat{\mathbf{b}}_0 - \hat{\mathbf{b}}_0^H\mathbf{R_{hy}} - \hat{\mathbf{b}}_0^H\mathbf{R_h}\hat{\mathbf{b}}_0\right) \tag{5.59}$$

$$\hat{\sigma}_1^2 = \frac{1}{N_y N_s}\Big(\mathbf{y}^H\mathbf{C}\mathbf{y} - \mathbf{R_{sy}}^H\hat{\mathbf{a}} - \mathbf{R_{hy}}^H\hat{\mathbf{b}}_1 + \hat{\mathbf{a}}^H\big(\mathbf{R_s}\hat{\mathbf{a}} + \mathbf{R_{hs}}^H\hat{\mathbf{b}}_1 - \mathbf{R_{sy}}\big) + \hat{\mathbf{b}}_1^H\big(\mathbf{R_{hs}}\hat{\mathbf{a}} + \mathbf{R_h}\hat{\mathbf{b}}_1 - \mathbf{R_{hy}}\big)\Big) \tag{5.60}$$

here $\hat{\sigma}_0^2$ and $\hat{\sigma}_1^2$ are the MLEs of noise variance under hypothesis H_0 and H_1 respectively. Using $\hat{\sigma}^2$, $\hat{\mathbf{a}}$ and $\hat{\mathbf{b}}$, the test statistic for the proposed target detector is written as

$$\mathbb{T} = \frac{\max\limits_{\sigma^2,\mathbf{b}} f(\mathbf{y}|\mathbf{b},\sigma^2,H_0)}{\max\limits_{\sigma^2,\mathbf{a},\mathbf{b}} f(\mathbf{y}|\mathbf{a},\mathbf{b},\sigma^2,H_1)} = \left(\frac{\hat{\sigma}_1^2}{\hat{\sigma}_0^2}\right)^{N_y N_s} \underset{H_1}{\overset{H_0}{\gtrless}} \gamma \tag{5.61}$$

Substituting $\hat{\sigma}_0^2$ and $\hat{\sigma}_1^2$ and correlation matrices defined in equations Equation 5.46 to Equation 5.49 gives the desired test statistic as

$$\mathbb{T} = \frac{q_1}{q_0} \underset{H_1}{\overset{H_0}{\gtrless}} \sqrt[N_y N_s]{\gamma} \tag{5.62}$$

where q_0 and q_1 are given by,

$$q_0 = \mathbf{y}^H\mathbf{C}\mathbf{y} - \mathbf{R_{hy}}^H\mathbf{R}_h^{-1}\mathbf{R_{hy}} \tag{5.63}$$

$$q_1 = \mathbf{y}^H\mathbf{C}\mathbf{y} - \mathbf{R_{hy}}^H\mathbf{R}_h^{-1}\mathbf{R_{hy}} + \hat{\mathbf{a}}^H\mathbf{R_{hs}}^H\mathbf{R}_h^{-1}\mathbf{R_{hs}}\hat{\mathbf{a}} - \mathbf{R_{sy}}^H\hat{\mathbf{a}} - \hat{\mathbf{a}}^H\mathbf{R_{sy}} + \hat{\mathbf{a}}^H\mathbf{R_s}\hat{\mathbf{a}} + \mathbf{R_{hy}}^H\hat{\mathbf{b}}_1 + \hat{\mathbf{b}}_1^H\mathbf{R_{hy}} - 2\hat{\mathbf{b}}_1^H\mathbf{R_h}\hat{\mathbf{b}}_1 \tag{5.64}$$

To optimise the test statistic in Equation 5.62, Equation 5.63 and Equation 5.64 are solved by using the measurement coefficients defined in Equation 5.56. This leads to generating the test statistic coefficients given by,

$$\boldsymbol{\chi}_0 = \mathbf{C} - \boldsymbol{\nabla}_2^H \mathbf{R}_\mathbf{h} \boldsymbol{\nabla}_2 \tag{5.65}$$

$$\boldsymbol{\chi}_1 = \boldsymbol{\chi}_0 + (\boldsymbol{\nabla}_3^H + \boldsymbol{\nabla}_3) - (\boldsymbol{\nabla}_4^H + \boldsymbol{\nabla}_4) - (\boldsymbol{\nabla}_3 - \boldsymbol{\nabla}_4)\mathbf{C}^{-1}\boldsymbol{\nabla}_4^H \tag{5.66}$$

here $q_0 = \mathbf{y}^H \boldsymbol{\chi}_0 \mathbf{y}$ and $q_1 = \mathbf{y}^H \boldsymbol{\chi}_1 \mathbf{y}$. Therefore, the optimised test statistic for the proposed target detector is,

$$\mathbb{T} = \left(\frac{\mathbf{y}^H \boldsymbol{\chi}_1 \mathbf{y}}{\mathbf{y}^H \boldsymbol{\chi}_0 \mathbf{y}} \right) \underset{H_1}{\overset{H_0}{\gtrless}} \sqrt[N_y N_s]{\gamma} \tag{5.67}$$

5.6.3 Case 3: Detector Design With Unknown σ^2 and n Interfering Nodes

Here a target detector has been designed for a generalised scenario with unknown noise variance and multiple interfering nodes i.e., $b_n = n$. Since the interfering waveforms are mutually independent, estimating the unknown impulse responses from each interfering waveform allows to dynamically adopt to any changes in the choice of transmit waveforms within the neighbourhood of the sensing node. The probability density functions of the received signal under hypothesis H_0 Equation 5.68 and H_1 Equation 5.69 are given by,

$$f(\bar{\mathbf{y}}|\mathbf{b}_1, \mathbf{b}_2 \ldots \mathbf{b}_n, \sigma^2, H_0) = \left(\frac{1}{\pi\sigma^2 |\mathbf{C}^{-1}|} \right)^{N_y N_s/2} exp\left[\frac{-1}{2\sigma^2} \left((\mathbf{y} - \sum_{k=1}^{b_n} \mathbf{H}_k \mathbf{b}_k)^H \mathbf{C} \right.\right.$$
$$\left.\left. (\mathbf{y} - \sum_{k=1}^{b_n} \mathbf{H}_k \mathbf{b}_k) \right) \right] \tag{5.68}$$

$$f(\bar{\mathbf{y}}|\mathbf{b}_1,\mathbf{b}_2\dots\mathbf{b}_n,\mathbf{a},\sigma^2,H_1)=\left(\frac{1}{\pi\sigma^2|\mathbf{C}^{-1}|}\right)^{N_yN_s/2}exp\left[\frac{-1}{2\sigma^2}\left((\mathbf{y}-\sum_{k=1}^{t_n}\mathbf{S}\mathbf{a}_k-\sum_{k=1}^{b_n}\mathbf{H}_k\mathbf{b}_k)^H\mathbf{C}\right.\right.$$
$$\left.\left.(\mathbf{y}-\sum_{k=1}^{t_n}\mathbf{S}\mathbf{a}_k-\sum_{k=1}^{b_n}\mathbf{H}_k\mathbf{b}_k)\right)\right] \quad (5.69)$$

The test statistic for the proposed detector in this scenario can be written as

$$\mathbb{T}=\frac{\max\limits_{\sigma^2,\mathbf{b_1},\mathbf{b_2}\dots\mathbf{b_n}} f(\mathbf{y}|\sigma^2,\mathbf{b}_1,\mathbf{b}_2\dots\mathbf{b}_n,H_0)}{\max\limits_{\sigma^2,\mathbf{a},\mathbf{b_1},\mathbf{b_2}\dots\mathbf{b_n}} f(\mathbf{y}|\sigma^2,\mathbf{a},\mathbf{b}_1,\mathbf{b}_2\dots\mathbf{b}_n,H_1)}\underset{H_1}{\overset{H_0}{\gtrless}}\gamma \quad (5.70)$$

The unknown estimates of $\mathbf{b}_1,\mathbf{b}_2\dots\mathbf{b}_n$ under hypothesis H_0 and H_1 are obtained by performing the procedure described in Equation 5.43 and Equation 5.44 recursively for each known interfering waveform. However, this requires solving a complex n^{th} order differential equation which is computationally intense. Since it is necessary to estimate each interfering signal independently, to obtain a generalised solution recursive correlation matrices for the j^{th} interfering signal have been defined as

$$\begin{bmatrix}\mathbf{R}_{\mathbf{h}jk}\\ \mathbf{R}_{\mathbf{h}js}\\ \mathbf{R}_{\mathbf{h}jy}\end{bmatrix}=\mathbf{H}_j^H\mathbf{K}_j\begin{bmatrix}\mathbf{H}_k\\ \mathbf{S}\\ \mathbf{y}\end{bmatrix} \quad (5.71)$$

here $\mathbf{K}_j$ is the projection matrix for j^{th} interfering signal which is measured as

$$\mathbf{K}_j=(\prod_{l=1}^{j}\boldsymbol{\psi}_{l-1})^H\mathbf{C}(\prod_{l=1}^{j}\boldsymbol{\psi}_{l-1}) \quad (5.72)$$

$$\boldsymbol{\psi}_n = \mathbf{I}-\mathbf{H}_n\mathbf{R}_{\mathbf{h}nn}^{-1}\mathbf{H}_n^H\mathbf{K}_n \quad \text{n}\neq 0 \quad (5.73)$$

$$\boldsymbol{\psi}_0 = \mathbf{I} \quad (5.74)$$

Generalised solutions for the recursive impulse response estimates of the j^{th} interfering signal under hypothesis H_0 and H_1 are written as

$$\begin{aligned}\hat{\mathbf{b}}_{j0} &= (\mathbf{H}_j^H\mathbf{K}_j\mathbf{H}_j)^{-1}\mathbf{H}_j^H\mathbf{K}_j(\mathbf{y} - \sum_{k=j+1}^{n}\mathbf{H}_k\hat{\mathbf{b}}_k) \\ &= \mathbf{R}_{\mathbf{h}jj}^{-1}(\mathbf{R}_{\mathbf{h}jy} - \sum_{k=j+1}^{n}\mathbf{R}_{\mathbf{h}jk}\hat{\mathbf{b}}_k) \end{aligned} \tag{5.75}$$

$$\begin{aligned}\hat{\mathbf{b}}_{j1} &= (\mathbf{H}_j^H\mathbf{K}_j\mathbf{H}_j)^{-1}\mathbf{H}_j^H\mathbf{K}_j(\mathbf{y} - \mathbf{S}\hat{\mathbf{a}} - \sum_{k=j+1}^{n}\mathbf{H}_k\hat{\mathbf{b}}_k) \\ &= \mathbf{R}_{\mathbf{h}jj}^{-1}(\mathbf{R}_{\mathbf{h}jy} - \mathbf{R}_{\mathbf{hs}j}\hat{\mathbf{a}} - \sum_{k=j+1}^{n}\mathbf{R}_{\mathbf{h}jk}\hat{\mathbf{b}}_k) \end{aligned} \tag{5.76}$$

While the process of estimating the unknown parameters recursively seems to be a tedious procedure, substituting these ML estimates in Equation 5.68 and Equation 5.69 respectively and subsequent mathematical analysis reveals that a simple generalised solution can be obtained. Substituting the ML estimates of the interfering signals, Equation 5.68 and Equation 5.69 can be rewritten as

$$f(\mathbf{y}|\sigma^2, H_0) = \left(\frac{1}{\pi\sigma^2|\mathbf{C}^{-1}|}\right)^{N_yN_s/2} exp\left[\frac{-1}{2\sigma^2}\left(\mathbf{y}^H\mathbf{K}_{n+1}\mathbf{y}\right)\right] \tag{5.77}$$

$$f(\mathbf{y}|\mathbf{a}, \sigma^2, H_1) = \left(\frac{1}{\pi\sigma^2|\mathbf{C}^{-1}|}\right)^{N_yN_s/2} exp\left[\frac{-1}{2\sigma^2}\left((\mathbf{y}-\sum_{k=1}^{t_n}\mathbf{S}\mathbf{a}_k)^H\mathbf{K}_{n+1}(\mathbf{y}-\sum_{k=1}^{t_n}\mathbf{S}\mathbf{a}_k)\right)\right] \tag{5.78}$$

From Equation 5.72, the subscript $n+1$ for the interference projection matrix $\mathbf{K}$ is chosen to accommodate all n interfering waveforms. The interference projection matrix can be obtained during the initialisation stage using the known information regarding clutter and interfering waveforms. Hence, the number of interfering nodes has no impact on the computational complexity of the target

detection procedure during the operational phase. The control centre gathers the received signal data from all the sensing nodes within its cluster to detect the existence of targets. The amount of power consumed during the data transmission process between sensing nodes and the control centre has a significant impact on the lifetime of the sensing nodes. To reduce the transmission costs, compressive sensing has been considered where the sensing nodes are only required to transmit compressed received signal samples to the control centre. The received signal data at the i^{th} sensing node is compressed by projecting it onto a measurement matrix $\boldsymbol{\phi}_i$ such that $\bar{\mathbf{y}}_i = \boldsymbol{\phi}_i \mathbf{y}_i$, where $\bar{\mathbf{y}}_i$ represents the compressed data. The dimensions $M \times N_y$ of $\boldsymbol{\phi}_i$ are chosen such that $M \ll N_y$. $\boldsymbol{\phi}_i$ is usually orthogonal i.e., $\boldsymbol{\phi}_i \boldsymbol{\phi}_i^H = \mathbf{I}$. A compression ratio which is defined by $\mu = \frac{M}{N_y}$, is a measure of compressibility. The choice of compression ratio μ is chosen as a trade-off between the transmission costs and target detection reliability. The compressed received signal data at the control centre can be written as

$$\begin{aligned} \bar{\mathbf{y}} &= [\boldsymbol{\phi}_1 \mathbf{y}_1, \boldsymbol{\phi}_2 \mathbf{y}_2, \ldots, \boldsymbol{\phi}_{Ns} \mathbf{y}_{Ns}]^T \\ &= [\bar{\mathbf{y}}_1, \bar{\mathbf{y}}_2, \ldots, \bar{\mathbf{y}}_{Ns}]^T \end{aligned}$$

Therefore, the probability density functions under hypothesis H_0 and H_1 with the compressed received signal samples are,

$$f(\bar{\mathbf{y}}|\sigma^2, H_0) = \left(\frac{1}{\pi\sigma^2|\mathbf{C}^{-1}|}\right)^{N_y N_s/2} exp\left[\frac{-1}{2\sigma^2}\left(\bar{\mathbf{y}}^H \boldsymbol{\phi} \mathbf{K}_{n+1} \boldsymbol{\phi}^H \bar{\mathbf{y}}\right)\right] \tag{5.79}$$

$$f(\bar{\mathbf{y}}|\mathbf{a}, \sigma^2, H_1) = \left(\frac{1}{\pi\sigma^2|\mathbf{C}^{-1}|}\right)^{N_y N_s/2} exp\left[\frac{-1}{2\sigma^2}\left((\bar{\mathbf{y}} - \sum_{k=1}^{t_n} \bar{\mathbf{S}}\mathbf{a}_k)^H \boldsymbol{\phi} \mathbf{K}_{n+1} \boldsymbol{\phi}^H (\bar{\mathbf{y}} - \sum_{k=1}^{t_n} \bar{\mathbf{S}}\mathbf{a}_k)\right)\right] \tag{5.80}$$

where $\bar{\mathbf{S}} = \boldsymbol{\phi}\mathbf{S}$ and n is the number of interfering nodes. The ML estimates $\hat{\mathbf{a}}$ and $\hat{\sigma}^2$ can now be obtained as discussed previously.

$$\left(\bar{\mathbf{S}}^H(\boldsymbol{\phi}\mathbf{K}_{n+1}\boldsymbol{\phi}^H)\bar{\mathbf{S}}\right)\sum_{k=1}^{t_n}\hat{\mathbf{a}}_k = \bar{\mathbf{S}}^H(\boldsymbol{\phi}\mathbf{K}_{n+1}\boldsymbol{\phi}^H)\bar{\mathbf{y}} \tag{5.81}$$

$$\hat{\sigma}_0^2 = \frac{1}{MN_s}\left(\bar{\mathbf{y}}^H(\boldsymbol{\phi}\mathbf{K}_{n+1}\boldsymbol{\phi}^H)\bar{\mathbf{y}}\right) \tag{5.82}$$

$$\hat{\sigma}_1^2 = \frac{1}{MN_s}\left((\bar{\mathbf{y}} - \sum_{k=1}^{t_n}\bar{\mathbf{S}}\hat{\mathbf{a}}_k)^H(\boldsymbol{\phi}\mathbf{K}_{n+1}\boldsymbol{\phi}^H)(\bar{\mathbf{y}} - \sum_{k=1}^{t_n}\bar{\mathbf{S}}\hat{\mathbf{a}}_k)\right) \tag{5.83}$$

Substituting the ML estimates in Equation 5.70 gives the test statistic for the proposed target detector. To optimise the target detection procedure, a measurement coefficient, $\boldsymbol{\nabla}$ has been defined for the test statistic as

$$\boldsymbol{\nabla} = (\boldsymbol{\phi}\mathbf{K}_{n+1}\boldsymbol{\phi}^H)\bar{\mathbf{S}}\left(\bar{\mathbf{S}}^H(\boldsymbol{\phi}\mathbf{K}_{n+1}\boldsymbol{\phi}^H)\bar{\mathbf{S}}\right)^{-1}\bar{\mathbf{S}}^H(\boldsymbol{\phi}\mathbf{K}_{n+1}\boldsymbol{\phi}^H) \tag{5.84}$$

Therefore, the optimised test statistic, $\mathbb{T}$ for the proposed target detector is expressed as

$$\mathbb{T} = \left(\frac{\bar{\mathbf{y}}^H\boldsymbol{\chi}_1\bar{\mathbf{y}}}{\bar{\mathbf{y}}^H\boldsymbol{\chi}_0\bar{\mathbf{y}}}\right)\underset{H_1}{\overset{H_0}{\gtrless}} \sqrt[N_yN_s]{\gamma} \tag{5.85}$$

here $\boldsymbol{\chi}_0$ and $\boldsymbol{\chi}_1$ are test statistic coefficients given by,

$$\boldsymbol{\chi}_0 = \boldsymbol{\phi}\mathbf{K}_{n+1}\boldsymbol{\phi}^H \tag{5.86}$$

$$\boldsymbol{\chi}_1 = \boldsymbol{\chi}_0 - 2\boldsymbol{\nabla} + \boldsymbol{\nabla}(\boldsymbol{\phi}\mathbf{K}_{n+1}\boldsymbol{\phi}^H)^{-1}\boldsymbol{\nabla} \tag{5.87}$$

5.7 Performance Analysis

In this section, the target detection performances of the target detectors proposed in this chapter have been demonstrated for WSN in the presence of interference and clutter. Target detection performance is quantised in terms of P_d and P_{fa}. A

WSN has been considered where the clusters of transmitting and receiving nodes are deployed within the sensing region with each cluster accounting for surveillance within its range. Each cluster is assumed to consist of a transmitting primary node which is referred to as a control centre and receiving nodes. Through simulation results, it has been shown that having multiple receiving within each cluster increases the reliability with which the presence of targets can be detected. For simulations, moderate and aggressive deployment strategies have been considered. In a moderate deployment strategy, the individual clusters are widely spaced and the interference caused by the neighbouring clusters is relatively low. However, this is achieved as a trade-off with the target detection reliability as this strategy results in poor coverage within the sensing region and hence may lead to increased miss detections. In aggressive deployment strategy, while better coverage within the sensing region maybe ensured, however the sensing nodes experience increased interference from the neighbouring clusters. The presence of a cluttered background environment is also considered. Existing threshold based detection strategies for WSN fail to provide reliable target detection performance in the presence of clutter. It has been shown that the proposed target detector provides a more reliable target detection performance in the presence of clutter. The target detection performance of the proposed target detector is compared with a simple GLRT detector under similar sensing conditions. Simulations are performed based on Monte-Carlo techniques and thresholds are evaluated to ensure required maximum false alarm rate by resorting to $100/P_{fa}$ independent simulations. Acceptable false alarm rate is assumed to be 10^{-4}. The length N_t of the transmit signal vector $\mathbf{s}$ is assumed to be 32 samples within each cluster and N_a is assumed to be 4. A summary of assumptions made within simulations is provided in Table 5.1.

Parameter	Assumption
N_T	1
N_a	4
N_t	32, 64, 96
N_y	35, 67, 99
P_{fa}	10^{-4}
N_s	1, 2, 3
μ	0.4, 0.6
SCR	3dB, -3dB
SIR	3dB, -3dB

TABLE 5.1: Summary of assumptions within simulations

5.7.1 Primary Detection

In this section, that target detection performance of the hybrid matched filter detector proposed in Section 5.5 has been analysed. In the presence of clutter, the energy detector fails to perform reliably due to the nature of its operating principle. The performance of the proposed H-MFD detector is compared with the performance of a conventional GLRT detector under similar sensing conditions. The test statistic for the proposed H-MFD detector is derived in Equation 5.39. In Figure 5.5, the performance of the proposed H-MFD is plotted with 35 received signal samples and 3dB Signal to Clutter Ratio (SCR) and 3dB SIR. The target detection performance of the proposed detector is compared with the performance of a GLRT detector. Under is said sensing conditions, the proposed target detector narrowly outperformed the GLRT detector with 1.5dB improvement at 80% probability of detection which can be observed in Figure 5.5.

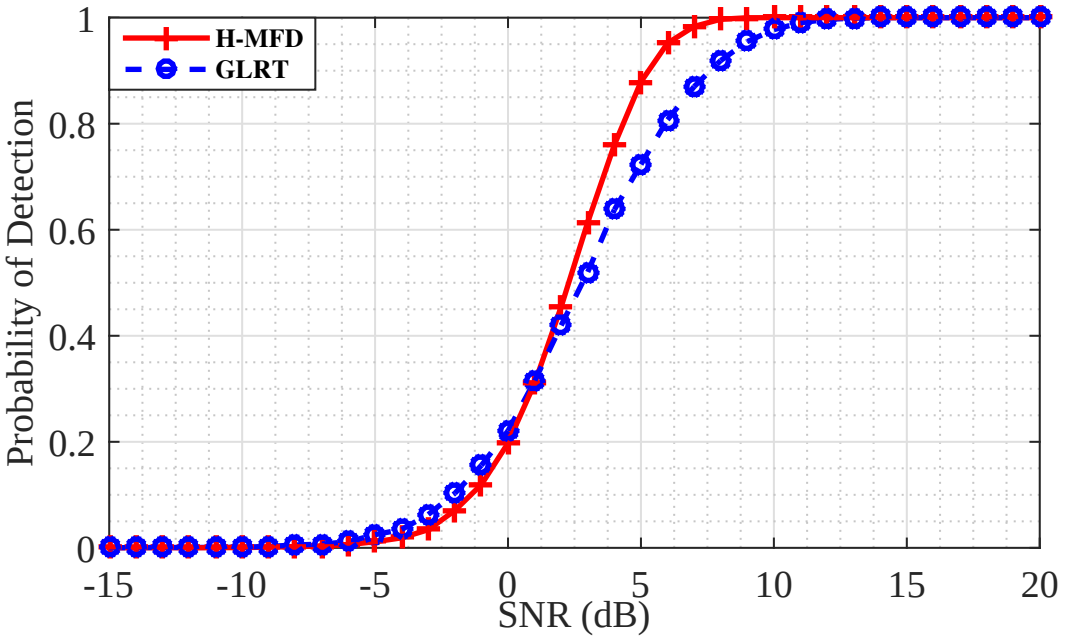

FIGURE 5.5: Target detection performance of the proposed hybrid matched filter detector for primary detection with 35 received signal samples and 3dB SCR

In Figure 5.6, the target detection performance of the proposed H-MFD and the GLRT detectors are simulated under harsh sensing conditions with stronger clutter returns. For this scenario, the sensing conditions with -3dB SCR is assumed. It can be observed that under harsh sensing conditions, while the GLRT detector completely to provide any detection performance, the proposed h-MFD detector managed to provide reasonably good target detection performance thereby outperforming the GLRT detector by a significant margin.

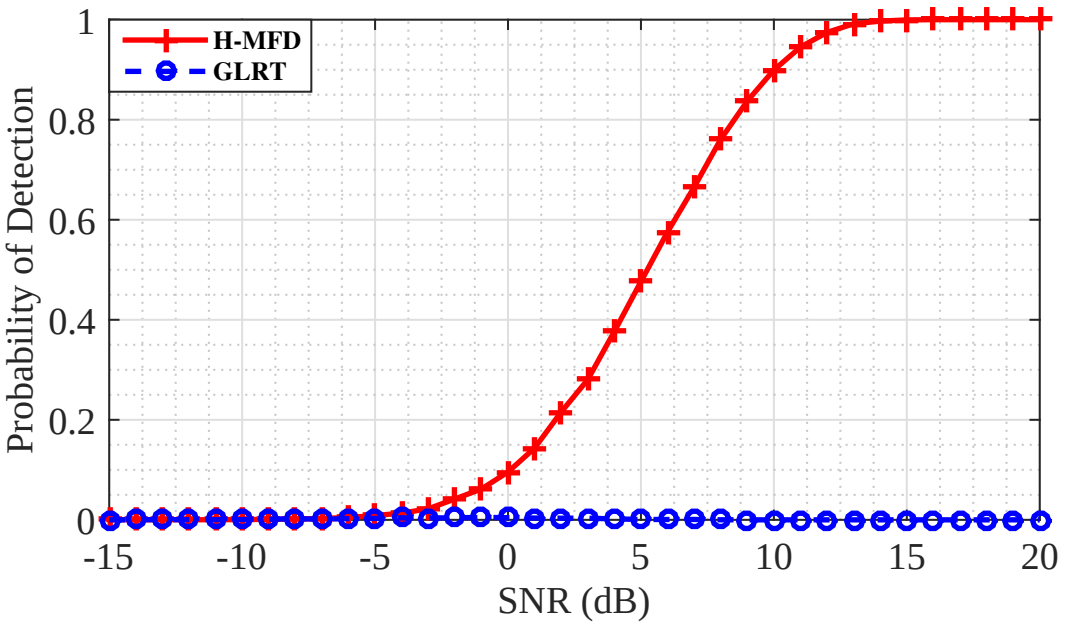

FIGURE 5.6: Target detection performance of the proposed hybrid matched filter detector for primary detection with 35 received signal samples and -3dB SCR

To analyse the impact of the number of received signal samples on the target detection performance of the primary detector, in Figure 5.7 the proposed H-MFD and GLRT detectors are simulated with 67 received signal samples. At 3dB SCR, H-MFD and GLRT detectors produced nearly similar target detection performances.

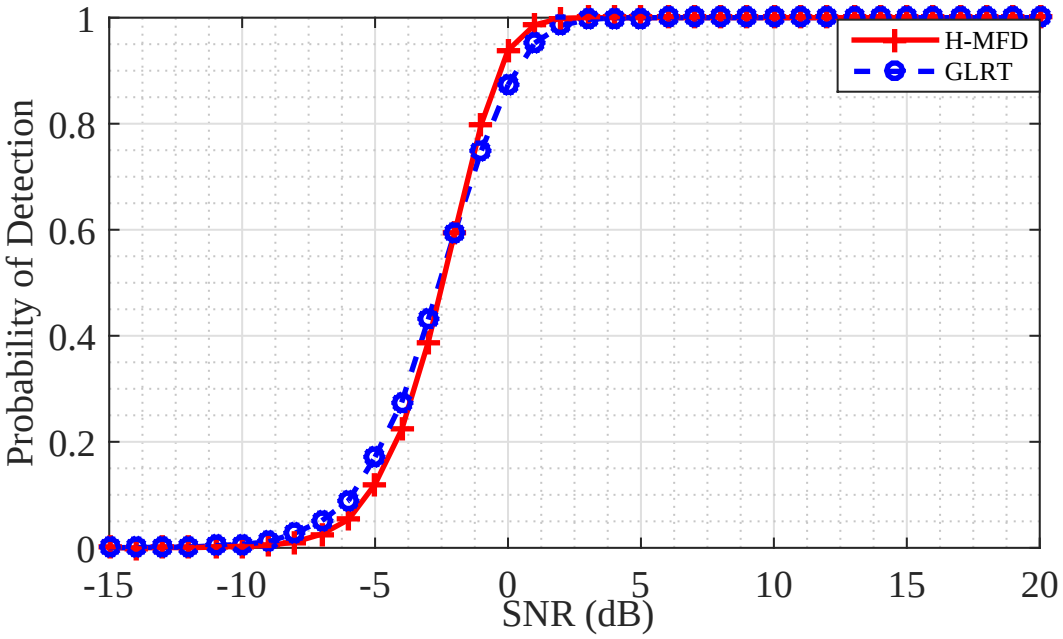

FIGURE 5.7: Target detection performance of the proposed hybrid matched filter detector for primary detection with 67 received signal samples and 3dB SCR

However as shown in Figure 5.8 at -3dB SCR, the GLRT detector sill failed to achieve reliable target detection rates. The number of received signal samples are further increased to 99 and the simulation results are plotted in Figure 5.9 and Figure 5.10. In Figure 5.9, at 3dB SCR, the GLRT detector again slightly outperformed the proposed H-MFD detector. However, at harsher sensing conditions with -3dB SCR, the proposed H-MFD outperformed the GLRT detector by 2.5dB at 80% probability of detection. Clearly, under harsher sensing conditions in the presence of cluttered background, the proposed H-MFD is the suitable choice. The proposed H-MFD also significantly less number of received signal samples than the conventional GLRT detector to provide similar target detection performances.

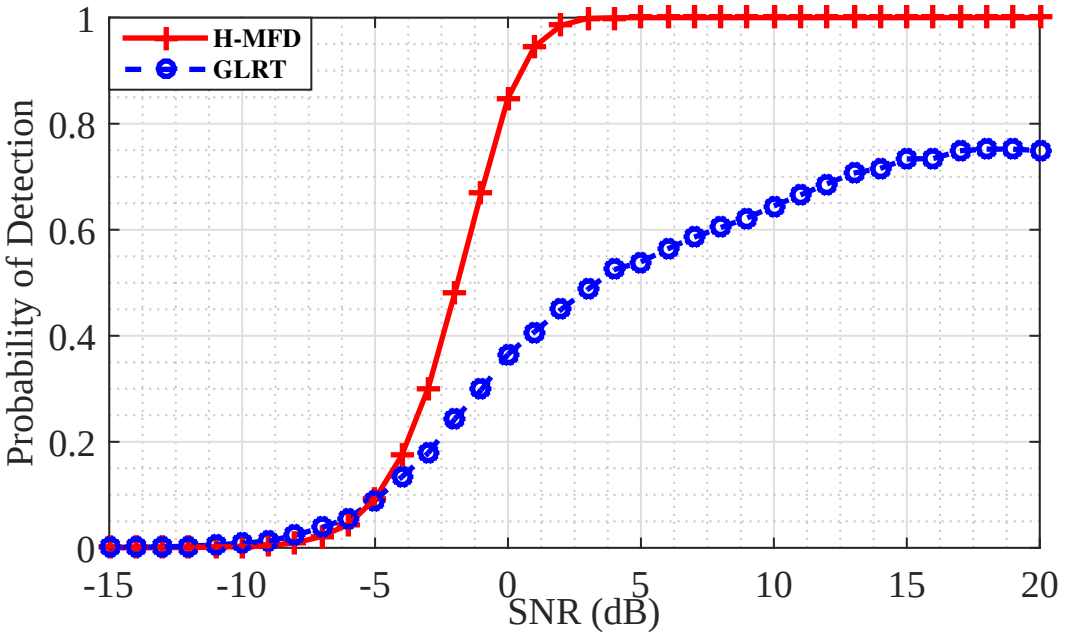

FIGURE 5.8: Target detection performance of the proposed hybrid matched filter detector for primary detection with 67 received signal samples and -3dB SCR

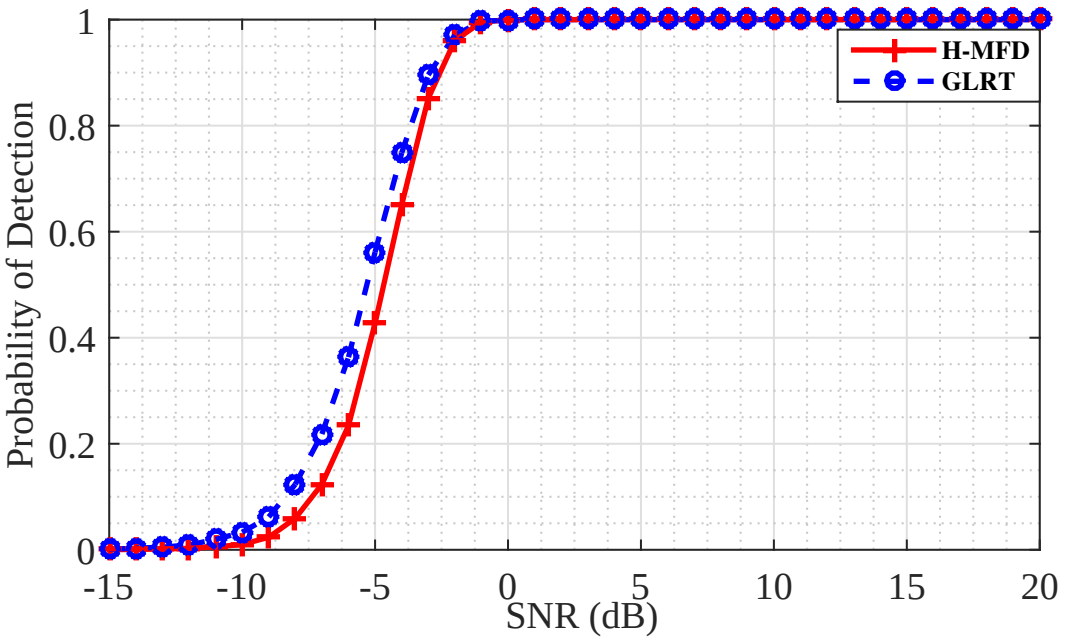

FIGURE 5.9: Target detection performance of the proposed hybrid matched filter detector for primary detection with 99 received signal samples and 3dB SCR

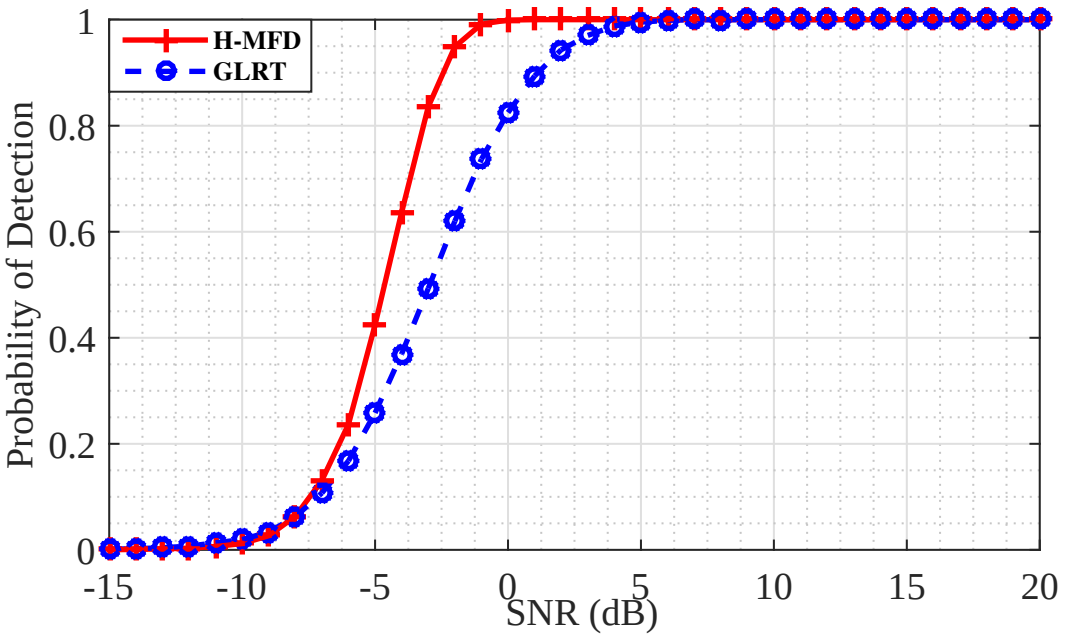

FIGURE 5.10: Target detection performance of the proposed hybrid matched filter detector for primary detection with 99 received signal samples and -3dB SCR

5.7.2 Secondary Detection

Due to cooperative nature of WSN, the control centre is assumed to have the knowledge of the transmit waveforms from the neighbouring sensing nodes which contribute to interference. However due to spatial displacement of the sensing nodes, the phase of the interfering waveform is assumed to be unknown. The target detection performances for three different scenarios related to the sensing conditions have been analysed. In case 1, the target detection performance of the proposed target detector in the presence of interference and clutter respectively has been simulated and its performance is compared with that of a GLRT detector in each scenario. In case 2, a harsh sensing environment has been considered with both clutter and interference being present. In case 3, the performance of the proposed detector with compressive sensing and its effect on target detection reliability has been analysed.

5.7.2.1 Case 1

In this case, the performances of the proposed detector in the presence of interference and clutter respectively have been analysed. In Figure 5.11 the target detection performances of the proposed AIE detector and a GLRT detector are shown.

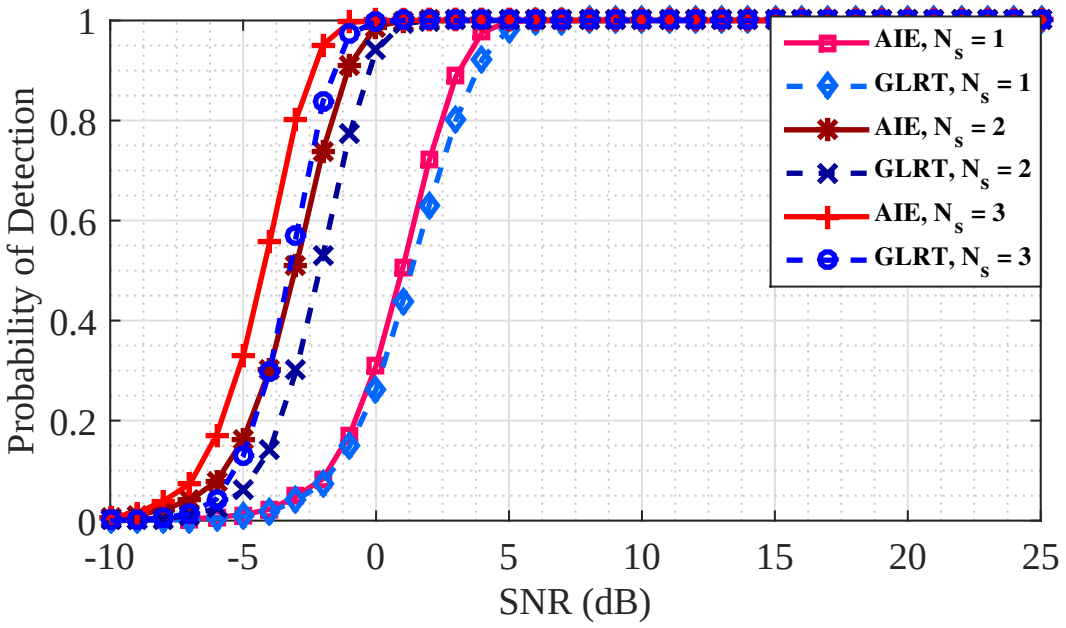

FIGURE 5.11: Target detection performance of the proposed AIE detector vs conventional GLRT detector in the presence of interference at SIR = 3dB

Results are simulated for the case of 1,2 and 3 receiving sensing nodes. SIR is assumed to be 3dB and the interfering waveform is assumed to be G4 which is defined in Equation 3.23. SIR at the detector is measured as

$$SIR = \frac{\|\mathbf{Sa}\|^2}{\|\sum_{k=1}^{b_n} \mathbf{H}_k \mathbf{b}_k\|^2} \tag{5.88}$$

This is a relatively moderate sensing environment in the absence clutter. The test statistic for AIE detector defined in Equation 5.84-Equation 5.87 can be modified for this scenario as

$$\mathbb{T} = \left(\frac{\mathbf{y}^H \boldsymbol{\chi}_0 \mathbf{y}}{\mathbf{y}^H \boldsymbol{\chi}_1 \mathbf{y}} \right) \underset{H_0}{\overset{H_1}{\gtrless}} \sqrt[N_y N_s]{\gamma} \tag{5.89}$$

where χ_1 and χ_2 are test statistic coefficients given in Equation 5.86 and Equation 5.87. The new measurement coefficients for this case are,

$$\mathbf{K}_j = (\prod_{l=1}^{j} \boldsymbol{\psi}_{l-1})^H (\prod_{l=1}^{j} \boldsymbol{\psi}_{l-1}) \tag{5.90}$$

$$\boldsymbol{\psi}_n = \mathbf{I} - \mathbf{H}_n \mathbf{R}_{\mathbf{h}_{nn}}^{-1} \mathbf{H}_n^H \mathbf{K}_n \quad \text{n}\neq 0 \tag{5.91}$$

$$\boldsymbol{\psi}_0 = \mathbf{I} \tag{5.92}$$

In moderate sensing conditions with low interfering signal strengths, the target detection performances of the proposed AIE detector and GLRT detector are nearly identical with AIE detector slightly outperforming the GLRT detector. In Figure 5.12, the performances of AIE and GLRT detectors are compared in much harsher sensing environment at SIR = -3dB. Under harsher sensing conditions, the proposed AIE detector significantly outperformed the conventional GLRT detector.

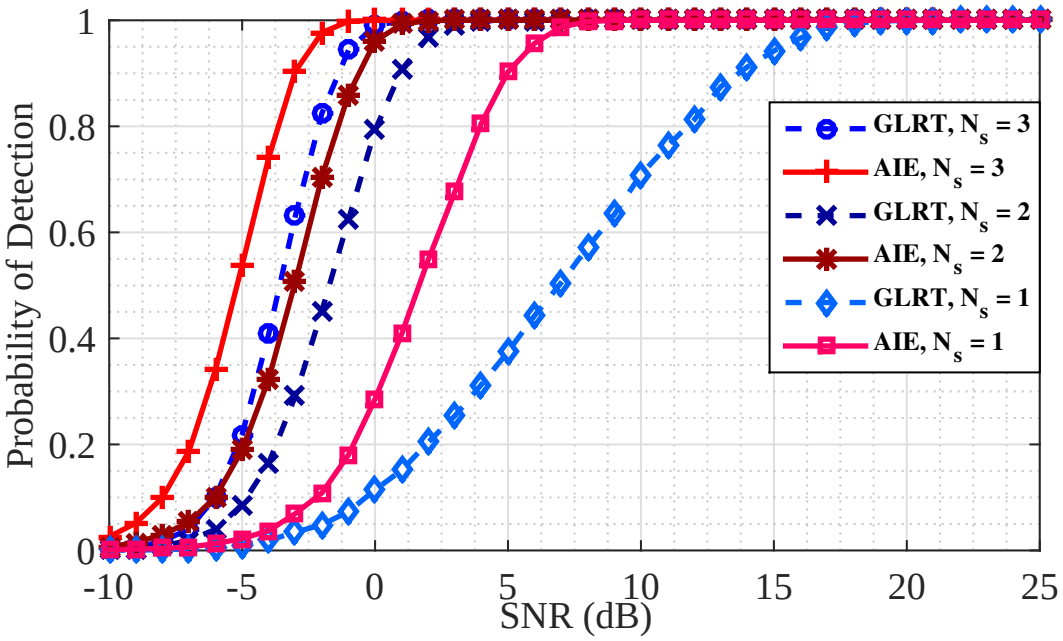

FIGURE 5.12: Target detection performance of the proposed AIE detector vs conventional GLRT detector in the presence of interference at SIR = -3dB

TABLE 5.2: Performance analysis of the proposed detector in case 1

Signal to Interference/Clutter Ratio (dB)	**Receiving Nodes**	**SNR at 100% P_d**		**Performance Gain**	**SNR at 80% P_d**		**Performance Gain**
		AIE	GLRT		AIE	GLRT	
SIR = 3dB	$N_s = 1$	5.9dB	7dB	1.1dB	2.5dB	3dB	0.5dB
	$N_s = 2$	1.7dB	2.8dB	1.1dB	-1.6dB	-0.8dB	0.8dB
	$N_s = 3$	-0.1dB	1dB	1dB	-3.2dB	-2.2dB	0.8dB
SIR = -3dB	$N_s = 1$	9.1dB	21.1dB	12dB	3.9dB	11.8dB	7.9dB
	$N_s = 2$	3dB	5dB	2dB	-1.4dB	0.2dB	1.6dB
	$N_s = 3$	0dB	2dB	2dB	-3dB	-2.2dB	1.4dB
SCR = 3dB	$N_s = 1$	6dB	11dB	5dB	2.6dB	5 dB	2.4dB
	$N_s = 2$	1.5dB	4.8dB	3.3dB	-1.6dB	-0.7dB	0.9dB
	$N_s = 3$	0dB	1.9dB	1.9dB	-3.2dB	-2.7dB	0.5dB
SCR = -3dB	$N_s = 1$	12dB	N/A	N/A	6.4dB	N/A	N/A
	$N_s = 2$	3dB	N/A	N/A	-0.6dB	N/A	N/A
	$N_s = 3$	0.3dB	N/A	N/A	-2.9dB	10.8dB	13.7dB

In Table 5.2 target detection performances of AIE and GLRT detectors are summarised. It has been observed that deploying additional receiving nodes within the sensing region increases the efficiency of the target detector. However, beyond a certain upper threshold any additional receiving nodes yield no significant performance gain. Similarly, in In Figure 5.13 and Figure 5.14, the performances of AIE and GLRT detectors in the presence of clutter have been plotted. While the GLRT detector experienced a severe deterioration in the target detection performance in the presence of clutter, the target detection performance of the proposed AIE detector remained robust. From Figure 5.14 it can be seen that in the presence of strong clutter, the GLRT detector completely failed to provide reliable detection performance while the proposed detector showed robust performance. This clearly validates the significance of the clutter projection matrix in Equation 5.22 to overcome clutter.

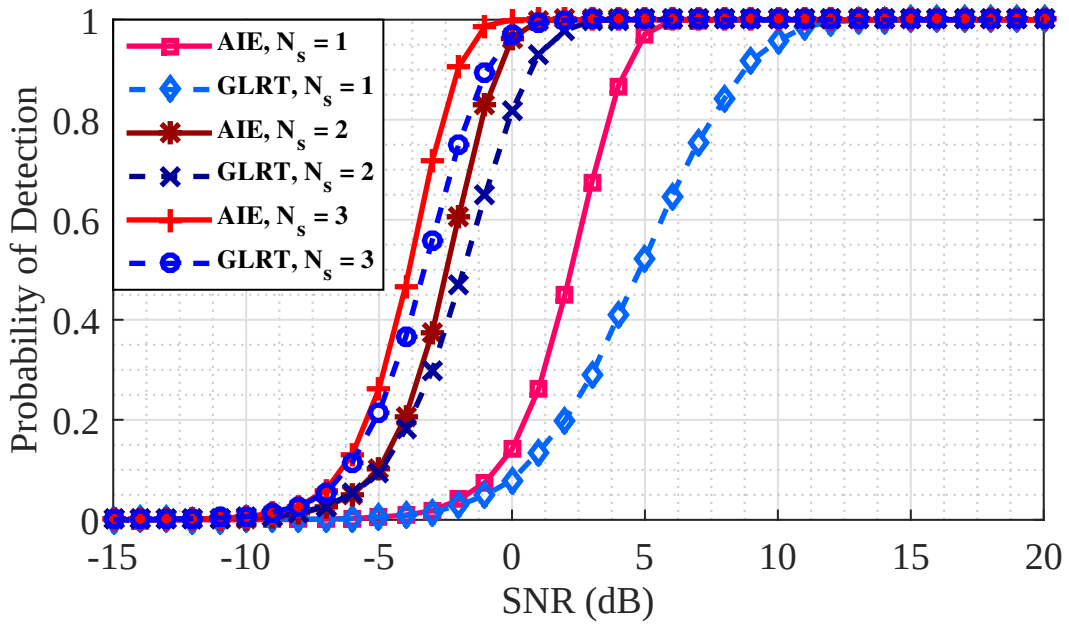

FIGURE 5.13: Target detection performance of the proposed AIE detector in the presence of clutter at SCR = 3dB

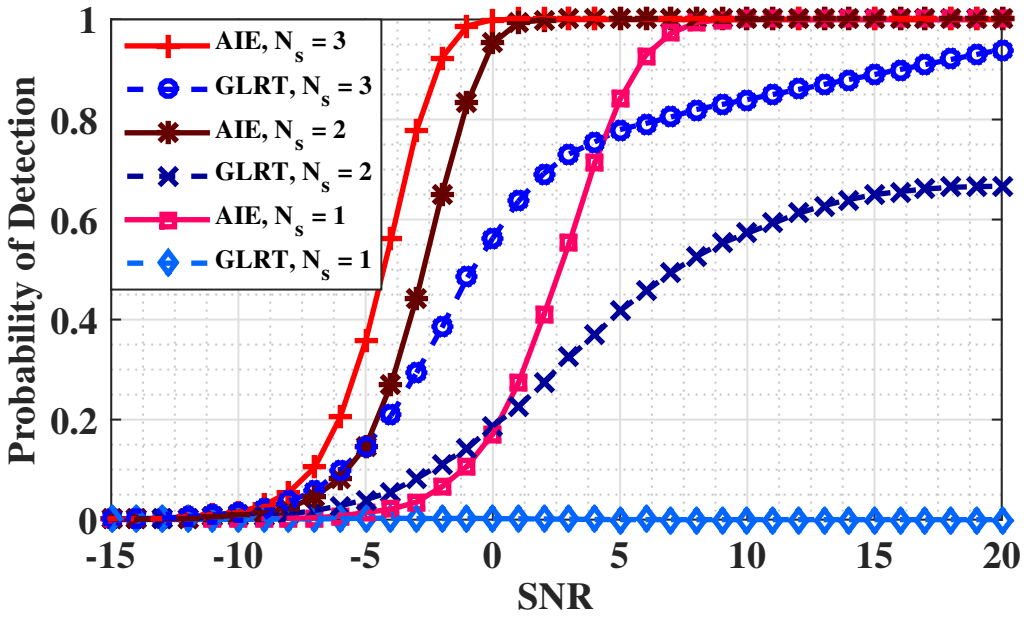

FIGURE 5.14: Target detection performance of the proposed AIE detector in the presence of clutter at SCR = -3dB

5.7.2.2 Case 2

Here a sensing environment which consists of clutter and interference has been simulated to analyse the performance of the proposed target detector. In Figure 5.15, the presence of relatively weak clutter and interfering signals has been considered and the target detection performances of AIE and GLRT detectors are compared. Similarly, in Figure 5.16 and Figure 5.17 the target detection performances of AIE and GLRT detectors in the presence of strong clutter and interference respectively have been compared. GLRT detector failed to achieve reliable detection rates in harsh sensing conditions and the proposed AIE detector outperformed the GLRT detector by a significant margin.

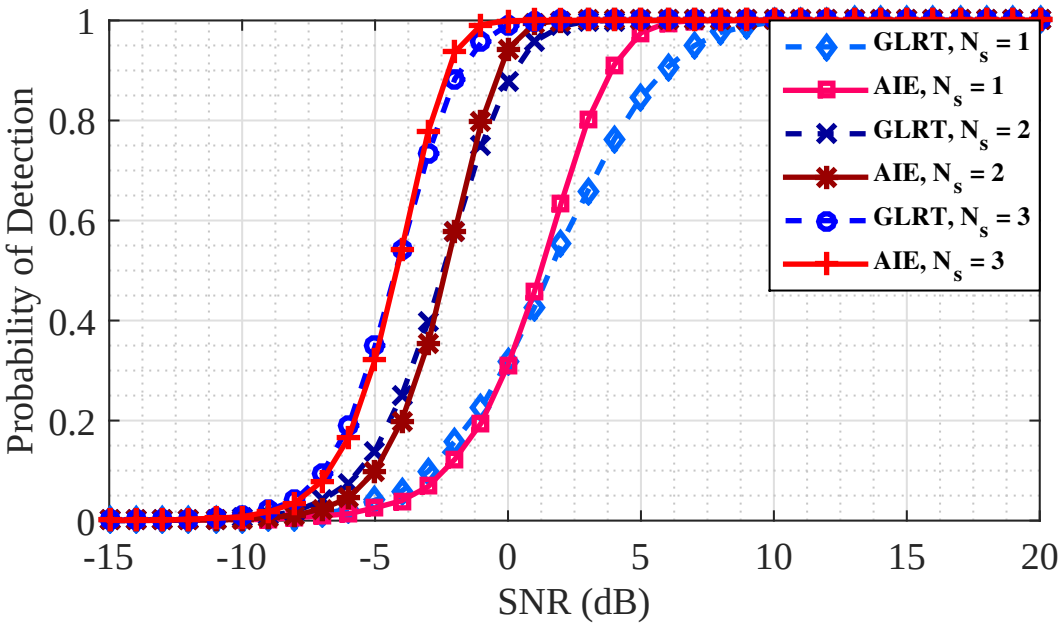

FIGURE 5.15: Target detection performances of AIE and GLRT detectors in the presence of interference and clutter at SIR = 3dB and SCR = 3dB

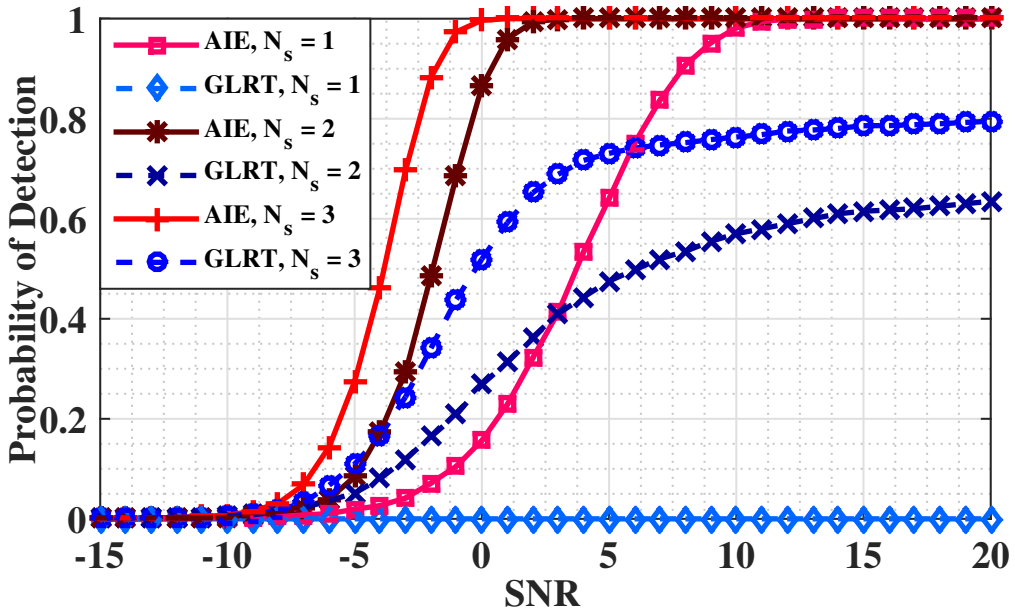

FIGURE 5.16: Target detection performances of AIE and GLRT detectors in the presence of interference and clutter at SIR = 3dB and SCR = -3dB

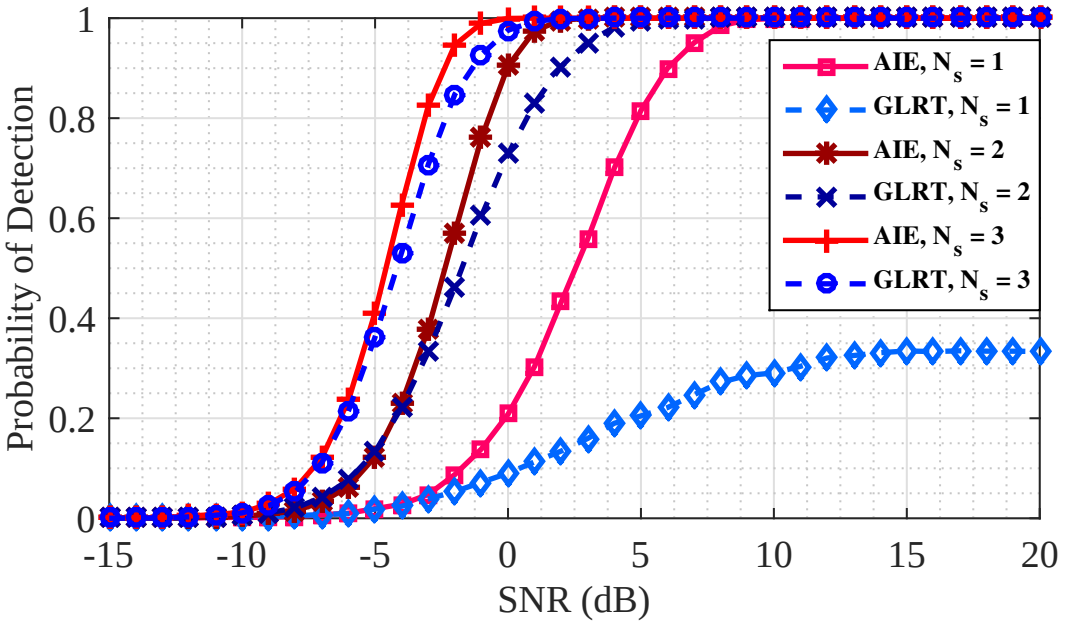

FIGURE 5.17: Target detection performances of AIE and GLRT detectors in the presence of interference and clutter at SIR = -3dB and SCR = 3dB

The performance evaluations in this case are summarised in Table 5.3. In Figure 5.18, Figure 5.19 and Figure 5.20, the performance of the proposed detector in

the presence of multiple interfering nodes is shown. From the simulation results, performance deterioration with increasing number of interfering nodes is observed. This has occurred due to the assumption that the phase of the interfering waveform is unknown due to spatial displacement of the receiving nodes. There is a possibility to improve the detection performance in this section and the authors aim to address this issue in the future work.

TABLE 5.3: Performance analysis of the proposed detector in case 2

Disturmance (dB)	**Receiving Nodes**	**SNR at 100% P_d**		**Performance Gain**	**SNR at 80% P_d**		**Performance Gain**
		AIE	GLRT		AIE	GLRT	
[SIR SCR] = [3 3]dB	$N_s = 1$	7.9dB	13.8dB	5.9dB	3dB	5.9dB	2.9dB
	$N_s = 2$	2.9dB	5dB	2.1dB	-1dB	-0.6dB	0.4dB
	$N_s = 3$	0.6dB	2.2dB	1.6dB	-2.9dB	-2.4dB	0.58dB
[SIR SCR] = [3 -3]dB	$N_s = 1$	13.5dB	N/A	N/A	6.7dB	N/A	N/A
	$N_s = 2$	3.9dB	N/A	N/A	-0.3dB	N/A	N/A
	$N_s = 3$	1dB	N/A	N/A	-2.4dB	N/A	N/A
[SIR SCR] = [-3 3]dB	$N_s = 1$	11.1dB	N/A	N/A	4.9dB	N/A	N/A
	$N_s = 2$	4dB	7.7dB	3.7dB	-0.7dB	0.7dB	1.4dB
	$N_s = 3$	2.5dB	6dB	3.5dB	-1.8dB	-0.5dB	0.3dB

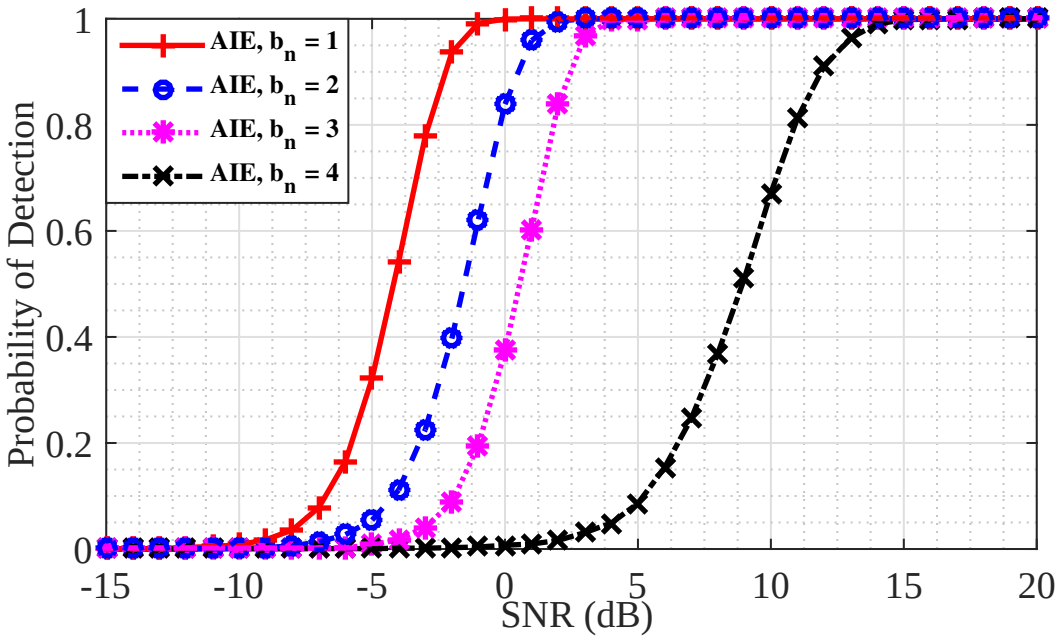

FIGURE 5.18: Target detection performance of AIE detector in the presence of multiple interfering nodes and 3 receiving nodes at SIR = 3dB and SCR = 3dB

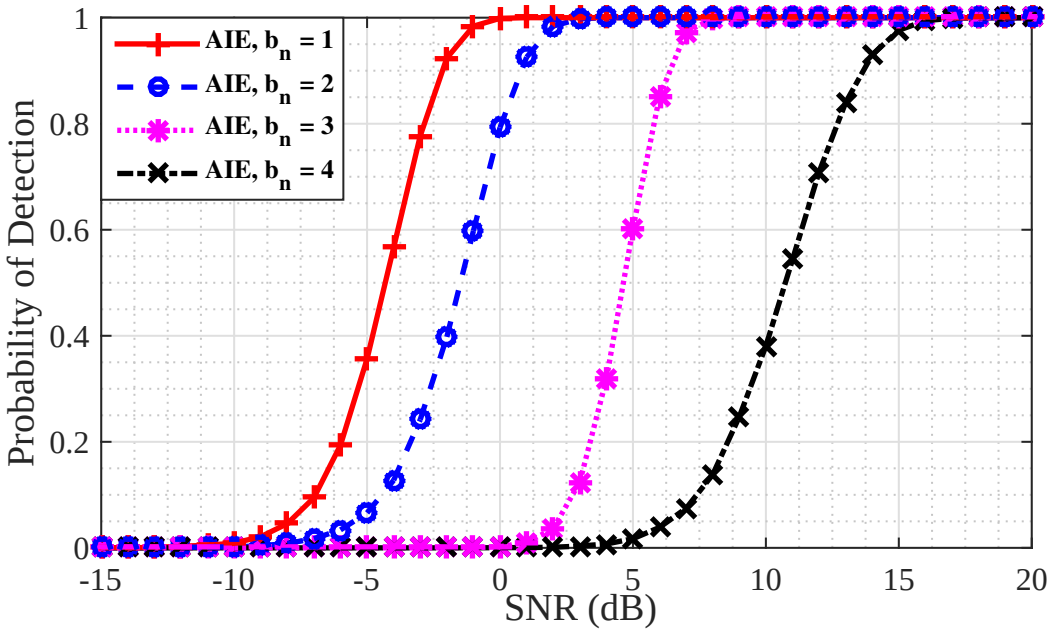

FIGURE 5.19: Target detection performance of AIE detector in the presence of multiple interfering nodes and 3 receiving nodes at SIR = -3dB and SCR = 3dB

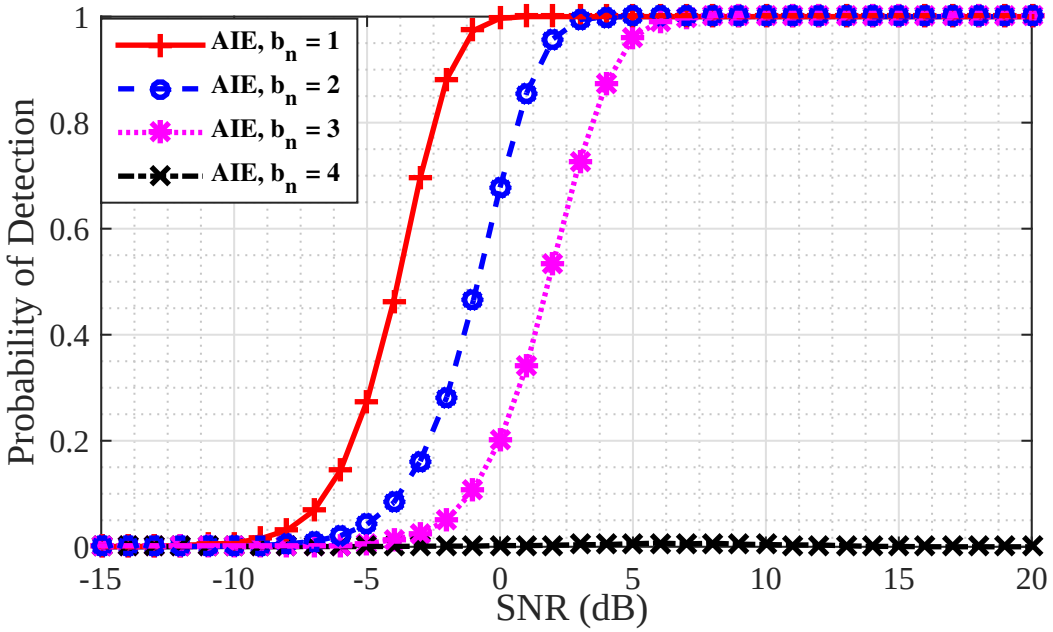

FIGURE 5.20: Target detection performances of AIE detector in the presence of multiple interfering nodes and 3 receiving nodes at SIR = -3dB and SCR = -3dB

TABLE 5.4: Performance analysis of the proposed detector in case 3 at 40% compression

SNR	N_s	**Probability of Detection** (P_d)		**Tradeoff**	**Probability of Detection** (P_d)		**Tradeoff**
		GLRT	**C-GLRT**		**AIE**	**C-AIE**	
0	1	0.3200	0.0102	0.3098	0.3112	0.0441	0.2671
	2	0.8794	0.0436	0.8358	0.9434	0.1808	0.7626
	3	0.9913	0.3602	0.6311	0.9997	0.5927	0.4070
5	1	0.8463	0.0250	0.8213	0.9754	0.1543	0.8211
	2	1	0.2317	0.7683	1	0.7673	0.2327
	3	1	0.8850	0.1150	1	0.9985	0.0015
10	1	0.9973	0.0256	0.9717	1	0.3138	0.6862
	2	1	0.4351	0.5649	1	0.9975	0.0025
	3	1	0.9970	0.0030	1	1	0
15	1	1	0.0103	0.9897	1	0.4920	0.5080
	2	1	0.5185	0.4815	1	1	0
	3	1	1	0	1	1	0

5.7.2.3 Case 3

Within resource constrained WSN, the sensing nodes are expected to operate independently with limited amount of available power. The lifetime of the sensing nodes is of utmost importance to ensure longevity of the WSN. It has already been established in the existing literature that a major share of the available power is consumed during data transmission between the sensing nodes and the control centre. Transmitting compressed received signal samples to the control centre is observed to be a potential solution to reduce the power consumption. However, data compression is achieved as a trade-off with the target detection reliability. Here the performance of the proposed target detector using compressed received signal samples has been plotted. In Figure 5.21, the target detection performances of the AIE and GLRT detectors using compressed received signal samples at 40% compression have been shown and the results are summarised in Table 5.4. The amount of detection loss which occurred due to compression is also shown in Table 5.4 to justify the significance of compressive sensing and the sensing conditions at which the target detection performances of C-AIE and AIE detectors converge are shown while the GLRT detector failed to achieve convergence within the simulated range of SNR. Similarly, in Figure 5.22 performances of the AIE and

GLRT detectors are compared at 60% compression and corresponding summary of detection performances are shown in Table 5.5

TABLE 5.5: Performance analysis of the proposed detector in case 3 at 60% compression

SNR	N_s	Probability of Detection (P_d)		Tradeoff	Probability of Detection (P_d)		Tradeoff
		GLRT	C-GLRT		AIE	C-AIE	
0	1	0.3200	0.0035	0.3165	0.3112	0.0096	0.3016
	2	0.8794	0.0152	0.8642	0.9434	0.0554	0.8880
	3	0.9913	0.0958	0.8955	0.9997	0.2043	0.7954
5	1	0.8463	0.0038	0.8605	0.9754	0.0291	0.9535
	2	1	0.0692	0.9308	1	0.2724	0.7276
	3	1	0.4996	0.5004	1	0.8059	0.1941
10	1	0.9973	0.0030	0.9943	1	0.0305	0.9695
	2	1	0.1344	0.8656	1	0.5750	0.4250
	3	1	0.8253	0.1747	1	0.9969	0.0031
15	1	1	0.0035	0.9965	1	0.0124	0.9876
	2	1	0.1448	0.8552	1	0.7646	0.2354
	3	1	0.9319	0.0681	1	1	0

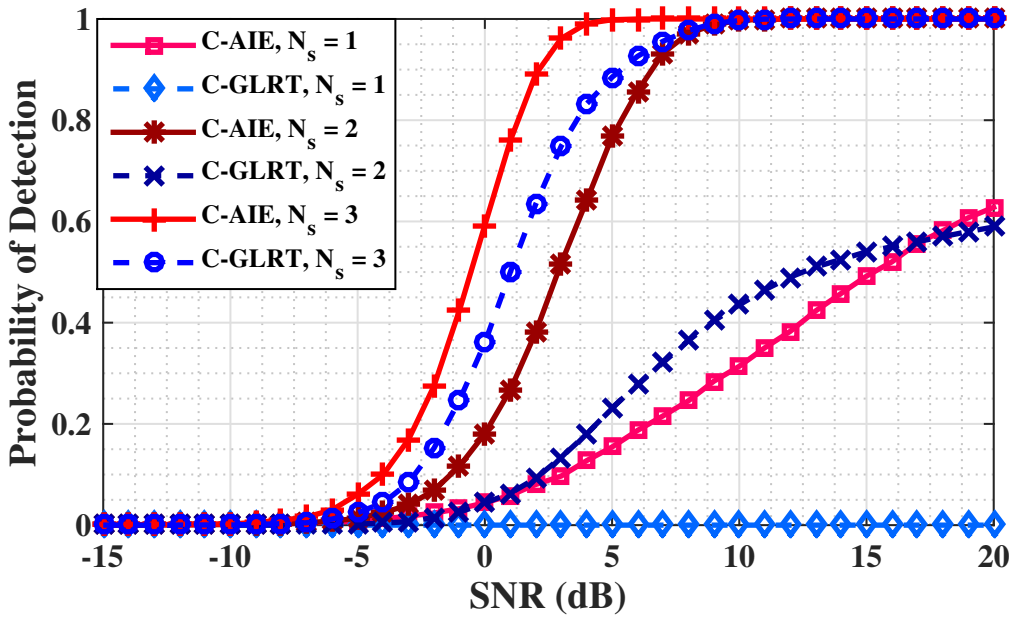

FIGURE 5.21: Target detection performances of AIE and GLRT detectors in the presence of interference and clutter at SIR = 3dB and SCR = 3dB and 40% compression

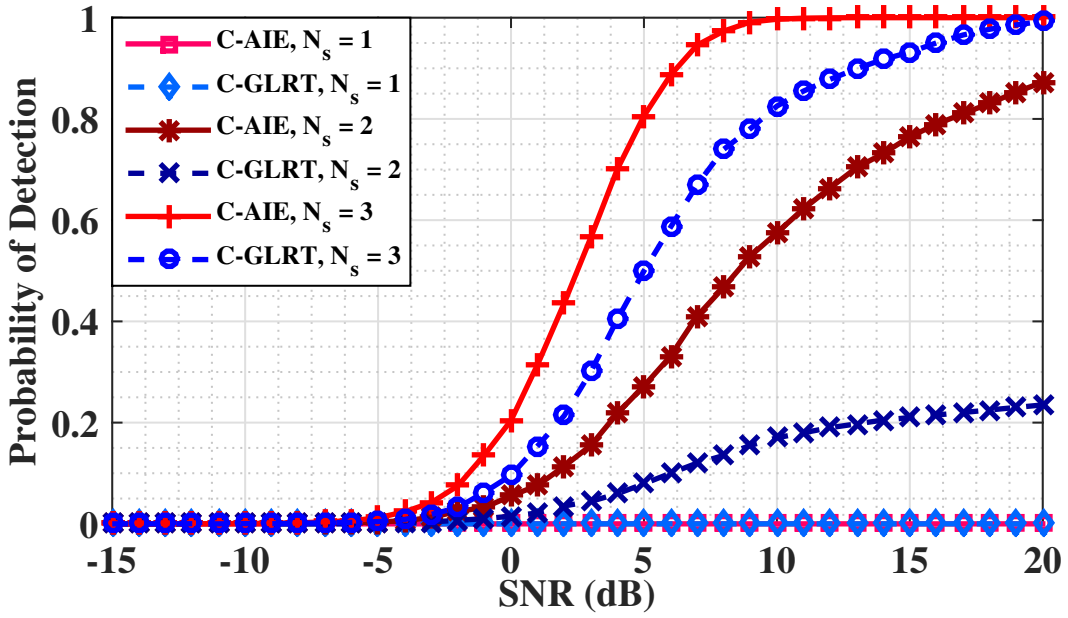

FIGURE 5.22: Target detection performances of AIE and GLRT detectors in the presence of interference and clutter at SIR = 3dB and SCR = 3dB and 60% compression

Effect of sample size on the performance of the proposed AIE detector is shown in Figure 5.23. For theoretical analysis, a comparison of the target detection performance of the proposed detector with other existing detectors is provided in Figure 5.24. Simulations are performed under the assumption that there are $N_s = 3$ receiving nodes and SIR = 3dB, SCR = 3dB and SNR = -3dB. The corresponding ROC curves for sensitivity analysis are shown in Figure 5.25.

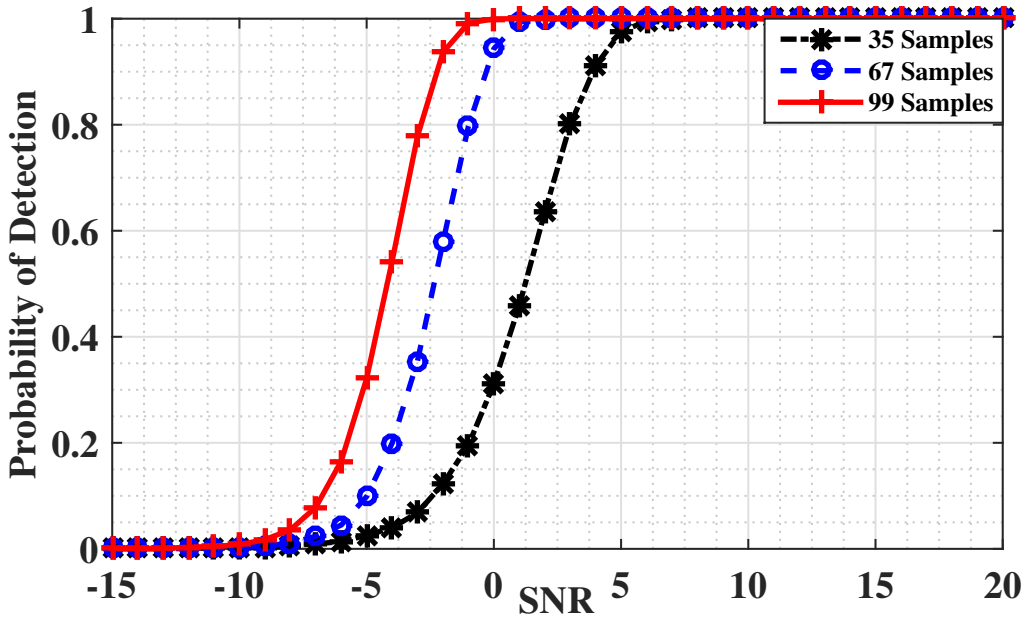

FIGURE 5.23: Effect of sample size on the target detection performance of the proposed AIE detector

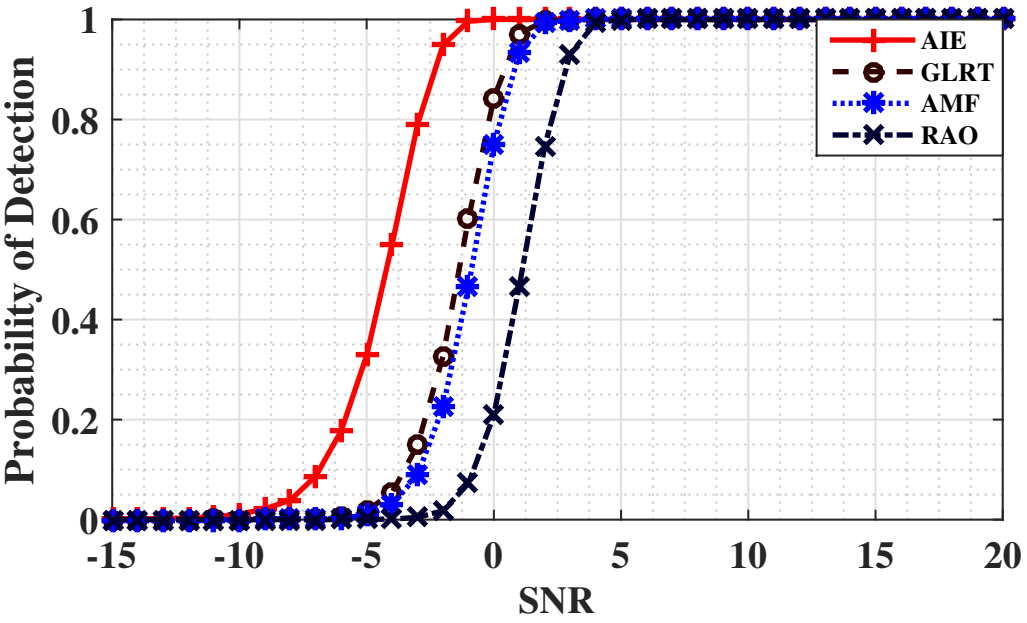

FIGURE 5.24: Target detection performances of proposed AIE compared with other existing detectors

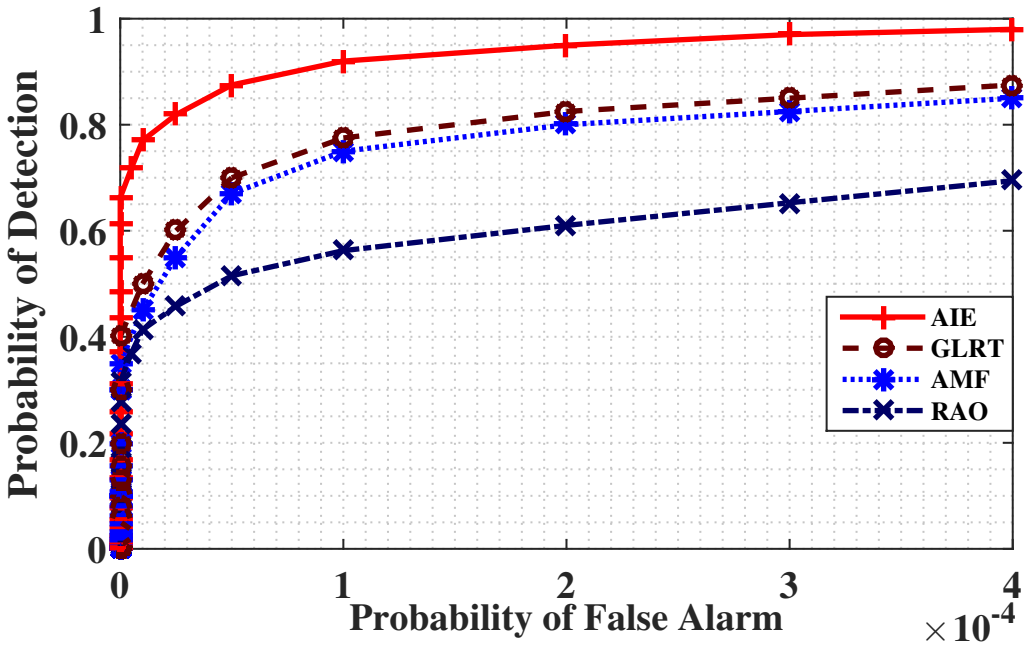

FIGURE 5.25: Sensitivity analysis of AIE, GLRT, AMF and RAO detectors

5.8 Summary

In this chapter, RF sensing based surveillance applications of WSN within heterogeneous sensing conditions have been addressed. An energy efficient target detection architecture, which is suitable for resource constrained WSN has been proposed. The sensing environments in which WSN are expected to operate have been considered while deriving the received signal models and the corresponding probability density functions. A two-step detection model has been proposed which optimises the energy efficiency of the target detector without compromising the detection reliability. This Two-step detection scheme, while reducing the computational burden also reduces the decision-making time. The proposed target detection model estimates the interfering signal strengths from each interfering node, which allows the sensing nodes to dynamically adopt to changes in interfering waveforms from the neighbouring clusters while providing reliable target detection performances. To reduce the transmission costs, compressive sensing scheme has been proposed where the sensing nodes are only required to transmit

compressed received signal samples to the control centre. It has been shown in the simulations results that under suitable sensing conditions compressive sensing can be used without any significant loss in target detection reliability. Finally, in Chapter 6, concluding remarks have been presented and the directions of the future work have been discussed.

Chapter 6

Conclusions and Future Directions

6.1 Conclusions

In this thesis, an RF sensing based target detection architecture for resource constrained WSN has been proposed. The proposed target detection architecture, which addresses the surveillance applications of WSN, is expected to be adaptable to fluctuating sensing conditions and provide optimum target detection performance. Unlike traditional WSN which use passive sensing devices for surveillance applications, in this research active sensing nodes have been proposed with radio frequency being the primary means of sensing. A hybrid distributed detection model has been proposed where the sensing nodes perform a preliminary detection and the control centre performs the secondary detection procedure to make the final decision regarding the existence of the targets.

6.1.1 Target Detection Optimisation Through Waveform Selection

The proposed target detection architecture uses sensing nodes with RF sensing based capabilities to detect the presence of targets. For the proposed target detection architecture, an RF signal is transmitted into the sensing environment. In principle, in the case of existence of a target, the transmitted RF signals are reflected from the target and the sensing nodes detect the reflect signals based on which a decision is made regarding the existence of the target. However, transmitting RF signals is associated with high energy consumption and significantly reduces the operating lifetime of the resource constrained WSN. Recent advancements in UWB technologies allowed development of low-cost UWB transmitting devices, which are suitable for WSN. UWB technologies allow generation of ultra-short UWB pulses, which are transmitted into the sensing region unlike the traditional RF sensing devices, which transmit narrowband signals. Due to ultra-short nature of UWB pulses, significantly reduces the transmit duration which in turn reduces the amount of power consumed during this procedure. Various UWB signals, which are suitable for RF sensing applications, are discussed in this thesis. With the knowledge of the transmit pulse shape available, the receiving nodes match the received data with the expected target signal. However, due to distributed nature of the WSN, multiple sensing nodes are expected to operate simultaneously within the sensing region. Within a sensing region with densely deployed sensing nodes, the RF signals transmitted from the neighbouring nodes interfere with each other. Due to the dynamic nature of the sensing environment, the received signals are usually corrupted versions of the transmitted signals. Under such scenarios, the choice of the transmit pulse defines the ability of the target detector to reliably detect the existence of the target signal within the received signal components in an energy efficient manner. In Chapter 3, a waveform selection criterion has been proposed which takes the sensing conditions and available

choices of transmit waveforms into account and generates an ease of detection index based on which an appropriate choice of the transmit waveform can be chosen. Simulations are performed under various sensing conditions and the target detection performances with different transmit waveforms are plotted. To validate the proposed model, the target detection performances with the transmit waveforms which are chosen based on the proposed ease of detection index are compared with the target detection performances of other waveforms

6.1.2 Target Detection Architecture for Homogeneous Sensing Environments

In Chapter 4, the problem of target detection within a homogeneous sensing environment has been considered. In this scenario, the sensing environment is assumed to be free of clutter and the total interference at the sensing nodes from the neighbouring sensing nodes remains uniform. A system model for the proposed distributed target detection architecture for WSN has been discussed and operational specifications for the experimental setup have been specified. Target detection procedure has been identified as a binary hypothesis testing problem and the received signal models under the respective hypothesis have been mathematically modelled. A two-stage target detection model, which is a hybrid combination of centralised and decentralised target detection architectures, has been proposed to reduce the operational and transmission burden on the sensing nodes while achieving desirable reliability in target detection process. Target detection process has been classified into primary and secondary detections with sensing nodes performing the primary detection and control centre performing the secondary detection. Primary detection has been proposed for WSN to restrict the undesirable wireless transmissions between sensing nodes and the control centre. Primary detector makes a preliminary decision regarding the existence or absence of the target and the detected information is transmitted to the control centre only if a decision is made in favour of existence of the target. A matched subspace detector

has been proposed for primary detection. The proposed matched subspace detector makes a decision regarding the existence of the target based on the known knowledge of the transmitted signal. Due to limited storage capacity, the sensing nodes have to operate without the knowledge of the interfering signals. To reduce the probability of missed detections at the primary detector, thresholds are adjusted to tolerate increased false alarms. The performance of the proposed target detector is compared with the performance of a conventional energy detector for WSN under similar sensing conditions. The target detection performances of the proposed primary detectors have been simulated under varying number of received signal samples.

For secondary detection, a new target detector namely AIE has been proposed. The secondary detector at the control centre is designed to provide increased target detection reliability. To reduce the processing complexity and decision making time, the target detection procedure at the control centre is performed in two phases namely initialisation and operational phases. During initialisation phase, the control centre gathers preliminary data regarding the sensing conditions, which is used during operational phase to increase the target detection reliability. Compressive sensing techniques have been introduced to restrict the data transmissions and the processing complexity. A new target detector namely C-AIE has been proposed which has the ability to perform secondary detection based on the compressed received signal samples. Simulations are performed and the target detection performances of the proposed target detectors are compared with the performance of a conventional GLRT detector, which is also considered to be a suitable detector for resource constrained WSN.

6.1.3 Target Detection Architecture for Heterogeneous Sensing Environments

In Chapter 5, RF sensing applications of a WSN in heterogeneous sensing environments has been considered. Heterogeneous sensing environments are associated

with non-uniform interferences from neighbouring sensing nodes and the presence of clutter. Estimating the clutter and interfering signal strengths under such scenarios is challenging and computationally intense procedure. The sensing nodes are required to detect the reflected echoes of the transmitted signals, which are corrupted by noise, interference and clutter. A system model for the proposed target detection architecture has been discussed. Estimation the information regarding clutter statistics from the secondary data is a computationally intense procedure. A clutter estimation procedure from the secondary data has been proposed which is computationally less intense than the existing clutter estimation procedures. The primary detector is provided with limited information regarding the clutter statistics and hybrid matched filter detector has been proposed for primary detection. Due to cooperative nature of the WSN, the control centre is assumed to have the knowledge of the transmitted interfering waveforms from the neighbouring sensing nodes. The proposed secondary detector at the control centre exploits the known knowledge of the interfering waveforms and makes a final decision regarding the existence or absence of the targets, while meeting the desired reliability requirements.

6.2 Future Directions

This research contributes to developing an RF sensing based target detection architecture for surveillance applications of resource constrained WSN. Various resource constraints are addressed and suitable target detectors have been proposed which can optimise the target detection reliability while operating within the bounds of the identified resource constraints of WSN. There are several aspects improvements within the proposed work, which can be extended in the future, some of which are as follows,

- It has been observed from the simulation results that the target detection performance is closely related to the number of received signal samples and number of sensing nodes within the cluster within the given constraints of the

sensing environment. Analytical and mathematical models can be developed to identify the optimum balance between number of required received signal samples and number of sensing nodes within the cluster to optimise the lifetime of the WSN.

- In the current work, a waveform selection procedure has been proposed to optimise the target detection reliability within the given set of sensing conditions. The proposed model identifies the optimum choice of the transmit waveform from the available transmit waveforms. This model has been proposed to meet the limited capabilities of the transmitting devices within the resource constrained WSN. With emerging technologies in wireless transmitter design significant advancements are being made in developing ultra-low power transmitting devices [163, 164]. When sufficiently capable transmitting devices are available, waveform design techniques can be developed in the context of the sensing conditions of WSN to achieve improved target detection reliabilities. Within the immediate future, reconfigurable and dynamic waveform selection feature for the target detector can be developed to achieve increased the detection reliability while meeting the resource constraints of WSN.

- It has been observed from the current research that compressive sensing based target detectors while reducing the transmission and computational costs, also suffer a significant deterioration in the target detection performance. The loss in the detection rate further pronounced within harsher sensing conditions. The primary responsibility for this detection loss has been attributed to the choice of random measurement matrix, which is used to compressed the received signal samples. Currently available measurement matrix design techniques are unsuitable for resource constrained WSN. Computationally efficient measurement matrix design techniques can be addressed in the future work to improve the reliability of compressive sensing techniques while reducing the transmission costs.

References

[1] Jayavardhana Gubbi, Rajkumar Buyya, Slaven Marusic, and Marimuthu Palaniswami. Internet of things (IoT): A vision, architectural elements, and future directions. *Future Generation Computer Systems*, 29(7):1645 – 1660, 2013. ISSN 0167-739X.

[2] Fernando Martincic and Loren Schwiebert. *Introduction to wireless sensor networking*, volume 1. chapter, 2005.

[3] Amit Sinha and Anantha P Chandrakasan. Energy aware software. In *Thirteenth International Conference on VLSI Design*, pages 50–55. IEEE, 2000.

[4] Th. Arampatzis, J. Lygeros, and S. Manesis. A survey of applications of wireless sensors and wireless sensor networks. In *Proceedings of the IEEE International Symposium on, Mediterrean Conference on Control and Automation*, pages 719–724, June 2005. doi: 10.1109/.2005.1467103.

[5] Tatiana Bokareva, Wen Hu, Salil Kanhere, Branko Ristic, Neil Gordon, Travis Bessell, Mark Rutten, and Sanjay Jha. Wireless sensor networks for battlefield surveillance. In *Proceedings of the land warfare conference*, pages 1–8, 2006.

[6] Dan Li, K.D. Wong, Yu Hen Hu, and A.M. Sayeed. Detection, classification, and tracking of targets. *IEEE Signal Processing Magazine*, 19(2):17–29, Mar 2002. ISSN 1053-5888. doi: 10.1109/79.985674.

[7] C. Meesookho, S. Narayanan, and C.S. Raghavendra. Collaborative classification applications in sensor networks. In *Sensor Array and Multichannel Signal Processing Workshop Proceedings*, pages 370–374, Aug 2002. doi: 10.1109/SAM.2002.1191063.

[8] Liljana Gavrilovska, Srdjan Krco, Veljko Milutinovic, Ivan Stojmenovic, and Roman Trobec. *Application and multidisciplinary aspects of wireless sensor networks: concepts, integration, and case studies*. Springer Science & Business Media, 2010.

[9] M. Ali, A. Bhm, and M. Jonsson. Wireless sensor networks for surveillance applications - a comparative survey of mac protocols. In *The Fourth International Conference on Wireless and Mobile Communications*, pages 399–403, July 2008. doi: 10.1109/ICWMC.2008.53.

[10] F. T. Jaigirdar and M. M. Islam. A new cost-effective approach for battlefield surveillance in wireless sensor networks. In *International Conference on Networking Systems and Security (NSysS)*, pages 1–6, Jan 2016. doi: 10.1109/NSysS.2016.7400694.

[11] F. T. Jaigirdar, M. M. Islam, and S. R. Huq. An efficient and cost effective maximum clique analysis based approximation in military application of wireless sensor network. In *14th International Conference on Computer and Information Technology (ICCIT)*, pages 85–90, Dec 2011. doi: 10.1109/ICCITechn.2011.6164879.

[12] S. Azevedo and T.E. McEwan. Micropower impulse radar. *IEEE Potentials*, 16(2), April 1997.

[13] Yingfei Diao, Minyue Fu, and Huanshui Zhang. An overview of range detection techniques for wireless sensor networks. In *8th World Congress on Intelligent Control and Automation (WCICA)*, pages 1150–1155, July 2010. doi: 10.1109/WCICA.2010.5554706.

[14] P.K. Dutta, A.K. Arora, and S.B. Bibyk. Towards radar-enabled sensor networks. In *The Fifth International Conference on Information Processing in Sensor Networks*, pages 467–474, 2006. doi: 10.1109/IPSN.2006.243915.

[15] M. Ditzel and F.H. Elferink. Low-power radar for wireless sensor networks. In *3rd European Radar Conference*, pages 139–141, Sept 2006. doi: 10.1109/EURAD.2006.280293.

[16] S. Fedor and M. Collier. On the problem of energy efficiency of multi-hop vs one-hop routing in wireless sensor networks. In *21st International Conference on Advanced Information Networking and Applications Workshops*, volume 2, pages 380–385, May 2007. doi: 10.1109/AINAW.2007.272.

[17] M. Neugebauer, J. Ploennigs, and K. Kabitzsch. Evaluation of energy costs for single hop vs. multi hop with respect to topology parameters. In *IEEE International Workshop on Factory Communication Systems*, pages 175–182, 2006. doi: 10.1109/WFCS.2006.1704148.

[18] Wei Ye, John Heidemann, and Deborah Estrin. An energy-efficient mac protocol for wireless sensor networks. In *Twenty-first annual joint conference of the IEEE computer and communications societies (INFOCOM)*, volume 3, pages 1567–1576. IEEE, 2002.

[19] Arati Manjeshwar and Dharma P Agrawal. Teen: Arouting protocol for enhanced efficiency in wireless sensor networks. In *ipdps*, volume 1, page 189, 2001.

[20] An Liu, Mihui Kim, Leonardo B Oliveira, and Hailun Tan. Wireless sensor network security, 2013.

[21] Adrian Perrig, John Stankovic, and David Wagner. Security in wireless sensor networks. *Communications of the ACM*, 47(6):53–57, 2004.

[22] Sonia Sharma. Wireless sensor network and security. In *3rd International Conference on Computing for Sustainable Global Development (INDIACom)*, pages 3301–3304. IEEE, 2016.

[23] Advantica, Inc, . *TWR-ISM-002-I Radar: Hardware User's Manual 2002.*

[24] Setia Budi, Paulo de Souza, Greg Timms, Vishv Malhotra, and Paul Turner. Optimisation in the design of environmental sensor networks with robustness consideration. *Sensors*, 15(12):29765–29781, 2015.

[25] C. Y. Chang, C. T. Chang, Y. C. Chen, and H. R. Chang. Obstacle-resistant deployment algorithms for wireless sensor networks. *IEEE Transactions on Vehicular Technology*, 58(6):2925–2941, July 2009. ISSN 0018-9545. doi: 10.1109/TVT.2008.2010619.

[26] M. Cardei, M. T. Thai, Yingshu Li, and Weili Wu. Energy-efficient target coverage in wireless sensor networks. In *Proceedings IEEE 24th Annual Joint Conference of the IEEE Computer and Communications Societies.*, volume 3, pages 1976–1984 vol. 3, March 2005. doi: 10.1109/INFCOM.2005.1498475.

[27] Peter Corke, Steven Hrabar, Ronald Peterson, Daniela Rus, Srikanth Saripalli, and Gaurav Sukhatme. Autonomous deployment and repair of a sensor network using an unmanned aerial vehicle. In *Proceedings of the IEEE 2004 International Conference on Robotics and Automation*, Volume 4, pages 3602–3608. IEEE Computer Society Press, May 2004.

[28] Nissanka B Priyantha, Anit Chakraborty, and Hari Balakrishnan. The cricket location-support system. In *Proceedings of the 6th annual international conference on Mobile computing and networking*, pages 32–43. ACM, 2000.

[29] Lewis Girod, Martin Lukac, Vlad Trifa, and Deborah Estrin. The design and implementation of a self-calibrating distributed acoustic sensing platform.

In *Proceedings of the 4th international conference on Embedded networked sensor systems*, pages 71–84. ACM, 2006.

[30] J-F Chamberland and Venugopal V Veeravalli. Asymptotic results for decentralized detection in power constrained wireless sensor networks. *IEEE Journal on selected areas in communications*, 22(6):1007–1015, 2004.

[31] Biao Chen, Lang Tong, and Pramod K Varshney. Channel-aware distributed detection in wireless sensor networks. *IEEE Signal Processing Magazine*, 23 (4):16–26, 2006.

[32] Ana Paula R. da Silva, Marcelo H. T. Martins, Bruno P. S. Rocha, Antonio A. F. Loureiro, Linnyer B. Ruiz, and Hao Chi Wong. Decentralized intrusion detection in wireless sensor networks. In *Proceedings of the 1st ACM International Workshop on Quality of service & Security in Wireless and Mobile Networks (Q2SWINET'05)*, pages 16–23. ACM Press, 2005.

[33] Bin Liu and Biao Chen. Decentralized detection in wireless sensor networks with channel fading statistics. *EURASIP Journal on Wireless Communications and Networking*, 2007(1):062915, 2006.

[34] S. Rajasegarar, C. Leckie, M. Palaniswami, and J. C. Bezdek. Distributed anomaly detection in wireless sensor networks. In *10th IEEE Singapore International Conference on Communication Systems*, pages 1–5, Oct 2006. doi: 10.1109/ICCS.2006.301508.

[35] W. Li and H. Dai. Distributed detection in wireless sensor networks using a multiple access channel. *IEEE Transactions on Signal Processing*, 55(3): 822–833, March 2007. ISSN 1053-587X. doi: 10.1109/TSP.2006.887563.

[36] C. Savarese, J. M. Rabaey, and J. Beutel. Location in distributed ad-hoc wireless sensor networks. In *IEEE International Conference on Acoustics, Speech, and Signal Processing. Proceedings (Cat. No.01CH37221)*, volume 4, pages 2037–2040 vol.4, 2001. doi: 10.1109/ICASSP.2001.940391.

[37] I.F. Akyildiz, W. Su, Y. Sankarasubramaniam, and E. Cayirci. Wireless sensor networks: a survey. *Computer Networks*, 38(4):393 – 422, 2002. ISSN 1389-1286.

[38] Robert Kozma, Lan Wang, Khan Iftekharuddin, Ernest McCracken, Muhammad Khan, Khandakar Islam, Sushil R. Bhurtel, and R. Murat Demirer. A radar-enabled collaborative sensor network integrating cots technology for surveillance and tracking. *Sensors*, 12(2):1336, 2012. ISSN 1424-8220. doi: 10.3390/s120201336.

[39] The samraksh company. user manual for the bumblebee: A low-power, mote-scale pulsed doppler radar sensor board. https://samraksh.com/index.php/products/sensors/32-product-pages/products-sensors/71-bumblebee-radar, . (Accessed on: 18-10-2016).

[40] Seapahn Meguerdichian, Farinaz Koushanfar, Gang Qu, and Miodrag Potkonjak. Exposure in wireless ad-hoc sensor networks. In *Proceedings of the 7th Annual International Conference on Mobile Computing and Networking*, MobiCom '01, pages 139–150, 2001. ISBN 1-58113-422-3.

[41] V. Phipatanasuphorn and Parameswaran Ramanathan. Vulnerability of sensor networks to unauthorized traversal and monitoring. *IEEE Transactions on Computers*, 53(3):364–369, Mar 2004. ISSN 0018-9340. doi: 10.1109/TC.2004.1261841.

[42] Tian He, Sudha Krishnamurthy, John A. Stankovic, Tarek Abdelzaher, Liqian Luo, Radu Stoleru, Ting Yan, Lin Gu, Jonathan Hui, and Bruce Krogh. Energy-efficient surveillance system using wireless sensor networks. In *Proceedings of the 2Nd International Conference on Mobile Systems, Applications, and Services*, MobiSys '04, pages 270–283, 2004. ISBN 1-58113-793-1.

[43] Pramod K. Varshney. *Distributed Detection and Data Fusion*. Springer-Verlag New York, Inc., Secaucus, NJ, USA, 1st edition, 1996. ISBN 0387947124.

[44] J. Liang and Q. Liang. Design and analysis of distributed radar sensor networks. *IEEE Transactions on Parallel and Distributed Systems*, 22(11): 1926–1933, Nov 2011. ISSN 1045-9219. doi: 10.1109/TPDS.2011.45.

[45] O. Younis and S. Fahmy. Distributed clustering in ad-hoc sensor networks: a hybrid, energy-efficient approach. In *Twenty-third AnnualJoint Conference of the IEEE Computer and Communications Societies (INFOCOM)*, volume 1, page 640, March 2004. doi: 10.1109/INFCOM.2004.1354534.

[46] Lakshmish Ramaswamy, B. Gedik, and L. Liu. A distributed approach to node clustering in decentralized peer-to-peer networks. *IEEE Transactions on Parallel and Distributed Systems*, 16(9):814–829, Sept 2005. ISSN 1045-9219. doi: 10.1109/TPDS.2005.101.

[47] C. Liu, K. Wu, Y. Xiao, and B. Sun. Random coverage with guaranteed connectivity: joint scheduling for wireless sensor networks. *IEEE Transactions on Parallel and Distributed Systems*, 17(6):562–575, June 2006. ISSN 1045-9219. doi: 10.1109/TPDS.2006.77.

[48] S.K. Bolisetti, K. Ahmed, M. Patwary, and M. Abdel-Maguid. Compressive parametric glrt detector for airborne mimo radar. In *International Conference on Wireless Communications and Signal Processing, WCSP*, pages 1 –5, nov. 2011. doi: 10.1109/WCSP.2011.6096735.

[49] N.B. Pulsone and M.A. Zatman. A computationally efficient two-step implementation of the GLRT. *IEEE Transactions on Signal Processing*, 48 (3):609 –616, Mar 2000. ISSN 1053-587X. doi: 10.1109/78.824657.

[50] E. Conte, A. De Maio, and G. Ricci. GLRT-based adaptive detection algorithms for range-spread targets. *IEEE Transactions on Signal Processing*, 49(7):1336 –1348, Jul 2001. ISSN 1053-587X. doi: 10.1109/78.928688.

[51] Bin Liu, Biao Chen, and J.H. Michels. A glrt for radar detection in the presence of compound-gaussian clutter and additive white gaussian noise. In *Sensor Array and Multichannel Signal Processing Workshop Proceedings*, pages 87 – 91, Aug. 2002. doi: 10.1109/SAM.2002.1191005.

[52] K. Ahmed, S. Kothuri, M. Patwary, and M. Abdel-Maguid. Subspace compressive glrt detector for airborne mimo radar. In *16th Asia-Pacific Conference on Communications (APCC)*, pages 302 –306, 31 2010-nov. 3 2010. doi: 10.1109/APCC.2010.5679718.

[53] Siva Karteek Bolisetti, Mohammad Patwary, Khawza Ahmed, Abdel-Hamid Soliman, and Mohamed Abdel-Maguid. Subspace compressive glrt detector for mimo radar in the presence of clutter. *The Scientific World Journal*, 2015.

[54] Antonio Moschitta and Igor Neri. Power consumption assessment in wireless sensor networks. In Giorgos Fagas, Luca Gammaitoni, Douglas Paul, and Gabriel Abadal Berini, editors, *ICT - Energy - Concepts Towards Zero - Power Information and Communication Technology*, chapter 09. InTech, Rijeka, 2014. doi: 10.5772/57201.

[55] E. J. Duarte-Melo and Mingyan Liu. Analysis of energy consumption and lifetime of heterogeneous wireless sensor networks. In *IEEE Global Telecommunications Conference, GLOBECOM.*, volume 1, pages 21–25 vol.1, Nov 2002. doi: 10.1109/GLOCOM.2002.1188034.

[56] R. Subramanian and F. Fekri. Sleep scheduling and lifetime maximization in sensor networks: fundamental limits and optimal solutions. In *5th International Conference on Information Processing in Sensor Networks*, pages 218–225, April 2006. doi: 10.1145/1127777.1127813.

[57] M. Bala Krishna and N. Vashishta. Energy efficient data aggregation techniques in wireless sensor networks. In *5th International Conference and Computational Intelligence and Communication Networks*, pages 160–165, Sept 2013. doi: 10.1109/CICN.2013.143.

[58] Xiang-Yang Li, Wen-Zhan Song, and Weizhao Wang. A unified energy-efficient topology for unicast and broadcast. In *Proceedings of the 11th Annual International Conference on Mobile Computing and Networking*, MobiCom '05, pages 1–15, 2005. ISBN 1-59593-020-5.

[59] P. Lohan and R. Chauhan. Geography-informed sleep scheduled and chaining based energy efficient data routing in wsn. In *IEEE Students' Conference on Electrical, Electronics and Computer Science (SCEECS)*, pages 1–4, March 2012. doi: 10.1109/SCEECS.2012.6184802.

[60] Guoliang Xing, Tian Wang, Weijia Jia, and Minming Li. Rendezvous design algorithms for wireless sensor networks with a mobile base station. In *Proceedings of the 9th ACM International Symposium on Mobile Ad Hoc Networking and Computing*, MobiHoc '08, pages 231–240, 2008. ISBN 978-1-60558-073-9.

[61] C. K. Tan, S. Y. Liew, H. G. Goh, and I. Andonovic. A fast, adaptive, and energy-efficient multi-path-multi-channel data collection protocol for wireless sensor networks. In *International Conference on Recent Advances in Signal Processing, Telecommunications Computing (SigTelCom)*, pages 33–38, Jan 2017. doi: 10.1109/SIGTELCOM.2017.7849791.

[62] L. Xiang, J. Luo, and A. Vasilakos. Compressed data aggregation for energy efficient wireless sensor networks. In *8th Annual IEEE Communications Society Conference on Sensor, Mesh and Ad Hoc Communications and Networks*, pages 46–54, June 2011. doi: 10.1109/SAHCN.2011.5984932.

[63] G. Quer, R. Masiero, D. Munaretto, M. Rossi, J. Widmer, and M. Zorzi. On the interplay between routing and signal representation for compressive sensing in wireless sensor networks. In *2009 Information Theory and Applications Workshop*, pages 206–215, Feb 2009. doi: 10.1109/ITA.2009.5044947.

[64] D. Friboulet, H. Liebgott, and R. Prost. Compressive sensing for raw rf signals reconstruction in ultrasound. In *IEEE International Ultrasonics Symposium*, pages 367–370, Oct 2010. doi: 10.1109/ULTSYM.2010.5935766.

[65] Joachim H.G. Ender. On compressive sensing applied to radar. *Signal Processing*, 90(5):1402 – 1414, 2010. ISSN 0165-1684. Special Section on Statistical Signal & Array Processing.

[66] C. R. Berger, Z. Wang, J. Huang, and S. Zhou. Application of compressive sensing to sparse channel estimation. *IEEE Communications Magazine*, 48 (11):164–174, November 2010. ISSN 0163-6804. doi: 10.1109/MCOM.2010.5621984.

[67] Y. Yu, A. P. Petropulu, and H. V. Poor. Measurement matrix design for compressive sensing based mimo radar. *IEEE Transactions on Signal Processing*, 59(11):5338–5352, Nov 2011. ISSN 1053-587X. doi: 10.1109/TSP.2011.2162328.

[68] M. Marzinzik and B. Kollmeier. Speech pause detection for noise spectrum estimation by tracking power envelope dynamics. *IEEE Transactions on Speech and Audio Processing*, 10(2):109 –118, feb 2002. ISSN 1063-6676. doi: 10.1109/89.985548.

[69] Rainer Martin. An efficient algorithm to estimate the instantaneous snr of speech signals. *in Proc. EUROSPEECH*, 1, 1993.

[70] A. Fisher and V.Stahl. On improvement measures for spectral subtraction applied to robust automatic speech recognition in car environments. *in Proc.*

Workshop Robust Methods Speech Recognition in Adverse Conditions, pages 75 –78, May 1999.

[71] Jitendra Padhye, Sharad Agarwal, Venkata N. Padmanabhan, Lili Qiu, Ananth Rao, and Brian Zill. Estimation of link interference in static multi-hop wireless networks. In *Proceedings of the 5th ACM SIGCOMM Conference on Internet Measurement*, IMC, pages 28–28, 2005.

[72] Martin Oberkönig and Ralph Tanbourgi and Friedrich Jondral. Co-channel interference limitations of ofdm communication-radar networks. *EURASIP J. Wireless Comm. and Networking*, 2013:207, 2013.

[73] Wen-Qin Wang and Huaizong Shao. Radar-to-radar interference suppression for distributed radar sensor networks. *Remote Sensing*, 6(1):740–755, 2014. ISSN 2072-4292. doi: 10.3390/rs6010740.

[74] Pu Wang, Hongbin Li, and B. Himed. Moving target detection using distributed mimo radar in clutter with nonhomogeneous power. *IEEE Transactions on Signal Processing*, 59(10):4809–4820, Oct 2011. ISSN 1053-587X. doi: 10.1109/TSP.2011.2160861.

[75] K. Gerlach. Spatially distributed target detection in non-gaussian clutter. *IEEE Transactions on Aerospace and Electronic Systems*, 35(3):926–934, Jul 1999. ISSN 0018-9251. doi: 10.1109/7.784062.

[76] A. Breloy, G. Ginolhac, F. Pascal, and P. Forster. Robust estimation of the clutter subspace for a low rank heterogeneous noise under high clutter to noise ratio assumption. In *IEEE International Conference on Acoustics, Speech and Signal Processing (ICASSP)*, pages 66–70, May 2014. doi: 10.1109/ICASSP.2014.6853559.

[77] A. Breloy, G. Ginolhac, F. Pascal, and P. Forster. Numerical performances of low rank stap based on different heterogeneous clutter subspace estimators.

In *International Radar Conference*, pages 1–5, Oct 2014. doi: 10.1109/RADAR.2014.7060426.

[78] L. Bai, S. Roy, and M. Rangaswamy. Compressive radar clutter subspace estimation using dictionary learning. In *IEEE Radar Conference*, pages 1–6, April 2013. doi: 10.1109/RADAR.2013.6586160.

[79] A.G. Jaffer, B. Himed, and P.T. Ho. Estimation of range-dependent clutter covariance by configuration system parameter estimation. In *IEEE International Radar Conference*, pages 596–601, May 2005. doi: 10.1109/RADAR.2005.1435868.

[80] R.S. Raghavan. Statistical interpretation of a data adaptive clutter subspace estimation algorithm. *IEEE Transactions on Aerospace and Electronic Systems*, 48(2):1370–1384, APRIL 2012. ISSN 0018-9251. doi: 10.1109/TAES.2012.6178068.

[81] W. L. Melvin and G. A. Showman. An approach to knowledge-aided covariance estimation. *IEEE Transactions on Aerospace and Electronic Systems*, 42(3):1021–1042, July 2006. ISSN 0018-9251. doi: 10.1109/TAES.2006.248216.

[82] E. Conte, A. De Maio, and G. Ricci. Covariance matrix estimation for adaptive cfar detection in compound-gaussian clutter. *IEEE Transactions on Aerospace and Electronic Systems*, 38(2):415–426, Apr 2002. ISSN 0018-9251. doi: 10.1109/TAES.2002.1008976.

[83] F. Gini. Sub-optimum coherent radar detection in a mixture of k-distributed and gaussian clutter. *IEE Proceedings - Radar, Sonar and Navigation*, 144 (1):39–48, Feb 1997. ISSN 1350-2395. doi: 10.1049/ip-rsn:19970967.

[84] D. C. Schleher. Radar detection in weibull clutter. *IEEE Transactions on Aerospace and Electronic Systems*, AES-12(6):736–743, Nov 1976. ISSN 0018-9251. doi: 10.1109/TAES.1976.308352.

[85] S. Watts. Radar detection prediction in sea clutter using the compound K-distribution model. *IEE Proceedings (Communications, Radar and Signal Processing)*, 132:613–620(7), December 1985. ISSN 0143-7070.

[86] E. Conte, M. Lops, and G. Ricci. Asymptotically optimum radar detection in compound-gaussian clutter. *IEEE Transactions on Aerospace and Electronic Systems*, 31(2):617–625, April 1995. ISSN 0018-9251. doi: 10.1109/7.381910.

[87] R. A. Romero and N. A. Goodman. Waveform design in signal-dependent interference and application to target recognition with multiple transmissions. *IET Radar, Sonar Navigation*, 3(4):328–340, August 2009. ISSN 1751-8784. doi: 10.1049/iet-rsn.2008.0146.

[88] Y. Yang and R. S. Blum. Mimo radar waveform design based on mutual information and minimum mean-square error estimation. *IEEE Transactions on Aerospace and Electronic Systems*, 43(1):330–343, January 2007. ISSN 0018-9251. doi: 10.1109/TAES.2007.357137.

[89] B. Friedlander. Waveform design for mimo radars. *IEEE Transactions on Aerospace and Electronic Systems*, 43(3):1227–1238, July 2007. ISSN 0018-9251. doi: 10.1109/TAES.2007.4383615.

[90] C. Y. Chen and P. P. Vaidyanathan. Mimo radar waveform optimization with prior information of the extended target and clutter. *IEEE Transactions on Signal Processing*, 57(9):3533–3544, Sept 2009. ISSN 1053-587X. doi: 10.1109/TSP.2009.2021632.

[91] D. DeLong and E. Hofstetter. On the design of optimum radar waveforms for clutter rejection. *IEEE Transactions on Information Theory*, 13(3):454–463, July 1967. ISSN 0018-9448. doi: 10.1109/TIT.1967.1054038.

[92] F. Elbahhar, A. Rivenq-Menhaj, J. M. Rouvaen, M. Heddebaut, and T. Boukour. Comparison between ds-cdma and modified gegenbauer functions for a multiuser communication ultra-wideband system. *IEE Proceedings - Communications*, 152(6):1021–1027, Dec 2005. ISSN 1350-2425. doi: 10.1049/ip-com:20045236.

[93] L. B. Michael, M. Ghavami, and R. Kohno. Multiple pulse generator for ultra-wideband communication using hermite polynomial based orthogonal pulses. In *IEEE Conference on Ultra Wideband Systems and Technologies*, pages 47–51, May 2002. doi: 10.1109/UWBST.2002.1006316.

[94] L Sakkila, A Rivenq, C Tatkeu, F ElBahhar, JM Rouvaen, and Y ElHillali. *Short Range Radar Based on UWB Technology*. INTECH Open Access Publisher, 2010.

[95] Laila Sakkila, Atika Rivenq, Charles Tatkeu, Yassin Elhillali, Jean-Pierre Ghys, et al. Performances of micropower uwb radar using orthogonal waveforms. *Wireless Engineering and Technology*, 5(03):74, 2014.

[96] William A Kissick et al. *The temporal and spectral characteristics of ultrawideband signals*. US Department of Commerce, National Telecommunications and Information Administration, 2001.

[97] V.I. Kostylev. Energy detection of a signal with random amplitude. In *IEEE International Conference on Communications*, volume 3, pages 1606 – 1610 vol.3, 2002. doi: 10.1109/ICC.2002.997120.

[98] I.M.G. Lourtie and G.C. Carter. Signal detection in a multiple time delay environment. *IEEE Transactions on Signal Processing*, 40(6):1587 –1590, jun 1992. ISSN 1053-587X. doi: 10.1109/78.139268.

[99] E.J. Kelly. An adaptive detection algorithm. *IEEE Transactions on Aerospace and Electronic Systems*, AES-22(2):115 –127, march 1986. ISSN 0018-9251. doi: 10.1109/TAES.1986.310745.

[100] A. De Maio. Rao test for adaptive detection in gaussian interference with unknown covariance matrix. *IEEE Transactions on Signal Processing*, 55 (7):3577 –3584, july 2007. ISSN 1053-587X. doi: 10.1109/TSP.2007.894238.

[101] O.F. Rodriguez, S. Primak, and V. Kontorovich. On performance of the wald test in partially coherent cognitive radio channels. In *International Conference on Communications and Information Technology (ICCIT)*, pages 214 –217, march 2011. doi: 10.1109/ICCITECHNOL.2011.5762685.

[102] E. Conte, M. Lops, and G. Ricci. Adaptive matched filter detection in spherically invariant noise. *IEEE Signal Processing Letters*, 3(8):248 –250, aug. 1996. ISSN 1070-9908. doi: 10.1109/97.511809.

[103] R. S. Schlunt and H. P. Schmid. An adaptive matched filter. In *IEEE Conference on Decision and Control including the 17th Symposium on Adaptive Processes*, volume 17, pages 608 –609, jan. 1978. doi: 10.1109/CDC.1978.268000.

[104] H. Urkowitz. Energy detection of unknown deterministic signals. *Proceedings of the IEEE*, 55(4):523 – 531, april 1967. ISSN 0018-9219. doi: 10.1109/PROC.1967.5573.

[105] F. F. Digham, M.-S. Alouini, and M. K. Simon. On the energy detection of unknown signals over fading channels. *IEEE Transactions on Communications*, 55(1):21 –24, jan. 2007. ISSN 0090-6778. doi: 10.1109/TCOMM.2006.887483.

[106] Gerhard Doblinger. Computationally efficient speech enhancement by spectral minima tracking in subbands. *in Proc. 4th Eur. Conf. Speech Communication Technology EUROSPEECH*, pages 1513 –1516, Sept 1995.

[107] R.R. Nadakuditi and J.W. Silverstein. Fundamental limit of sample generalized eigenvalue based detection of signals in noise using relatively few signal-bearing and noise-only samples. *IEEE Journal of Selected Topics*

in Signal Processing, 4(3):468 –480, june 2010. ISSN 1932-4553. doi: 10.1109/JSTSP.2009.2038310.

[108] L. C. Zaho, P. R. Krishnaiah, and Z. D. Bai. On detection of the number of signals when the noise covariance matrix is arbitary. *J. Multivariate Analysis*, 20(1):26 – 49, 1986.

[109] M. Wax and T. Kailath. Detection of signals by information theoretic criteria. *IEEE Transactions on Acoustics, Speech and Signal Processing*, 33(2): 387 – 392, apr 1985. ISSN 0096-3518. doi: 10.1109/TASSP.1985.1164557.

[110] R.R. Nadakuditi and A. Edelman. Sample eigenvalue based detection of high-dimensional signals in white noise using relatively few samples. *IEEE Transactions on Signal Processing*, 56(7):2625 –2638, july 2008. ISSN 1053-587X. doi: 10.1109/TSP.2008.917356.

[111] J.T. Durham and N.H. Younan. Neyman-pearson detector design for steady point targets with known phase detection. In *Proceedings of the Thirtieth Southeastern Symposium on System Theory*, pages 130 –133, mar 1998. doi: 10.1109/SSST.1998.660032.

[112] E. Conte, A. De Maio, and C. Galdi. Signal detection in compound-gaussian noise: Neyman-pearson and cfar detectors. *IEEE Transactions on Signal Processing*, 48(2):419 –428, feb 2000. ISSN 1053-587X. doi: 10.1109/78.823969.

[113] A. Yazi andci and, A.C. Hamurcu, and B. Baykal. The detection performance of neyman-pearson detector for mimo radar in k-distributed sea clutter. In *IEEE 18th Signal Processing and Communications Applications Conference (SIU)*, pages 165 –168, april 2010. doi: 10.1109/SIU.2010.5649973.

[114] G.L. Armstrong. Performance of the neyman-pearson detector for correlated input samples. *Proceedings of the IEEE*, 54(9):1190 – 1191, sept. 1966. ISSN 0018-9219. doi: 10.1109/PROC.1966.5069.

[115] V.P. Jilkov, J.R. Katkuri, and H.K. Nandiraju. Design of bayesian signal detectors using gaussian-mixture models. In *42nd Southeastern Symposium on System Theory (SSST)*, pages 286 –289, march 2010. doi: 10.1109/SSST.2010.5442823.

[116] Emmanuelle Jay, Jean-Philippe Ovarlez, David Declercq, and Patrick Duvaut. Bayesian optimum radar detector in non-gaussian noise. In *IEEE International Conference on Acoustics, Speech, and Signal Processing (ICASSP)*, volume 2, pages II–1289 –II–1292, may 2002. doi: 10.1109/ICASSP.2002.5744038.

[117] J. Boutros, S. Chaillou, and R. Vallet. A posteriori probability detection of pulse position modulated signals under imperfect channel estimation. In *International Zurich Seminar on Communications*, pages 72 – 75, 2004. doi: 10.1109/IZS.2004.1287391.

[118] Jinho Choi. On the partial map detection with applications to mimo channels. *IEEE Transactions on Signal Processing*, 53(1):158 – 167, jan. 2005. ISSN 1053-587X. doi: 10.1109/TSP.2004.838951.

[119] T.F. Ayoub and A.R. Haimovich. Modified glrt signal detection algorithm. *IEEE Transactions on Aerospace and Electronic Systems*, 36(3):810 –818, jul 2000. ISSN 0018-9251. doi: 10.1109/7.869498.

[120] P. Wang, Hongbin Li, and B. Himed. A new parametric glrt for multichannel adaptive signal detection. *IEEE Transactions on Signal Processing*, 58(1): 317 –325, jan. 2010. ISSN 1053-587X. doi: 10.1109/TSP.2009.2030835.

[121] A. Broumandan, J. Nielsen, and G. Lachapelle. Glrt signal detection performance of a synthetic array. In *23rd Canadian Conference on Electrical and Computer Engineering (CCECE)*, pages 1 –5, may 2010. doi: 10.1109/CCECE.2010.5575114.

[122] Pu Wang, Hongbin Li, and B. Himed. Bayesian parametric glrt for knowledge-aided space-time adaptive processing. In *IEEE Radar Conference*, pages 329 –332, may 2011. doi: 10.1109/RADAR.2011.5960553.

[123] Chengpeng Hao, Long Cai, Changlong Si, and Qi Xu. A new two-stage rao test detector. In *IEEE 10th International Conference on Signal Processing (ICSP)*, pages 1232 –1235, oct. 2010. doi: 10.1109/ICOSP.2010.5655302.

[124] Kwang June Sohn, Hongbin Li, and B. Himed. Multichannel parametric rao detector. In *IEEE International Conference on Acoustics, Speech and Signal Processing. ICASSP Proceedings*, volume 4, page IV, may 2006. doi: 10.1109/ICASSP.2006.1661165.

[125] Antonio De Maio. A new derivation of the adaptive matched filter. *IEEE Signal Processing Letters*, 11(10):792 – 793, oct. 2004. ISSN 1070-9908. doi: 10.1109/LSP.2004.835464.

[126] A. Sabharwal and L. Potter. Wald statistic for model order selection in superposition models. *IEEE Transactions on Signal Processing*, 50(4):956 –965, apr 2002. ISSN 1053-587X. doi: 10.1109/78.992145.

[127] J. Rissanen. Modeling by shortest data description. *Automatica*, 14:465 –471, 1978.

[128] Christ D. Richmond. Performance of a class of adaptive detection algorithms in nonhomogeneous environments. *IEEE Transactions on Signal Processing*, 48(5):1248 –1262, may 2000. ISSN 1053-587X. doi: 10.1109/78.839973.

[129] C.D. Richmond. Performance of the adaptive sidelobe blanker detection algorithm in homogeneous environments. *IEEE Transactions on Signal Processing*, 48(5):1235 –1247, may 2000. ISSN 1053-587X. doi: 10.1109/78.839972.

[130] F. Bandiera, D. Orlando, and G. Ricci. A subspace-based adaptive sidelobe blanker. *IEEE Transactions on Signal Processing*, 56(9):4141 –4151, sept. 2008. ISSN 1053-587X. doi: 10.1109/TSP.2008.926193.

[131] F. Bandiera, O. Besson, D. Orlando, and G. Ricci. An improved adaptive sidelobe blanker. *IEEE Transactions on Signal Processing*, 56(9):4152 –4161, sept. 2008. ISSN 1053-587X. doi: 10.1109/TSP.2008.926191.

[132] N.B. Pulsone and C.M. Rader. Adaptive beamformer orthogonal rejection test. *IEEE Transactions on Signal Processing*, 49(3):521 –529, mar 2001. ISSN 1053-587X. doi: 10.1109/78.905870.

[133] A.R. Barron and T.M. Cover. Minimum complexity density estimation. *IEEE Transactions on Information Theory*, 37(4):1034 –1054, jul 1991. ISSN 0018-9448. doi: 10.1109/18.86996.

[134] S. Kraut, L.L. Scharf, and R.W. Butler. The adaptive coherence estimator: a uniformly most-powerful-invariant adaptive detection statistic. *IEEE Transactions on Signal Processing*, 53(2):427 – 438, feb 2005. ISSN 1053-587X. doi: 10.1109/TSP.2004.840823.

[135] S. Bidon, O. Besson, and J.-Y. Tourneret. The adaptive coherence estimator is the generalized likelihood ratio test for a class of heterogeneous environments. *IEEE Signal Processing Letters*, 15:281 –284, 2008. ISSN 1070-9908. doi: 10.1109/LSP.2007.916044.

[136] E.J. Candes and M.B. Wakin. An introduction to compressive sampling. *IEEE Signal Processing Magazine*, 25(2):21 –30, march 2008. ISSN 1053-5888. doi: 10.1109/MSP.2007.914731.

[137] Shihao Ji, Ya Xue, and L. Carin. Bayesian compressive sensing. *IEEE Transactions on Signal Processing*, 56(6):2346 –2356, june 2008. ISSN 1053-587X. doi: 10.1109/TSP.2007.914345.

[138] Zhongmin Wang, G.R. Arce, and B.M. Sadler. Subspace compressive detection for sparse signals. In *IEEE International Conference on Acoustics, Speech and Signal Processing. ICASSP*, pages 3873 –3876, 31 2008-april 4 2008. doi: 10.1109/ICASSP.2008.4518499.

[139] J. Haupt and R. Nowak. Compressive sampling for signal detection. In *IEEE International Conference on Acoustics, Speech and Signal Processing. ICASSP*, volume 3, pages III–1509 –III–1512, april 2007. doi: 10.1109/ICASSP.2007.367135.

[140] F. Chen, F. Lim, O. Abari, A. Chandrakasan, and V. Stojanovic. Energy-aware design of compressed sensing systems for wireless sensors under performance and reliability constraints. *IEEE Transactions on Circuits and Systems I: Regular Papers*, 60(3):650–661, 2013. ISSN 1549-8328. doi: 10.1109/TCSI.2012.2215738.

[141] N. Kimura and S. Latifi. A survey on data compression in wireless sensor networks. In *International Conference on Information Technology: Coding and Computing. ITCC*, volume 2, pages 8–13 Vol. 2, 2005. doi: 10.1109/ITCC.2005.43.

[142] S. Puthenpurayil, Ruirui Gu, and S.S. Bhattacharyya. Energy-aware data compression for wireless sensor networks. In *IEEE International Conference on Acoustics, Speech and Signal Processing. ICASSP*, volume 2, pages II–45–II–48, 2007. doi: 10.1109/ICASSP.2007.366168.

[143] Chaoyu Wang, Hongtao Li, Xiaohua Zhu, and Yapeng He. Robustly blind sparsity signal recovery algorithm for compressive sensing radar. In *3rd International Conference on Consumer Electronics, Communications and Networks (CECNet)*, pages 573–576, Nov 2013. doi: 10.1109/CECNet.2013.6703396.

[144] Amiya Nayak and Ivan Stojmenovic. Wireless sensor and actuator networks. *John-Whiley & sons*, 2010.

[145] Qi Cheng Riuxin Niu, Pramod K. Varshney. Distributed detection in a large wireless sensor network. *Special Issue on the Seventh International Conference on Information Fusion-Part I*, 7(4):380 – 394, 2006. ISSN 1566-2535.

[146] Haitao Zhang and Cuiping Liu. A review on node deployment of wireless sensor network. *International Journal of Computer Science Issues*, 9(6): 378–383, 2012.

[147] L. Sakkila, A. Rivenq, C. Tatkeu, Y. ElHillali, F. Boukour, and J. M. Rouvaen. Comparison of classical and orthogonal uwb waveforms for radar applications. In *6th International Colloquium on Signal Processing its Applications*, pages 1–5, May 2010. doi: 10.1109/CSPA.2010.5545276.

[148] T. Aittomki and V. Koivunen. Improved mimo radar channel estimation using spatial coding. In *IEEE International Conference on Acoustics, Speech and Signal Processing*, pages 4120–4124, May 2013. doi: 10.1109/ICASSP.2013.6638434.

[149] H. Hashemi. Impulse response modeling of indoor radio propagation channels. *IEEE Journal on Selected Areas in Communications*, 11(7):967–978, Sep 1993. ISSN 0733-8716. doi: 10.1109/49.233210.

[150] S. U. Pillai, D. C. Youla, H. S. Oh, and J. R. Guerci. Optimum transmit-receiver design in the presence of signal-dependent interference and channel noise. In *Conference Record of the Thirty-Third Asilomar Conference on Signals, Systems, and Computers (Cat. No.CH37020)*, volume 2, pages 870–875 vol.2, Oct 1999. doi: 10.1109/ACSSC.1999.831834.

[151] Chun-Yang Chen and PP Vaidyanathan. Mimo radar waveform optimization with prior information of the extended target and clutter. *IEEE Transactions on Signal Processing*, 57(9):3533–3544, 2009.

[152] L. L. Scharf and L. T. McWhorter. Adaptive matched subspace detectors and adaptive coherence estimators. In *Conference Record of the Thirtieth Asilomar Conference on Signals, Systems and Computers*, pages 1114–1117 vol.2, Nov 1996. doi: 10.1109/ACSSC.1996.599116.

[153] Todd McWhorter and Louis Scharf. Matched subspace detectors for stochastic signals. Technical report, COLORADO STATE UNIV FORT COLLINS, 2003.

[154] N. A. Goodman, P. R. Venkata, and M. A. Neifeld. Adaptive waveform design and sequential hypothesis testing for target recognition with active sensors. *IEEE Journal of Selected Topics in Signal Processing*, 1(1):105–113, June 2007. ISSN 1932-4553. doi: 10.1109/JSTSP.2007.897053.

[155] D. A. Garren, M. K. Osborn, A. C. Odom, J. S. Goldstein, S. U. Pillai, and J. R. Guerci. Enhanced target detection and identification via optimised radar transmission pulse shape. *IEE Proceedings - Radar, Sonar and Navigation*, 148(3):130–138, Jun 2001. ISSN 1350-2395. doi: 10.1049/ip-rsn:20010324.

[156] L. P. Roy and R. V. R. Kumar. Accurate k-distributed clutter model for scanning radar application. *IET Radar, Sonar Navigation*, 4(2):158–167, April 2010. ISSN 1751-8784. doi: 10.1049/iet-rsn.2009.0108.

[157] L. P. Roy and R. V. R. Kumar. A glrt detector in partially correlated texture based compound-gaussian clutter. In *Communications (NCC), 2010 National Conference on*, pages 1–5, Jan 2010. doi: 10.1109/NCC.2010.5430182.

[158] Richard Kelmn. *Principles of space-time adaptive processing*. The Institution of Electrical Engineers, London, United Kingdon, 2002.

[159] S. Kraut, L. T. McWhorter, and L. L. Scharf. A canonical representation for distributions of adaptive matched subspace detectors. In *Conference Record of the Thirty-First Asilomar Conference on Signals, Systems amp; Computers*, volume 2, pages 1331–1335 vol.2, Nov 1997. doi: 10.1109/ACSSC.1997.679120.

[160] S. Kraut and L. L. Scharf. The cfar adaptive subspace detector is a scale-invariant glrt. *IEEE Transactions on Signal Processing*, 47(9):2538–2541, Sep 1999. ISSN 1053-587X. doi: 10.1109/78.782198.

[161] S. Kraut, L. L. Scharf, and L. T. McWhorter. Adaptive subspace detectors. *IEEE Transactions on Signal Processing*, 49(1):1–16, Jan 2001. ISSN 1053-587X. doi: 10.1109/78.890324.

[162] Kenneth S. Miller. On the inverse of the sum of matrices. *Mathematics Magazine*, 54(2):67–72, 1981. ISSN 0025570X, 19300980.

[163] H. Wang, P.C.P. Liang, C.H. Peng, and H.C. Huang. Rf transmitter, integrated circuit device, wireless communication unit and method therefor, June 28 2016. US Patent 9,379,742.

[164] Trung-Kien Nguyen, Nam-Jin Oh, Seok-Kyun Han, and Sang-Gug Lee. A low power cmos rf transmitter front-end for 2.4 ghz zigbee applications. In *IEEE Radio and Wireless Symposium*, pages 43–46, Jan 2006. doi: 10.1109/RWS.2006.1615090.